CHARACTERIZATION OF RIPARIAN WETLAND SOILS AND ASSOCIATED METAL CONCENTRATIONS AT THE HEADWATERS OF THE STILLWATER RIVER, MONTANA

by

Steven Allen Cook

A thesis submitted in partial fulfillment
of the requirements for the degree

of

Master of Science

in

Land Resources and Environmental Sciences

MONTANA STATE UNIVERSITY-BOZEMAN
Bozeman, Montana State University

April, 2007

© COPYRIGHT

by

Steven Allen Cook

2007

All Rights Reserved

APPROVAL

of a thesis submitted by

Steven Allen Cook

This thesis has been read by each member of the thesis committee and has been found to be satisfactory regarding content, English usage, format, citations, bibliographic style, and consistency, and is ready for submission to the Division of Graduate Education.

Dr. Brian L. McGlynn
(chair)

Approved for the Department of Land Resources and Environmental Sciences

Dr. Jon M. Wraith

Approved for the Division of Graduate Education

Dr. Carl A. Fox

STATEMENT OF PERMISSION TO USE

In presenting this thesis in partial fulfillment of the requirements for a master's degree at Montana State University-Bozeman, I agree that the Library shall make it available to borrowers under rules of the Library.

If I have indicated my intention to copyright this thesis by including a copyright notice page, copying is allowable only for scholarly purposes, consistent with "fair use" as prescribed in the U.S. Copyright Law. Requests for permission for extended quotation from or reproduction of this thesis in whole or in parts may be granted only by the copyright holder.

Steven Allen Cook

April, 2007

ACKNOWLEDGEMENTS

I wish to thank the U.S. Forest Service, which provided financial support for lab analysis, field support, and numerous discussions throughout the research effort. Special thanks go to U.S. Forest Service employees Mary Beth Marks, Joe Gurrieri, Henry Shovic, Mark Story, Janet Kempff, Kathryn Kaufman, and Leland Fuhrig. Additional thanks goes to George Furniss from the Montana Department of Environmental Quality for his invaluable input and field support, Kelsey Jencso for field survey assistance, and Marlene Renwick for assistance in describing the vegetation of the wetland.

I also wish to thank the following reviewers of early drafts of the manuscript:

Mike Wireman – U.S. Environmental Protection Agency

Mike Cormier – Maxim Technologies, Inc.

Bill Olsen – U.S. Fish and Wildlife Service

David Nimick – U.S. Geological Survey

I am especially thankful to my committee members:

Dr. Brian McGlynn – Chair

Dr. Clain Jones

Dr. Catherine Zabinski

Dr. Dave Brown – Former committee member

TABLE OF CONTENTS

LIST OF TABLES …… viii

LIST OF FIGURES …… ix

ABSTRACT …… x

1. INTRODUCTION …… 1

History of New World Mining District …… 1
Site Description …… 4
Acid Rock Drainage …… 6
Study Objective and Hypothesis …… 11
Project Design …… 13
XRF and ICP Metal Analysis …… 13
Spatial Distribution of Metals …… 15
Vertical Distribution of Metals …… 16
Statistical Analysis of XRF:ICP Data …… 16
Age Dating …… 17
Hydrologic Units …… 22
Piezometers and Monitoring Wells …… 22
Topographic Survey …… 24
Conclusion …… 27

2. LITERATURE REVIEW …… 29

Introduction …… 29
New World Mining District …… 31
Geology …… 31
Acid Rock Drainage …… 32
Daisy Creek and Stillwater River …… 36
Fisher Creek …… 38
Miller Creek and Soda Butte Creek …… 39
Regional Studies …… 42
Glaciation …… 42
Climate …… 43
Flooding …… 43
^{210}Pb Age Dating …… 44
Wetland Processes …… 46
Conclusion …… 49

TABLE OF CONTENTS CONTINUED

3. CHARACTERIZATION OF RIPARIAN WETLAND SOILS AND ASSOCIATED METAL CONCENTRATIONS AT THE HEADWATERS OF THE STILLWATER RIVER, MONTANA ……..…….....50

Introduction ……..……..... 50
Site Description ……..... 53
Materials and Methods …..……..... 56
Hydrologic Units ….....……..…….....56
Soil Metal Analysis ...……..……..... 57
Spatial and Vertical Metal Distribution ……...…..…… ……57
XRF and ICP Analysis ……...…… 58
Organic Carbon/Nitrogen/pH Analysis …….……..... 61
Soil Age Dating …….……...……...…….....61
^{14}C Analysis …… ……...……...…...…….……..... 62
^{210}Pb Analysis …….....……..... …...63
Hydrology …. ……..……...64
Groundwater Gradients and Chemistry ……...…….……..64
Topographic Map with Flood Elevations ……..……..……...65
Results …..……...……..……..……... 66
Hydrologic Units and Vegetation …. ……..…… 66
Soil Metal Analysis ...……...……..……...68
Spatial Distribution of Metals ……...……..... 68
Regression Analysis of XRF:ICP Data ……...……...…….....69
Vertical Distribution of Metals …….…….....… 72
Stream Channel Distribution of Metals ……..…….…….....79
Bivariate Metal Analysis …...……..... 80
Soil Age Dating …….……..... 82
^{14}C Analysis ...……..…… 82
^{210}Pb Analysis ……...……...……..... 84
Hydrology …… …..……..... 89
Vertical Hydraulic Gradients …….…….....…..... 89
Groundwater Chemistry……. ……..... 89
Flooding Potential…….……..……..... 91
Discussion …..……..……..... 92
Conceptual Model of Metal Deposition ……..……...…….. 97
Conclusion …...…….……..... 99

4. HAND-PORTABLE X-RAY FLORESCENCE APPLICATION TO METALS CHARACTERIZATION IN A RIPARIAN WETLAND IMPACTED BY ACID ROCK DRAINAGE ……....101

TABLE OF CONTENTS CONTINUED

Introduction ……...101

Site Description ……..…….104
Materials and Methods ……..…....106
Soils ……..……...……..... 106
Metal Analysis ……..…….…….... 107
Results ……..……..109
Duration Test ……..……...…….. 110
XRF:ICP Error……... ……..……... .112
Regression Analysis ……..……..114
Spatial Maps ……..……..116
Discussion ……..……..... ..…..119
Conclusion ……...…….……....…..125

5. SUMMARY ……..126

REFERENCES CITED …….……..…..129

APPENDICES …….……..... 135

APPENDIX A: Metals Data …….……...……..... 136

APPENDIX B: Soil Age Data …...……..……...…….. 179

APPENDIX C: Vegetation and Well Data ……...……...……. 195

LIST OF TABLES

Table Page

1. Statistics for the active floodplain metals (ICP adjusted XRF) by depth .. …… 72
2. Statistics for the beaverpond marsh metals (ICP adjusted XRF) by depth ……..73
3. 2004 In-stream sediment sample results for Daisy Creek and Stillwater River .....…. 80
4. Summary of average sedimentation estimates calculated from ^{210}Pb analysis …..... 84
5. Statistics for pre-mining and post-mining metal concentrations ……..…. 88
6. Monitoring wells chemistry data . ……..…. 90
7. Selected trace metal concentrations for the Western U.S. and Stillwater watershed....95
8. Daisy Creek and Stillwater River surface water chemistry …….. ……..…..95
9. Box plot and descriptive statistics for copper, lead, and zinc …..…….....113
10. ICP recovery results for duplicate soil samples ……..…….…… 115
11. ICP % difference analysis for duplicate soil samples ……….....117
12. Survey data for soil sample locations ……..…… 137
13. XRF Data for soil samples collected in 2003 …..……...……..... 143
14. ICP Data for soil samples collected in 2003 ……..……..144
15. XRF Data for soil samples collected in 2004 ……....……..... 146
16. ICP Data for soil samples collected in 2004 ……..……...167
17. Carbon and nitrogen data for soil samples collected in 2004 ……..... 169
18. Stream sediment data for lower Daisy Cr. and upper Stillwater River ……170
19. ANOVA results for pre-mining and post-mining metals in the marsh soils ……171
20. ANOVA results for pre-mining and post-mining metals in the floodplain soils ….172
21. ANOVA results (LSD) for copper concentrations by depth in the marsh ……..173
22. ANOVA results (LSD) for lead concentrations by depth in the marsh ……..... 174
23. ANOVA results (LSD) for zinc concentrations by depth in the marsh ……... 175
24. ANOVA results (LSD) for copper concentrations by depth in the floodplain …….176
25. ANOVA results (LSD) for lead concentrations by depth in the floodplain …….177
26. ANOVA results (LSD) for zinc concentrations by depth in the floodplain …….178
27. Data and ages from ^{210}Pb analysis …….....….184
28. Results of ^{14}C analysis from Beta Analytic……..... 187
29. Survey data for monitoring wells and piezometer nest locations …… 199
30. Well evacuation data for monitoring well M1 …….....200
31. Water chemistry data for monitoring well M1 ……..……..... 200
32. Well evacuation data for monitoring well M2 ……201
33. Water chemistry data for monitoring well M2 ……..... 201
34. Well evacuation data for monitoring well M3 …….....202
35. Water chemistry data for monitoring well M3 …….....202
36. Well evacuation data for monitoring well M5 ……203
37. Water chemistry data for monitoring well M5 …… 203
38. Well evacuation data for monitoring well M11 ……...204
39. Water chemistry data for monitoring well M11 ……...204

LIST OF FIGURES

Figure Page

1. Location map of the Stillwater wetland study area 5
2. The potential metal transport pathways from the source to sink 10
3. Areal soil and stream sediment sampling locations 19
4. Soil sampling locations for age-dating 20
5. Vegetation habitat types for the hydrological units 23
6. Piezometer design and completion data 25
7. Monitoring well design and completion data 25
8. Location of monitoring wells and piezometers 26
9. Topographic survey locations 27
10. Location map of the Stillwater wetland study area 51
11. Study area and soil sampling locations for metal and age dating analysis 54
12. Location of monitoring wells, piezometers and hydrologic units 55
13. Spatial maps of copper, lead, and zinc concentrations 68
14. Cross-section depth profiles for copper, lead, and zinc 70
15. Copper, lead, and zinc box plots by depth for the marsh and active floodplain 71
16. Regression plot of ICP vs XRF for copper 74
17. Metal/depth plots for the two dominant settings in the Stillwater wetland 76
18. Percent carbon, nitrogen and pH depth profiles for three sample sites 78
19. Metal/depth profiles for the Daisy Creek and Stillwater River reference sites 79
20. Bivariate plots of copper, lead, and zinc concentrations 81
21. Copper levels, and ^{14}C and ^{210}Pb ages for peat and charcoal samples 83
22. Plots showing metal levels, ^{210}Pb data, and sedimentation estimates 85
23. Copper, lead, and zinc concentrations for the marsh and active floodplain 87
24. Flood inundation maps of the wetland at three flood stages 91
25. Location map of the Stillwater wetland study area and soil sampling locations 103
26. Plot of optimum time to analyze samples 111
27. ICP error results from the analysis of soil standard 2710 116
28. Regression residual plot of ICP vs XRF for copper, lead and zinc 118
29. Histograms of predicted residuals of copper, lead, and zinc 119
30. Spatial map of XRF and ICP copper concentrations 120
31. Plots of all the ^{210}Pb profiles for the Stillwater wetland 183
32. Calibration plot for ^{14}C ages for sample PS1 (180-190 cm) 189
33. Calibration plot for ^{14}C ages for sample PS2 (70-90 cm) 190
34. Calibration plot for ^{14}C ages for sample PS2 (90-110 cm) 191
35. Calibration plot for ^{14}C ages for sample PS2 (110-130 cm) 192
36. Calibration plot for ^{14}C ages for sample PS3 (120-130 cm) 193
37. Calibration plot for ^{14}C ages for sample PS4 (90-100 cm) 194

ABSTRACT

I investigated the spatial and vertical distribution of metals in an alpine riparian wetland downstream of acid rock drainage in the New World Mining District, Cooke City, Montana. The McLaren ore deposit was discovered on Fisher Mountain in 1933, and underground and open-cut mining occurred until 1953. Fisher Mountain is the primary source of acid rock drainage in this part of the New World Mining District. Both natural and mining related processes released acidity and metals (particularly copper, lead, and zinc) into Daisy Creek and the upper Stillwater River in the form of dissolved metals and metal-rich sediment. The Stillwater River flows through the 66-hectare Stillwater wetland before entering the Beartooth Wilderness Area. This wetland has had the potential to accumulate metals beginning with retreat of the glaciers from the Beartooth plateau approximately 11,000 years ago.

I investigated the spatial and vertical distribution of metals (copper, lead, and zinc) using XRF and ICP-AES laboratory analysis, and the timing of metal deposition using ^{14}C and ^{210}Pb age-dating techniques. The 66-hectare wetland was sampled on a 100 by 100 meter grid (105 samples) and along 7 detailed transects (887 samples). The metal concentrations ranged from 38 to 7088 mg/kg for copper, 29 to 114 mg/kg for lead, and 43 to 775 mg/kg for zinc. The results of metal mapping and age-dating highlighted two metal deposition settings. The active floodplain had the highest copper and zinc concentrations in the 20 cm. of the soil profile and had estimated soil ages that predated the earliest mining activity. Soils in the wetland marsh had copper and zinc concentrations that increased with depth and were older than the mining activity. Radiocarbon analysis indicated a peat layer in the wetland was thousands of years old (2770 to 8710 years BP) and contained metals, suggesting a long history of metal deposition. This investigation integrates XRF plus ICP metal analysis and ^{14}C and ^{210}Pb age dating for characterizing metal concentrations in a riparian wetland impacted by acid rock drainage.

INTRODUCTION

History of New World Mining District

Gold and other valuable minerals were discovered near Cooke City, Montana in 1869 by four trappers, whose reports brought prospectors to the area the following summer (Lovering, 1929). Mining occurred over the next 100 years at numerous locations in the area using underground and surface mining techniques. This region, named the New World Mining District, is adjacent to Yellowstone National Park and the Beartooth Wilderness Area, and consists of an alpine landscape with steep mountains and deep forested valleys. The McLaren ore deposit, which was discovered in 1933, was the main location of mining activity in the Daisy Creek watershed. The ore body was initially mined with a number of underground tunnels starting in 1934, and by open cut methods from 1938 until 1953 (Elliot et al., 1992). The isolation of the New World Mining District, long harsh winters, and distance from major transportation corridors prevented the development of large scale mining operations and population growth. Today, the region serves as a recreational destination, and Cooke City has a population of several hundred residents.

While the scale of the mining activity was small compared to modern operations, the environmental impacts have been significant. One of the biggest impacts is acid rock drainage, which results in high metal concentrations and acidity in water resources downstream of the ore bodies. Sulfide deposits often contain pyrite which when exposed to oxygen and water generates acidity thereby releasing metals into surface runoff and

groundwater. This process, which occurs naturally and is often enhanced by mining activity, is a major problem in mining districts throughout the western U.S. and the world.

Two of the watersheds in the New World Mining District with headwaters originating on Fisher Mountain are impacted by acid rock drainage. Fisher Creek begins near the Glengary Adit, and has iron-stained cobbles for several kilometers downstream (Kimball et al., 1999). Daisy Creek starts downslope of the McLaren ore deposit and has iron-stained cobbles its entire length (Nimick et al., 2001). Daisy Creek flows into the Stillwater River, which flows through a 66 hectare wetland before entering the Beartooth wilderness area. Upstream of the confluence with Daisy Creek, the Stillwater River has high quality water resources, but downstream of the confluence the river has high concentrations of aluminum, copper, iron, and zinc (Gurrieri, 1998). At an established water quality sampling station (SW-7) on the Stillwater River at the lower end of the wetland, copper and aluminum exceeded the acute and/or chronic aquatic life standards during some of the sampling dates (Maxim, 2003 and 2007). The Stillwater River carries this metal load as it meanders through the wetland. During spring runoff and flood events, these metals can be deposited across the wetland. Only after several tributaries flow into the Stillwater River downstream of the wetland does the water quality meet Montana water quality standards.

Crown Butte Mining, Inc. did exploratory drilling in Fisher Mountain in the late 1980's and determined that over two million ounces of ore deposits still remained in the McLaren deposit (Nimick et al., 2001). Crown Butte also conducted a number of

reclamation activities in the 1990's as part of their exploration work. Crown Butte Mining, Inc. was in the process of permitting a large underground mine under Fisher Mountain in the 1990's when the U.S. government bought their mining claims due to public concerns about the impact of the mining activities on the waters and wildlife of Yellowstone National Park. The government purchased Crown Butte's mineral leases in 1996 and the New World Mining District Response and Restoration Project was implemented as a Superfund project under the Comprehensive Environmental Response, Compensation, and Liability Act (CERCLA), with the U.S. Forest Service (USFS) as the agency responsible for managing the cleanup. This buyout on August 12, 1996 committed $22,500,000 to clean up of historic mining impacts. The Consent Decree, which was signed in June, 1998, finalized the terms of the agreement and made funds available for restoration activities (Maxim, 2003). The New World Mining District Response and Restoration Project was initiated in 1999 and has addressed many of the major inputs by sealing adits and mining tunnels, and consolidating mining waste into repositories.

While the upstream mining deposits have been studied in great detail since their discovery in the 1870's, the Stillwater wetland has received little scientific study. The wetland has been suspected of being both a sink and source for metals (Gurrieri, 1998). However, no extensive investigation has been conducted to determine the actual levels of metal concentrations within the wetland soils. Some investigative work occurred in the 1990's as the mineral resources of the area were being evaluated by Crown Butte Mining, Inc. (Hydrometrics, 1994). Still, the areal and vertical metal concentrations (and the

timing of metal deposition) within the wetland soils was unknown. Because major reclamation activities were occurring on the upstream areas impacted by mining, an understanding of the metal concentrations present in the wetland was important to evaluating the downstream legacy of mining activities.

My research addressed some of these concerns and consisted of an extensive soil study to characterize the metal concentrations in the wetland soils and the timing of metal deposition. Soil samples were collected throughout the wetland and analyzed for metal content, with a subset selected for age-dating using ^{14}C and ^{210}Pb techniques. The hydrology of the wetland was also studied with the installation of monitoring wells, piezometers and topographic surveying.

Site Description

The Stillwater wetland is located at latitude 45º 04' 40" N and longitude 109º 59' 45" W. The wetland is approximately 66 hectares in size, and is located in a glacier carved valley at an elevation of 2585 meters. The wetland is adjacent to the Beartooth Wilderness Area and just over 4 kilometers from Yellowstone National Park (Figure 1). The study area (150-hectares) was comprised of the active floodplain of the Stillwater River; an alluvial fan formed by an unnamed stream flowing into the wetland from the western edge; and marshy areas with abundant beaver ponds. The bedrock surrounding the wetland is Paleozoic sedimentary rocks (predominately limestone, dolomite and shale) that have been intruded by Eocene volcanic dikes, sills and laccoliths (Lovering, 1929; Elliot et al., 1992). Glacial features dominate the surrounding landscape, with

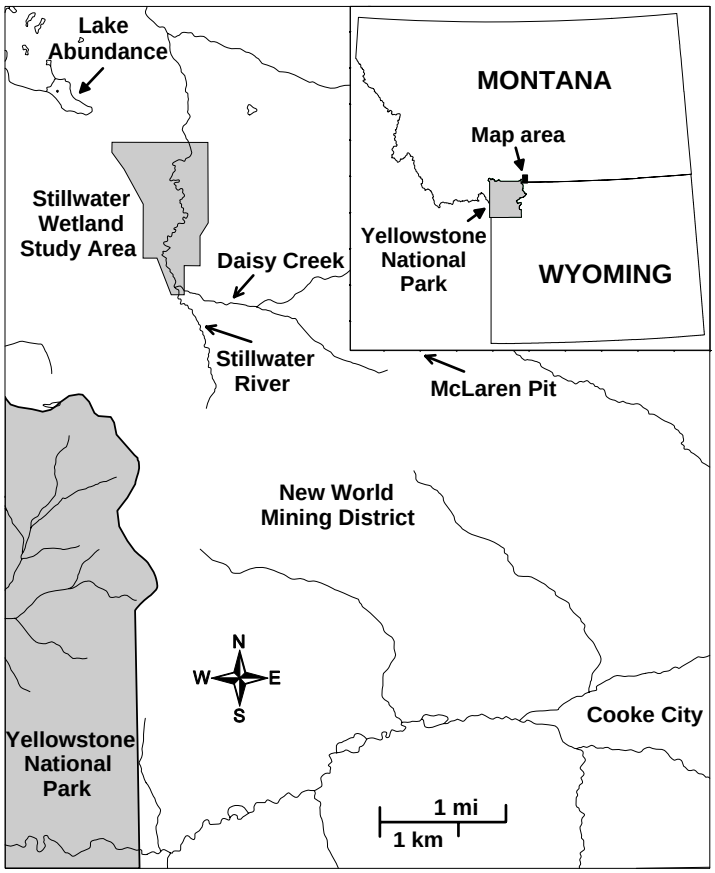


Figure 1. Map of the Stillwater wetland study area.

moraines covering the hillsides surrounding the wetland. The area is typically snow covered for up to six months per year, and has a cool summer alpine climate.

The marsh areas of the wetland are dominated by planeleaf willow (*Salix planifolia)* and water sedge (*Carex aquatilis)*, whereas the drier portions of the wetland are dominated by wolf's willow (*Salix wolfii)* and water sedge. The alluvial fan transitions from willow thickets and sedges, to grasses and forbs, to an engelmann spruce (*Picea engelmannii*) and subalpine fir (*Abies lasiocarpa)* forest near the upslope edge of the wetland. The marsh areas are typically underlain by clay and silty soils, whereas the floodplain and alluvial fan contain more sands and fine gravel. The bed material of the

Stillwater River is armored with iron-stained cobbles from the confluence with Daisy Creek to the lower end of the study area. Beaver ponds are abundant throughout the lower half of the wetland and have helped sustain near surface water tables throughout much of this area. Air photos (taken on 8-7-96) of the wetland show numerous abandoned channels surrounding the beaver ponds, indicating long-term beaver activity.

Acid Rock Drainage

The geology of the New World Mining District is important to understanding the processes of metal transport and deposition in the Stillwater wetland. The bedrock in the New World Mining District is igneous and sedimentary rock of Precambrian and Paleozoic ages that was uplifted during the Laramide orogeny to form the Beartooth Mountains (Elliot et al., 1992). These rocks were intruded by Eocene volcanic and intrusive rocks, which altered the Paleozoic limestone with hydrothermal fluids that led to precipitation of sulfide deposits (Johnson et al., 1994). Quaternary glaciation then altered the landscape, leaving behind the landscape that we see today (Lovering, 1929; Pierce, 1979).

The Paleozoic bedrock is nearly 2000 feet in thickness, and consists predominately of limestone with interbedded dolomite, shale, and sandstone. Eocene igneous activity intruded into these rocks with extensive replacement of the original rock and mineralization of sulfide metals. These intrusions of stocks, laccoliths, sills and dikes created economically viable deposits of copper, gold, and silver. The McLaren deposit is a gold bearing copper skarn that also contains significant quantities of silver (Johnson et

al., 1994). The primary ore body is associated with quartz-pyrite rocks in the Meagher formation. Significant ore deposits are also found along faults and in limestone blocks incorporated into intrusive breccias (Elliot et al., 1992; Johnson et al., 1994).

These ore bodies and the altered bedrock contain other sulfides including pyrite and chalcopyrite. Oxidation of these sulfide minerals (particularly pyrite) by surface weathering processes releases metals and acidity into surface runoff and groundwater. The process is facilitated by microbes, which accelerates the generation of acidity (Stumm and Morgan, 1996). Pyrite comprises 95% of the sulfides present in the ore deposit, which accounts for the extensive acid rock drainage in the Daisy and Fisher Creek watersheds (Johnson et al., 1994). The source of the acid rock drainage in the Daisy Creek drainage is the McLaren ore deposit that is located on Fisher Mountain. Large areas of Fisher Mountain are acid generating. The open-pit mining added to these naturally occurring processes. Fisher Mountain is heavily fractured and has a major geological fault bounding the deposit, forming groundwater pathways that are complex and poorly understood (Johnson et al., 1994; Nimick et al., 2001). The chemical equilibrium reactions below describe generally accepted pyrite oxidization reactions (Stumm and Morgan, 1996, p. 691):

$$FeS_2(s) + 7/2O_2 + H_2O = Fe^{+2} + 2SO_4^{2-} + 2H^+ \qquad \text{(equation 1)}$$

$$Fe^{+2} + 1/4O_2 + H^+ = Fe^{+3} + 1/2H_2O \qquad \text{(equation 2)}$$

$$Fe^{+3} + 3H_2O = Fe(OH)_3(s) + 3H^+ \qquad \text{(equation 3)}$$

$$FeS_2(s) + 14Fe^{+3} + 8H_2O = 15Fe^{+2} + 2SO_4^{2-} + 16H^+ \qquad \text{(equation 4)}$$

Equation 1 represents the initial reaction of pyrite with water and oxygen, which produces ferrous iron, sulfate and acidity. The ferrous iron is converted through oxidation to ferric iron in equation 2. The ferric iron then hydrolyzes to ferric hydroxide, producing more acidity in equation 3. Ferric hydroxide is the iron species that coats the streambed sediments. Equation 4 represents the oxidation of pyrite by the additional ferric iron. This cyclic oxidation of pyrite is catalyzed by a species of autotrophic bacteria, *Thiobacillus ferroxidans*, which accelerates the conversion of ferrous iron to ferric iron (equation 2).

Acidity produced by pyrite oxidation dissolves metals contained in the rock matrix, which are transported by surface runoff and groundwater to streams and wetlands where they can severely impact aquatic fauna and flora. Dilution by less impacted waters eventually raises the pH of the stream, and metals in solution adsorb to suspended iron hydroxides and clay particles. These colloids eventually form particles large enough to settle to the bottom of the stream and form coatings on the streambed sediments (Amacher et al., 1995). Over time these coatings can undergo chemical transformations to become amorphous minerals that permanently bind the metals. Under the right conditions, these iron coatings can become thick enough to cement rock particles together and form a conglomerate rock called ferricrete, which is common along Daisy Creek (Furniss et al., 1999).

Acidic metal-rich water eventually reaches Daisy Creek, which begins with several springs at the base of Fisher Mountain (Furniss et al., 1999). The acidity of Daisy Creek reaches neutrality within several kilometers, but the metal load in the water column and the accumulation on stream bed sediments is still large in the Stillwater River

downstream of the confluence with Daisy Creek (Gurrieri, 1998). Figure 2 shows the dominant chemical processes and expected metal species along the flow pathways from Fisher Mountain (source) to the Stillwater wetland (sink). As the pH of the water rises, iron precipitates out of solution and coats the rocks in the stream channel with iron oxyhydroxide deposits (Furness et al., 1999). These iron stained stream sediments coat the streambed of Daisy Creek and the Stillwater River for some distance below the Stillwater wetland. Over time, the iron deposits can cement the stream sediments into ferricrete. Extensive ferricrete deposits found along Daisy and Fisher Creek indicate that this process has been occurring since the retreat of the glaciers. Radiocarbon dates of wood found in these ferricrete deposits range in age from 310 to 8840 years B.P. (Furness et al., 1999).

An ongoing study in the Daisy and Fisher Creek drainages has been investigating the age and chemical relationships of these deposits. Furniss and Gurrieri (in press) are developing a model for estimating pre-mining water quality in catchments impacted by acid rock drainage. Previous work has shown that the generation of acid rock drainage has been ongoing in the New World Mining District since the end of the last ice age, when these deposits were left exposed to the surface (Furniss et al., 1999).

The acidity produced by weathering of these sulfide deposits is partially balanced by the alkaline buffering provided by the abundant limestone in the Stillwater River watershed (Gurrieri, 1998). Limestone is present in the streambed cobbles and surrounding soils. Several small streams enter Daisy Creek along its path to the Stillwater River, and these influxes of water greatly reduce the acidity of Daisy Creek through both

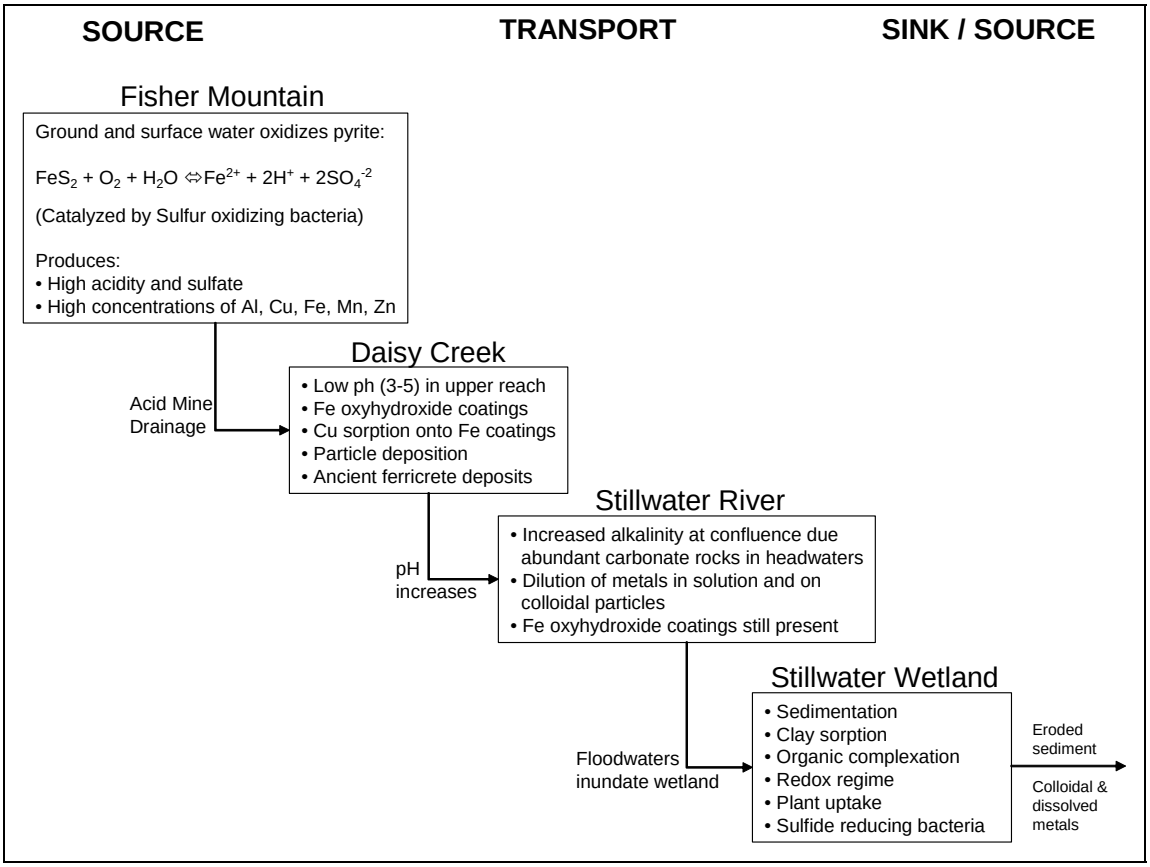


Figure 2. The potential metal transport pathways from the source at the McLaren ore deposit to the Stillwater wetland. Each box shows the dominant processes and expected metal speciation.

dilution and increased acid neutralizing capacity. At the confluence of the Daisy Creek and the Stillwater River, the water quality improves dramatically, and the pH of the water is neutral with the metals predominately in colloidal suspension. The Stillwater River upstream of the confluence with Daisy Creek is typical of a high quality Rocky Mountain stream, whereas downstream of the confluence, water quality impacts are significant (Gurrieri, 1998). Below the confluence, the only aquatic life present in the stream are metal-tolerant invertebrates. Concentrations of copper, aluminum and zinc at the lower end of the project area exceed Montana's acute aquatic water quality standards (Maxim, 2003).

One of the major efforts in the New World restoration project was the capping of the McLaren Pit which started in 2002 and was finished in 2003. This involved placing all the surrounding tailings back into the existing pit, and then capping the site with a liner and soil similar to that used in reclaiming landfills (Maxim, 2001). This was the largest reclamation effort that has occurred in the Daisy Creek watershed with significant potential to reduce acid rock drainage and improve water quality. The purpose of the reclamation work was to prevent weathering and oxidization of the sulfides in the waste rock and ore deposit. It is thought that by allowing the water to drain off the surface instead of infiltrating into the bedrock, acid rock drainage will be significantly curtailed. An important question is whether this really addresses the problem since there is an extensive fault and fracture system that transports groundwater under the capped tailings. Also, the added runoff may actually increase erosion downslope of the reclaimed area. An extensive network of monitoring wells has been in place in the McLaren Pit area which will be tested for water quality on a regular basis (Maxim, 2001). Together with surface water sampling of Daisy Creek, water quality monitoring will be used to evaluate the success of the reclamation effort.

Study Objective and Research Questions

The impact of acid rock drainage has been studied in some detail in the McLaren Pit area and along Daisy Creek, but the status of the Stillwater wetland soils remained unknown. Limited studies suggest that metals have always existed in the wetland sediments, but no extensive soils investigations have occurred. An important question is

whether the historic mining activity has enhanced the naturally occurring acid generating processes occurring on Fisher Mountain. Acid rock drainage has been impacting the Daisy Creek watershed for thousands of years (Furniss et al., 1999) and the mining activity at the McLaren ore deposit was of relatively short duration and of a limited scale. Since a major restoration project is ongoing in the New World Mining District, a better understanding of the metal concentrations in the Stillwater wetland is important for remediation and monitoring activities. The Stillwater wetland provides an excellent opportunity to gain new understanding of mining impacts on alpine riparian wetlands. These issues provide the context for my research objective, which was to quantify the vertical and spatial extent and timing of metal deposition in the riparian wetlands along the Stillwater River below the confluence of Daisy Creek.

I sought to address the following questions: (1) what are the spatial and vertical patterns of metal concentrations across the wetland; and (2) are the metal concentrations in the post-mining sediments higher than those in pre-mining sediments? I used a combination of metal analysis and dating of soil samples, measurements of water levels and water chemistry from piezometers and monitoring wells, and topographic and vegetation surveys. This allowed development of metal distribution maps and age-dated soil depth profiles to describe the concentration and timing of deposition of metals in the Stillwater wetland. Water levels and water quality data from the wells contributed to a basic understanding the movement of groundwater within the wetland. The topographic survey allowed development of maps that showed areas of the wetland that would be covered by water from several levels of flooding (based on elevation).

Project Design

XRF and ICP Metal Analysis

I investigated the concentration and timing of metal deposition utilizing an extensive soil sampling survey that mapped the spatial and vertical distribution of metals. Results from the metal analysis guided selection of characteristic vertical soil profiles for ^{210}Pb age dating. The USFS provided an X-Ray Fluorescence (Niton Xli 700 XRF) instrument for rapid assessment of metal concentrations that was used to analyze almost 1000 soil samples. A subset of these soil samples was analyzed with inductively coupled plasma atomic emission spectroscopy (ICP) to further quantify the metal concentrations and to evaluate the data quality provided by the XRF instrument.

Soil samples were collected using a hand-auger and stored in Ziploc plastic bags for transport back to the laboratory. The soil samples were either air-dried or dried in an oven at 45 ºC to prevent combustion of organic material. The gravel-sized particles and any visible vegetation fragments were separated from the dried soil samples by hand, and the remaining material was ground to a fine powder (~ 45 microns) using a SPEX CentriPrep 8000D ball-mill grinder so that a consistent particle size would be used in all analyses. Two possible sources of contamination were small particles from the grinding vial itself or metals that stick to the surface of the grinding vial during the grinding process. A grinding protocol was followed that was designed to reduce the potential for cross-contamination.

I used zirconium vials and an acid bath wash to reduce the potential for cross-contamination of soil samples. Zirconium vials are extremely hard, and even if particles

from the vials contaminated the soil sample, the metal was of no concern in the Stillwater wetland soil analysis. Dilute hydrochloric acid was used to dissolve any metals that might adhere to the surface of the grinding vial. The following process was used to grind all the soil samples that were collected from the Stillwater wetland:

1. Brush out residue from grinding vials.
2. Grind with fine sand for 2 minutes.
3. Rinse grinding vials in soapy water.
4. Rinse grinding vials in deionized water.
5. Rinse grinding vials for 5 minutes in a 4 molar hydrochloric acid /deionized water solution.
6. Rinse grinding vials in deionized water.
7. Dry grinding vials with Kimwipes.
8. Grind soil sample for 5 minutes.
9. Empty soil sample into 20 ml glass or HDPE sample bottle.

The ICP analysis used a strong acid digestion that followed the EPA 3050B protocol. The method is not a total digestion, since the elements bound to silicate structures (which are not normally mobile) will not be dissolved (U.S. EPA Method 3050B, 1996). The metals of interest in this research were copper, lead and zinc, although arsenic, cadmium, chromium, iron, manganese, and nickel concentrations were also quantified. Samples selected for ^{210}Pb analysis were also analyzed for pH, and total carbon and nitrogen content. The ICP and C/N analyses were performed by the Montana

State University Soil Analytical Laboratory. The MSU Lab used an Accuris model 3500 ICP instrument manufactured by Fisons Instruments for metal analysis, and a Leco TruSpec CN instrument for carbon and nitrogen. I added soil duplicates (5% of the soil samples) and eleven soil standards (Montana Soil SRM 2710) to the set of soils sent to the laboratory. These duplicates and standards were used to evaluate the quality of the data provided by the analytical laboratory.

Spatial Distribution of Metals

During the 2003 field season, we sampled the wetland soils utilizing a 100 x 100 meter grid, and collected a total of 105 soil samples (Figure 3a). The top 20 centimeters of the soil at each location was collected for a consolidated sample. After the soils were dried and ground, they were analyzed with both XRF and ICP analysis for metal concentrations. The data were used to produce spatial maps of metal concentrations. The spatial concentrations of copper, lead, and zinc were then mapped. I also performed an initial linear regression analysis of the XRF:ICP data to better understand the precision and accuracy of the data provided by the XRF instrument.

Maxim Technologies, Inc., which is the lead engineering firm for the New World restoration project, conducted a stream sediment sampling survey in 2005 that included the upper reaches of the Stillwater River (Figure 3c). I included this dataset in my research to better understand the spatial distribution of metals in the wetland. These stream sediments provide a major potential source of metals that can be remobilized during floods and re-deposited in those areas outside of the active stream channel.

Vertical Distribution of Metals

Spatial mapping of metal concentrations in the wetland revealed that the highest concentrations were located in the active floodplain and beaver pond marsh. Based on this information, I sampled those areas with the highest concentrations using vertical soil sampling during the 2004 field season. Seven transects (Figure 3b) were located in the active floodplain and beaver pond marsh hydrologic units. At each sample location, soil was collected at 10 cm intervals to a depth of 50 cm, and at 25 cm intervals to a depth of 100 cm. At a number of locations, it was not possible to sample to the 100 cm depth due to the presence of gravel. Samples were also collected from other locations: the McLaren Pit, adjacent to Daisy Creek, and next to the Stillwater River upstream of the confluence with Daisy Creek.

A total of 887 soil samples were collected, which were dried, ground and analyzed with the XRF instrument. Cross-sections of the transects were plotted as depth intervals versus metal concentration for copper, iron, lead, manganese, and zinc. The vertical metal concentrations were mapped along cross-sections. The cross-sections revealed trends in the metal concentrations, both horizontally and vertically. Based on the results of these cross-sections, we selected a subset of the soil samples for ICP, pH, carbon and nitrogen analysis, and ^{210}Pb dating.

Statistical Analysis of XRF:ICP Data

Simple linear regression analysis was used to evaluate the relationship between the XRF and ICP data. I assumed the ICP data reflected the “most accurate” measurement of true metal concentration, that it could be used to provide a measure of

the data quality provided by the XRF, and that it could be used to test the effectiveness of the XRF as a laboratory analysis tool. I used the regression equations to adjust the XRF data for mapping and plotting purposes. Plots of the residuals of observed and predicted ICP values showed that metal concentrations were normally distributed, and supported using ANOVA analysis and linear regression for XRF:ICP data.

Box plots of XRF:ICP data along with the sediment age estimates helped build a conceptual model of metal distribution within the wetland. I categorized the metals data into pre-mining versus post-mining for the active floodplain and beaver pond marsh hydrologic units. I used ANOVA (SPSS 13.0, Lead Technologies, Inc., 2001) to determine whether there were differences in the spatial and vertical metal concentrations between these two hydrologic units. I used the Levene's test to evaluate the homogeneity of variances of the XRF:ICP data.

Age Dating

I dated 7 soil samples using ^{14}C analysis and 74 samples using ^{210}Pb analysis (Figure 4). Each dating technique provides a unique dating window: ^{14}C measurements are on the scale of thousands of years; whereas ^{210}Pb measurements have a maximum of 100 to 150 years of applicability (Shukla, 2002). Since mining activity started in 1933 at the McLaren ore deposit, metal deposition cannot be attributed to mining activity for a soil sample with high metal concentrations greater than 73 years old. If sediment with high metal concentrations was less than 73 years old, then both natural processes and mining activity may have been the source of metals. Metal concentrations were

considered high if they were of the same order of magnitude as those found at the McLaren ore deposit.

Since mining of the McLaren ore deposit occurred within the last 100 years, the ^{210}Pb dating method provided a useful diagnostic tool for differentiating between pre-mining and post-mining wetland sediments. In my analysis, I used the calendar year 1933 (73 years ago) as the cutoff between pre-mining and post-mining sediment. The ^{210}Pb technique provided sediment ages of soil profiles in detail and age range (young) that ^{14}C could not provide (because of the ^{14}C requirement for organic matter, cost of analysis, and temporal resolution). The ^{210}Pb technique does not require special soil sample handling techniques, and the lower costs of analysis allowed dating of a larger number of samples. The ability to date all the samples from a single soil profile (which was typically 5 to 7 soil samples) also allowed calculation of sedimentation rates.

An assumption of my research is that the concentration of metals in the soil today represents concentrations comparable to those at the time of deposition. This is a common assumption in soils that not extremely acidic (Gambrell, 1994). Soil mapping revealed two characteristic metal concentration profiles: (1) high metal concentrations (particularly copper and zinc) in the shallow floodplain sediments; and (2) high metal concentrations (particularly copper and zinc) in the beaver pond marsh. Soil samples were selected for ^{210}Pb dating to define the timing of these two depositional settings.

Four initial samples were selected and analyzed by the U.S. Geological Survey Center for Coastal and Regional Marine Studies (St. Petersburg, FL) to evaluate whether the ^{210}Pb technique was appropriate for the Stillwater wetland soils (e.g. if any of the soil

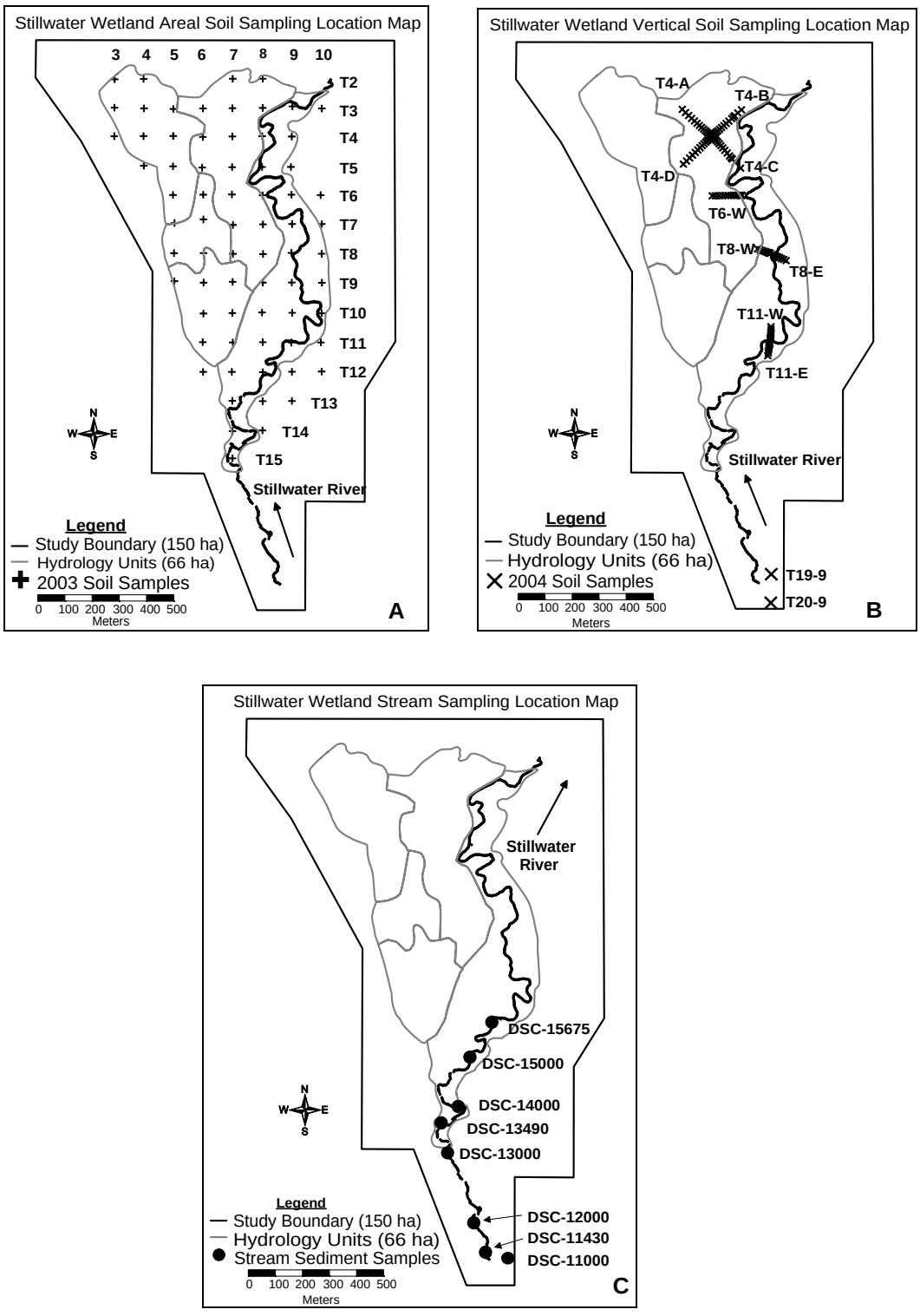


Figure 3. (a) Shallow (0-20 cm) soil samples collected in 2003. (b) Deeper soil transects (0-100 cm) collected in 2004. (c) Stream sediment sampling locations conducted by Maxim Technologies in 2005.

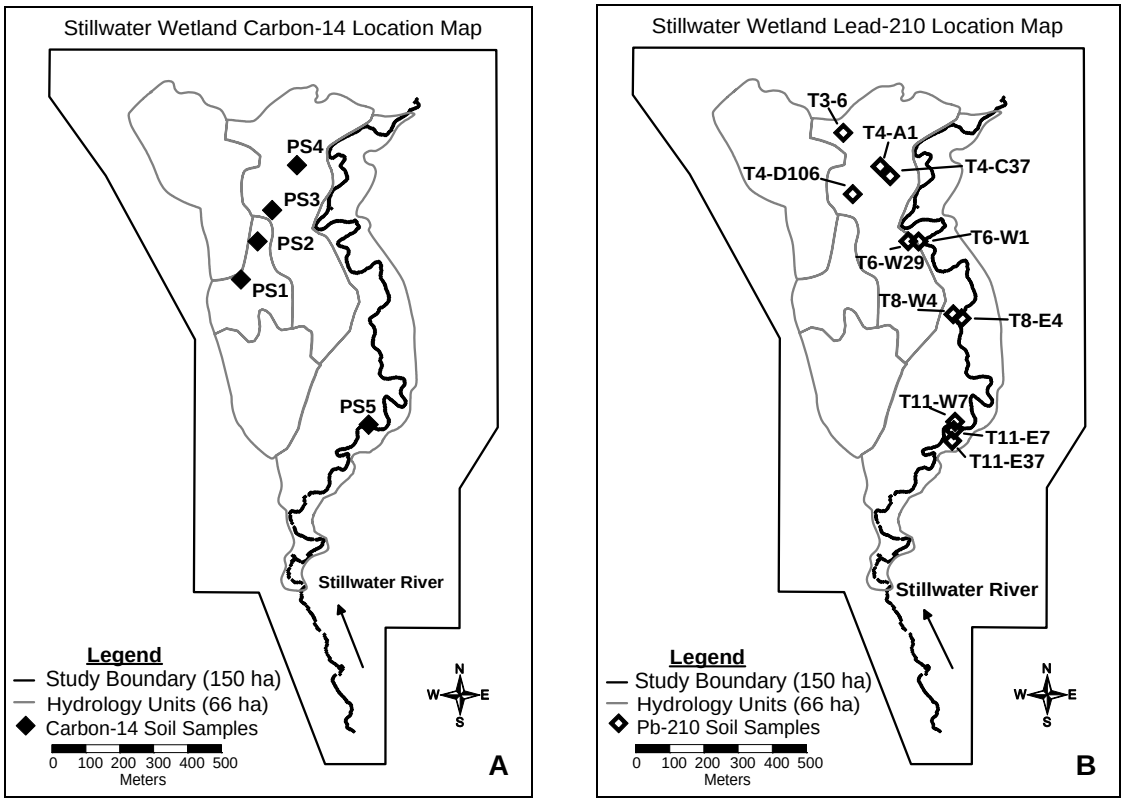


Figure 4. (a) Locations of the samples for ^{14}C age dating. (b) Location of the samples for ^{210}Pb age dating.

samples were still in a state of disequilibrium). Disequilibrium indicates that the soil samples contain an excessive and detectable amount of ^{210}Pb activity. The samples were selected based on the metal concentration profiles and location within the two primary depositional settings of interest. The results of the preliminary analysis indicated that the technique was appropriate for these wetland soils. I then selected eleven soil profiles (74 samples) for analysis at the U.S.G.S. Center for Coastal and Regional Marine Studies laboratory for ^{210}Pb dating. Radioactive activity of ^{210}Pb, ^{226}Ra, and ^{137}Cs was measured using gamma spectroscopy, which was then used to calculate calendar dates for each soil sample.

During the 2005 field season, I collected peat samples for ^{14}C dating. While installing one of the monitoring wells, we augered through a peat layer that was at the same depth as sediment with elevated metal concentrations (copper and zinc). I sampled this organic layer along a transect and collected six samples across 4 sample sites (PS1-PS4) at a depth ranging from 70 to 190 cm (Figure 4a). The average distance between sample sites was 116 m; with a total transect length of 348 m. I also collected a charcoal sample (PS5) at a depth of 80-90 cm from a sample location adjacent to the Stillwater River.

Spatial mapping of metal concentrations confirmed that these areas were important to understanding the timing of metal deposition within the wetland. I believe this is a continuous peat layer that provided a range of dates showing that metal deposition in this part of the wetland has been active for thousands of years. One of the sample sites contained a thicker peat deposit which yielded three separate samples that were dated. These samples provided the data necessary to estimate gross sedimentation rates.

The soil sample collected next to the Stillwater River contained small fragments of a charcoal-like material. This sample site was located within several meters of the stream and was on the active floodplain. The active floodplain was shown to have high metal concentrations in the upper section of the soil profile relative to the deeper sections of the profile. The charcoal-like material selected for radiocarbon dating came from the 80-90 cm depth range, and was below sediment layers with the highest metal concentrations. The soil profile was a mixture of sand, silt and pea to cobble-sized gravel.

The organic samples were collected using a hand auger and stored in Ziploc bags until they were dried. They were oven dried at 45 ºC on plastic plates to prevent carbon contamination and combustion of organic material. Five of the samples were dated from consolidated peat samples, and two were dated from single wood fragments. These samples were analyzed by Beta Analytic Radiocarbon Dating Laboratory (Miami, FL). Beta Analytic used standard acid/alkali/acid wash techniques to prepare the samples, and Accelerator Mass Spectrometry (AMS) for measuring the radioactivity of the samples.

Hydrologic Units

The wetland was divided into five hydrologic units (units of similarity) based on geomorphic and hydrological properties (Figure 5). These units were first delineated from stereoscopic air photographs using changes in elevation, vegetation, and surface hydrology. The boundaries were then verified and/or adjusted during field reconnaissance. The vegetation habitat types were described in 2005 with the aid of Marlene Renwick (U.S.F.S. plant ecologist), who provided a detailed description of each unit (Appendix C). The vegetation survey helped to delineate the hydrologic units and to evaluate whether high metal concentrations were having an impact on the wetland plants. The active floodplain hydrologic unit includes the present stream channel and the area of the wetland that would be covered by water (~1 meter) during a small to moderate flood event above the constricted wetland outlet elevation.

Piezometers and Monitoring Wells

I investigated the groundwater hydrology and chemistry of the Stillwater wetland

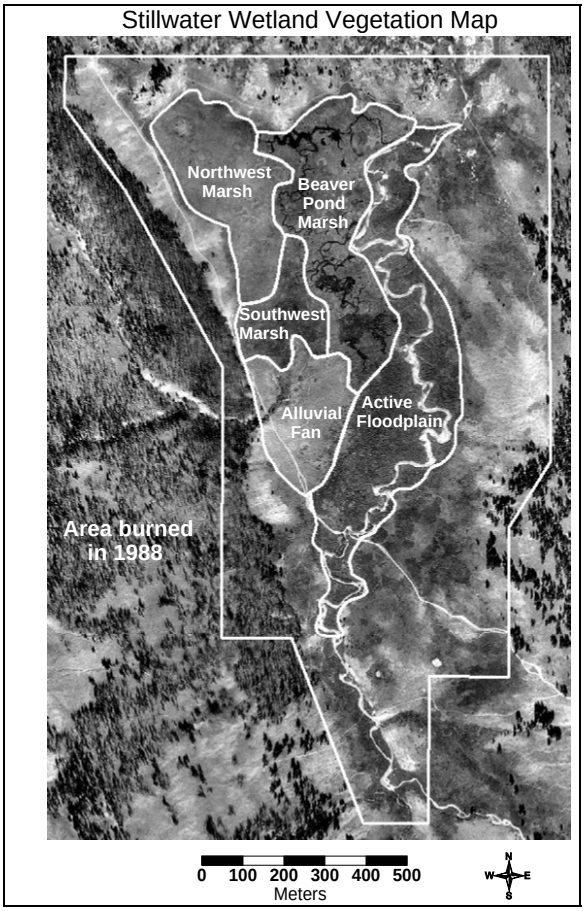


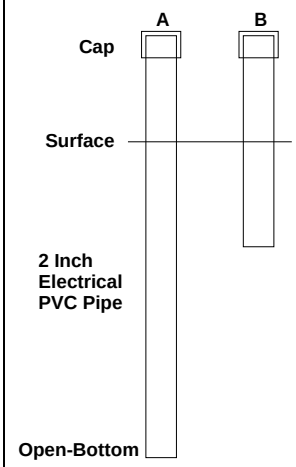
Figure 5. Vegetation habitat types for the five hydrologic units of the Stillwater wetland. Vegetative habitat types for each hydrologic unit are the following: Northwest Marsh Unit - Planeleaf Willow/Water Sedge; Beaver Pond Marsh Unit - Planeleaf Willow/Water Sedge; Active Floodplain Unit – Wolf's Willow/Tufted Hairgrass; Southwest Marsh Unit – Wolf's Willow/Water Sedge; Alluvial Fan Unit – Wolf's Willow/Tufted Hairgrass.

using monitoring wells and piezometers. Figures 6 and 7 show the well configurations and installation dates and figure 8 shows the locations of these wells. Piezometers and monitoring wells were installed by hand with a combination of augers and driven piezometers. Field properties of all the wells included water elevations, temperature, pH and electrical conductivity. The monitoring wells were sampled in 2005 for anions, cations, and metal analysis.

Topographic Survey

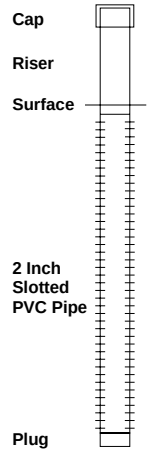
The topography of the Stillwater wetland partially controls and reflects the movement of surface water across the wetland complex. Beaver ponds play an important role in the wetland by storing water in an extensive pond network, which helps support a saturated environment throughout much of the wetland. The surface topography partially determines which areas of the wetland will receive overbank flow during flooding events. Investigation of metal concentrations and topography provided context for understanding the likely mechanisms for deposition of metals in the wetland. A topographic survey of the wetland was used to build flood inundation maps based on the valley bedrock constriction at the downstream end of the wetland. In my analysis, areas with the same elevation had the same potential for inundation. While I suspected that the highest metal concentrations would be found along the channel, the entire lower end of the wetland appeared to be more susceptible to flooding. Flooding has the potential for dispersing metal-rich sediment and dissolved metals across the wetland.

The largest scale U.S.G.S. topographic map (1:24000 with a contour interval of 40 feet) shows no topographic relief in the wetland even though there is significant micro-topography and a gradual elevation gradient from the upper to lower end of the wetland. Therefore, a topographic survey was conducted using conventional survey equipment (Pentax PTS-V3 Total Station and Husky FS/2 Data Collector with Tripod Data Systems Software) and survey-grade GPS equipment (Trimble Total Station with model 5700 base station and model 5800 rover). A total of 1784 survey points were collected during 5 days of surveying during the 2003 and 2004 field seasons (Figure 9).



Piezometer Name	Ground Surface Elevation (meters)	Completion Depth (meters) A	Completion Depth (meters) B	Installation Date
P1	2575.60	2.04	1.00	7/29/2003
P2	2575.25	2.11	1.00	7/30/2003
P3	2579.23	2.06	1.00	7/31/2003
P4	2579.67	2.03	1.00	7/30/2003
P5	2579.62	2.05	1.00	7/31/2003

Figure 6. Piezometer design and completion data.



Monitoring Well Name	Ground Surface Elevation (meters)	Completion Depth (meters)	Installation Date
M1	2575.66	3.16	8/14/2003
M2	2575.44	2.90	8/14/2003
M3	2575.14	1.68	8/13/2003
M5	2579.32	2.03	8/13/2003
M11	2779.36	1.48	8/14/2003

Figure 7. Monitoring well design and completion data.

The survey data points included every soil sample and well location, the main channel of the Stillwater River, and a large number of points scattered throughout the wetland. The data was gridded in Surfer (Golden Software, Inc.) mapping software to produce topographic maps. Data from the U.S.G.S. 10-meter digital elevation model (DEM) was used to control the area outside the surveyed area of the wetland during interpolation. The

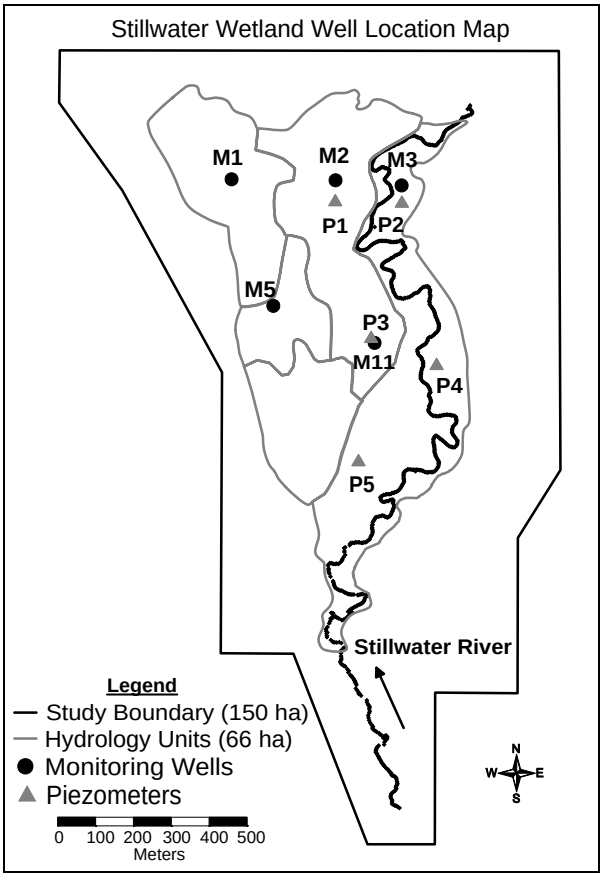


Figure 8. Location of monitoring wells and piezometers.

minimum curvature algorithm, which is used extensively by earth scientists, generated the most realistic topographic surface matching field observations of the wetland. This algorithm generates a thin, linearly elastic plate passing through each of the data values with a minimum amount of bending. The algorithm attempts to honor the data as closely as possible, but is not an exact interpolator (Surfer 8.01 Documentation, 2002). A total of 10,907 data points were used to produce the wetland and surrounding landscape topographic coverage. The fine scale topography allowed for an improved depositional model and an understanding of the mechanisms of metal accumulation within the wetland.

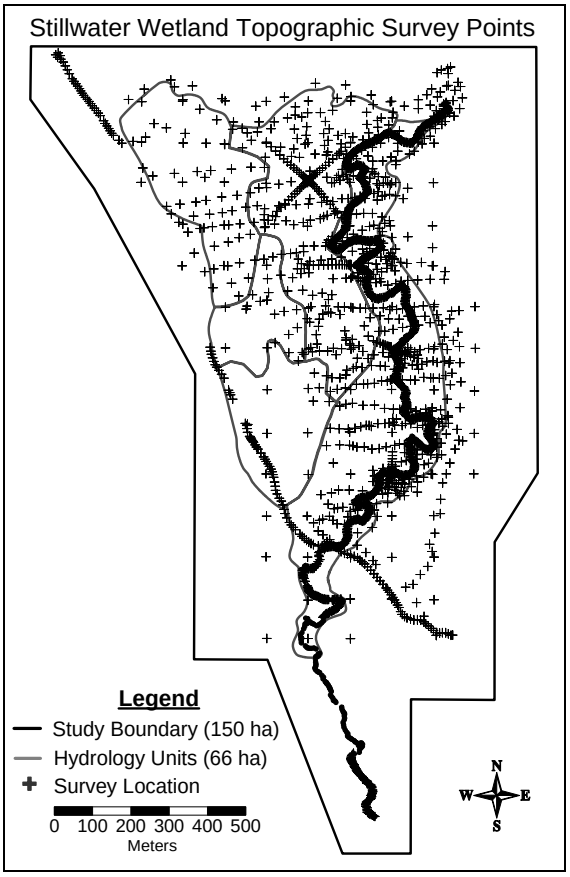


Figure 9. Topographic survey points.

Conclusion

Acid rock drainage (natural and mining related) has impacted the Daisy Creek and upper Stillwater River watersheds, and my research employed innovative techniques to investigate these impacts on a downstream alpine riparian wetland. I utilized the XRF instrument and ^{210}Pb age-dating method to address the spatial and vertical distribution of metals in the wetland soils, and their timing of deposition. I also used ICP-AES metal analysis, ^{14}C age-dating, monitoring wells, nested piezometers, and topographic surveying to add to my understanding of the status of the wetland soils. The statistical

analysis of the XRF:ICP data provided an evaluation of the data quality of the XRF instrument, which is becoming an accepted tool in mining-related reclamation activities.

LITERATURE REVIEW

Introduction

The geology of the New World Mining District has been extensively studied due to the rich mineral resources of the area. The surrounding area, which includes Yellowstone National Park, has also been the subject of a broad range of scientific studies due to the unique geology and relatively undisturbed ecosystem. Studies that investigated the impact of mining activities on the waters of the upper Stillwater River and the wetland that the river flows through before entering the Beartooth Wilderness Area are more limited.

This literature review summarizes the relevant research that has occurred in the New World Mining District and the surrounding area. These studies describe geologic, climatic, and biogeochemical processes that control the levels of metal concentrations within wetlands. The bedrock geology at the headwaters of Daisy Creek results in acid rock drainage that releases metals which are then transported by surface runoff and groundwater to the Stillwater River and wetland. Mining activity has been indicated as the primary cause of environmental degradation, but research on ancient ferricrete deposits suggest that this process has been going on since the end of the last ice age (Furniss et al., 1999).

The major streams that flow from the mining district have been the subject of several studies focused on the movement of metals in the watershed. Daisy Creek, Fisher Creek, and Miller Creek have been sites for tracer injection and synoptic sampling

surveys performed by the U.S. Geological Survey (USGS) for quantification of metal loads (Kimball et al., 1999; Nimick et al., 2001; Cleasby et al., 2002). The wetlands in Fisher Creek have also been investigated to evaluate the potential for natural wetlands to remediate copper contaminated water (MacHardy-Mitman, 2002). Wetlands are known sinks (and potential sources) of metals, and MacHardy-Mitman (2002) found that the wetlands downstream of the Glengary adit were had high metal concentrations in the sediments, functioning as a metal sink.

Regional studies have focused on glaciation, vegetation, fire, and metal distribution due to flooding events, with the research primarily located in Yellowstone National Park. The glacial history of the area has been extensively studied, particularly by Ken Pierce of the USGS (Pierce, 1979). Pierce showed that the axis of the icecap on the Beartooth uplift was directly over the Stillwater wetland, which was covered by a layer of ice almost 800 meters thick. Whitlock (1993) studied the climatic and vegetative changes of the Yellowstone region primarily through pollen analysis, providing a clearer picture of the post-glacial climate in the region.

Meyers and coworkers have studied the impact of climatic change and fires on geomorphic processes, primarily in the Soda Butte Creek area (Meyer et al., 1995; Marcus et al., 2001; Meyers, 2001). The collapse of a tailings pond dam in 1950 due to a major flooding event carried metals downstream into Yellowstone National Park. Their research has mapped the distribution of these metals as they relate to geomorphic processes. They have also studied the impact of fires on the frequency of flooding events (Meyer et al., 1995).

A unique area of research in the region has been conducted by Furniss, Gurrieri, and their coworkers on the depositional processes of ferricrete, iron-rich sedimentary layers generated by acid rock drainage. They have mapped and dated ferricrete deposits in the area and are working on a model to determine pre-mining metal concentrations and acidity in mining-impacted streams (Furniss and Gurrieri, in press). Dating of these deposits indicate that ferricrete deposition has been an ongoing process for at least 8000 years. Their research also suggests that these deposits were deposited during periods of wetter climate which released more acid rock drainage to the surrounding streams (Furniss et al., 1999).

Revegetation research plays a key role in reducing erosion which helps mitigate the impacts of mining. Forest Service researcher Ray Brown dedicated his career to high altitude revegetation, particularly those areas impacted by mining. His research in the Cooke City area has provided invaluable information for reclaiming these types of sites, and forms the basis for present-day alpine revegetation strategies (Brown et al., 2003).

New World Mining District

Geology

The geology of the New World Mining District has been extensively studied by government and university scientists and mining companies interested in mineral extraction. T.S. Lovering was the first geologist to perform a detailed investigation of the area, and spent a number of years evaluating the mineral resources and the regional geology for the U.S.G.S. (Lovering, 1929). U.S.G.S. geologist J.E. Elliot produced a

more detailed geologic map of the area (Elliot, 1979). The gold-copper-silver deposits of the New World District were described in further detail in the Guidebook for the Red Lodge-Beartooth Mountains-Stillwater Area (Elliot et al., 1992). An extensive description of the McLaren ore deposit describing the gold-copper-silver skarn and replacement mineralization was published in 1994 (Johnson and Meinert, 1994). Crown Butte Mining Company performed an extensive drilling program during the 1990's to evaluate the subsurface geology of their mining claims for a potential underground mine.

The geology of the Cutoff Mountain area, which borders the western edge of the study area, was the subject of research by David Courtis at the University of Michigan (Courtis, 1965). This landscape is the headwaters for the small stream that deposited the large alluvial fan in the Stillwater wetland. This research provided a clearer understanding of the geology of the southern slope of the Beartooth Mountains. Courtis believed the volcanic intrusives of Cutoff Mountain were evidence that the Eocene igneous activity did not end with the eruption of volcanic rocks in the Absaroka Mountains. The researcher also indicated that the Heart Mountain Detachment thrust zone was the result of gravity sliding, which is the accepted theory today.

Acid Rock Drainage

One of the first studies that examined the impact of acid rock drainage in the New World Mining District was the Acid Mine Drainage Control-Feasibility Study conducted by the Montana Department of Natural Resources (DNRC) in the 1970's. They contracted the Montana Bureau of Mines and Geology (MBMG) to conduct a hydrogeological and water quality study and investigate the feasibility of rehabilitation of

the McLaren pit, the Glengary mine, and the mill area near Cooke City (Sonderegger et al., 1975). The MBMG performed water studies from July 1973 through September 1975, and concluded that dissolved iron and aluminum were the greatest problem in the McLaren pit area. Annual iron loads of 13.15 metric tons and aluminum loads of 12.47 metric tons were entering the watershed from the McLaren mine area. The important conclusions concerning the Daisy Creek watershed were that the factors influencing acid rock drainage included mining methods, topographic setting, type of mineralization, and geologic setting. They also determined that Daisy Creek was much more severely impacted from acid rock drainage than Fisher Creek.

Amacher and co-workers looked at element speciation of water and sediment samples from Daisy and Fisher Creeks in 1989 and 1990 (Amacher et al., 1995). Their analysis included sequential extractions to determine the amount of each metal associated with specific solid phases, and use of the equilibrium chemical speciation program MINTEQA2 to analyze the stream data for possible geochemical controls on element concentrations. They showed that iron concentrations are controlled by iron hydroxide; that an adsorption edge exists for copper that is pH dependent; and that copper adsorbs on iron hydroxide at pH > 4.5. The sequential extraction results showed significant amounts of heavy metals in the organic matter + sulfide + residual fraction of the tested sediments. These metals are susceptible to leaching into streamwater and will continue to be a source of metals until natural weathering reduces their concentrations to background levels. They also made a number of recommendations for reducing the acid rock drainage, which

included sealing of all adits, backfilling all pits, burying acid generating material, revegetation, and lining drainage channels with limestone.

Hinman and coworkers investigated the background chemistry of mineral-rich drainages in Montana (Hinman et al., 2000). They studied modern and ancient mineral compositions from Stevens Creek in the Heddleston Mining District near Lincoln, Montana and Daisy Creek in the New World Mining District. Their objective was to determine whether the composition of the precipitated metals can be correlated with the water solution metal composition, and if there was a detectable trend in the natural variability of the stream chemistry with age and location. They selected samples from stream sediments and adjacent exposed sediment deposits, and also collected precipitate coatings from glass beads that were left in the stream for several months. The mineralogy and crystallinity were analyzed to measure aging of the oxides and evaluate chemical remobilization. They used MINTEQA2 to model solution composition and pH correlations to the solid composition. Their geochemical models and linear regression analysis failed to show any relationships, but did provide a direction for further research.

Furniss and coworkers used radiocarbon-dated ferricrete deposits in the New World Mining District to interpret paleoclimatic changes and demonstrate that natural acid rock drainage has been occurring for thousands of years (Furniss et al., 1999). Ferricrete forms in waters with low pH and high metal concentrations in many mineralized areas throughout the western United States. Using ^{14}C dates of wood fragments embedded in the deposits allows determining the age of deposition of these sediments, and provides insight into the climate at the time of deposition. Their results

show that natural acid rock drainage has been occurring at least since ~8840 years before present. They also suggest that these deposits correlate with warmer and wetter climatic periods, which have been corroborated with other paleoclimatic records. Finally, they speculate that these oldest ferricrete deposits were deposited just after the glacial ice melted, which suggests that glaciers may have persisted in the high alpine valleys of the New World Mining District 2000 to 5000 years longer than those in other parts of Yellowstone National Park (Pierce, 1979).

Poage and others (2000) used isotopic evidence from ferricrete deposits in the New World Mining District to interpret Holocene climate change in the northern Rockies. They used oxygen isotope ratios (^{18}O) of the mineral goethite present in ferricrete deposits to interpret localized climatic changes. The mineral composition was determined using x-ray diffraction and the ^{18}O values were measured using a gas-source mass spectrometer. Ages of the wood fragments imbedded in these ferricrete deposits were determined using ^{14}C age-dating. The oxygen isotope ratios showed an increase of ~3% over the last 9000 years, suggesting a regional increase in summer precipitation since the early Holocene. These results correlate well with palynology data from the Yellowstone Region that indicates that summers were drier 9000 years ago (Whitlock et al., 1993).

Furniss and Gurrieri (in press) describe an empirical model for estimating pre-mining water quality in catchments with acid rock drainage and ferricrete deposits. Their research sites included the Daisy Creek and Fisher Creek drainages, and an unmined drainage with ferricrete deposits in the Upper Blackfoot Mining Complex near Lincoln,

Montana. They use trace metal concentrations of stream water, ferricrete deposits, and modern Fe-oxyhydroxide precipitates to develop equations to model pre-mining pH and metal concentrations. These estimates can be used to monitor the progress of restoration efforts, and provide an expected baseline for water quality improvement.

Daisy Creek and Stillwater River

While extensive scientific work exists on the economic geology of New World mining district, studies concerning the environmental impacts of mining activity are limited. Research has focused primarily on water quality, since this has the largest impact on aquatic resources. The Stillwater River has received less attention because the foci has been more on the more heavily impacted Daisy and Fisher Creeks.

Some of first efforts to address the impact of mining at the McLaren mine were carried out by Ray Brown and his co-workers (Brown et al., 2003). They established a research site at the McLaren Mine in 1976 to test methods for high altitude restoration of sites disturbed by mining. This research provided valuable techniques for reestablishing native plant habitat at alpine mining disturbed sites. These included appropriate soil handling techniques, proper selection of native plant species, fertilization rates, and monitoring activities to determine success or failure of the restoration efforts.

In 1994, Hydrometrics, Inc. completed a report on sediment metal characterization of Daisy Creek for Crown Butte Mines, Inc. (Hydrometrics, 1994). The chemical characteristics of the sediments in Daisy Creek and the upper section of the Stillwater River and the impact of historical acid mine drainage were the focus of this report. Crown Butte Mines, Inc. was interested in how these sediments would impact

post-remediation water quality efforts. Hydrometrics hand augered two holes to look at overbank sediments in the Stillwater wetland. These samples were analyzed for metal concentrations and used to describe a generalized stratigraphy of sediments next to the Stillwater River.

The next major study was conducted in 1994 by Joe Gurrieri for the Montana Department of Environmental Quality (Gurrieri, 1998). This study evaluated the distribution of metals in the water and sediments in the upper Stillwater basin and their effects on the aquatic biota in the river. The study looked extensively at the aquatic community in the stream above and below the confluence of Daisy Creek and the Stillwater River. This study also provided an overview of the hydrogeological conditions of the Stillwater wetland and possible metal movement through the wetland. The study documented a severely impaired biological community downstream of the confluence with Daisy Creek. The study also concluded that water quality of the Stillwater River improved dramatically downstream of the confluence with Goose Creek, due to the influx of clean water and sediment.

In 1999, the USGS investigated metals loads in Daisy Creek and the Stillwater River using tracer injections and synoptic sampling (Nimick et al., 2001). The tracer injection method allowed accurate measurement of streamflow and the synoptic water quality sampling provided concentrations of major ions and metals. They concluded that the most significant copper loading occurred in the upper portion of Daisy Creek and was dominated by subsurface flow and surface inflows from areas impacted by the mining activity. They also demonstrated that cadmium, copper, lead, and zinc are present in

lethal concentrations for aquatic life in Daisy Creek, and at potentially toxic levels for aquatic life in parts of the upper Stillwater River.

Fisher Creek

The Fisher Creek drainage has also been impacted by acid rock drainage. Fisher Creek starts near the Glengary adit, which is one of the main point sources for metal loads in the stream. The cobbles of the stream channel are iron-stained to the confluence with the Upper Clark's Fork of the Yellowstone River. The aquatic community is also severely impacted. In 1997, the USGS investigated metals loads in Fisher Creek using tracer injections and synoptic sampling (Kimball et al., 1997). They concluded that the stream receives inflows from both surface and groundwater sources and that just reclaiming the Glengary adit would not solve the stream's water quality problems. Significant metal loads from subsurface flow would still leave Fisher Creek with metal concentrations exceeding aquatic water standards.

MacHardy-Mitman (2002) investigated a wetland next to Fisher Creek to evaluate the potential for natural wetlands to remediate copper contaminated water. The objective of their research was to determine whether two natural wetlands along Fisher Creek near Cooke City, Montana and Copper Gulch near Jefferson City, Montana had the potential to remove and store metals from metal-rich streamwater. The study included field hydrological investigations and laboratory experiments, which helped to evaluate the wetland's capacity to absorb copper. She determined that the Fisher Creek wetland contains large amounts of metals, particularly copper and iron, which have been accumulating over geologic time. Much of the copper is in a readily exchangeable

carbonate form that is highly susceptible to remobilization, with the remaining forms being metallic copper, sulfides, and chelates. The iron is stored as ferricrete deposits and oxides. The wetland still has the capacity to remove copper and iron from contaminated water, but not with 100% efficiency (the effluent water leaving the wetlands exceeded Montana aquatic standards for copper).

Researchers from Dartmouth College conducted a combined flooding and geochemical analysis of metal fluxes along the upper reaches of Fisher Creek (Hren et al., 2001). They used geochemical analysis of the spatial distribution of metals in overbank deposits, streamflow modeling, and dendrochronology to develop a model of the spatial and temporal distribution of metals along Fisher Creek. They concluded that the sediments contain an ~8000 year record of metal deposition and that sediments pre-dating mining activity contain metal concentrations equal to those found in modern sediments. They also determined that the natural metal-rich sediments found throughout the floodplain are independent of flood occurrence. They estimated that Fisher Creek has not experienced a flood greater than the 100 year event during or after initiation of mining activity (based on HEC-RAS modeling and dendrochronology) (Hren et al., 2001).

Miller Creek and Soda Butte Creek

The Miller Creek watershed is the least impacted drainage in the New World Mining District. A small lead-zinc deposit near the headwaters was mined in the early 1900's, but has had limited impact on water quality. Even though the U.S. government purchased the mining claims of the proposed Crown Butte mine in the 1990's, the mineral withdrawal is subject to review every 20 years. There is concern that any future

mining could impact the water quality of Miller Creek, which flows into Soda Butte Creek and in turn into Yellowstone National Park.

Durst (1999) investigated the geologic controls on spring discharge in the Miller Creek basin to determine whether spring discharge in the upper parts of watershed was derived from the bedrock aquifer or the surficial aquifer. Durst used specific electrical conductivity (SC) to determine whether the source of the water was shallow or deep, since each source had a unique SC signature. Bedrock aquifers were a significant contributor (>50%) to springflow, especially during the early summer. As the summer progresses, the bedrock contribution decreases to 40-50%. He concluded that any mining activity that intersected the bedrock aquifer has greater potential for impact to water quality in the early summer than in the fall.

In 1999, the USGS investigated metal loads into Soda Butte Creek upstream of Yellowstone National Park using tracer injections, synoptic sampling, and retrospective analysis of previous research in the watershed (Boughton, 2001). Soda Butte Creek flows into Yellowstone National Park, and was impacted by the collapse of a tailings pond dam in 1950. The McLaren mine tailings impoundment was just upstream of Cooke City and was the site where ore from the McLaren mine was processed. The floodwaters spread metals across the floodplain for some distance downstream of Cooke City. They concluded that the McLaren tailings was one of three major sources of metals entering Soda Butte Creek and that removing these sediments may not reduce metal loads to acceptable levels. They also indicated that flooding remains the biggest threat for delivering these metals to Soda Butte Creek.

In 2000, the U.S.G.S. investigated metal loading to Miller Creek using tracer injections and synoptic sampling (Cleasby et al., 2002). Cadmium, copper, lead, and zinc concentrations in the stream water were below Montana water quality aquatic standards, with only one exception. A water sample just downstream of a mine adit where lead and zinc were mined in small quantities was above aquatic standards for lead. Their study concluded that metal loads were small and did not have a significant impact on water quality.

The Montana Bureau of Mines and Geology and the USGS investigated the hydrology of the upper Soda Butte Creek basin (Metesh et al., 1999). They investigated geology, streamflow, groundwater, climatic data, and water chemistry to evaluate the status of Soda Butte Creek at the watershed scale. They also incorporated tritium-helium age-dating of water and modeling of streamflow to better understand the hydrologic balance of the watershed. One of the major conclusions was that the water balance of the upper Soda Butte Creek watershed was dominated by surface runoff (49.8%) and evapotranspiration (47.8%) and that groundwater accounted for only 2.3% of the water budget and consumptive use 0.1%. They determined that a major limitation in their research was a lack of groundwater data, which was limited to domestic wells. Their research incorporated a range of data sources and provides an excellent baseline to evaluate restoration efforts occurring upstream of Cooke City.

Regional Studies

Glaciation

Research by Pierce on the glaciation in the Yellowstone region provides a foundation for understanding the impact of the glaciers on the topography of the New World Mining District (Pierce, 1979). He mapped geologic evidence of the last two ice ages (Bull Lake which ended ~150,000 years ago, and the Pinedale glaciation that ended ~11-13,500 years ago). An interesting aspect of this work that relates to my research is that the axis of the icesheet that covered large parts of the Yellowstone area was directly over Lake Abundance, which is several hundred meters from the northwestern edge of the Stillwater wetland. A layer of ice approximately 800 meters thick at the peak of the Pinedale glaciation covered the Stillwater wetland. More recent work refined some of the dates of the Pinedale glaciation using cosmogenic ^{3}He and ^{10}Be chronologies (Licciardi et al., 2001). They suggest that the Pinedale glaciation maximum (~14,000 years ago) in the northern Yellowstone region was significantly younger than previously documented.

Furniss and others (1999) speculated that the valley glaciers may have persisted in the alpine regions of the New World Mining District for an additional 2000 to 5000 years, based on their ferricrete research. The ^{14}C dates go back a maximum of 8840 years BP, suggesting that this was when the sulfide deposits in the watershed were first exposed to oxidation and the release of acid rock drainage. Prior to that time, the deposits would have been sealed off from the atmosphere by glacial ice.

Climate

Numerous paleoclimatic studies have focused on the Yellowstone Park region, with significant work being produced by Meyer (Meyer, 2001; Meyer et al., 1995 and 2003), Marcus (Marcus et al., 2001), Whitlock (Whitlock et al., 1993) and their co-workers. Their investigations have focused on the time period since the end of the last ice age. Whitlock has used pollen studies and the earth's orbital oscillations to infer past climatic conditions and the resulting vegetation communities, whereas Meyer and Marcus have studied the relationships between flooding, fire, and climate as primary controls on geomorphic changes in the floodplain. Meyer's and Marcus's research has focused in the northeastern section of the park, and includes Soda Butte Creek, which has been impacted by mining activity.

Present-day weather in the Yellowstone Park region is dominated by two climate patterns; a summer-wet/winter-dry cycle in the northern part of the park and a summer-dry/winter-wet cycle in the southern area of the park. Whitlock suggests that these same climate regimes existed throughout the Holocene, though the intensity of the differences and the dominant mechanism between the two regimes has changed through time. Topography is also a key factor and must be taken into account when looking at different spatial scales.

Flooding

Flooding is the dominant agent of geomorphic change in the floodplain, and impacts both the channel and the floodplain and the associated vegetation. The frequency, size, and length of the flooding events are key factors controlling the magnitude of

change and are strongly linked to climatic conditions. The largest historical floods in the region have resulted from rain on a melting snowpack or intense summer storms (Meyer, 2001). Meyer and co-workers have focused on alluvial chronology and climatic controls on geomorphic processes, with a strong emphasis on fire-induced sediment pulses (Meyer et al., 1995; Meyer et al., 2003). Their mapping of stream terraces using ^{14}C dating combined with documented flooding events established that major floods occurred in 1790, 1873, 1918, 1950 and 1996-1997.

The role of flooding on the distribution of metals has also been investigated by Meyer and coworkers (Meyer, 2001; Marcus et al., 2001). Meyer studied the geomorphic controls on metal contamination and the implications for the recovery of these fluvial systems. The sulfide metal-rich tailings from the 1950 tailings dam failure continue to impact the downstream aquatic resources to this day.

^{210}Pb Age Dating

The ^{210}Pb age-dating technique was first described by Goldberg (1963), who used the method to measure sedimentation rates on a glacial icesheet. Goldberg also used ^{210}Pb values of river waters from the Colorado and Sacramento rivers to model lead removal and ^{210}Pb values of marine waters to study mixing rates in a simple oceanic model. He did not assign actual dates to glacial ice at each depth, but calculated a sedimentation rate of ~70 cm/yr of ice, which agreed with that determined by stratigraphic analysis. Goldberg established the main assumptions that form the basis for the two most popular dating models: (1) a constant rate of ^{210}Pb accumulation from the atmosphere, but a non-

constant sedimentation rate (Constant Initial Concentration – CIC model); and (2) a constant rate of ^{210}Pb accumulation from the atmosphere and a constant sedimentation rate (Constant Rate of Supply – CRS Model).

The use of the ^{210}Pb age-dating technique increased in the late 1970's and early 1980's. Appleby and Oldfield described the CRS model and explored the applicability of the dating method to lakes and their drainage basins (Appleby et al., 1978 and 1983), and expanded their research into paleolimnology and paleoecology (Oldfield et al., 1984). Robbins (1978) investigated the geochemical and geophysical applications of ^{210}Pb age-dating, and with coworkers used the technique in their Great Lakes research (Robbins et al., 1975 and 1978). The use of the ^{210}Pb age-dating technique has expanded in the last 20 years, and there are a large number of papers in the literature documenting the importance of the method in environmental studies, including papers focused on calculation and uncertainty analysis (Binford, 1990).

An important application of the ^{210}Pb dating technique is in mining impacted environments. The USGS used the method to determine pre-mining geochemical conditions and paleoecology in the Animas River watershed in Colorado (Church et al., 1999). Knowledge of the pre-mining geochemical baseline helped in establishment of restoration goals and measurement of success. They used the ^{210}Pb method to establish the chronology of stream terrace deposition. Those terraces older than 100-150 years old were assumed to have metal concentrations equal to pre-mining conditions. These pre-mining terraces helped define the increase in metal concentrations in modern deposits and to develop appropriate restoration goals for the streams in their watershed.

Shukla provided an extensive discussion of measuring sedimentation rates through ^{210}Pb age dating of sediments (Shukla, 2002). His book explores the merits of the constant initial concentration (CIC), CRS, and advection diffusion equation (ADE) models that are most often used to calculate ^{210}Pb dates. Variable sedimentation rates and diffusion coefficients are discussed in detail as is how they are used in the new porosity variation (PV) model. Statistical methods are provided for interpreting the results from each of the models. The book also discusses the issue of ^{137}Cs mobility, which is measured along with ^{210}Pb and used as an independent dataset for calibration of the age dates.

Wetland Processes

Numerous examples of wetlands as a source of metal enrichment exist throughout the world. Bog deposits have been mined since Roman times for elements such as copper and iron. Wetlands, due to the unique biogeochemical processes that operate within them, tend to be sinks for metals. An important characteristic of wetlands is their typically high organic content. Wetlands in cooler climates tend to accumulate more organic matter than in drier climates due to the lower rates of decomposition caused by the slower rates of microbial respiration and/or shorter warm seasons.

Gambrell (1994) describes trace and toxic metals in wetlands and the processes that affect metal mobility and bioavailability. One of the key conclusions that relates to my research is that fine-grained soils containing organic matter will tend to accumulate metals. Another important factor in wetlands is that oxidized soils can become anaerobic

when flooded and the pH will trend toward neutrality, which favors immobilization. Organic matter in wetlands is effective at immobilizing metals, as are oxides of iron, manganese, and aluminum. They concluded that the association of trace metals with organic matter and a near neutral pH due to flooded soils will cause more metal immobilization than upland soil conditions.

Weis and Weis (2002) reviewed wetland plant dynamics and concluded that wetland sediments are generally a sink for metals, though they can be a source of metals through plant activities (sediment oxidation and plant uptake). The root rhizosphere zone oxidizes the sediments near the roots and can affect metal concentration and bioavailability. There is also evidence that bacteria, fungi and periphyton can play a significant role in the root zone (increasing and decreasing bioavailability), but research is limited. Typically, the roots cannot extend very far into the anoxic zone, where the metals will be in a reduced state with low bioavailability.

The scientific literature contains many papers that discuss adsorption processes of metal on sediments, both in soils and water. Bradl (2004) described adsorption of heavy metal ions on soils and soil constituents, and discussed copper, lead, and zinc in detail. The paper describes the theoretical models and mechanisms of adsorption and complexation and the importance of pH and soil type. Copper has a high affinity for organic matter and also iron and manganese oxides. Lead is strongly adsorbed to manganese oxides and to a lesser degree organic matter. Zinc is most strongly influenced by soil properties such as cation exchange capacity (CEC), soil particle size, and pH. The paper concluded that adsorption is a key process in the accumulation of metals and that

there will be less metal mobility at high soil pH, and that coarse grained soil will have a lower tendency for metal adsorption than fine-grained soils.

Metal attenuation due to adsorption processes in streambed sediments was investigated at the abandoned Spenceville copper mine in California (Ranville et al., 2003). Sequential extractions were used to characterize speciation of metals and their potential for bioavailability. Metals associated with carbonates, iron, manganese, and aluminum hydroxides were considered bioavailable. The carbonates and hydroxides were effective at scavenging metals from the water, but loosely bound metals were also susceptible to remobilization. They concluded that copper and zinc had the highest potential for mobility, followed by cadmium, lead, and aluminum.

August and others (2002) researched the seasonal variability of metal transport through a wetland impacted by acid mine drainage near Leadville, Colorado. They investigated a wetland receiving iron, zinc, and manganese from an abandoned mine tunnel. They found that the amount of metals leaving the wetland during the summer was reduced by 90% for iron, 65% for zinc, and 25% for manganese when compared to the amount of metals leaving the wetland during the autumn and winter. During the autumn and winter, zinc and manganese loads leaving the wetland were greater than the metal loads entering the wetland from the mine tunnel. Spring runoff increased the level of metals entering the wetland to twice the normal load and the wetland was not effective at significantly reducing the metal load. They showed that the wetland was a sink in the summer and a source during the winter. They concluded that wetlands can be used to treat mine drainage, but that they also require maintenance.

Conclusion

Wetlands with high metal concentrations occur throughout the world, and are often both a sink and source for metals. The introduction described the research objectives and methodology we used to investigate the Stillwater wetland. The following chapter presents the results of my research, and focuses on the spatial and vertical distribution of metals in the wetland, and the timing of their deposition. The final chapter presents the results of the XRF:ICP analysis. The XRF instrument provided significant cost savings to my research effort, and the data collected in my research allowed a rigorous evaluation of the quality of the data of the XRF instrument. The XRF chapter will be of interest to the U.S.F.S., since they are using the instrument extensively in their restoration projects.

CHARACTERIZATION OF RIPARIAN WETLAND SOILS AND ASSOCIATED METAL CONCENTRATIONS AT THE HEADWATERS OF THE STILLWATER RIVER, MONTANA

Introduction

Historic mining activity has impacted water and land resources throughout the western United States. The rich history and environmental impact of mineral exploitation in the Rocky Mountains is well documented. These regions contain numerous mineralized bodies of gold, silver, copper, lead, zinc, and other metals of economic value. Pyrite is often present in these rocks, which when exposed to oxygen and water produces acidity that releases metals present in the rock matrix. These metals can travel to streams and rivers, where aquatic life can be severely impacted. Ore bodies are often exposed at the land-atmosphere interface, where weathering processes naturally produce acid rock drainage that ends up in streams. Mining activities can enhance this process by exposing more of the ore body to an oxidizing environment or by bringing acid producing rock to the surface. Waste rock was often deposited on the surface near mine entrances, or stored in tailing ponds. Underground tunnels also exposed susceptible rocks to oxidizing conditions, which generates acid rock drainage that can enter the groundwater. Erosion of metal enriched soils and scavenging of precipitates add to the supply of mobilized metals that can be re-deposited within the watershed or exported. Acid rock drainage is a difficult and expensive problem to address and continues to impact water and associated land resources throughout the western United States.

Areas downstream of mineralized ore bodies frequently had elevated levels of metals before mining activity commenced so that attempting to restore/reclaim impacted soils or waters to metal concentrations less than what was naturally present may not be technically or economically feasible (Runnels et al., 1992). Knowledge of the areal and depth distribution of metals, the age of deposition, and their mobility provide context for understanding environmental risks associated with these areas. We investigated a wetland at the headwaters of the Stillwater River, Montana, which has been impacted by acid rock drainage from both natural sources and historic mining activities. The Stillwater wetland is located in the New World Mining District near Cooke City, Montana (Figure 10).

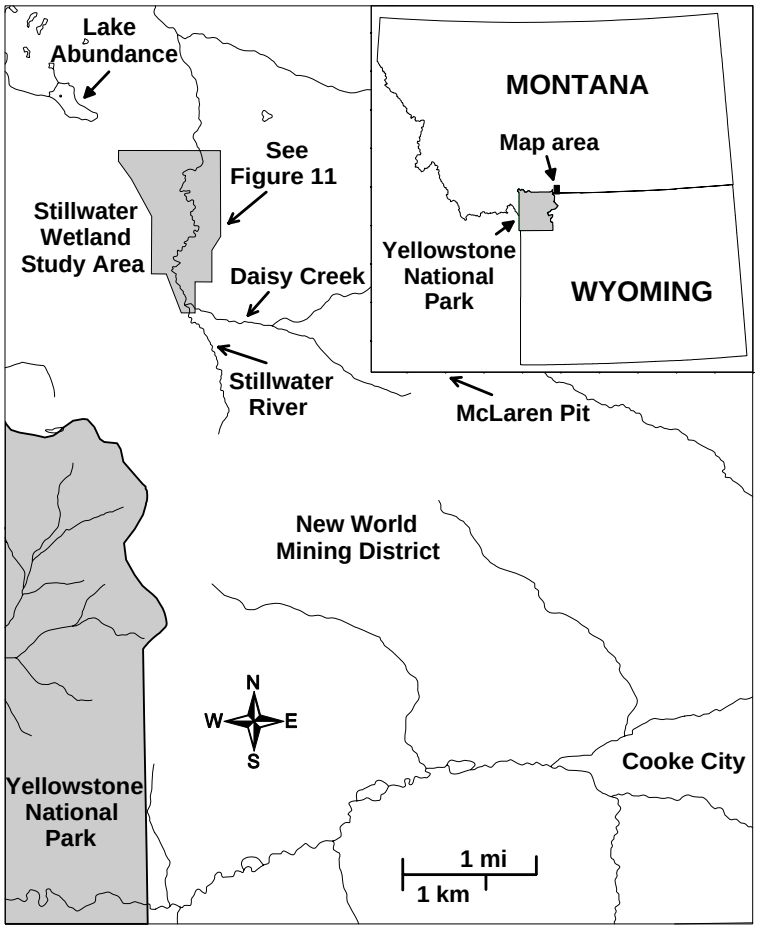


Figure 10. Map of the Stillwater wetland study area.

Gold, silver, and copper were discovered in the area in the 1870's, and various mining activities have occurred there through the 1990's. The McLaren ore deposit, which was discovered in 1933, was the main location of mining activity in the Daisy Creek watershed. The ore body was initially mined with a number of underground tunnels starting in 1934 and by open cut methods from 1938 until 1953 (Elliot et al., 1992). No reclamation requirements existed at that time, so the exposed waste rock and open pit added to the acid rock problem in the watershed (Brown et al., 2003).

Surface runoff and groundwater with low pH and high metal concentrations reaches Daisy Creek and is carried downstream to the Stillwater River. Iron-stained cobbles line the streambed of Daisy Creek and the upper reaches of the Stillwater River (Gurrieri, 1998; Nimick et al., 2001). The New World Mining District Response and Restoration Project started addressing the environmental impacts of the historical mining activities in 1999, with the U.S. Forest Service (U.S.F.S.) as the agency responsible for managing site assessment and cleanup. This research is part of the reclamation effort, and focuses on quantifying the impact of acid rock drainage and metal enriched sediments to the Stillwater wetland.

The Stillwater wetland has been receiving acid rock drainage since the end of the last ice age (Furniss et al., 1999), but the influence of mining activities (or even the level of metals within the wetland soils) was unknown. Concerned citizens and reclamation experts have questioned whether the historic mining at the McLaren ore deposit has had a direct impact on the concentration of metals within the wetland. My research focused on quantifying the extent and timing of metal deposition in the riparian wetlands along the

Stillwater River below the confluence of Daisy Creek. Copper, lead, and zinc were the key metals of interest in my research, since previous studies (Gurrieri, 1998; Nimick et al., 2001; Maxim, 2001) showed that these metals were at potentially toxic levels to aquatic life in the upper reaches of the Stillwater River.

I sought to address the following questions: (1) what are the spatial and vertical patterns of metal concentrations across the wetland; and (2) are the metal concentrations in the post-mining sediments higher than those in pre-mining sediments? We investigated these questions using a combination of spatial and soil profile metal analysis, sediment age dating, measurements of water levels and water chemistry from piezometers and monitoring wells, and topographic and vegetation surveys.

Site Description

The Stillwater wetland is located at 45º 04' 40" N latitude and 109º 59' 45" W longitude. The study area is 150 hectares in size, with the Stillwater wetland (the area within the five hydrologic units) totaling 66 hectares (Figures 11 and 12). The study area is in the northwest corner of the New World Mining District, and is ~5 km downstream of the McLaren Pit. The McLaren Pit and the surrounding landscape on Fisher Mountain is the source of the acid rock drainage that enters Daisy Creek and the Stillwater River. There is an extensive beaver pond network at the center and lower ends of the wetland, and the Stillwater River flows along the eastern side of the wetland.

The Stillwater wetland is in a glacier carved valley at an elevation of 2585 meters. The wetland is adjacent to the Beartooth Wilderness Area and just over 4 kilometers

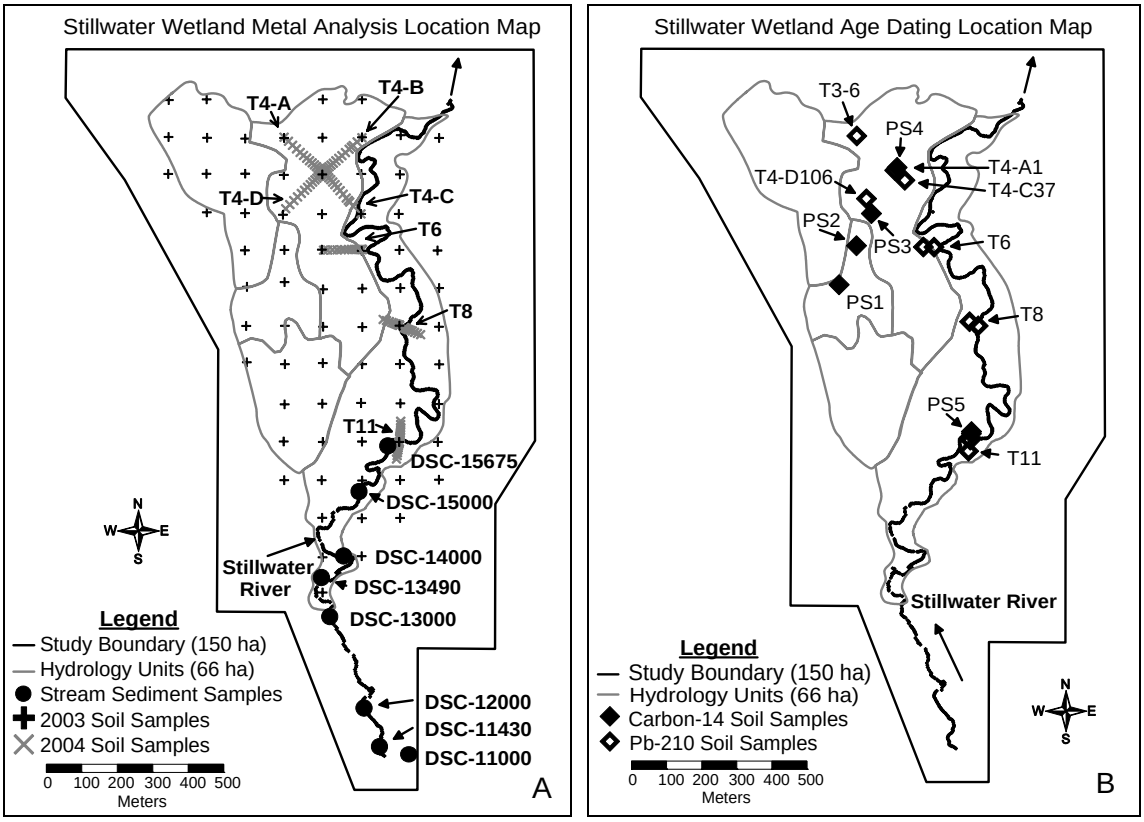


Figure 11. (a) The study area, hydrologic units, and the soil sampling locations for metal analysis at the research site. The vertical depth transects (2004 soil samples) are labeled. (b) Soil sample locations selected for ^{14}C and ^{210}Pb age dating. The arrows show the flow direction of the Stillwater River.

northeast of Yellowstone National Park. The study area is comprised of the active floodplain of the Stillwater River, an alluvial fan formed by an unnamed stream flowing into the wetland from the western edge, and marshy areas with abundant beaver ponds. The vegetation of the study area is a sedge willow marsh complex that transitions into a spruce/fir forest. The soils comprising the sedge marsh sections of the wetland range from clay to silt with occasional interbedded gravel. The alluvial floodplain consists of sand and gravels. The surrounding bedrock is Paleozoic sedimentary rocks (predominately limestone, dolomite and shale) that have been intruded by Eocene

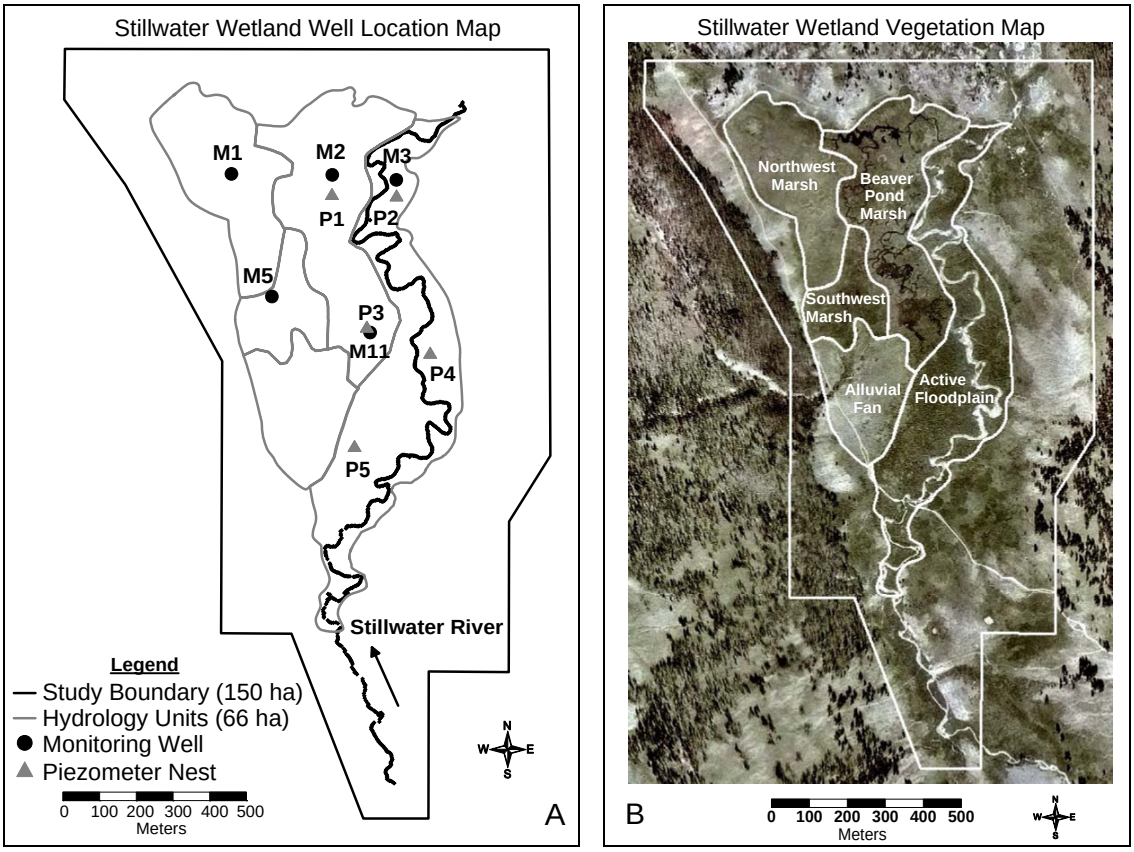


Figure 12. (a) Location of monitoring wells, piezometers and hydrologic units in the study area. The arrow shows the flow direction of the Stillwater River. (b) Orthophoto map of the wetland and the hydrologic units. Vegetative habitat types for each hydrologic unit include: Northwest Marsh Unit - Planeleaf Willow/Water Sedge; Beaver Pond Marsh Unit - Planeleaf Willow/Water Sedge; Active Floodplain Unit – Wolf's Willow/Tufted Hairgrass; Southwest Marsh Unit – Wolf's Willow/Water Sedge; Alluvial Fan Unit– Wolf's Willow/Tufted Hairgrass.

volcanic dikes, sills, and laccoliths (Lovering, 1929; Elliot et al., 1992). The Stillwater wetland was under ~800 meters of ice during the Pinedale glaciation (Pierce, 1979), which ended approximately 11,000 years ago. Glacial features dominate the landscape with abundant moraines covering the hillsides surrounding the wetland.

Igneous activity formed the sulfide ore bodies that produce the acid rock drainage in the mining district. The ore in the New World district often occurs as copper skarn deposits that contain major deposits of copper, gold, and silver (Elliot, 1979; Johnson et

al., 1994). The McLaren deposit is a gold-copper-silver skarn and replacement deposit that occurs at the contact between the Tertiary Fisher Mountain intrusive complex and the dolomitic and calcareous shale of the Cambrian Meagher Formation (Johnson and Meinert, 1994). These deposits contain abundant pyrite, which is the source of the acidity that releases high concentrations of metals into surface runoff and groundwater. Daisy Creek begins at the base of the McLaren ore deposit and is severely impacted by acid rock drainage. The Stillwater River begins in a glacial cirque containing non-mineralized Paleozoic carbonates and is in a pristine condition above the confluence with Daisy Creek. The unnamed stream that enters the western side of the wetland also has its source in non-mineralized Paleozoic carbonates. The Stillwater River downstream of Daisy Creek supports limited aquatic life until some distance into the wilderness area, where incoming streams dilute the elevated concentration of metals (Gurrieri, 1998).

Materials and Methods

Hydrologic Units

We delineated the Stillwater wetland into hydrologic units (units of similarity) using stereoscopic air photographs and field mapping (Figure 12b). Each unit was delineated using geomorphic and hydrological properties to define areas where similar hydrologic processes were occurring. The dominant geomorphic processes were the Stillwater River and its active channel/floodplain which flows along the eastern margin of the wetland, a small stream that enters the wetland from the west and has formed an alluvial fan, and numerous beaver ponds that cover much of the lower and middle

sections of the wetland. These units provided the framework for defining areas where similar patterns of metal concentrations were expected.

The vegetation of the wetland was also surveyed to describe the dominant plant community within each hydrologic unit (Figure 12b). The vegetation data also helped determine whether invasive species were present in the wetland, which was of importance to the USFS. The habitat types were described using *Classification and Management of Montana's Riparian and Wetland Sites* by Hansen et al. (1995).

Soil Metal Analysis

Spatial and Vertical Metal Distribution We investigated the spatial distribution of metal concentrations using shallow (0-20 cm), composite soil sampling. We sampled on a 100 m by 100 m grid (Figure 11a) in 2003 to collect shallow (0-20 cm) soil samples. The vegetation was scraped away from the surface prior to collecting the soil samples and the soil was then collected with a hand auger. The vertical metal distribution was investigated with a series of transects that sampled the wetland sediments to a depth of 1-meter. The samples were stored in labeled zip-lock bags for transport to the laboratory. Soil samples were dried, ground with a ball-mill grinder, and then analyzed for total metal concentration using X-ray fluorescence (XRF) and inductively coupled plasma atomic emission spectroscopy (ICP).

Shallow soil total metal concentrations were mapped to identify areas for more detailed soil sampling. The metals of interest were copper, lead, and zinc, with areas of high copper concentrations having the highest priority for further soil sampling. Based on

the spatial soil maps, areas of high copper concentration were sampled in 2004 using a series of transects to better evaluate the spatial and vertical distribution of metals (Figure 11a). Soil samples were collected using a hand auger down to a depth of one meter where possible, and typically produced 7 samples per location (0-10, 10-20, 20-30, 30-40, 40-50, 50-75, 75-100 cm). Soil samples were analyzed for total metal concentration using XRF, with a subset analyzed for metals with ICP, carbon and nitrogen content, and pH.

XRF and ICP Analysis The soil samples were either air dried or oven dried at 45 ºC to avoid organic matter combustion. The gravel-sized particles and any visible vegetation fragments were separated from the dried soil samples by hand and the remaining material was ground to a fine powder (~ 45 microns) using a ball-mill grinder. The grinding process provided a consistent soil particle size and a homogeneous sample. We followed a grinding protocol that was designed to reduce the potential for cross-contamination. Two possible sources of contamination were small particles from the grinding vial itself and metals that adhered to the surface of the grinding vial during the grinding process. We used zirconium vials and an acid bath wash in between samples. Zirconium vials are extremely hard, and even if particles from the vials contaminated the soil sample, the metal was of no interest in the Stillwater wetland soil analysis. A dilute hydrochloric acid solution was used to dissolve any metals that might adhere to the surface of the grinding vial. The zirconium vials and the acid bath wash helped reduce the potential for contamination. All prepared samples were then analyzed for total metal concentration using XRF and a subset of the samples was analyzed with ICP. We were primarily interested in the total concentrations of each individual metal present in the

wetland sediments and comparison of the XRF data to those measured using ICP analysis.

We utilized a Niton Xli 700 XRF instrument in the field on a limited basis. We primarily used the XRF in the lab on the same set of samples that were analyzed with ICP. This instrument provided an opportunity for rapid and low-cost metal analysis of the wetland soils. ICP measurements of a subset of the soil samples provided data that was used for mapping and to assess the XRF unit's precision and accuracy. A total of 992 soil samples were analyzed with XRF, of which 179 were analyzed with ICP to assess the analytical performance of the Niton Xli XRF instrument on mining impacted soils.

The 179 soils samples analyzed with ICP included all the shallow (0-20 cm) samples used for spatial mapping, and the vertical depth samples selected for ^{14}C and ^{210}Pb age dating. The ICP analysis was performed by the Montana State University Plant and Soil Analysis Laboratory using a Fisons Instruments Accuris model 3500 instrument. The ICP analysis used a strong acid digestion that followed the EPA 3050B protocol. We chose this method because it dissolves almost all the elements that are "environmentally available". The method is not a total digestion, since the elements bound to silicate structures (which are not normally mobile) will not be dissolved (U.S. EPA Method 3050B, 1996). The metals of interest in this research were copper, lead, and zinc, although arsenic, cadmium, chromium, iron, manganese, and nickel concentrations were also analyzed.

We used soil standard NIST SRM 2710 and sample duplicates for quality control of the MSU lab ICP analysis. SRM 2710 is a highly contaminated soil from a mining

impacted site in Montana, and provided a measure of the accuracy of the ICP analysis, since the true metal concentrations are precisely known. Splitting soil samples provided a measure of the ICP precision from the repeat measurements of the same soil sample. We split 11 soil samples for duplicate analysis, and added 11 soil standards to the set of soil samples submitted to the MSU lab. The industry-accepted criteria used to evaluate the results of the soil standard analysis is percent recovery of the known metal concentration, which should range from 80 to 120 percent. The accepted criteria for sample duplicates is percent difference between the two samples, which should be $\leq$ 20 percent (U.S. EPA, 2006).

We compared the XRF to the ICP results with simple linear regression analysis (SigmaPlot 8.0. SPSS Inc., 2001). This comparison provided information on the quality of data that the XRF produces. This was particularly important because the USFS uses the XRF extensively to perform onsite metal analysis during reclamation activities. The data used in the regression (179 XRF:ICP comparisons) provided a basis for comparison. We also evaluated the residuals of the predicted ICP values, which showed that data did not violate the assumption of normality for linear regression.

The regression analysis allowed calculation of equations which were used to adjust the XRF data. The correction equations calculated new XRF values based on the linear regression line from the XRF:ICP data. We also performed ANOVA (SPSS 13.0, Lead Technologies Inc., 2001) on the XRF data and the ICP data with ^{14}C and ^{210}Pb age dates. The ICP data was categorized into pre-mining and post-mining for the beaver pond marsh and active floodplain and ANOVA was used to determine whether there were

statistically significant differences between the datasets. The corrected XRF data was categorized by depth for the beaver pond and active floodplain, and ANOVA was used to determine whether there were statistically significant differences between the metal concentrations at each depth for the two hydrologic units.

Organic Carbon/Nitrogen/pH Analysis Carbon and nitrogen for 90 soil samples were measured by the Montana State University Plant and Soil Analysis Laboratory using a Leco TruSpec CN instrument. The pH of these 90 soil samples was measured using a Fisher Scientific Accumet Research AR15 pH meter following method 8C(1) from the Soil Survey Laboratory Methods Manual (USDA-NRCS, 1996). These samples included those selected for ^{210}Pb and ^{14}C age dating, and reference sites T19-9 and T20-9. The amount of carbon in the soil samples was of particular interest, since some metals (including copper) have an affinity for organic matter. These metals forms complexes with large molecular weight organics that help reduce the mobility of these metals (Gambrell, 1994).

Soil Age Dating

A subset of the wetland samples (11 sample locations and 74 samples total) from the vertical soil sampling transects was selected for ^{210}Pb age dating (Figure 11b). The ^{210}Pb dating technique is a widely used method for dating soil and sediment less than 100-150 years old, and is particularly useful in studying the impacts of mining activity in the western U.S. (Church et al., 1999). A separate sampling transect was used to collect peat samples for ^{14}C dating (Figure 11b). The two techniques complement each other in

that the ^{14}C method can be used for soils that are thousands of years old, whereas ^{210}Pb method is most useful for sediments less than 150 years old. The dating techniques provide estimations of sedimentation rates where two or more soil samples were available for age dating at the same sampling site (profile). The ^{210}Pb dates provided evidence of whether the sediment sample pre-dated or post-dated the onset of mining activity and was used to estimate sediment deposition rates. If the sediment sample was older than 70 years, then the metal concentration was likely due to natural acid rock drainage (since the primary mining activity in the Daisy Creek watershed occurred at the McLaren Pit ~50-70 years ago). Soil samples younger than 70 years old have possibly been impacted by both mining activities and natural processes.

^{14}C Analysis A peat layer was discovered during soil sampling and was sampled for ^{14}C sample age dating along a transect (Figure 11b). This peat layer (samples P1-P4) proved to be extensive in the lower wetland marsh where high metal concentrations were identified in the deeper sections of the soil profile. The peat layer was located between one and two meters in depth and was present in a number of sample sites over a distance of several hundred meters. The peat layer was over 0.3 m thick at one sample site (PS2) where three samples were selected for ^{14}C analysis. At the other sample sites, the buried peat layer was ~0.1 m thick and provided only a single sample. A charcoal sample was also collected from a site adjacent to the Stillwater River (sample P5) at a depth of 70-80 cm. A total of 7 samples were ^{14}C dated by Beta Analytical using accelerator mass spectrometry (AMS) with an uncertainty of +/- 40 years BP. These same soil samples were also analyzed for metal concentration with ICP.

^{210}Pb Analysis Eleven soil profiles, based on metal concentration and location within the wetland, were selected for ^{210}Pb soil age dating (Figure 11b). These dates were used to tie in with the ^{14}C dates and provide estimated sediment ages for the younger wetland deposits. These soil profiles provided six to seven individual dates for each location, for a total of 74 ^{210}Pb ages. The dating analysis was performed by the U.S. Geological Survey (U.S.G.S.) Center for Coastal and Regional Marine Studies in St. Petersburg, Florida using gamma spectroscopy. Sediment ages and sedimentation rates were calculated by the USGS following techniques described by Appleby and Oldfield (1978), Robbins (1978), Kotarba, Lokas and Wachniew (2002), and Shukla (2003).

The most common methods for calculating ^{210}Pb sediment ages and sedimentation rates are the constant initial concentration (CIC) and the constant rate of supply (CRS) models (Shukla, 2003). Both the CIC and CRS models assume a constant rate of supply of unsupported ^{210}Pb to the sediment. The CIC model also assumes a constant sedimentation rate, whereas the CRS model assumes a variable sedimentation rate. The CRS model uses the total amount of unsupported ^{210}Pb activity present in the core, and the amount of unsupported ^{210}Pb activity present in the core below a given depth for calculating ages. The CIC Model uses the total amount of unsupported ^{210}Pb activity present at the surface, and the amount of unsupported ^{210}Pb activity present in the core at a given depth for calculating ages. The USGS method uses a technique that first calculates a new ^{210}Pb depth profile from the measured ^{210}Pb excess activities to eliminate the impact of negative excess values while still matching the original data. This method then uses the constant initial concentration (CIC) method to calculate the

sediment dates from the new ^{210}Pb depth profile (Chuck Holmes, U.S.G.S., personnel communication). The dates used in my research were calculated by the USGS, although we also calculated sedimentation rates using the CIC and CRS model, to better understand the ^{210}Pb dating technique.

Hydrology

Groundwater Gradients and Chemistry We installed 5 piezometers nests and 5 monitoring wells in the wetland during the 2003 field season (figure 12a). Each piezometer nest consisted of two 4.0 cm inner diameter unslotted PVC pipe open only at the completion depth. The deepest piezometer of each nest pair was installed to a depth of 2 meters, and the shallow piezometer was installed to a depth of 1 meter. The monitoring wells were slotted 4.0 cm inner diameter PVC pipe with capped bottoms that were installed in hand-augered holes that ranged in depth from 1.48 to 3.16 meters. The depth of installation was determined by auger refusal. The monitoring wells were developed with a bailer to remove excess sediment. All wells were sealed with clay at the surface to prevent water from percolating down the sides of the well.

Three monitoring wells were located adjacent to each piezometer nest (M2, M3, and M11). Field data gathered from the wells included water levels (5-7 measurements in 2003 and 2004), pH, electrical conductivity (EC), salinity, and temperature (2 measurements in 2003). Water levels were measured in the piezometers to determine the vertical hydraulic gradient at each location. The monitoring wells were sampled on 7/12/2005 by Maxim Technologies, Inc. and the analysis of water chemical parameters

was performed by Northern Analytical Laboratories, Inc. in Billings, Montana using the standard New World Response and Restoration Project water analysis protocol (Maxim, 1999). This included major metal concentrations, dissolved oxygen, redox potential, acidity, and alkalinity.

Topographic Map with Flood Elevations The topographic survey was conducted in 2003 and 2004 using conventional survey equipment (Pentax PTS-V3 Total Station and Husky FS/2 Data Collector with Tripod Data Systems Software) and survey-grade GPS equipment (Trimble Total Station with model 5700 base station and model 5800 rover). A total of 1,784 wetland locations were surveyed, including all soil sampling and well locations, and the active channel zone of the Stillwater River. This survey data was interpolated and gridded using a minimum curvature algorithm to a grid size of 35 by 35 meters. The areas outside of the surveyed section were constrained by the 10 meter DEM to control edge effects during interpolation.

The existing 10 meter Digital Elevation Model (DEM) and the USGS 1:24000 Cooke City Quadrangle were of insufficient resolution for mapping the flood inundation potential of the wetland. The topographic survey was used to create a topographic map to explore likely bedrock channel constriction flooding patterns due to damming at the wetland outlet. We assumed that areas of the wetland with equal elevation had the same potential for flooding.

Results

Hydrologic Units and Vegetation

The wetland contains five distinct hydrological units that were delineated by stereoscopic air photos and field investigation (Figures 11 and 12). The wetland was divided into the channel and active floodplain, the northwest, southwest, and beaver pond marshes, and the alluvial fan. The marsh areas were predominately planeleaf willow (*Salix planifolia*) and water sedge (*Carex aquatilis*), whereas the drier sections of the wetland were mostly wolf's willow (*Salix wolfii*) and water sedge (*Carex aquatilis*). The alluvial fan transitioned from willow thickets and sedges to grasses and forbs, and into an engelmann spruce (*Picea engelmannii*) /subalpine fir (*Abies lasiocarpa*) forest from the downslope to the upland edge of the wetland. The marsh areas were typically underlain by clay and silty soils, whereas the floodplain and alluvial fan contained more sands and fine gravel. The bed material of the Stillwater River was armored with iron-stained cobbles from the confluence with Daisy Creek to the lower end of the study area. Beaver ponds were abundant throughout the lower half of the wetland, and the water table was at or near the surface throughout much of this area.

Dominant vegetation and habitat types were described for each of the hydrologic units of the Stillwater wetland (Figure 12b). The dominant vegetation, soils, surface hydrology and topographic features are described as follows:

- Northwest Marsh – This unit is a planeleaf willow (*Salix planifolia*)/water sedge (*Carex aquatilis*) plant community growing on predominately clayey and silty soils. There was a small glacial depositional feature in the northwestern corner of the unit

composed of till and small boulders. A network of paleochannels filled in with sediment and vegetation covered the southeastern section of the unit. Surface water was present in the lower elevations of the unit throughout much of the summer.

• Beaver Pond Marsh – This unit was a planeleaf willow (*Salix planifolia*)/water sedge (*Carex aquatilis*) plant community growing on predominately clayey and silty soils. This unit was dominated by beaver ponds, and surface water was present in most of the unit throughout most of the snow-free season.

• Active Floodplain – This unit was a wolf's willow (*Salix wolfii*)/tufted hairgrass (*Deschampsia cespitosa*) plant community growing on predominately sandy and gravelly soils. This unit is the active floodplain of the Stillwater River, and has numerous abandoned channels. The topographically higher sections of the floodplain had little surface water saturation during this study.

• Southwest Marsh – This unit was a wolf's willow (*Salix wolfii*)/water sedge (*Carex aquatilis*) plant community growing on predominately clayey and silty soils, with inclusions of sandy and gravelly soils. The unit receives water from the small stream that enters the wetland from the west and drains to the beaver ponds. A network of paleochannels filled in with sediment and vegetation covered much of the unit. Flowing and standing surface water were present in much of the unit.

• Alluvial Fan – This unit was a wolf's willow (*Salix wolfii*)/tufted hairgrass (*Deschampsia cespitosa*) plant community growing on predominately sandy and gravelly soils. The large alluvial fan was formed by the small stream that enters the wetland from the west. The unit had no surface water saturation except for the small stream channel.

Soil Metal Analysis

Spatial Distribution of Metals Spatial patterns of copper, lead, and zinc (0-20 cm soil depth), as measured by ICP were plotted on the contour map generated from the topographic survey data (Figure 13). The circles represent concentration levels (size proportional to concentration - specific to each metal) at each sample location. The highest levels of copper were found in the active floodplain sediments, although there were several locations with high concentrations in the beaver pond marsh unit. The lead and zinc patterns were different than copper, with high concentrations more evenly dispersed throughout the active floodplain and beaver pond hydrologic units and the two

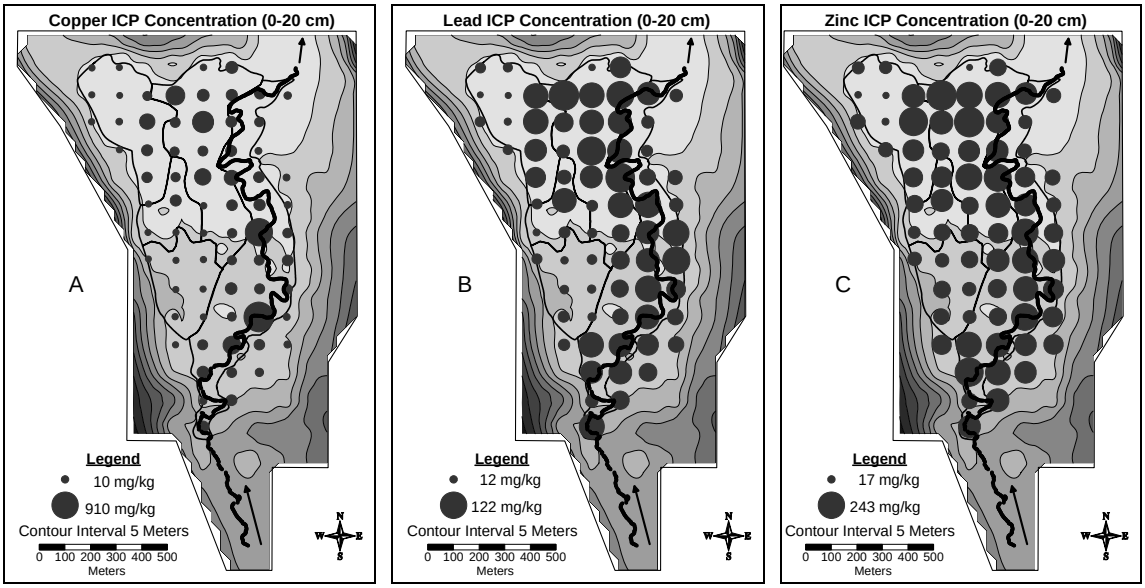


Figure 13. (a)-(c) Spatial maps of copper, lead, and zinc concentrations for upper 0-20 cm of the soil profile (for soil samples collected in 2003). The largest grey circle in each plot represents the highest measured ICP value for each metal, with the rest of the circle sizes scaled to that concentration. Note that each map has a different range of metal concentrations. The plots show the highest metal concentrations are in the active floodplain and the marsh units of the wetland. The plots also show that copper levels drop off more rapidly away from the floodplain than either lead or zinc.

metals had similar spatial patterns. The alluvial fan and northwest corner of the wetland had the lowest metal concentrations.

The areas with the highest copper concentrations were selected for deeper (0-100 cm) soil profile sampling transects (Figure 11a). These transects provided sample locations between the grid points (Figure 14). Higher concentrations of copper and zinc were found in the upper 20 cm of the active floodplain profiles (Figure 15 and Tables 1 and 2) than indicated by the spatial maps generated from the 100 meter grid samples (Figure 13). The lead concentrations in the upper 20 cm of the transect profiles were consistent with the spatial data, though the mean lead levels (0-20 cm) in the marsh were lower (mean of 66.5 mg/kg) than those in the active floodplain (mean of 88.5 mg/kg).

Regression Analysis of XRF:ICP Data The regression plots for copper, lead, and zinc show the regression lines and correlation coefficients for the XRF and ICP data, and the equation that is used to predict the ICP values (Figure 16). These plots also include a 1:1 line where the data would all fall if XRF and ICP measured exactly the same value for each sample. The regression lines show that as the concentration increased, the amount of deviation from the 1:1 line increased for all three metals. Copper had the highest range of concentrations and a high r^2 of 0.97. Zinc had a much lower range of values, with an r^2 of 0.86. Lead, which had the smallest range of concentrations, had the lowest r^2 value of 0.45. The analysis showed that the XRF underpredicts copper and zinc values and overpredicts the lead values at the concentrations measured in the wetland.

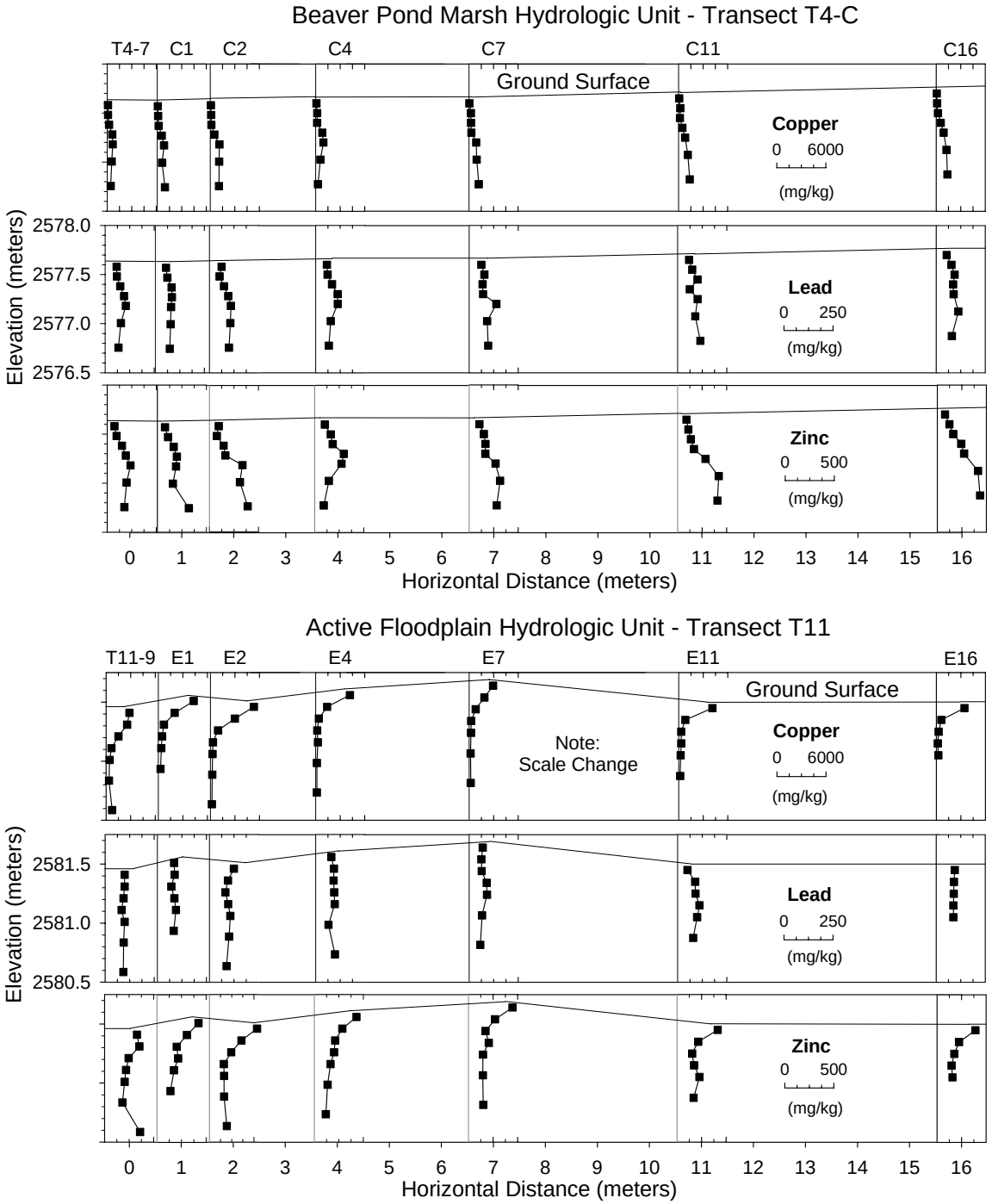


Figure 14. Cross-section depth profiles of ICP adjusted XRF values for copper, lead, and zinc. Transect T4-C was located in the beaver pond marsh and showed copper increasing with depth at most sample locations. Transect T11 is at the upper end of the active floodplain and showed the highest copper concentrations near the surface at all sample locations.

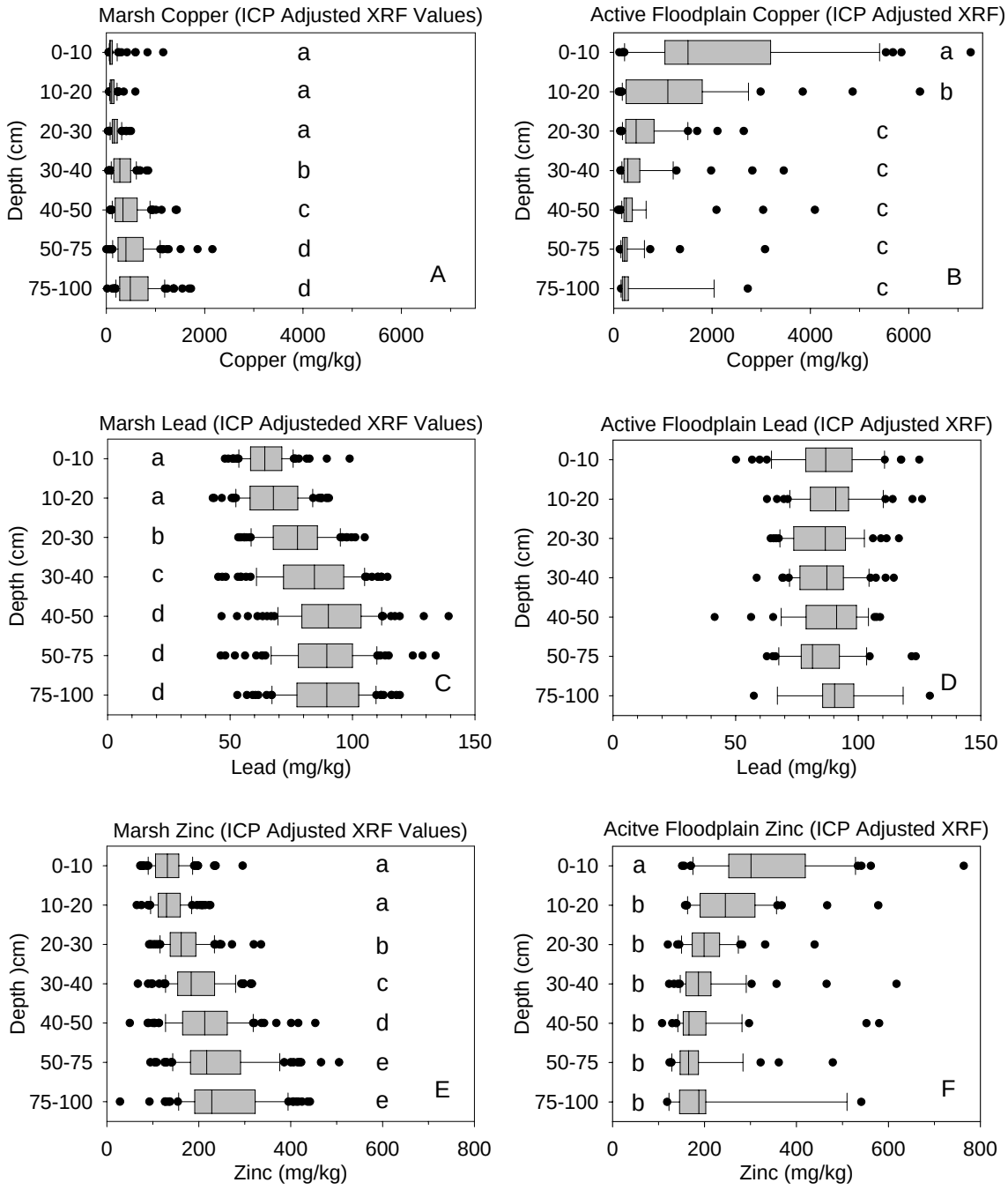


Figure 15. (a)-(f) Copper, lead, and zinc box plots by depth for the combined soil profiles in the beaver pond marsh and active floodplain hydrologic units. The ICP adjusted XRF values were from all the vertical depth sampling transects. The beaver pond marsh had higher metal levels at depth, whereas the floodplain had the highest metal levels near the surface. The lowercase letters designate which depths are significantly different in metal concentration.

[a]Boxes indicate 25th and 75th percentile with median line, and whiskers indicate 90th and 10th percentiles.

Table 1. Statistics for the active floodplain metals (ICP adjusted XRF) by depth.

	Mean (mg/kg)	Std. Dev (mg/kg)	Std. Err (mg/kg)	95% Conf. (mg/kg)	98% Conf. (mg/kg)	n	Min (mg/kg)	Max (mg/kg)
Copper								
0-10	2233	1811	270	544	727	45	116	7258
10-20	1312	1271	189	382	510	45	107	6229
20-30	641	554	83	166	222	45	133	2647
30-40	536	675	102	205	274	44	139	3459
40-50	493	798	128	259	346	39	92	4092
50-75	361	544	96	196	264	32	125	3079
75-100	472	715	198	432	606	13	152	2728
Lead								
0-10	87	16	2	5	7	45	50	125
10-20	90	14	2	4	6	45	63	126
20-30	86	13	2	4	5	45	64	117
30-40	87	13	2	4	5	44	59	115
40-50	88	15	2	5	7	39	41	109
50-75	85	14	2	5	7	32	63	124
75-100	91	16	4	10	13	13	57	129
Zinc								
0-10	330	129	19	39	52	45	151	764
10-20	259	86	13	26	35	45	158	578
20-30	208	55	8	17	22	45	120	440
30-40	208	89	13	27	36	44	123	618
40-50	195	95	15	31	41	39	108	580
50-75	183	73	13	26	36	32	124	479
75-100	221	129	36	78	109	13	119	541

Vertical Distribution of Metals The vertical depth transects were located across the active floodplain and beaver pond hydrologic units based on the spatial patterns of copper. The cross-sections of ICP- adjusted XRF metal concentration show two patterns of vertical distribution of metals present in the beaver pond and active floodplain wetland settings (Figure 14). The sediments on the active floodplain (Transect T11) had higher concentrations of copper and zinc near the surface, whereas those sediments in beaver

Table 2. Statistics for the beaverpond marsh metals (ICP adjusted XRF) by depth.

	Mean (mg/kg)	Std. Dev (mg/kg)	Std. Err (mg/kg)	95% Conf. (mg/kg)	98% Conf. (mg/kg)	n	Min (mg/kg)	Max (mg/kg)
Copper								
0-10	136	166	18	36	47	86	46	1159
10-20	129	76	8	16	22	86	59	593
20-30	183	95	10	20	27	86	35	505
30-40	317	200	22	43	57	86	40	855
40-50	434	315	34	68	90	86	75	1435
50-75	542	410	44	88	117	85	5	2158
75-100	600	396	44	88	116	81	19	1725
Lead								
0-10	65	9	1	2	3	86	48	99
10-20	68	12	1	2	3	86	43	90
20-30	77	13	1	3	4	86	53	105
30-40	84	17	2	4	5	86	45	114
40-50	91	17	2	4	5	86	47	139
50-75	89	17	2	4	5	85	46	134
75-100	89	16	2	4	5	81	53	119
Zinc								
0-10	136	40	4	9	11	86	73	296
10-20	138	35	4	7	10	86	65	225
20-30	169	46	5	10	13	86	92	336
30-40	194	56	6	12	16	86	68	316
40-50	217	75	8	16	21	86	50	454
50-75	240	86	9	19	25	85	95	505
75-100	253	90	10	20	26	81	29	442

pond marsh (Transect T4-C) had increased copper and zinc concentrations with depth in most of the soil profiles. The lead profiles show no dominant trend in either of the wetland transects (Figure 14).

The highest copper concentrations were found on the active floodplain, though we also measured high metal concentrations in the deeper sediments in the beaver pond marsh area of the wetland. Maximum copper levels in the floodplain profiles ranged from

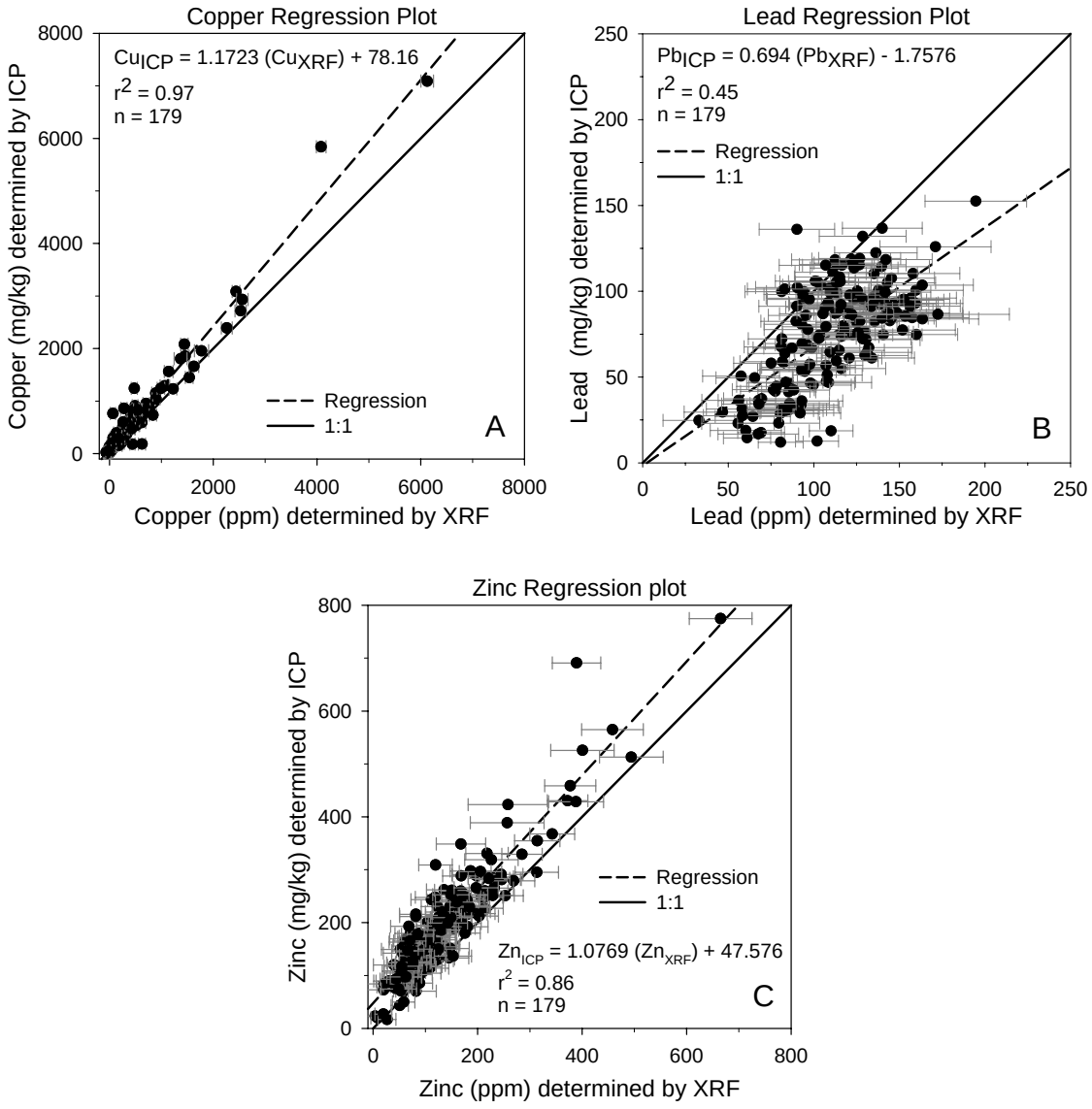


Figure 16. (a)-(c) Regression plots of XRF vs ICP for copper, lead, and zinc. The plots show the XRF and ICP values for each soil sample, regression line and 1:1 lines, and the regression equation and r^2. The plots show that the XRF under-predicts the values as measured by ICP of copper and zinc, but over-predicts the lead values.

575 to 7088 mg/kg and 545 to 1957 mg/kg in the marsh soil profiles. We found copper concentrations ranging from 223 to 1469 mg/kg in the peat samples we collected for ^{14}C age dating, which were located at depth in the marsh area (Figure 11b). The highest

copper concentrations in the active floodplain were at 0-20 cm in depth, whereas the highest levels of copper in the rest of the wetland marsh area ranged from 50-185 cm in depth.

Metal concentration profiles (as measured by ICP analysis) from six soil locations show the difference in metal distribution between the active floodplain and the beaver pond marsh (Figure 17). Metal concentrations increased with depth in soil profiles from the beaver pond marsh (Figure 17a-c), whereas soil profiles from the active floodplain had the highest concentrations near the surface (Figure 17d-f). The upper end of the wetland (T11-W7) had higher surface metal concentrations than those locations further downstream (T8-W4 and T6-W1).

The vertical pattern of copper in the active floodplain (Figure 15 and Table 2) has mean values of 2233 mg/kg (0-10 cm) and 1312 mg/kg (10-20 cm) which decrease to a mean of 361 mg/kg at a depth of 50-75 cm. Zinc follows a similar pattern with a mean of 330 mg/kg (0-10 cm) and 259 mg/kg (10-20 cm) which decrease to a mean of 183 mg/kg at 50-75 cm. The mean concentrations for lead ranged from 86 to 91 mg/kg in the active floodplain soil profiles. There were significant differences between the 0-10 cm and the deeper depths for copper and zinc, but no significant difference for lead concentrations at any of the depths (Figure 15b,d,f).

The vertical pattern of copper in the beaver pond marsh (Figure 15 and Table 1) is the opposite of the active floodplain. These profiles have mean values of 136 mg/kg (0-10 cm) and 126 mg/kg (10-20 cm) which increase to a mean of 600 mg/kg at a depth of 75-100 cm. Zinc follows a similar pattern with a mean of 136 mg/kg (0-10 cm) and 138

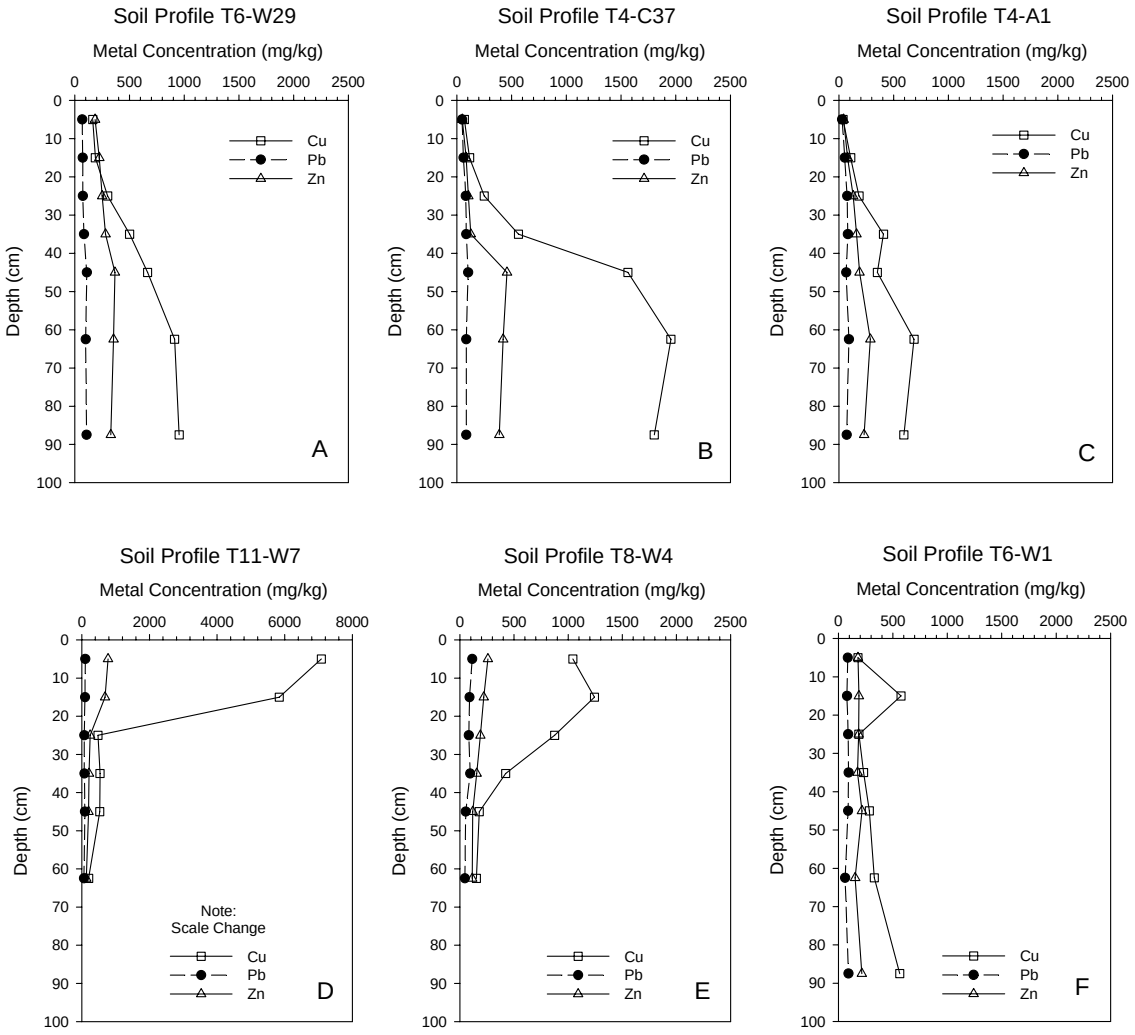


Figure 17. Concentration/depth plots for individual soil profiles in the beaver pond marsh and active floodplain hydrologic units. (a)-(c) Data for sample sites on the beaver pond marsh hydrologic unit of the wetland with metal levels that increase with depth. (d)-(f) Data for sample sites on the active floodplain hydrologic unit with the highest metals levels near the surface.

mg/kg (10-20 cm) which increase to a mean of 253 mg/kg at 75-100 cm. The mean concentrations for lead ranged from 65 to 91 mg/kg in the active floodplain soil profiles. There were significant differences between the 0-50 cm. and 50-100 cm depths for copper and zinc, and the 0-40 cm. and 40-100 cm. depths for lead (Figure 15a,c,e).

The ICP-adjusted XRF data for all the vertical depth soil sampling locations in the active floodplain (45 profiles - 263 depth samples) and the beaver pond marsh (86 profiles - 596 depth samples) show the differences in metal profiles for the beaver pond and active floodplain units (Figure 14). All three metals of interest showed an increase in concentration with depth in the beaver pond marsh, though lead reached a maximum at ~90 mg/kg (median) at depths $\geq$ 40 cm. On the active floodplain, copper and zinc had the highest concentrations in the shallow sediments, whereas lead had median values ranging from ~80 to ~90 mg/kg for all the depths and showed no visible trend. Copper concentrations (range of 92 to 7258 mg/kg and a mean of 993 mg/kg) were higher on the active floodplain compared to those in the beaver pond marsh (range of 5 to 2158 mg/kg and a mean of 332 mg/kg). Zinc also had higher concentrations on the active floodplain (range of 108 to 764 mg/kg and a mean of 233 mg/kg) compared to the beaverpond marsh (range of 29 to 505 mg/kg and a mean of 192 mg/kg).

Carbon and nitrogen fractions, and pH depth profiles from these locations showed the variability within and between the beaver pond and active floodplain units (Figure 18). The carbon profiles showed a similar pattern for the beaver pond marsh sediments (Figure 18a-c), but were less variable than the floodplain sediments (Figure 18d-f). The carbon fraction decreased to less than 1% in all the soil profiles at depths greater than 50 cm. The nitrogen fractions were low for all the soil profiles, but there was slightly more nitrogen in the marsh profiles than those in the floodplain. The pH depth profiles provided evidence that the carbon content was organic carbon, since the acidity of the soil would have consumed any inorganic carbon (eroded limestone particles) that would

have been present in the soil. The mean soil pH values ranged from 3.82 to 7.52 with a mean of 5.87. The beaver pond marsh soil pH values ranged from 3.82 to 6.65 with a mean of 5.60, and the floodplain soil pH values ranged from 4.41 to 7.52 with a mean of 6.16.

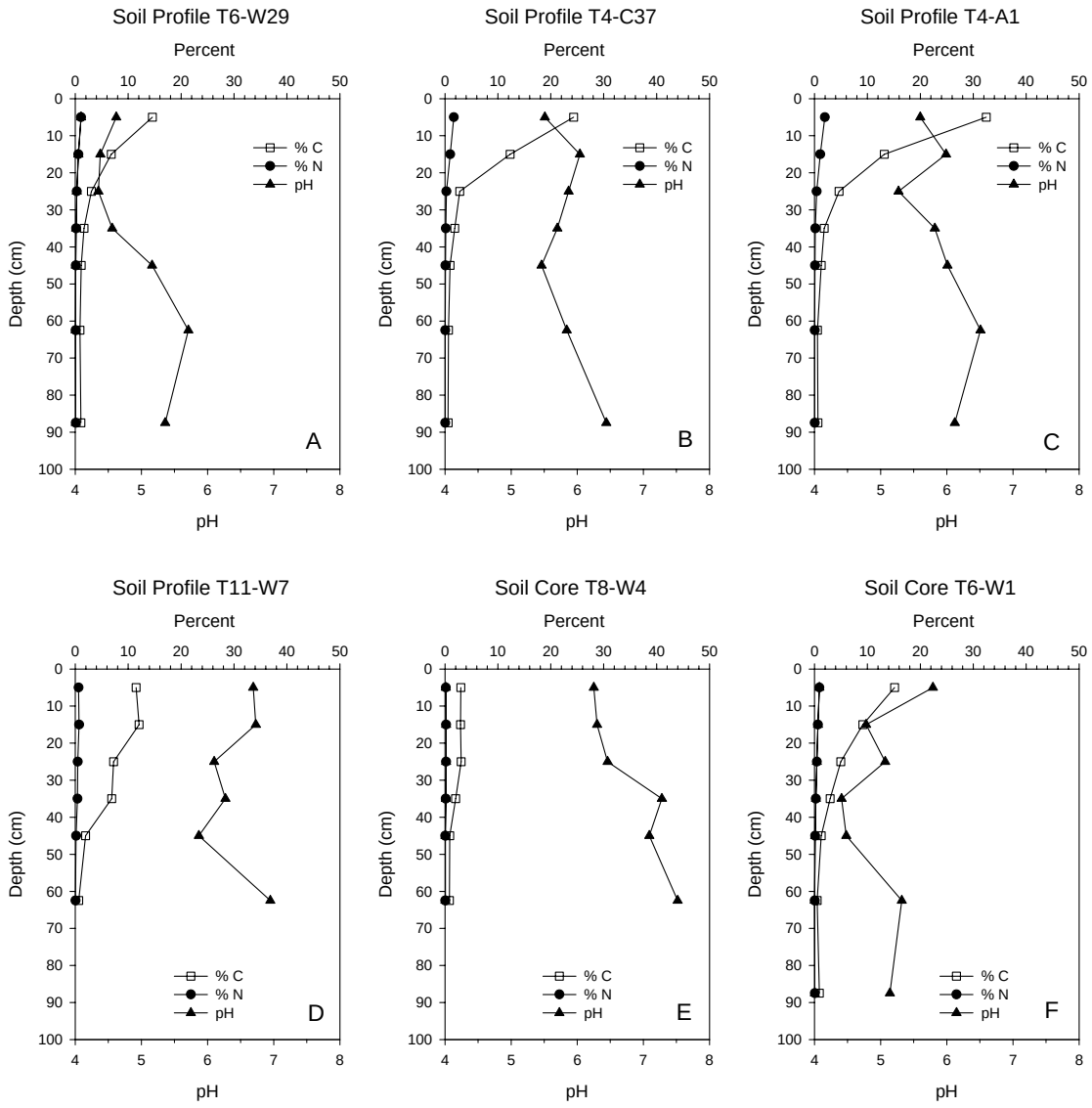


Figure 18. Carbon and nitrogen percent and pH depth profiles for the floodplain and beaverpond marsh hydrologic units. Plots (a)-(c) were in the beaver pond marsh and plots (d)-(f) were in the active floodplain.

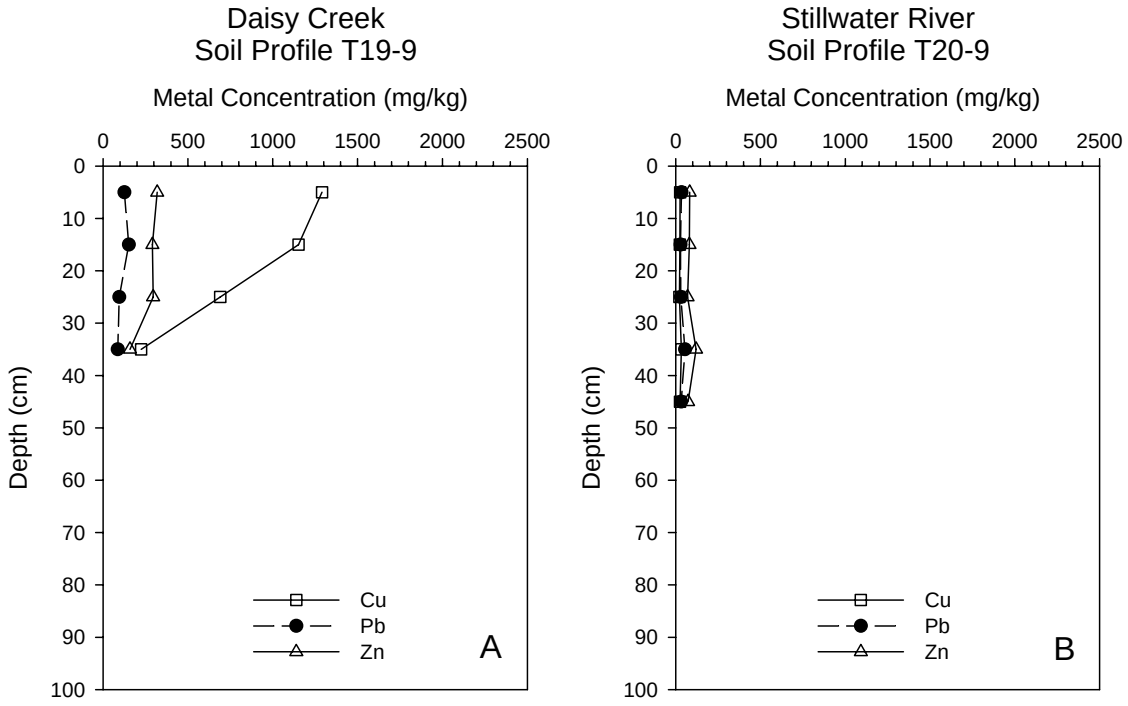


Figure 19. Metal/depth profiles for the Daisy Creek and Stillwater River reference sites. (a) Metal data for a sample site next to Daisy Creek and just above the confluence with the Stillwater River. (b) Metal data for a site on the Stillwater River above the confluence with Daisy Creek.

Stream Channel Distribution of Metals Metal data for two stream channel reference sites show contrasting concentration profiles (Figure 19). Sample site T19-9 was adjacent to Daisy Creek and just above the confluence with the Stillwater River. Profile T20-9 was next to the Stillwater River and above the confluence with Daisy Creek, and had low metal concentrations. Both sample locations were within a meter of the thalweg and flowing water and were on barren fluvial deposits of the respective streams. The maximum metal values for the Stillwater River soil profile T20-9 were 34 mg/kg copper, 56 mg/kg lead, and 120 mg/kg zinc, whereas the Daisy Creek soil profile. T19-9 had maximum values of 1291 mg/kg copper, 152 mg/kg lead, and 319 mg/kg zinc. T19-9 also showed a decrease in metal concentration with depth.

Table 3. In-stream sediment sample results for stream sediment collected in 2004 for Daisy Creek and Stillwater River (Maxim, 2005).

Maxim Sample Site[a]	Copper (mg/kg)	Lead (mg/kg)	Zinc (mg/kg)
DSC-11000	2060	86	404
DSC-11430	1140	83	297
DSC-12000	2030	76	401
DSC-13000	1440	69	324
DSC-13490	1110	88	287
DSC-14000	1110	82	312
DSC-15000	1180	64	320
DSC-15675	1200	54	321

[a]Stream sediment samples were collected on 9/29/04.

Stream sediment data was collected by Maxim Technology in 2005 as part of the New World Restoration Project (Table 3). These sample locations were located in the study area and provided another data set to correlate with my results (Figure 11a). DSC-11000 was on Daisy Creek and DSC-15676 was the furthest downstream sample site on the Stillwater River. Profile T19-9 was located between Maxim sample sites DSC-11000 and DSC-11430. The 0-10 cm copper value (1291 mg/kg) in profile T19-9 closely matches with the stream sediment concentration measured at site DSC-11430 (1140 mg/kg), as do the lead and zinc levels. Maxim site DSC-15675 was 35 meters upstream of transect T11, where I measured the highest copper concentrations in the wetland.

The copper concentration of 1200 mg/kg at this location was lower than those found in the upper sediments in the T11 soil profiles, but within the same order of magnitude in concentration.

Bivariate Metal Analysis We also analyzed the ICP metal data using bivariate plot (Figure 20). A non-linear correlation of pairs of metals would suggest the potential for

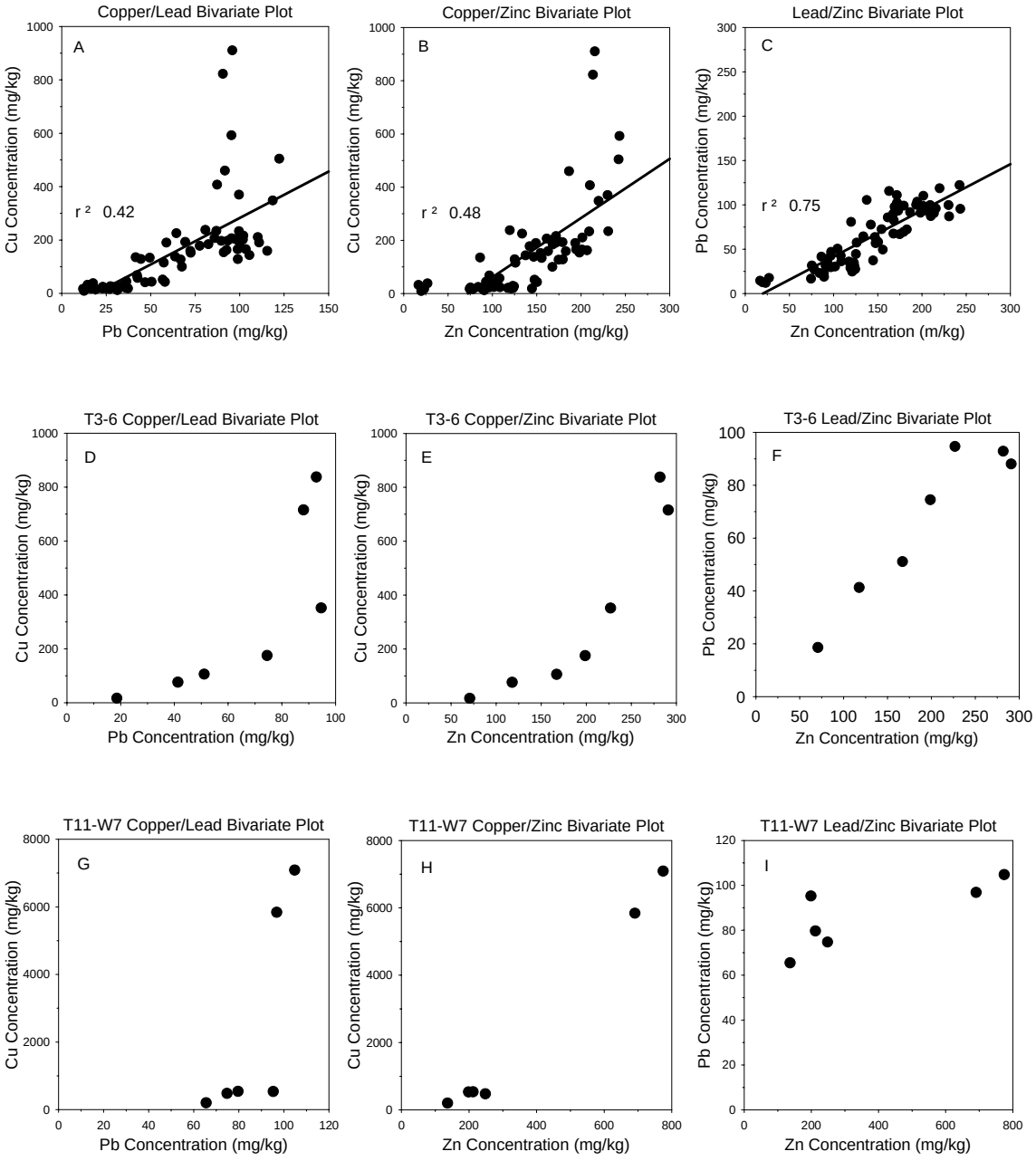


Figure 20. Bivariate plots of copper, lead, and zinc concentrations (mg/kg) as measured by ICP. (a)-(c) Metal data for all the shallow soil samples (0-20 cm depth soil samples collected in 2003) that were collected for spatial analysis. These plots include the simple linear regression line and r^2 value. (d)-(f) Metal data for sample location T3-6, which was located in the beaver pond hydrologic unit and had metal concentrations increasing with depth. (g)-(i) Metal data from sample location T11-W7, which was on the active floodplain hydrologic unit, and had highest metal concentrations near the surface.

mobility or concentration of individual metals. One set of bivariate plots included all the shallow (0-20 cm) soil samples metal concentrations (Figure 20a-c), and the other set of bivariate plots included two soil profiles used for ^{210}Pb age-dating (Figure 20d-i). This allowed comparison of the spatial metal data with the vertical depth data to see if the same pattern of linear correlation was present.

The bivariate plots (Figure 20a,b) for copper:lead, and copper:zinc in the shallow sediments (0-20 cm) shows a break in linear correlation at copper concentrations greater than ~300 mg/kg, whereas the lead:zinc plot (Figure 20c) shows strong linear correlation. The plots show that at high concentrations of copper, there is not a corresponding increase in lead and zinc. The linear correlation between lead and zinc suggests that the geochemical soil processes for both metals are similar within the wetland. The plots for sample sites T3-6 (Figure 20d-f), which were in the beaver pond marsh, show the same pattern. The plots for sample site T11-W7 (Figure 20g-i), which was on the active floodplain, show the same general pattern, though there is more scatter in the lead:zinc data.

Soil Age Dating

^{14}C Analysis The ^{14}C data for the Stillwater wetland is summarized in figure 21 and also includes the copper concentrations of the age-dated samples. Samples PS1, PS2, PS3 and PS4 were taken from the peat layer in the lower end of the wetland, and range in age from 2770 to 8710 years BP. Sample location PS2 had a thicker peat layer that

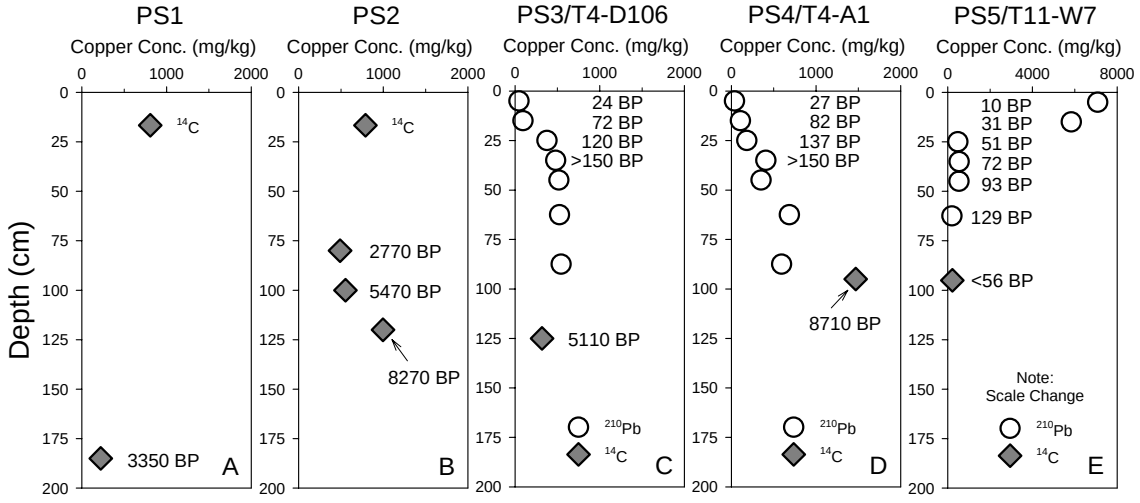


Figure 21. (a)-(e) The copper concentrations and soil ages for the ^{14}C and ^{210}Pb dated soil samples. Plots A-D show pre-mining copper concentrations in the marsh ranging from 223 to 1469 mg/kg for sediments dating from 2750 to 8710 years BP. Plot E show a site on the active floodplain with high copper concentrations near the surface that were younger than 150 years old. High concentrations of copper in the peat deposits may be due to copper's affinity for organic matter which would have increased the accumulation of copper. The ^{14}C date at PS5 (<56 years BP) was younger than the oldest ^{210}Pb date (129 years BP) at that location and could be due to either sampling or age-dating error.

provided three ^{14}C dates. The difference in the date intervals is 2250 and 2720 years, suggesting a very stable depositional environment for nearly 5000 years. The calculated sedimentation rates were 0.007 cm/year, which is at least an order of magnitude smaller than those calculated from the ^{210}Pb data, with an average profile range of 0.13 to 0.38 cm/yr in the upper sediment layers (0-100 cm) of the beaver pond marsh (Table 4).

Sample PS5 was taken next to the Stillwater River, and was reported in the pMC format. The value of 111.1 is percent modern carbon, meaning that the sample had more ^{14}C material than the modern (AD 1950) reference standard. This indicates that the organic material in the sample was still growing after the on-set of atmospheric nuclear

testing in the 1950's (Beta Analytic memo, 2005) and represents recent (< 56 years BP) deposition of this soil sample. This charcoal sample was 5 meters from a sample location (T11-7) that had a ^{210}Pb date of 129 years BP for sediment at 50-75 cm in depth. Sample location PS5 was also within 2 meters of the active channel of the Stillwater River, and this discrepancy in sediment ages was probably due to the variability of floodplain deposition.

^{210}Pb Analysis Metal concentrations, estimated ages, ^{210}Pb, ^{226}Ra, and ^{137}Cs activities, and sedimentation rates for soil profiles T8-E4 and T4-A1 represent the two characteristic vertical metal patterns present in the wetland (Figure 22). Sample site T8-E4 was adjacent to the Stillwater River and had high metal concentrations near the surface, whereas T4-A1 was near the center of the lower beaver pond marsh, and had metal concentrations increasing with depth.

Table 4. Summary of average sedimentation estimates (cm/yr) for each soil profile as determined from ^{210}Pb analysis.

Soil Profile	CRS Model (cm/yr)	CIC Model (cm/yr)	USGS Model (cm/yr)
Active Floodplain			
T6-W1	1.31	0.17	0.17
T8-W4	0.56	0.94	0.96
T8-E4	0.51	2.44	0.71
T11-W7	0.40	0.51	0.49
T11-E7	1.34	0.26	0.27
T11-E37	0.74	0.21	0.26
Beaver Pond Marsh			
T3-6	2.05	0.17	NA
T4-A1	0.72	0.33	0.18
T4-C37	0.50	1.31	0.38
T4-D106	0.76	0.20	0.21
T6-W29	1.10	0.13	0.13

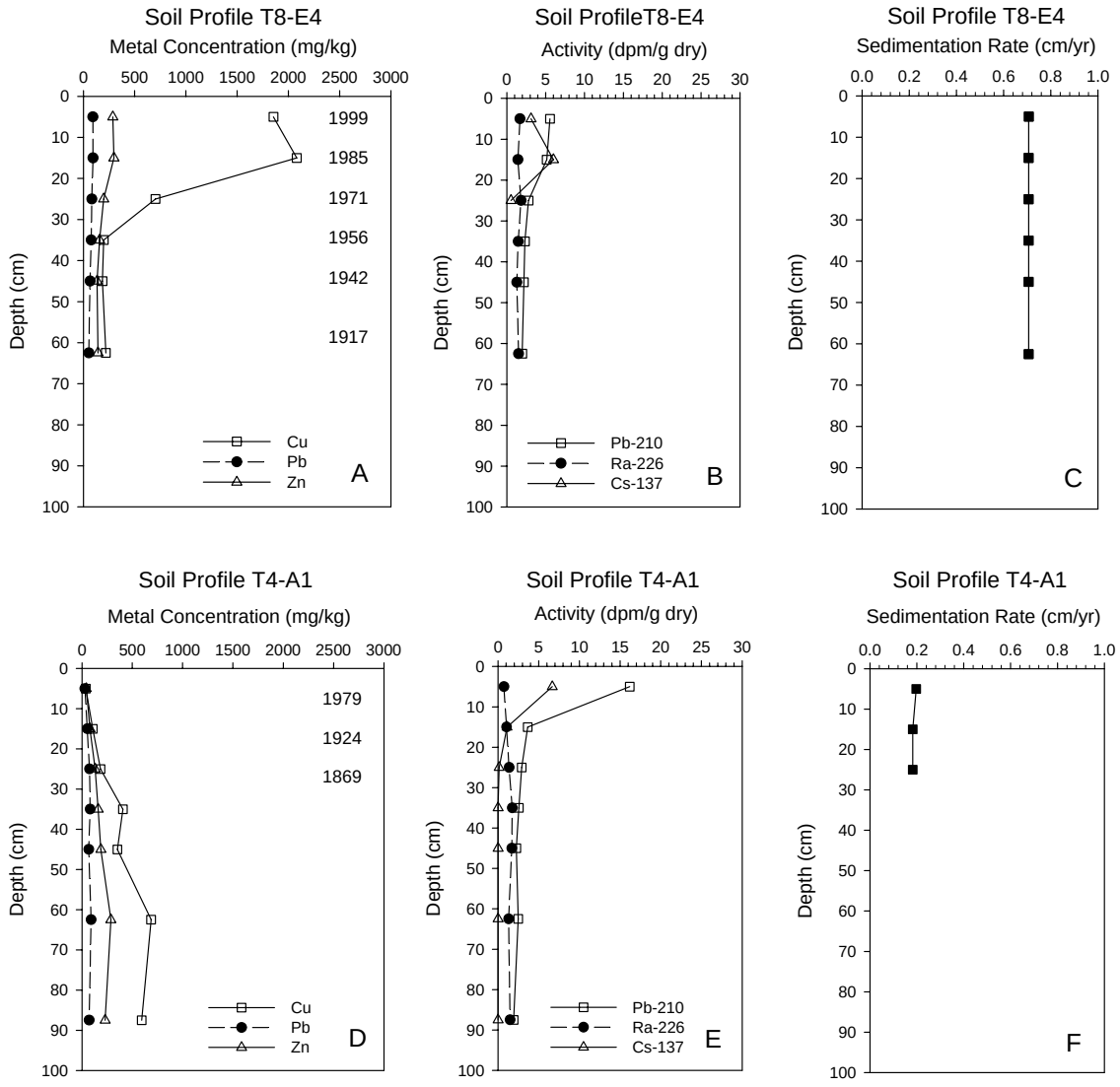


Figure 22. Metal concentrations, ^{210}Pb, ^{226}Ra, ^{137}Cs activities, and sedimentation estimates for soil profiles T8-E4 and T4-A1. (a)-(c) Data for a sample site in the active floodplain hydrologic unit that has high metals near the surface. (d)-(f) Data for a sample site in the beaver pond marsh hydrologic unit where metal levels increased with depth. Plots C and F show the differences in sedimentation estimates between the marsh and the floodplain, with T8-E4 having 3.5 times the rate of T4-A1.

Soil profile T8-E4 (Figure 22a) shows that the sediments with the highest concentrations of copper had ^{210}Pb dates less than 70 years old. The profile shows the ideal ^{137}Cs curve with a peak in activity in the subsurface (Figure 22b). The only other

soil profile that had a similar ^{137}Cs curve was T8-W4, which was along the same transect. Soil profile T4-A1 (Figure 22d-f) shows that the sediments with the highest copper concentrations had ^{210}Pb dates much older than 70 years. This profile shows the highest ^{137}Cs values near the surface, suggesting active deposition of sediment into the wetland (Figure 22e). This ^{137}Cs curve was characteristic of all the soil profiles except those along transect T8. The sedimentation rate for soil profile T8-E4 (Figure 22c) was 0.7 cm/yr, which is 3.5 times the rate of 0.2 cm/yr calculated for profile T4-A1 (Figure 22f), reflecting the differences in the depositional settings.

The ^{137}Cs data provides insight into depositional processes occurring in the wetland. Most of the wetland soil profiles had the highest concentration of ^{137}Cs at the surface, with the exceptions of two soil profiles that were next to the Stillwater River, which showed the peak in the subsurface. Since there is no appreciable ^{137}Cs deposition currently (Shukla, 2002), the highest ^{137}Cs activity should be in the subsurface. The presence of highest levels at the surface indicate that ^{137}Cs is being transported into the wetland through erosional/ depositional processes (Ritchie, 1990 et al., and Holmes, personnel communication) or that the upper soil layers have been removed through erosion. The U.S.G.S. ^{210}Pb sedimentation rate estimates (Table 4) ranged from 0.17 to 0.96 cm/yr on the active floodplain, and 0.13 to 0.38 cm/yr in the marsh. Sample location T6-W1, which was next to the outside bend of the Stillwater River and was being actively eroded, had a sedimentation estimate of 0.17 cm/yr, whereas soil sample location T8-W4, which is a point bar deposit, had a much higher sedimentation estimate of 0.94 cm/yr. My CIC sedimentations rates were similar to the USGS calculations in 8 of 11 soil profiles

(mean difference of 14.65%), supporting the use of this model for estimating sediment ages.

Figure 23 and table 5 categorize the metal concentrations found on the active floodplain and wetland marsh into pre-mining and post-mining sediment deposition. These box plots incorporate all the soil samples with age control (^{14}C and ^{210}Pb dates). The cutoff date for pre-mining vs. post-mining was 1933 (73 years old). All three metals

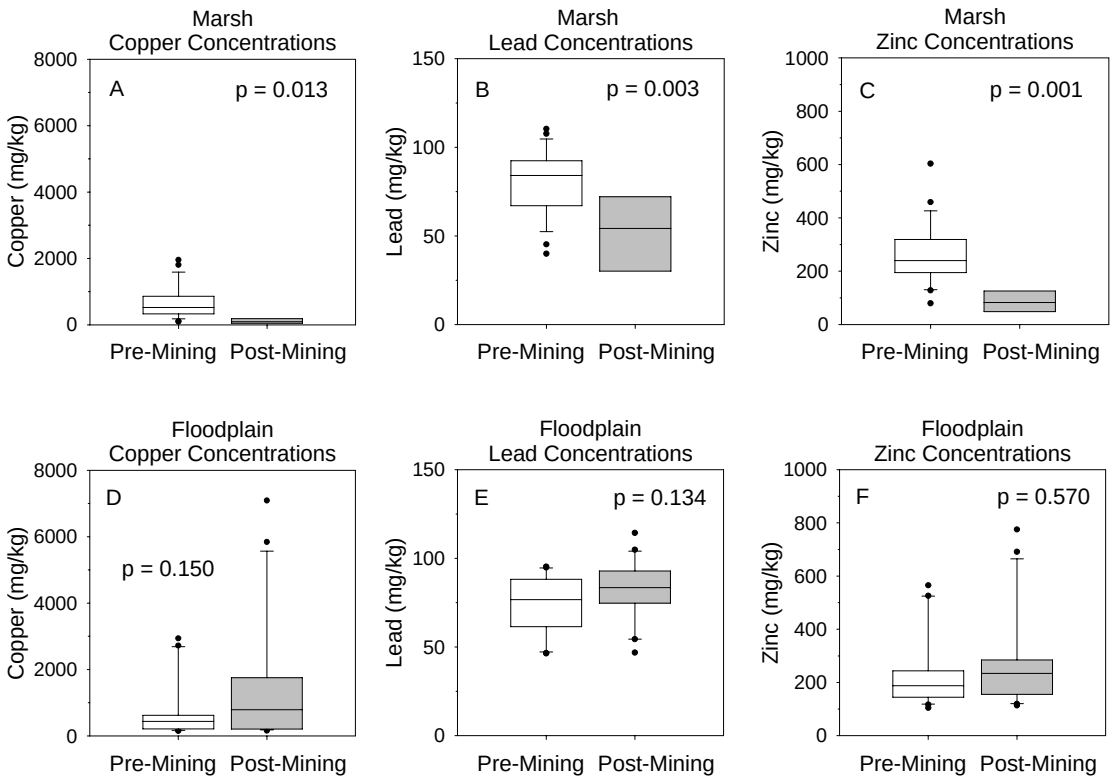


Figure 23. (a)-(f) Copper, lead, and zinc concentrations for the beaver pond marsh and active floodplain sediments. The shaded box plots represent the post-mining levels. The metal concentrations are higher in the pre-mining soils in the marsh (a)-(c), and higher in the post-mining sediments in the active floodplain (d)-(f). The metal results with age control were all located in the beaver pond marsh, southwest marsh, and active floodplain hydrologic units. ANOVA analysis shows the pre/post metal concentrations in the marsh soils are significantly different ($p < 0.05$), whereas the pre/post metal concentrations are not significantly different ($p > 0.05$) in the floodplain soils.

[a]Boxes indicate 25th and 75th percentile with median line, and whiskers indicate 90th and 10th percentiles.

Table 5. Statistics for pre-mining and post-mining copper, lead, and zinc concentrations for the beaver pond marsh and active floodplain.

	Mean (mg/kg)	Std. Dev (mg/kg)	Std. Err (mg/kg)	95% Conf. (mg/kg)	98% Conf. (mg/kg)	n	Min (mg/kg)	Max (mg/kg)
Marsh								
Pre-mine								
Copper	655	496	94	192	260	28	94	1957
Lead	80	19	4	7	10	28	40	110
Zinc	262	113	21	44	59	28	79	603
Post-mine								
Copper	114	82	33	86	135	6	38	250
Lead	53	21	9	22	35	6	29	82
Zinc	91	51	21	54	85	6	43	185
Floodplain								
Pre-mine								
Copper	765	895	200	419	573	20	147	2934
Lead	74	16	4	7	10	20	46	95
Zinc	240	144	32	67	92	20	104	565
Post-mine								
Copper	1453	1890	423	884	1209	20	153	7088
Lead	82	17	4	8	11	20	47	114
Zinc	269	176	39	82	113	20	114	775

in the floodplain (Figure 23d-f) showed a trend of higher concentrations in the post-mining sediments as compared to the pre-mining sediments, though they were not significantly different. The marsh sediments (Figure 23a-c), however, showed the

reverse, with pre–mining sediments having the highest metal concentrations for all three metals, and the differences were significant.

Hydrology

Vertical Hydraulic Gradients Vertical hydraulic gradients were computed for each piezometer nest for the 2003 field season. The water levels in these piezometers were measured only twice in 2004 (middle and end of July). Piezometers P1 and P3 were in the beaver pond hydrologic unit, and P2, P4 and P5 were in the active floodplain (Figure 12a). Piezometer P1 showed an upward gradient, whereas P2, P3 and P4 showed a downward gradient during the early part of the summer. Piezometers P1, P2, P3 and P4 show a reduction in hydrologic gradient as the summer progressed. P5 had a horizontal gradient throughout the measurement period.

Groundwater Chemistry Well chemical data from the monitoring wells (sampled on 7/12/05) showed that the pH of the water from the wells was circumneutral (pH ranged from 6.6 to 6.8), but that there were differences in the oxygen-reduction potential (ORP) and the EC (table 6). The middle area of the wetland (M5 and M11) had a positive ORP and similar EC values, whereas the lower area of the wetland (M1, M2, and M3) had negative ORP and a larger range of EC values. The EC was highest in the northwest part of the wetland (M1) and lowest in the active floodplain (M3).

While the piezometer data were limited, the piezometric gradient suggests that oxygenated water moves downward in the upper and middle of the wetland and upward

Table 6. Monitoring wells chemistry data. Wells M1, M2 and M3 are at the lower end of the wetland, and M5 and M11 are in the middle of the wetland[a] (Maxim, 2005).

Laboratory Parameter	**Test Units[b-d]**	**M1**	**M2**	**M3**	**M5**	**M11**
Specific Conductivity	µS/cm	562	342	109	185	203
pH	s.u.	6.8	6.7	6.6	6.6	6.7
Total Dissolved Solids	mg/l	351	218	78	127	124
Copper as Cu (Dissolved)	mg/l	0.002	<0.001	0.002	0.005	0.004
Lead as Pb (Dissolved)	mg/l	<0.001	<0.001	<0.001	<0.001	<0.001
Zinc as Zn (Dissolved)	mg/l	0.03	0.01	0.04	<0.01	0.06
Iron as Fe (Dissolved)	mg/l	24.5	27.4	0.48	1.05	0.1
Field Measurements		**M1**	**M2**	**M3**	**M5**	**M11**
Temperature	Deg. C	6.08	3.11	4.48	6.31	6.26
pH	s.u.	7.02	6.95	6.38	6.14	6.62
Specific Conductivity	µS/cm	603.00	423.00	117.00	183.00	210.00
Dissolved Oxygen	mg/l	6.03	0.40	1.77	5.10	5.61
Oxygen-Reduction Potential	millivolts	-66.80	-114.00	-94.20	65.20	113.00

[a]Wells were sampled on 7/12/2005
[b]mg/l = milligrams per liter
[c]s.u. = standard units
[d]µS/cm = microsiemens per centimeter at 25 degrees Celsius

at the lower end of the wetland. The lower end of the wetland would likely be a reducing environment due to the lack of oxygen. Wells M1 and M2 have the highest total dissolved solids (TDS) and concentrations of iron found in the monitoring wells, which also suggests a reducing environment. The concentrations of zinc were an order of magnitude higher than copper and lead in all of the monitoring wells.

Though the metal chemistry of the monitoring wells was only sampled once, the results provided important data. The monitoring well chemistry showed low concentrations of copper, lead, and zinc in the water extracted from all the wells. The hydraulic gradient in the piezometer nests showed a downward gradient at the upper end of the wetland and an upward gradient at the lower end of the wetland during the early

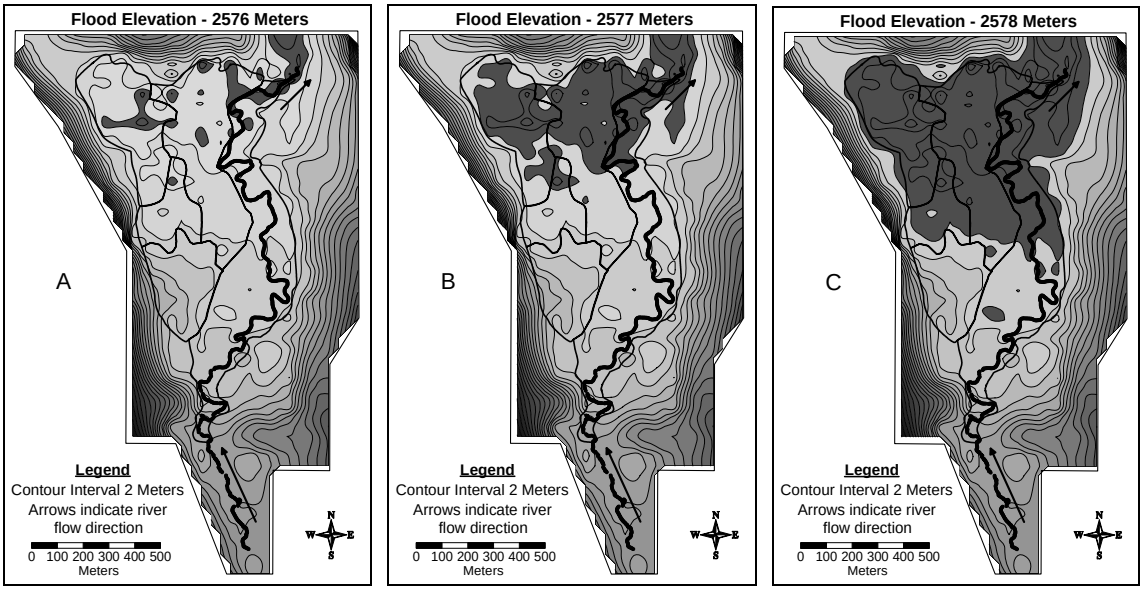


Figure 24. (a)-(c) Dark grey shading highlights the areas of the wetland that could be underwater at various flood stages. The Stillwater River exits at the northeast end of wetland where the valley narrows and the channel and valley constrained by igneous bedrock.

summer. These gradients in the soil profile decreased as the summer progressed, likely related to reduced groundwater recharge and snowmelt runoff. The dissolved oxygen and ORP measurements from the monitoring wells support this model of a downward hydraulic gradient of oxygen-rich water at the upper end of the wetland and an upward gradient of oxygen-deprived water at the lower end of the wetland. The high iron levels in the monitoring wells at lower end of the wetland (M1 and M2), plus the highest total dissolved solids, and conductivity values in these wells, suggests the presence of reducing conditions that correlate to hydrologic flowpaths and gradients.

Flooding Potential We developed three maps displaying the area potentially inundated under three flood stage scenarios (Figure 24). The plots show the areas of the wetland inundation for stage elevations of 2576, 2577, and 2578 meters AMSL (note that

the contour intervals are 2-meters). The Stillwater River exits the wetland at the northeast corner through a narrow bedrock constriction. These maps were based on the assumption that the narrowly-constricted Stillwater River could cause water to back up under ice-damming or high flow conditions and flood areas of equal elevation upstream.

Discussion

My research combined soil metal analysis, ^{14}C and ^{210}Pb age-dating techniques, topographic surveys, and groundwater investigations to describe the spatial and temporal variability of copper, lead, and zinc in the Stillwater wetland. My results showed differences in metal distributions between the active floodplain and the marsh, both spatially and vertically. I documented metal concentration profiles associated with pre-mining and post-mining sediments originating at the headwaters of the Stillwater watershed. I addressed the following questions:

(1) What are the spatial and vertical patterns of metal concentrations across the wetland?

Spatial and vertical mapping of metal concentration showed variation both across the wetland and with depth. Soil sampling in the shallow sediments (0-20 cm) showed that the highest concentrations of copper were found in the active floodplain, but that similar levels of lead and zinc were found throughout the active floodplain and lower marsh hydrologic units (Figure 13). The alluvial fan had low concentrations of copper, lead, and zinc compared to the rest of the wetland. The small stream that formed the alluvial fan begins in bedrock composed primarily of Paleozoic limestone that contains

no sulfide deposits. The northwest section of the wetland near the saddle between the wetland and Lake Abundance also showed low metals concentrations in shallow surface sediments relative to the rest of the wetland.

Copper, lead, and zinc do not show the same spatial pattern in the wetland soils. High concentrations of copper are not necessarily found in the same locations as are high zinc and lead concentrations. The difference in the spatial pattern of copper as compared to lead and zinc in the shallow sediment (0-20 cm) could be caused by a number of factors. The spatial differences between copper and lead/zinc could be due to mobility of lead and zinc from the upper layers of the soil profile. The bivariate plots in figure 20 show that at high concentrations of copper there are not corresponding high levels of lead and zinc. This relationship can be explained by either accumulation of more copper than lead and zinc, or the reverse process of lead and zinc leaching from the soil. While zinc can be mobile in soil, lead typically has low mobility in soils (Bradl, 2004; Matagi et al., 1998). Since lead and zinc have the same spatial pattern, leaching is a less probable mechanism for explaining the differences in the copper vs. lead/zinc concentration maps. A second possibility is that these differences in metal ratios reflect separate source rocks or areas within the watershed with different Cu:Pb:Zn ratios. The stream that enters the west side of the wetland carries sediment from non-sulfide Paleozoic carbonates and these sediments would have different Cu:Pb:Zn ratios than those eroded from the McLaren ore body. Circumneutral pH suggests this second scenario.

The difference in metal profiles between the active floodplain and beaver pond marsh soils includes the range of metal concentrations and whether the metal

concentrations increased or decreased with depth. The beaver pond marsh soils had copper concentrations of 5 to 2158 mg/kg and zinc concentrations of 29-505 mg/kg that increased with depth. The active floodplain had copper concentrations of 92 to 7258 mg/kg and zinc concentrations of 29-505 mg/kg that decreased with depth. The range of lead concentrations was almost the same between the two hydrologic units (43-139 mg/kg versus 41-129 mg/kg), though there was a slight increase in concentration with depth in the beaver pond marsh soils.

The stream sediments had the same level of metal concentrations as found in the active floodplain soils. Maxim Technologies sampled stream sediments in 2004 from upper Daisy Creek and the Stillwater River down to transect T11 (Maxim, 2005). The range of metal concentrations matched my data, especially at sample site T19-9, which was located on barren fluvial sediments adjacent to Daisy Creek and about 100 meters above the confluence with the Stillwater River. The Maxim stream sediment sample nearest T19-9 had a copper concentration of 1140 mg/kg (DSC-11430), which closely matches the 1300 mg/kg value we measured at 0-10 cm. The stream sediment copper value of 1200 mg/kg at Maxim site DSC-15675 was of a high magnitude as were those from transect T11, though these profiles had copper concentrations ranging from 2934 to 7088 mg/kg in the shallow sediments.

Geomorphic processes that transport metal-rich sediments can re-deposit these materials along the floodplain and out into the wetland marsh during extremely high flooding events. The stream sediments (Table 3) had copper, lead, and zinc concentrations that corresponded to the concentrations present in the McLaren ore

Table 7. Selected trace metal concentrations for the western U.S. and the upper Stillwater River watershed. Soil site T20-9 is above the confluence of Daisy Creek and the Stillwater River and located on the barren fluvial sediment adjacent to the stream. The metal concentrations in the Stillwater wetland and floodplain incorporated the shallow spatial and deeper soil profile transect data.

	Western US[a]	Soil Site T20-9	McLaren Deposit[b]	Daisy Creek Stillwater River Stream Sediment[b]	Marsh Bank/ Overbank[c]	Stillwater Wetland Floodplain	Stillwater Wetland Marsh
	Mean mg/kg	Mean mg/kg	Mean mg/kg	Breakpoint[d] mg/kg	Mean mg/kg	Mean mg/kg	Mean mg/kg
Copper	21	26	4069	521	393	1109	559
Lead	18	36	126	51	75	78	76
Zinc	51	85	140	182	210	245	232

[a]Shacklette et al., 1971.
[b]Gurierri, 1998.
[c]Hydrometrics, 1994.
[d]Upper limit of unpolluted or natural background conditions.

Table 8. Daisy Creek and Stillwater River surface water chemistry (Maxim, 2007).

Station ID	Sample Date	Flow Rate[a]	Cu Total[b]	Cu Dissolved[b]	Pb Total[b]	Pb Dissolved[b]	Zn Total[b]	Zn Dissolved[b]
DC-5	4/25/06	13.03	0.23	0.032	<0.001	<0.001	0.06	0.05
DC-5	6/27/06	446.84	0.21	0.011	<0.001	<0.001	0.04	<0.01
DC-5	9/27/06	7.93	0.79	0.049	0.001	<0.001	0.17	0.1
SW-7	4/25/06	57.77	0.003	<0.001	<0.001	<0.001	<0.01	<0.01
SW-7	6/27/06	1943.10	0.028	0.006	<0.001	<0.001	<0.01	<0.01
SW-7	9/27/06	55.22	0.003	<0.001	<0.001	<0.001	<0.01	<0.01

[a]l/s - liters per second
[b]mg/l - milligrams per liter

deposit (Table 7). These metals are likely bound to iron hydroxide coatings and colloids or are in solid phases within the stream sediment, though there are also dissolved metals in the stream water (Table 8). Transport and deposition of these sediments would explain why the highest metal concentrations are found on the active floodplain and in the lower wetland marsh that is susceptible to flooding (Figure 24). The spatial maps for lead and

zinc support the geomorphic deposition of metal-rich sediments along the floodplain and into the wetland marsh.

(2) Are the metal concentrations in the post-mining sediments higher than those in pre-mining sediments?

Soil metal concentration profiles were different between the active floodplain and the wetland marsh sediments in two respects: (1) high metal concentrations near the surface that decrease with depth on the active floodplain; and (2) low concentrations near the surface that increase with depth within the wetland marsh (Figures 14 and 15). These two profiles occur in different hydrologic settings and possess distinct profile-age relationships. The concentrations of the marsh metal deposits ranged from 38 to 1957 mg/kg copper, 10 to 29 mg/kg lead, and 43 to 603 mg/kg zinc in sediments deeper than 50 cm. The metal concentrations of the floodplain sediments ranged from 147 to 7088 mg/kg for copper, 46 to 114 mg/kg for lead, and 104 to 775 mg/kg for zinc in sediments less than 50 cm.

Figure 23 summarizes copper concentrations for pre-mining and post-mining deposition (based on ^{14}C and ^{210}Pb ages) for the marsh and floodplain sediments. The copper, lead, and zinc values show distinct ranges for each depositional setting. The highest metal concentrations in the marsh were in the pre-mining sediments for all three metals (> 30 cm depth) (Figure 23a-c). The differences between pre-mining and post-mining metal concentrations were not significantly different for the floodplain sediments, but there was a trend of higher metal concentrations are in the post-mining sediments for all three metals (< 20 cm depth) (Figure 23d-f). In soil profile T8-E4 (active floodplain)

(figure 22a), the highest copper concentrations were near the surface and are younger than 1933, whereas in soil profile T4-A1 (beaver pond marsh) (Figure 22d), the highest copper concentrations in the deepest depths and were older than 1869.

The ^{14}C data (Figure 21) corresponds to metal concentrations ranging from 223 to 1469 mg/kg for copper, 40 to 104 mg/kg for lead, and 196 to 603 mg/kg for sediments ranging in age from 2770 to 8710 BP. This data suggests that as far back as ~8000 years ago, acid rock drainage or erosion of metal rich soils was impacting the Stillwater wetland. These dates corroborate previous research in the watershed that indicated several episodes of ferricrete deposition in the Daisy and Fisher Creek drainages during the last 8000 years. That research suggested that these ferricrete deposits formed during more humid climatic periods which caused elevated erosion and increased acid rock drainage (Furniss et al., 1999; Hinman et al., 2000).

Conceptual Model of Metal Deposition

The wetland stratigraphy and depositional history of the Stillwater wetland were beyond the scope of this research. However, inferences can still be made from sampled sediment characteristics. The sediments of the marsh were predominantly clays and silts, with occasional interbedded gravels, while the floodplain was largely composed of sands and gravels. The fine sediments would have been likely deposited in either a lacustrine setting or from slow moving floodwaters. The gravels were likely deposited during overbank flooding and/or migration of the Stillwater River across the wetland. The peat samples indicate the presence of vegetation within several thousand years of the retreat of

the glaciers (~8000-10,000 years ago) and subsequent conditions that allowed burial of the plant material.

The peat deposits were associated with high copper, lead, and zinc concentrations equaling those found in the deeper beaver pond marsh soils. The metal concentrations in peat samples provide evidence that the Stillwater wetland has been receiving acid rock drainage for thousands of years. The possibility exists that these metals have leached through the soil profile and adsorbed to the organic matter, though the somewhat lower pH and ORP has likely desorbed metals from the sediment and immobilized the metals as sulfides. There is some potential for metal mobility at the lower soil pH values found in the wetland, but at the higher pH levels, copper, lead, and zinc will remain immobile in the soil.

The dominant process for distributing metals through the wetland has likely been channel migration and flood deposition. Erosion of metal rich sediments from upstream, plus metal precipitates and metals sorbed to stream sediments represent potential sources of metals. Even at the downstream end of the Stillwater wetland, the streamwater has a copper concentration (dissolved and particulate) ranging from 0.003 mg/l during low-flow to 0.028 mg/l during high-flow (Table 8). There is no difference in the low and high flow concentrations of lead (<0.001 mg/l) and zinc (<0.01 mg/l). We also observed an increase in water turbidity in the Stillwater River following several storm events, indicating an increase in the fine sediment load being transported by the streamwater following heavy rainfall. The Stillwater wetland is a sink for metal deposition, but may become a source of metals when streambank erosion occurs during flooding events. We

found the highest concentrations of metals in the shallow subsurface soils of the active floodplain. Erosion of these sediments could remobilize these metals during high runoff. Numerous abandoned channels demonstrate that the Stillwater River actively migrates within the floodplain. Therefore, the greatest potential for metal mobility in the Stillwater wetland is streambed remobilization and streambank erosion.

Conclusion

My research shows that metal concentrations varied spatially across the wetland, with depth and age of sediments. The XRF instrument provided a tool for rapid assessment and economical analysis of metal concentrations, and ^{14}C and ^{210}Pb age dating techniques provided a method for separating pre-mining sediments from post-mining sediments in the active floodplain and the wetland marsh.

I identified two distinct patterns: 1) high concentrations of metals (particularly copper) in the shallow post-mining floodplain sediments relative to the pre-mining floodplain sediments; and 2) high metal concentrations (particularly copper) in the deeper pre-mining marsh sediments relative to the shallow post-mining marsh sediments. Differences between the patterns could be due to different source areas for the sediments or metal mobility. These metals were likely distributed across the wetland through flooding and channel migration. While the higher concentrations in the active floodplain sediments correlate with historic mining activity, they can also be the result of reworking of metal-rich sediment found in the streambed or eroded from floodplain deposits. The occurrence of ferricrete deposits in the upper Daisy Creek indicate that metals have been

cycling through the drainage due to natural processes for thousands of years. My research included a broad survey of wetland sediments and identified those areas that have concentrations of metals that may be of concern. Further investigation may be required to map in more detail the floodplain sediments and to address the issue of potential metal mobility.

Numerous studies (Gurrieri, 1998; Furniss et al., 1999; Nimick et al., 2001) have shown that Daisy Creek continues to receive surface water and groundwater containing acid rock drainage and that the historic mining activity at the McLaren Pit is associated with increased metal loads in the streamwaters. Reclamation work has been occurring in the Daisy Creek watershed for the last 30 years and may improve the water quality of Daisy Creek and the Stillwater River. These activities include revegetation work by the Forest Service, the reclamation activities conducted by Crown Butte Mining, and the ongoing reclamation work that recently completed the capping of the McLaren Pit. Reducing the amount of acid rock drainage entering these waters should help limit the amount of metals entering the Stillwater wetland.

HAND-PORTABLE X-RAY FLORESCENCE APPLICATION TO METALS CHARACTERIZATION IN A RIPARIAN WETLAND IMPACTED BY ACID ROCK DRAINAGE

Introduction

Historic mining activity has impacted water and land resources throughout the western United States. The rich history and environmental impact of mineral exploitation in the Rocky Mountains is well documented. The bedrock in these regions contains numerous mineralized bodies of gold, silver, copper, lead, zinc, and other metals. Pyrite is often present in these rocks, which when exposed to oxygen and water produces acidity that releases metals present in the rock matrix. These metals often end up in streams and rivers, where aquatic life can be severely impacted. Acid rock drainage is a difficult and expensive problem to address and continues to impact water resources throughout the western United States.

Due to the large number of sites that are impacted by acid rock drainage and the costs associated with their reclamation, rapid assessment tools that are accurate and easy to use in the field are desirable. Rapid field assessment can provide significant cost savings in all phases of these projects, particularly during the investigative stages when expensive excavation equipment is active on-site. X-Ray Florescence (XRF) has become a valuable tool for rapid analysis of metal contamination (U.S. EPA, 2006). The XRF instruments have become reliable and relatively inexpensive in the context of the overall costs involved in most reclamation efforts. In-laboratory XRF analysis can also provide

valuable data at lower costs and can be especially efficient when dealing with a large number of samples.

I investigated a wetland at the headwaters of the Stillwater River, Montana, which has been impacted by acid rock drainage from both natural sources and processes, and historic mining activities. The Stillwater wetland is located in the New World Mining District near Cooke City, Montana (Figure 25a). Gold, silver, and copper were discovered in the area in the 1870's, and various mining activities have occurred there over the last one hundred years. Acid rock drainage occurs in the Fisher and Daisy Creek drainages. Iron stained cobbles line the streambed of both of these creeks in their upper reaches (Kimball et al., 1999; Nimick et al., 2001). The acid mine drainage originating at Fisher Mountain, due both to natural erosional processes and historic mining activity, impacts Daisy Creek and the Stillwater River. The main mining activity occurred at the McLaren ore deposit from the 1930's through the 1950's (Elliot, 1979). The New World Mining District Response and Restoration Project began addressing the environmental impacts of the historical mining activities in 1999, with the U.S. Forest Service (U.S.F.S.) as the agency responsible for managing the cleanup. This research was part of the restoration effort and focuses on quantifying the impact of acid mine drainage to the Stillwater wetland. I sampled the soils of the wetland to characterize the spatial and vertical extent and timing of metal deposition. The XRF instrument was used to measure metal concentrations of a much larger number of soil samples than would have been possible using standard laboratory techniques.

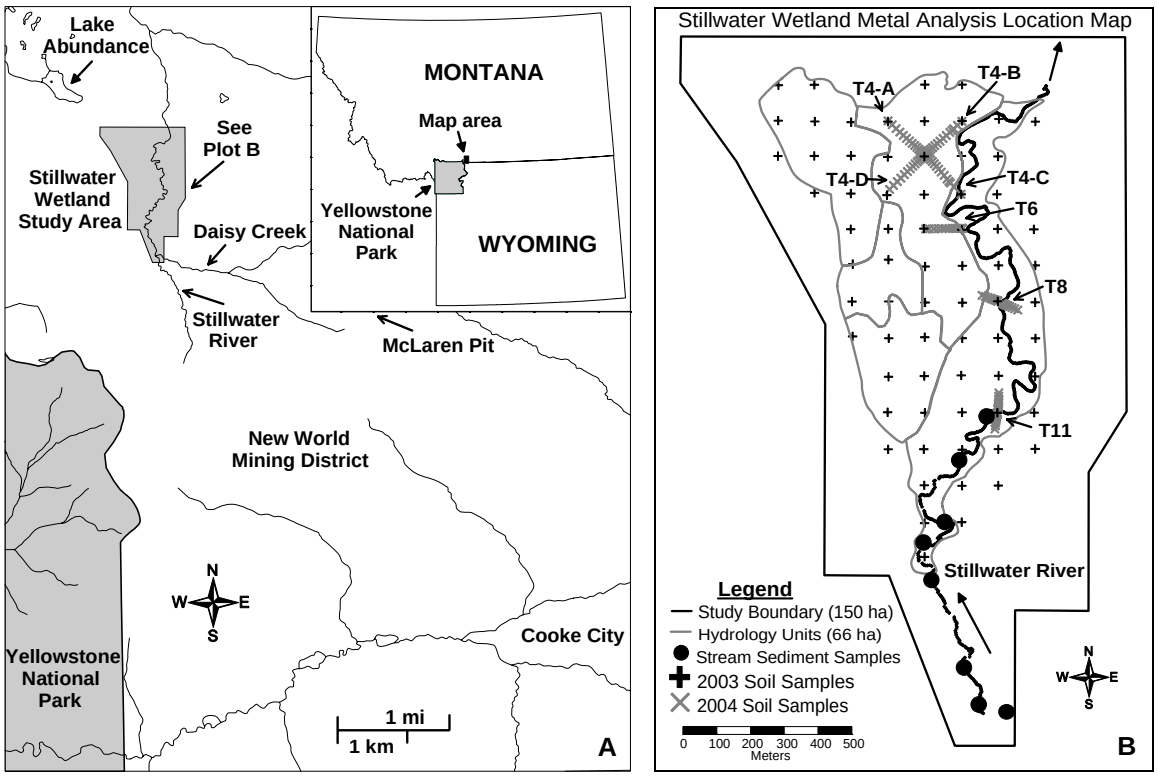


Figure 25. (a) Map of the Stillwater wetland study area. (b) Soil sampling locations in the study area and the hydrologic units that divided the wetland into areas with similar hydrology, vegetation, and soils.

I used the Niton Xli 700 XRF instrument extensively to measure metal concentration in wetland soils and analyzed ~1,000 samples during the project. I analyzed a subset of soil samples with inductively coupled plasma atomic emission spectrometry (ICP) analysis following the EPA 3050B protocol to assess the quality of the XRF data. I sought to assess the accuracy, precision, and bias of data provided by the XRF instrument. I addressed the following questions: 1) How can XRF data error be quantified, predicted, and incorporated into soil metal analysis and assessment; and 2) can the XRF data be useful in mapping and metal quantification efforts?

Site Description

The Stillwater wetland is located at 45º 04' 40" N latitude and 109º 59' 45" W longitude. The study area is 150 hectares in size, with the wetland area totaling 66 hectares. The Stillwater wetland is located in a glacier carved valley at an elevation of 2585 meters. The wetland is adjacent to and south of the Beartooth Wilderness Area and is located ~4 km northeast of Yellowstone National Park (Figure 25a). The study area is located in the northwest corner of the New World Mining District and is ~4 km downstream of the McLaren Pit. The McLaren Pit and the surrounding landscape are the sources of the acid rock drainage that enters Daisy Creek and the Stillwater River. The Stillwater River flows along the eastern edge of the wetland and an extensive beaver pond network covers much of the lower end of the wetland.

The study area is comprised of the active floodplain of the Stillwater River, an alluvial fan formed by an unnamed stream flowing into the wetland from the western edge, and marsh areas with abundant beaver ponds. The marsh areas were dominated by planeleaf willow (*Salix planifolia)* and water sedge (*Carex aquatilis*), whereas the drier parts of the wetland were dominated by wolf's willow (*Salix wolfii*) and water sedge (*Carex aquatilis)*. The alluvial fan transitioned from willow thickets and sedges to grasses and forbs, and into an engelmann spruce (*Picea engelmannii*)/subalpine fir (*Abies lasiocarpa*) forest near the upland edge of the wetland. The marsh areas were typically underlain by clay and silty soils, whereas the floodplain and alluvial fan contained more sands and fine gravel. The bed material of the Stillwater River was armored with iron-stained cobbles from the confluence with Daisy Creek to the lower end of the study area.

Beaver ponds dominate the lower half of the wetland (north), and impede drainage and help sustain the water table near the ground surface throughout much of this area.

The surrounding bedrock is Paleozoic sedimentary rocks (predominately limestone, dolomite, and shales) that have been intruded by Eocene volcanic dikes, sills, and laccoliths (Elliot, 1979; Lovering, 1929). The Stillwater wetland was under ~800 meters of ice during the Pinedale glaciation (Pierce, 1979), which ended approximately 11,000 years ago. Glacial features dominate the surrounding landscape with abundant moraines surrounding the wetland. The igneous activity formed the mineralized sulfide ore bodies that produce the acid rock drainage in the mining district. The rocks in the New World ore bodies are a copper skarn deposit that contains major deposits of copper, gold, and silver (Elliot, 1979; Johnson and Meinert, 1994). These deposits also contain abundant pyrite that when oxidized helps release high concentrations of metals into surface runoff and groundwater. The Stillwater River begins in a glacial cirque containing non-mineralized Paleozoic carbonates and is in pristine condition above the confluence with Daisy Creek. Daisy Creek begins at the base of the McLaren Deposit and is severely impacted by acid rock drainage. The Stillwater River downstream of the confluence with Daisy Creek supports limited aquatic life until some distance into the wilderness area, where incoming streams dilute the concentration of metals (Gurrieri, 1998).

Materials and Methods

Soils

We investigated the spatial distribution of metal concentrations using shallow (0-20 cm), composite soil sampling. We sampled on a 100 meter by 100 meter grid (Figure 25b). The vegetation was scraped away from the surface prior to soil sample collection by a hand auger. The samples were stored in labeled Ziploc bags for transport to the laboratory. The soil samples were either air dried or oven dried at 45ºC to avoid organic matter combustion. The gravel-sized particles and any visible vegetation fragments were separated from the dried soil samples by hand and the remaining material was ground to a fine powder (~ 45 microns) using a zirconium ball-mill grinder. The grinding process provided a consistent soil particle size and a representative sample of a larger amount of material.

We followed a grinding protocol designed to reduce potential for cross-contamination. Two possible sources of contamination are small particles from the grinding vial itself or metals that stick to the surface of the grinding vial during the grinding process. We used a procedure which utilized zirconium vials and an acid bath wash. Zirconium vials are extremely hard, and even if particles from the vials contaminated the soil sample, the metal was of no concern in the Stillwater wetland soil analysis. A dilute hydrochloric acid solution was used to dissolve any metals that might adhere to the surface of the grinding vial. The zirconium vials and the acid bath wash helped reduce the potential for contamination.

Metal Analysis

All prepared samples were analyzed for total metal concentration using XRF. A subset of the samples was analyzed with inductively coupled plasma atomic emission spectroscopy (ICP). We were primarily interested in the total concentration of metals present in the wetland sediments and sought to compare the results of the XRF data to those measured using ICP analysis. The ICP analysis used a strong acid digestion that followed the EPA 3050B protocol. We chose this method because it dissolves almost all the elements that are "environmentally available". The method is not a total digestion, since the elements bound to silicate structures (which are not normally mobile) will not be dissolved (U.S. EPA Method 3050B, 1996). The ICP analysis was performed by the Montana State University Soil Analytical Laboratory. The MSU Laboratory used an Accuris model 3500 ICP instrument manufactured by Fisons Instruments for metal analysis.

A total of 179 soil samples were analyzed using ICP techniques to quantify metal content. The metals of interest in this research were copper, lead and zinc. Arsenic, cadmium, chromium, iron, manganese, and nickel concentrations were also analyzed, but their concentration in the wetland soils were low and of less environmental concern. We used a soil standard (SRM NIST 2710) and sample duplicates for quality control of the MSU lab ICP analysis. The soil standard provided a measure of the accuracy of the ICP analysis, since the true metals concentrations are precisely known. Splitting soil samples provided provides a measure of the ICP precision from the repeat measurements of the same soil sample. We split 11 of the soil samples for duplicate analysis, and also added

11 soil standards to the set of soil samples submitted to the MSU laboratory. The industry accepted criteria used to evaluate the results of the soil standard analysis is percent recovery of the known metal concentration, which should range from 80 to 120 percent. The accepted criteria for sample duplicates is percent difference between the two samples, which should be $\leq$ 20 percent (U.S. EPA, 2006).

We used a Niton XLi 700 XRF hand unit for field and lab analysis. XRF analyzers use a radioactive source to produce x-rays, which irradiate the soil sample and cause various elements to release fluoresced x-rays due to electrons shifting from one orbit to another. When an electron is knocked out of the atomic orbit by a high energy photon such as an x-ray or gamma-ray, an electron from a higher level orbit fills the vacancy, and in the process releases energy in the form of a fluoresced x-ray. Since each element produces fluorescence x-rays at unique frequencies, this property can be used to identify which elements are present in a soil sample (Kalnicky et al., 2001). The instrument measures the various frequencies of these x-rays over a given amount of time and is able to compute the concentrations of each element present in the sample from the resulting spectra.

We deployed the XRF instrument in the field on a limited basis. We primarily used the XRF in the lab on the same set of samples that were analyzed with ICP (179 samples) as well as on an 804 additional XRF samples. This instrument provided a unique opportunity for rapid and low-cost metals analysis of the wetland soils. ICP measurements of the same soil samples provided data that was used to assess the XRF unit's precision and accuracy. A total of 983 soil samples were analyzed with XRF,

which would have been cost-prohibitive using ICP, while 179 samples were analyzed by both XRF and ICP.

An important step in using the XRF for metal analysis was to determine the optimum measurement time for each soil sample. The Niton XRF instrument uses a statistical algorithm based on measured frequencies over a length of time. The longer the soil is irradiated with x-rays, the more data that is gathered by the instrument, which allows averaging out the random variation in the x-ray emissions (U.S. EPA, 1995). Since a large number of samples were going to be analyzed, a tradeoff between error and duration of instrument analysis was required. We used NIST 2710 soil standard, which is a mining contaminated soil from Montana that is often used to evaluate data quality in these types of settings. The soil was measured by the XRF at 60 seconds (repeated 10 times) and 180, 300, 600, 1200 and 1800 seconds. Since the true concentrations of the NIST 2710 soil standard are known, we could determine the amount of reduction in error that occurred with each increase in analysis time. This duration test allowed determining the optimum XRF analysis time that would allow measurement of ~1000 soil samples.

Results

A total of 983 soil samples were analyzed using the XRF, with 179 of these samples analyzed both with XRF and ICP analyses. We first performed an XRF duration analysis on NIST 2710 soil standard to determine the ideal analysis time. The XRF instrument calculates a measurement error (+/- ppm error) that decreases as the length of analysis time increases. We wanted to reduce the amount of error and still process all the

samples in a reasonable amount of time. We then compared the XRF to ICP measurements with simple linear regression analysis. This comparison provided information on the quality of data provided by the XRF. The XRF data was also instrumental in producing spatial maps and vertical cross-sections for a large number of samples.

Duration Test

Figure 26 shows the plots that were used to determine the optimal sample analysis duration. Analysis duration optimality is a combination of precision, accuracy, and efficiency. Figure 26a shows error in measured metal concentration versus time of analysis for each of the metals of primary concern. This plot shows a break in slope at 300 seconds, with a significant reduction in error for all the metals when compared to measurements taken at 60 and 180 seconds. The plot also shows some interesting groupings of similar patterns of error. The top three curves are for chromium, iron, and manganese. For the lower sets of lines, copper and zinc have nearly identical error curves, as do arsenic and lead. Figure 26b shows the results for just copper, lead, and zinc which better illustrates the similarity in copper and zinc XRF measurement error. The total percent error and reduction in error for each time increment are also shown on this plot, and indicates a 55% reduction in XRF instrument error at 300 seconds.

Figures 26c-e show measured metal concentration versus time for copper, lead, and zinc in addition to the certified value for each metal (solid line) and the ICP value

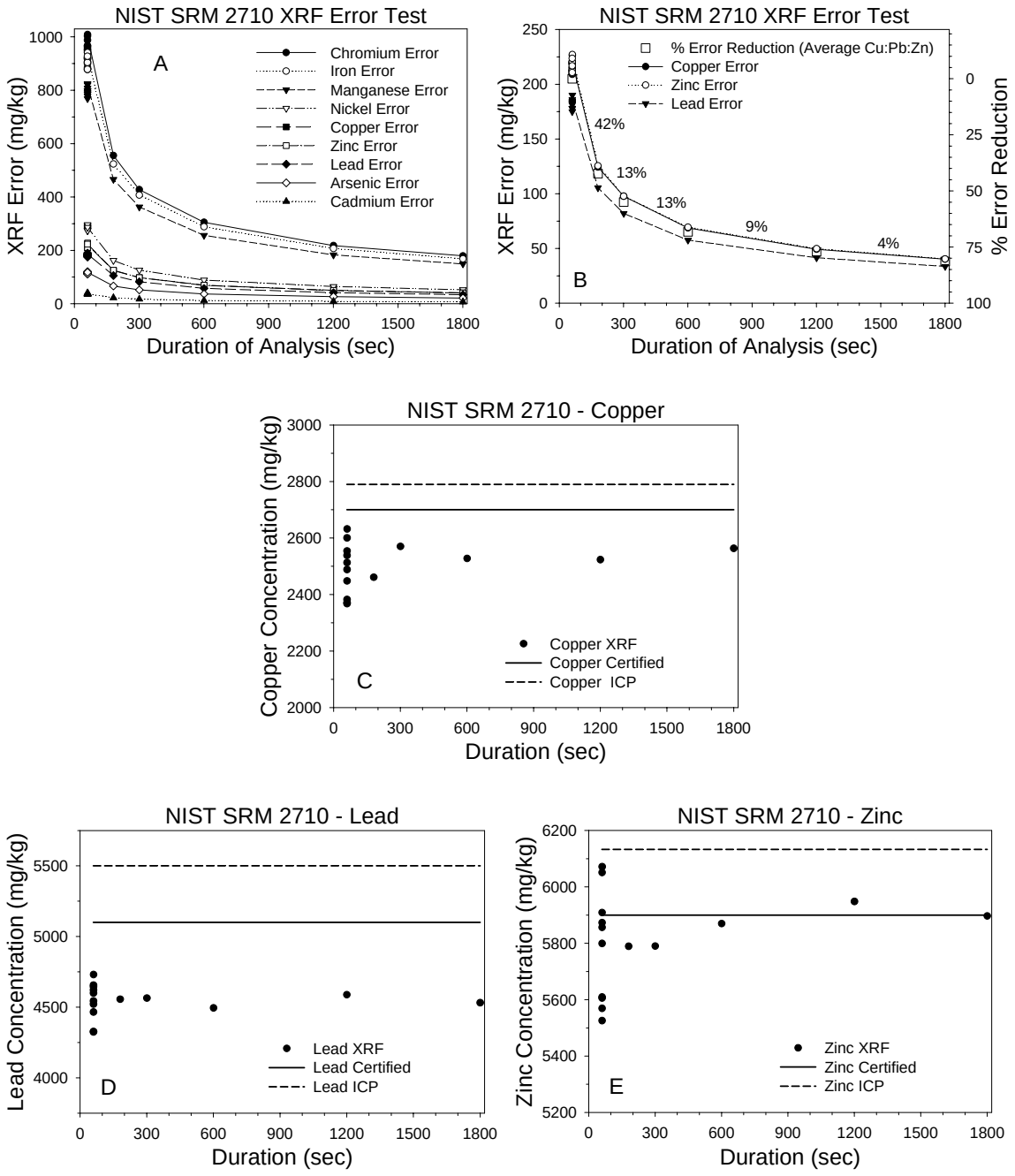


Figure 26. XRF duration analysis for SRM 2710 soil standard. (a) Error versus time for all metals analyzed using ICP. (b) Error versus time for copper, lead, and zinc. The percent values are the amount of error reduction per duration increment. (c)-(e) Metal concentration versus time for copper, lead and zinc. In plots C-E, the filled circles are the XRF values, the dashed line the measured ICP value, and the solid line the certified value for these soils. Plots C-E show 10 repeat XRF measurements at 60 seconds to illustrate the variability for a given time duration.

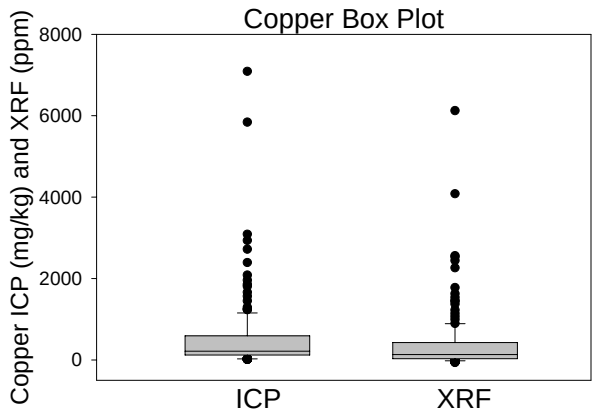
(dashed lined) that was measured by the MSU laboratory. These plots indicate that at 300 seconds, the XRF measured concentration value begins to stabilize. These plots also show that the XRF under predicts copper and lead, but provides more accurate zinc estimates. Based on the plots in figure 26, we determined that 300 seconds (55% reduction in XRF instrument error) provided a reasonable reduction of error for the amount of time available for analysis of nearly 1000 soil samples. Even doubling the analysis time to 600 seconds would reduce the XRF error by only another 13%, and even at 1800 seconds of instrument analysis time, the XRF values for copper and lead did not equal the certified values or the ICP results.

XRF:ICP Error

Table 9 shows the descriptive statistics for all the samples analyzed with XRF and ICP. The box plots show that the XRF values are lower than the ICP values for copper and zinc, and higher for lead. The paired t-test values indicate there are significant differences in the mean concentrations (all the p-values were less than 0.001). The XRF underpredicts copper and zinc, and overpredicts lead when compared to the ICP data. Copper had the largest range of concentrations, followed by zinc and then lead, which was reflected by the large standard deviations. The standard deviations were higher for the ICP values than for XRF values for all three metals.

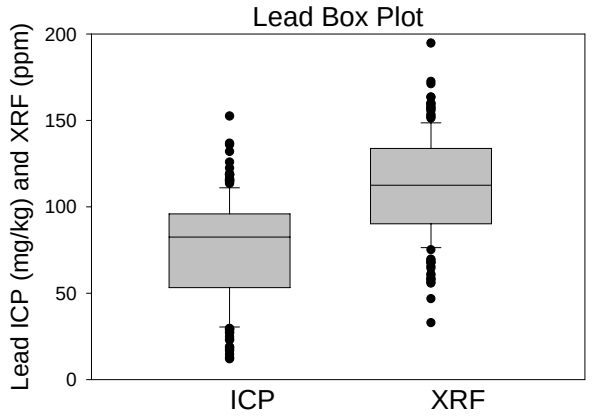
The ICP data for the NIST 2710 standards are summarized in table 10. The ICP recovery values for the soil standards show that all the results were acceptable for copper, lead, and zinc (<20% for environmental soil analysis) (U.S. EPA, 2006). Figure 27 shows

Table 9. (a)-(c) Box plot and descriptive statistics for copper, lead, and zinc.



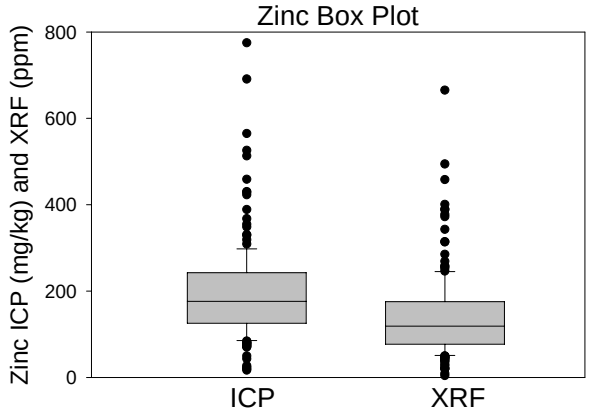
A

Copper	ICP (mg/kg)	XRF (mg/kg)
Mean	504.18	363.40
Std.Dev.	837.18	702.05
Std.Err.	62.57	52.47
95% Conf.	123.48	103.55
99% Conf.	162.94	136.64
Size	179	179
Min	9.59	-67.58
Max	7087.50	6124.27
Paired T-Test XRF vs ICP	T value	-9.64
	P value	0.00
	Deg. Freedom	178



B

Lead	ICP (mg/kg)	XRF (mg/kg)
Mean	75.56	111.40
Std.Dev.	29.96	28.89
Std.Err.	2.24	2.16
95% Conf.	4.42	4.26
99% Conf.	5.83	5.62
Size	179	179
Min	11.97	32.87
Max	152.50	194.70
Paired T-Test XRF vs ICP	T value	20.02
	P value	0.00
	Deg. Freedom	178



C

Zinc	ICP (mg/kg)	XRF (mg/kg)
Mean	196.08	137.90
Std.Dev.	109.59	94.42
Std.Err.	8.19	7.06
95% Conf.	16.16	13.93
99% Conf.	21.33	18.38
Size	179	179
Min	16.80	3.96
Max	774.70	665.02
Paired T-Test XRF vs ICP	T value	-18.76
	P value	0.00
	Deg. Freedom	178

[a]Boxes indicate 25th and 75th percentile with median line, and whiskers indicate 90th and 10th percentiles.

the difference between the ICP measurements and the certified values for the 11 NIST 2710 soil standards. The plot shows the clustering of the copper measurements, with one set of data trending higher than the certified value, and the other less than the certified value. The ICP data for the duplicate soil samples are summarized in table 11. The percent difference between the 11 duplicate samples was acceptable though there were 4 measurements above 20% difference. Four of the values were for cadmium, which had low concentrations less than 4 mg/kg, and the other two were lead and copper values.

Regression Analysis

We conducted simple linear regression analysis of XRF and ICP measurements for 179 soil samples collected from the wetland. We also evaluated the residuals of the predicted ICP values. Figure 28 shows regression and residual plots for the copper, lead, and zinc XRF and ICP data. The error bars in figures 28a,c,e are for the XRF data only. The XRF error bars show that while many of the data points do intersect the 1:1 line, there are obvious trends for all three metals. Regression plots (Figure 28a,c,e) show the regression lines and correlation coefficients for the XRF and ICP results, and the equation used to predict the ICP values. These plots also include a 1:1 line where the data would all fall if XRF and ICP measured exactly the same value for each sample. The regression lines show that as the concentration increases, the values deviated more from the 1:1 line for all 3 metals. Copper had the highest range of concentrations and an r^2 of 0.97. Zinc had a much lower range of values, with an r^2 of 0.86. Lead, which had the smallest range of concentrations, also had the lowest r^2 value of 0.45.

Table 10. ICP recovery results for soil standard NIST SRM 2710[a].

Sample ID	NIST 2710	SC-102		SC-103		SC-104		SC-105		SC-106	
	[b]		[c]		[c]		[c]		[c]		[c]
Cadmium	20	21.6	108	21.6	108	22.1	111	21.4	107	22.5	113
Chromium	19	20.0	105	19	100	20.0	105	19	100	20	105
Copper	2700	2781	103	2772	103	2826	105	2790	103	2759	102
Iron	2.7	2.68	99	2.63	97	2.67	99	2.72	101	2.7	100
Lead	5100	5416	106	5393	106	5499	108	5500	108	5522	108
Manganese	7700	7998	104	7904	103	8099	105	7934	103	7922	103
Nickel	10.1	32	297	31	307	33	327	33	327	35	347
Zinc	5900	6012	102	5996	102	6086	103	6133	104	6185	105

Sample ID	NIST 2710	SC-1001		SC-1002		SC-1003		SC-1004		SC-1005	
	[b]		[c]		[c]		[c]		[c]		[c]
Arsenic	590	510	86	516	86	505	86	517	88	511	87
Cadmium	20	18	91	18	91	18	91	19	95	18	92
Chromium	19	15	80	15	81	15	79	16	82	15	76
Copper	2700	2450	91	2447	91	2417	90	2446	91	2404	89
Iron	2.7	2.68	99	2.71	100	2.65	98	2.7	100	2.7	100
Lead	5100	5546	109	5658	111	5632	110	5790	114	5716	112
Manganese	7700	7877	102	8040	104	7847	102	8031	104	8005	104
Zinc	5900	6108	104	6221	105	6099	103	6231	106	6222	105

Sample ID	NIST 2710	SC-1014	
	[b]		[c]
Arsenic	590	504	85
Cadmium	20	19	93
Chromium	19	15	79
Copper	2700	2368	88
Iron	2.7	2.62	97
Lead	5100	5743	113
Manganese	7700	7713	100
Zinc	5900	5927	100

[a]All the metals are measured in mg/kg, except iron which is measured in %.
[b]Certified Leachable Concentrations (median value) using U.S. EPA Method 3050 values for
NIST SRM 2710 Montana soil standard.
[c] Percent recovery = (ICP Value/True Value) x 100

The residual plots (Figure 28b,d,f) show the difference between the predicted ICP value (calculated from the regression equation) and the measured ICP value. The plots indicate that the data is scattered around zero on the y-axis, and that there were few

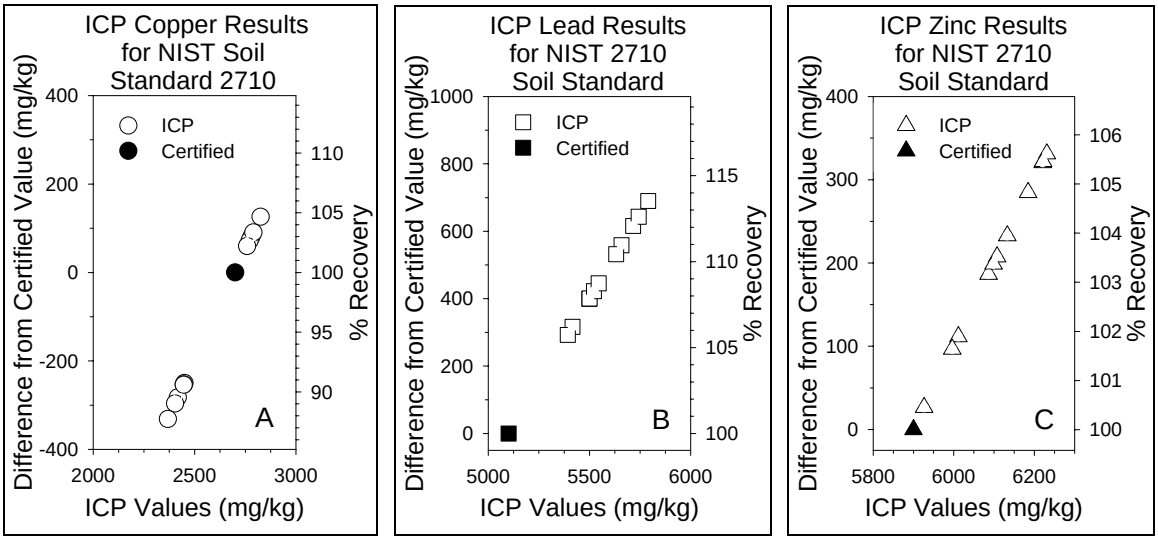


Figure 27. (a)-(c) ICP results from the analysis of NIST 2710 soil standards. Note that each plot has a different scale for the x and y axis. Eleven soil standards were included with the wetland soils samples to evaluate the accuracy of the MSU lab analysis. The results show the variability of the ICP analysis, even though the percent recovery was within the 80-120% range considered acceptable for environmental soil analysis (U.S. EPA, 2006).

outliers. The influence of any outliers is limited because of the large sample size (n= 179). The normalized residual histograms (Figure 29) show that the predicted residuals have acceptable normality, and that the assumptions supporting the use of linear regression are not violated.

Spatial Maps

A total of 96 soil samples were collected in 2003 to characterize the metal concentrations in the upper 20 centimeters of wetland soil across the wetland, and were analyzed with both XRF and ICP methods. The metal concentrations were plotted using Surfer software (Golden Software Inc., 2002) to produce maps showing the spatial distribution of metals. Figure 30 shows topographic maps with copper, lead, and zinc

Table 11. ICP % difference analysis for duplicate soil samples[a].

Sample ID	SC-97/SC-20			SC-98/SC-40			SC-99/SC-60			SC-100/SC-80			SC-97/SC-20		
			[b]			[b]			[b]			[b]			[b]
Cadmium	1.1	1.7	43	1.2	1.3	8	1.2	.8	40	2.7	2.5	8	1.7	1.3	27
Chromium	35	35	0	57	59	3	49	47	4	26	25	4	44	43	2
Copper	186	184	1	19	24	23	405	407	1	1223	1244	2	583	601	3
Iron	3.1	3.13	1	2.4	2.48	3	3.44	3.42	1	4.4	4.42	1	5.14	5.32	3
Lead	78	82	5	24	36	40	90	87	3	112	115	3	148	136	8
Manganese	857	891	4	650	703	8	267	261	2	1209	1170	3	481	480	1
Nickel	32	35	9	52	56	7	47	47	0	41	39	5	47	47	0
Zinc	166	168	1	93	109	16	214	210	2	280	262	7	306	309	1

Sample ID	SC-996/ SC-975			SC-997/ SC-545			SC-998/ SC-538			SC-999/ SC-121			SC-1000/ SC-995		
			[b]			[b]			[b]			[b]			[b]
Arsenic	28	27	2	21	21	-1	8	6	20	8	8	0	10	10	-4
Cadmium	4	3	24	1	1	-6	<1	<1	0	<1	<1	0	1	1	20
Chromium	22	22	2	33	35	-4	26	29	-8	42	41	4	26	26	0
Copper	1968	1957	1	639	665	-4	157	147	7	26	25	4	454	449	1
Iron	14.4	14.3	1	4.2	4.4	-4	2.6	2.6	0	2.7	2.8	-4	7.6	7.6	0
Lead	88	87	1	107	110	-3	53	46	13	29	29	1	371	402	-8
Manganese	571	559	2	193	194	-1	824	719	14	536	538	0	601	610	-1
Zinc	429	423	1	367	367	0	118	104	13	84	80	5	180	187	-4

Sample ID	SC-1013/SC-1010		
			[b]
Arsenic	8	9	-4
Cadmium	1	1	8
Chromium	44	45	-3
Copper	316	320	-1
Iron	2.6	2.6	0
Lead	60	61	-1
Manganese	120	120	0
Zinc	202	206	-2

[a] All the metals are measured in mg/kg, except iron which is measured in %.

[b] Percent Difference = $\frac{\text{(ICP Value 1 - ICP Value 2)}}{\text{(Average ICP Value 1 \& ICP Value2)}} * 100$

concentrations for the XRF and ICP data. The values are proportional to the size of the circle. Figure 30a-c shows the XRF data, and figure 30d-f show the ICP data. Both plots showed the highest metal concentrations were in the active floodplain and the lower (north) parts of the wetland. The plots also showed that the XRF values were less those of

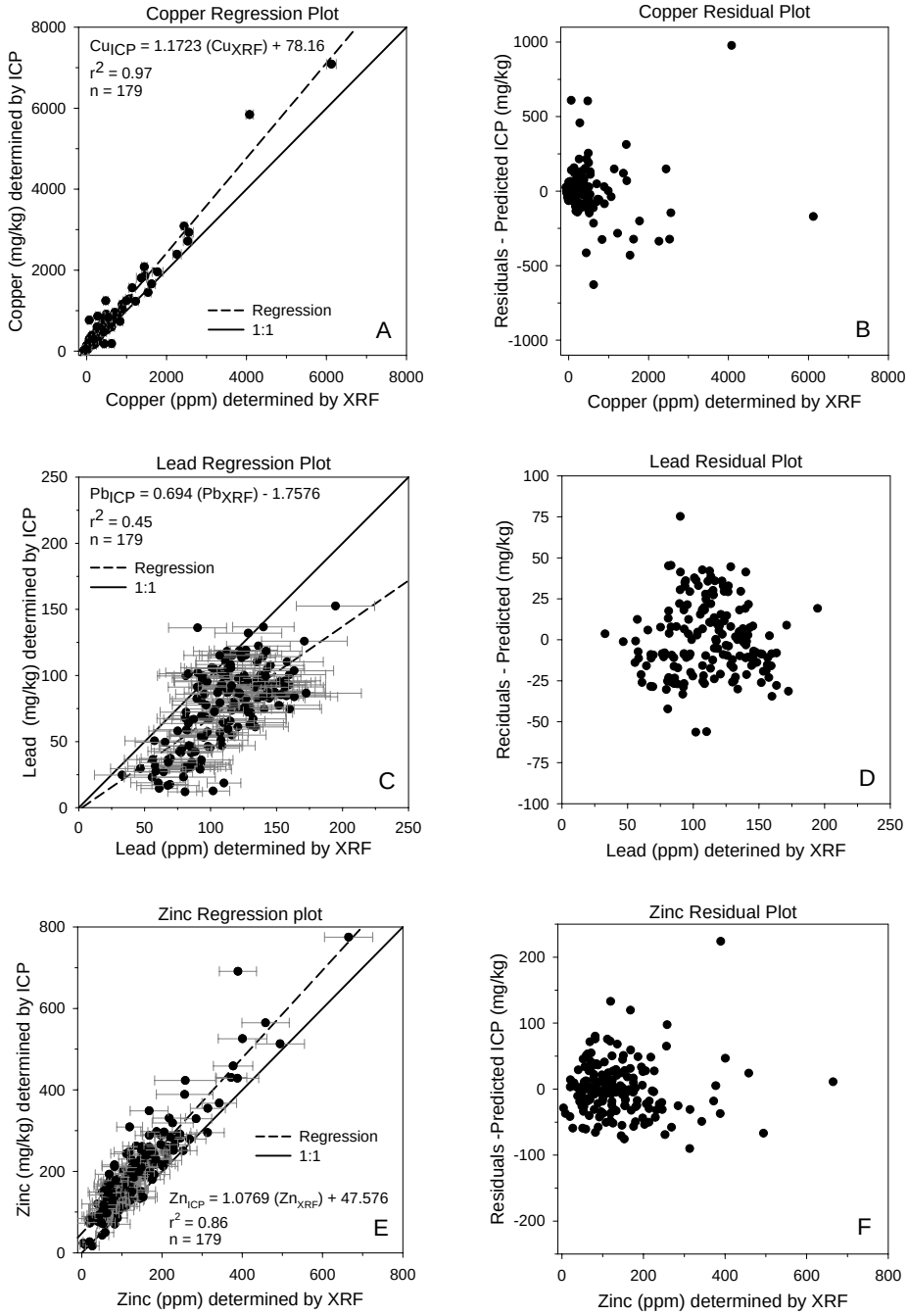


Figure 28. Regression and residual plots of ICP versus XRF for copper, lead, and zinc. (a),(c),(e) The XRF versus ICP values, XRF error associated with each data point, regression line and 1:1 line, plus the correction equation and r^2. The plots show that the XRF underpredicts copper and zinc values and overpredicts lead values at levels we measured in the wetland. (b),(d),(f) Residuals of the predicted ICP values versus the XRF values.

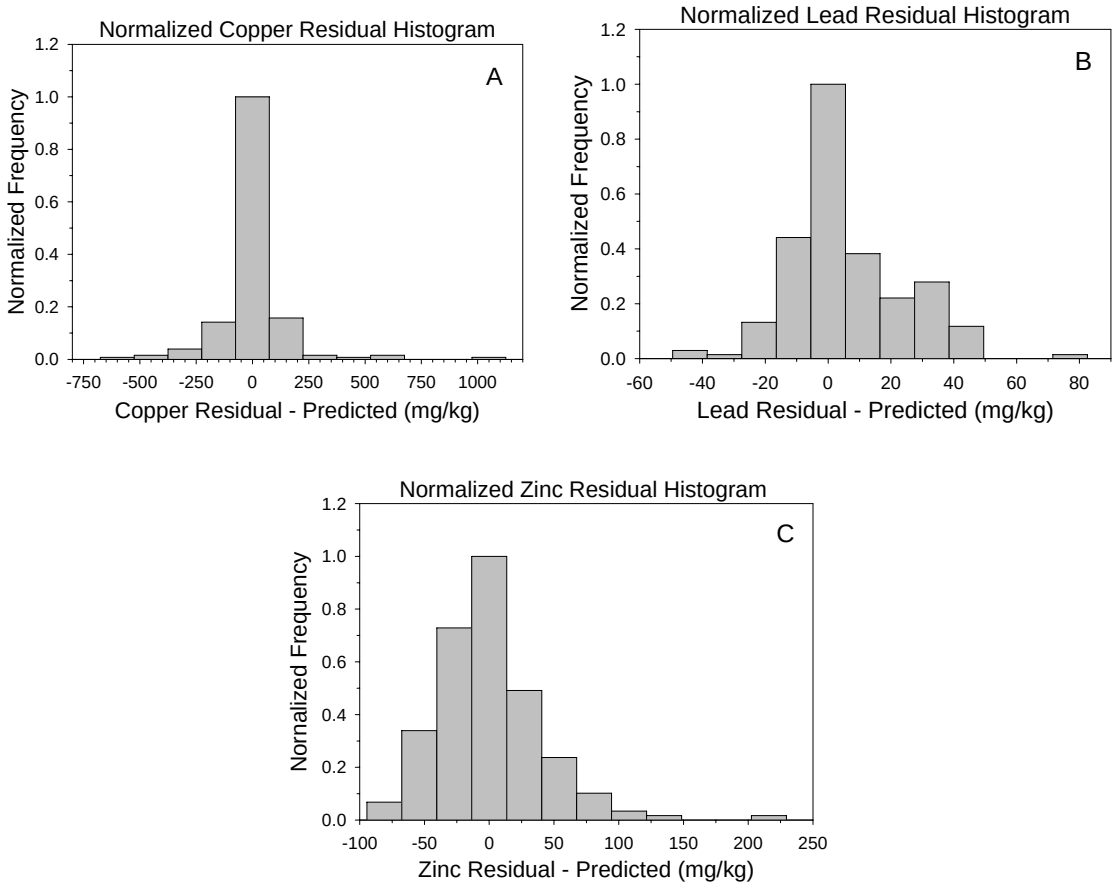


Figure 29. (a)-(c) Histograms of predicted residuals of copper, lead, and zinc for normality evaluation. The residuals for each metal represent the difference between the predicted regression value (based on the XRF:ICP linear regression equation) and the actual ICP value. None of the plots suggest normality inconsistencies. Several outliers exist at higher concentrations for all three metals, but due to an N=179, this is not problematic.

the ICP values, but that the overall spatial distribution is nearly identical.

Discussion

The XRF instrument provided timely and useful data on total metal concentrations during my research. The ICP results were available for only 18% of my soil samples, and most of the samples were still in the lab when I needed to make

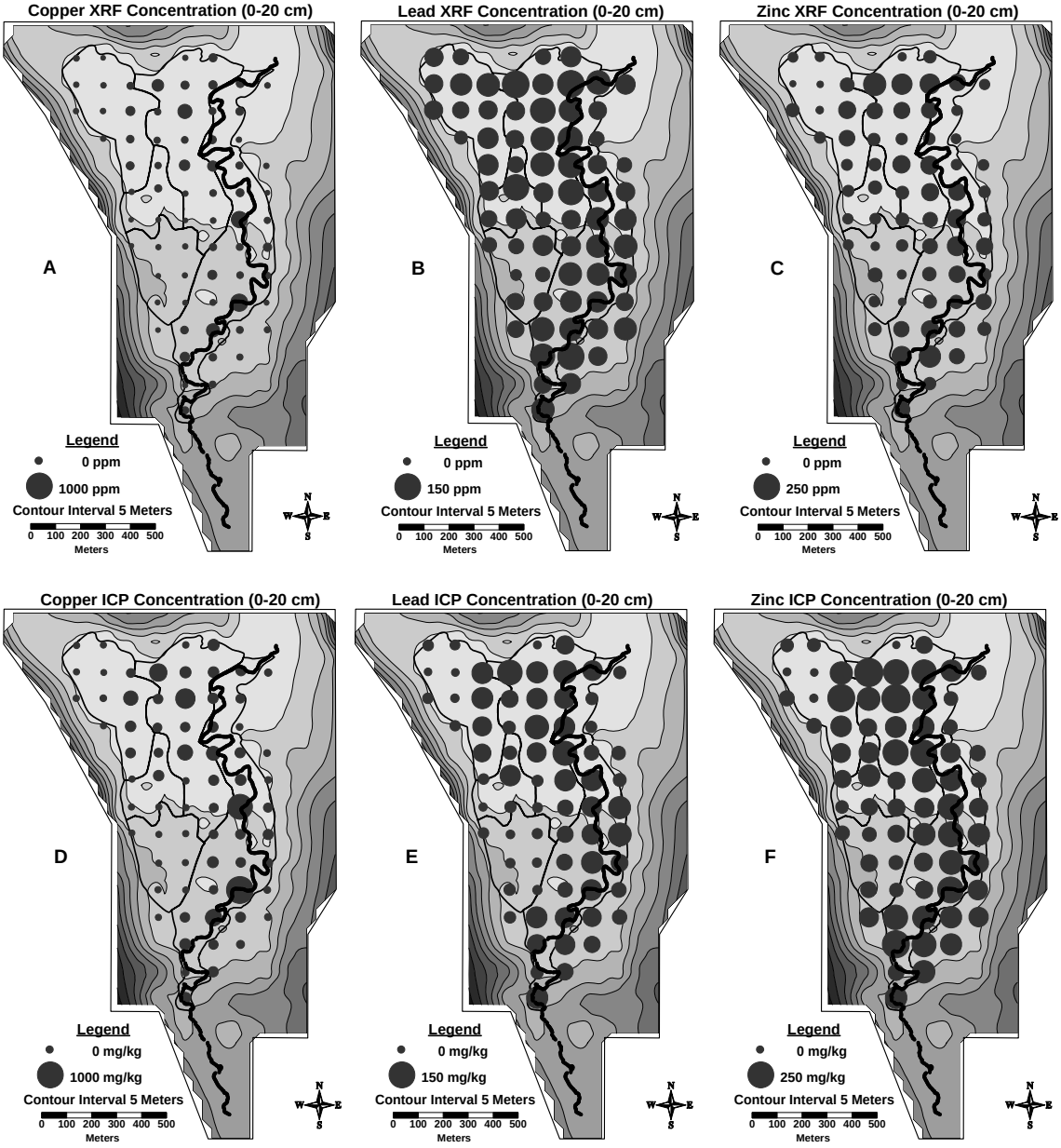


Figure 30. Spatial map of XRF and ICP copper concentrations for top 20 centimeter of soil. The values are proportional to the size of the circle. Plots (a)-(c) show the XRF data and plots (d)-(f) show the ICP data. Both sets of plots shows the highest metal concentrations are in the active floodplain and the lower parts of the wetland (north). The plots also show that the XRF values are less than those of the ICP values, but that the overall spatial pattern is comparable.

sampling decisions. Once I received the ICP data, there were no surprises and the XRF proved to be a good predictor of metal concentrations. All of the XRF trends were well correlated with the ICP results.

The XRF error is calculated by the instrument using an algorithm that averages the natural variation in the emissions. The longer the analysis time, the more data that is gathered by the instrument and used to calculate the average concentration. The XRF analysis time was an important factor in reducing the instrument error, which increased my confidence in the data. The duration test showed that at even an analysis time of 1800 seconds, the instrument would not produce results equal to the certified values for copper or lead. I concluded that the amount of error for the 300 second measurement duration was acceptable for my investigations.

1) How can XRF data error be quantified, predicted, and incorporated into soil metal analysis and assessment?

The duration test showed a reduction in error for all metals when the time of instrument analysis increased (Figure 26a,b). The soil standard was first analyzed 10 times for 60 seconds, which showed a range of measurements around an average value (Figure 26c,d,e). The test showed the largest decrease in error when we increased the analysis time from 60 to 180 seconds, with a decreasing amount of additional error reduction with each successive time step. The XRF data points approach an average value as the length of instrument analysis time increased up to 1800 seconds. Figures 26c-e shows that the measured XRF concentration never equaled the ICP value or the NIST 2710 soil standard certified value for copper or lead, but that the zinc XRF measurements

do come close to equaling the certified value as the duration time increased. We chose an analysis time of 300 seconds based on the reduction in XRF error and sample analysis efficiency.

There was measurable error associated with the ICP data based on the 11 quality control samples (NIST 2710 soil standard) that were included with the soil samples sent to the lab. There was a difference between the certified value and the ICP value, though the difference was within acceptable quality control standards (Table 10 and Figure 11). A criterion of acceptability of 80 to 120% recovery (or relative percent difference $\leq$ 20%) was used in this analysis (U.S. EPA, 2006). The soil samples from the wetland were sent to the soil lab in two groups. The ICP results for copper were interesting in that the results for the first set of soil samples ICP values were higher than the certified value, but lower for the second set of soil sample ICP values (Figure 27). The ICP values were higher than the certified value for lead and zinc for both groups of soil samples. The results of this analysis show that there is variability in the ICP analysis, even though the percent recovery was within acceptable guidelines.

Results for the simple linear regression analysis comparing the ICP:XRF data showed the strongest linear relationship for copper, followed by zinc and then lead (Figure 28). The XRF under-predicted the copper and zinc values, but over-predicted the lead values (at least in the range measured in the Stillwater wetland soils). The results for lead are interesting in that the regression analysis showed that the XRF over-predicted lead values, while the duration test on the NIST 2710 soil standard indicated that the XRF under-predicted lead values. The important difference is the lead concentration in the soil

standard, which was an order of magnitude higher (5500 mg/kg) compared to the wetland soils which averaged 75 mg/kg.

The ICP:XRF data was used to calculate calibration equations for correcting the XRF data (Figure 28a,c,e). These simple linear regression equations provided a statistical approximation for predicting the ICP value of the XRF measurement based on the XRF:ICP regression. An evaluation of the residuals between the predicted ICP values and the measured ICP values indicated that the assumptions of normality were valid and supported the use of linear regression. An important factor was the range of the metal concentration that was used in developing the calibration equations. Extrapolating the correction beyond the range of data used to develop the equations would have increased the error associated with the predicted ICP values. The copper and zinc regression plots (Figure 28a,e) have limited points at the highest concentrations, whereas the lead regression plot (Figure 28c) shows that the bulk of the lead concentrations range from 50 to 150 mg/kg. Both of these factors likely lead to increased error at high metal concentrations. These results illustrate the importance of building calibration curves with soil samples that have the expected range of metal concentration that will be analyzed.

The differences between lead levels in the wetland (Table 11) able and those in the NIST 2710 soil standard (Table 10) showed the potential for error if the correction equations were used on concentrations beyond the range of those used in the regression analysis. More ICP data over a wide range of metal concentrations would be required to address this problem. These regression equations reflect the metal concentrations and ratios present in the Stillwater wetland, and may not be valid for other locations/regions.

This would require soil sampling and metal analysis using XRF and ICP to calibrate the XRF corrections for each environmental setting.

2) Can the XRF data be useful in mapping and metal quantification efforts?

We analyzed two sets of soil samples with the XRF. This data allowed me to make timely sampling decisions not possible with the ICP analysis. Furthermore, XRF was economically efficient as resources for 1000 ICP sample analyses were not available. The XRF data was used to develop maps showing the areas of elevated metal concentrations that required more extensive soil sampling. The first set of ICP results was used for simple linear regression analysis to evaluate the error of the XRF data. These results then provided confidence levels for further mapping and sampling decisions.

The XRF data was also used to plot cross-sections of the transects conducted utilizing deeper soil sampling. These cross-sections showed that the soil layers with higher metal concentrations extended laterally over the wetland. These cross-sections were used to select soil profiles for ^{210}Pb age dating which helped us address the timing of metal deposition in the wetland. These samples selected for age dating were also analyzed with ICP, and the ICP results were added to dataset used for XRF:ICP linear regression analysis.

Figure 30 show spatial maps of shallow (0-20 cm) metal concentrations created using XRF and ICP data. The overall pattern is the same, though differences in the magnitude of metal concentrations are evident. These plots match the linear regression results showing that the XRF overpredicts lead and underpredicts copper and zinc. These

maps validate the relative effectiveness of the XRF for assessing spatial patterns of metal concentrations and concentration magnitudes.

Conclusion

The XRF instrument proved to be extremely useful in my research. I was able to analyze nearly 1000 soil samples in a timely matter, and to make sampling decisions based on near real-time XRF data. The ICP results provided a measure of the instrument analysis quality, and allowed calculation of correction equations for the XRF data. I also demonstrated the usefulness of the XRF for measuring total metal concentrations in a laboratory setting, and that the data was reliable for spatial mapping of metal concentrations.

The amount of error associated with the XRF instrument was acceptable for my research, because we were more concerned with the magnitude of metal concentrations rather than the exact values. The ICP data provided an independent dataset to evaluate the accuracy of the XRF instrument, and the regression analysis provided equations for correction of XRF values to more closely approximate true metal concentration. This type of combined analysis approach can provide an extensive dataset at a relatively low cost. The ICP data showed that the pattern and magnitude of the XRF values were acceptable for the objectives of my research.

SUMMARY

My research investigated the impact of acid rock drainage on an alpine riparian wetland using multiple techniques in combination. I mapped the spatial pattern of metal concentrations across the wetland and distinguished pre-mining metal levels from post-mining levels in the wetland soils at 16 locations. Topographic surveying was used to map the extent of the wetland that would likely be inundated with water at different flood stages. Monitoring wells and nested piezometers provided a basic understanding of groundwater flow and water chemistry in the wetland.

XRF metal concentration measurements allowed a larger number of soil samples (992) than would have been possible using ICP analysis. I measured metal concentrations of 179 of 992 soil samples with ICP to evaluate the quality of the XRF data. This comparison provided an estimate of the XRF instrument error, valid for the range of concentrations and soil composition at my research site, and allowed calculation of correction equations for the XRF data. For the wetland soils, the XRF under-estimated copper and zinc concentrations, but over-estimated lead concentrations (compared to ICP analysis). My research indicated the importance of performing the calibration procedure by measuring a set of soil samples with both XRF and ICP methods, since the amount of XRF measurement error may be different at other locations.

Spatial distribution maps of metal concentrations (copper, lead, and zinc) showed that on the active floodplain, the higher metal concentrations in the soil profile were near the surface, whereas the soils in the wetland marsh had increasing metal concentrations with depth. The ^{14}C and ^{210}Pb age-dating techniques provided soil age estimates that were

used to determine whether these metals were deposited before or after the onset of mining at the McLaren ore deposit. The ^{14}C soil dates were collected from a peat layer that was beneath marsh soils with metal concentrations increasing with depth. These soil ages were on the order of thousands of years old, indicating that the wetland has been receiving metals from natural acid rock drainage processes since the end of the last ice age.

The ^{210}Pb age estimates were selected from eleven soil profiles to compare the contrasting metal profiles found in the floodplain and marsh soils. The estimated soil ages provided a more refined age/metal profile of the last 100 years for these sample locations. The maximum range of applicability of the ^{210}Pb age dating technique is 100 to 150 years, which matched the time period of interest. Mining began in 1933 (73 years ago) at the McLaren ore deposit, which is the main source of acid rock drainage in the Daisy Creek/Stillwater River watershed. The ^{210}Pb age dates provided evidence that metal deposition on the active floodplain was younger than the onset of mining in the watershed, whereas the metals found in the deeper marsh soils were older than the earliest mining activity.

The piezometers and monitoring wells provided data on the direction of groundwater flow and basic groundwater chemistry. The hydraulic gradients from the piezometers suggested that the groundwater moves downward at the upper end of the wetland and moves upward at the lower end during the early part of the summer, but changes to a more horizontal flow as the summer progresses. This may be due to reduced recharge from snowmelt in the later part of the summer, though more research is needed

to fully understand the groundwater hydrology of the wetland. The limited water chemistry data supports this model, suggesting oxidizing conditions in the upper end of the wetland, and reducing conditions in the lower end.

The topographic survey provided a more detailed model of the wetland landscape and indicated those areas of the wetland that would be likely inundated under a few flood stage scenarios. The areas most susceptible to flooding were also the locations where we found higher metal concentrations (copper and zinc) outside of the active floodplain. This suggests that flooding is the main mechanism for transporting metals (both sediment bound and dissolved) to those areas beyond the active floodplain. Channel migration is also a likely mechanism for depositing metals throughout the wetland.

The ^{210}Pb and ^{14}C age dating techniques in addition to the XRF instrument provided an innovative approach to evaluating the environmental impact of acid rock drainage on a riparian wetland. The results showed that acid rock drainage has been impacting the wetland for thousands of years. My results also indicate metal-rich sediment deposition starting after the onset of mining in the watershed. We suggest areas for further study that include more detailed soil sampling and groundwater measurements. The mapping results indicated those areas with the highest copper, lead, and zinc concentrations, but more intensive sampling (spatially and with depth) may be required if the U.S. Forest Service is interested in removal of the soils with the highest metal concentrations.

REFERENCES CITED

Amacher, M.C., R.W. Brown, R.C. Sidle, J. Kotuby-Amacher, 1995. Effect of Mine Waste on Element Speciation in Headwater Streams, in Allen, H.E., Huang, C.P., Bailey, G.W., and Bowers, A.R., Metal Speciation and Contamination of Soil: Boca Raton, Lewis Publishers, p. 275-309.

Appleby, P.G., F. Oldfield, 1978. The Calculation of ^{210}Pb Dates Assuming a Constant Rate of Supply of Unsupported ^{210}Pb to the Sediment. Cantena 5:1-8.

Appleby, P.G., Oldfield, F., 1983. Assessment of ^{210}Pb From Sites with Varying Sediment Accumulation Rates, Hydrobiologia 103:29-35.

August, E.E., D.M. McKnight, D.C. Hrncir, K.S. Garhart, 2002. Seasonal Variability of Metals Through a Wetland Impacted by Mine Drainage in the Rocky Mountains, Environmental Science & Technology 36:3779-3786.

Bernick, M.B., D. Getty, G. Prince, M. Sprenger, 1995. Statistical Evaluation of Field-portable X-ray fluorescence Soil Preparation Methods, Journal of Hazardous Materials, 43:111-116.

Boughton, G.K., 1999. Metal Loading in Soda Butte Creek Upstream of Yellowstone National Park, Montana and Wyoming: A Retrospective Analysis of Previous Research; and Quantification of Metal Loading, August 1999. U.S. Geological Survey Water-Resources Investigations Report 01-4170, 68 p.

Bradl, H.B., 2004. Adsorption of Heavy Metal Ions on Soils and Soil Constituents, Journal of Colloid and Interface Science 277:1-18.

Brown, R.W., M.C. Amacher, W.F. Mueggler, J. Kotuby-Amacher, 2003. Reestablishing Natural Succession on Acidic Mine Spoils at High Elevation: Long-Term Ecological Restoration. USDA-FS Rocky Mountain Research Station, Research Paper RMRS-RP-41.

Burton, E.D., I.R. Phillips, D.W. Hawker, 2005. Geochemical Partitioning of Copper, Lead, and Zinc in Benthic, Estuarine Sediment Profiles, J. Environ. Qual. 34:263-273.

Church, S.E., D.L. Fey, E.M. Brouwers, C.W. Holmes, R. Blair, 1999. Determination of Pre-Mining Geochemical Conditions and Paleoecology in the Animas River Watershed, Colorado, U.S.G.S. Open-File Report 99-0038.

Courtis, D., 1965. Geology of the Cutoff Mountain Area, Park County, Montana, Masters Thesis, University of Michigan.

Cleasby, T.E., D.A. Nimick, 2002. Metal Concentrations and Sources in the Miller Creek Watershed, Park County, Montana, August 2000. U.S. Geological Survey Water-Resources Investigations Report 02-4148, 32 p.

Durst, A.D., 1999. Geologic Controls on Spring Discharge in the Miller Creek Basin, New World Mining District, Montana. Masters Thesis, Montana State University-Bozeman.

Elliot, J.E., 1979. Geologic Map of the Southwest Part of the Cooke City Quadrangle, Montana and Wyoming: U.S. Geological Survey Miscellaneous Investigations Series Map I-1084, 1 Sheet, Scale 1:24,000.

Elliot, J.E., A.R. Kirk, T.W. Johnson, 1992. Field Guide; Gold-Copper-Silver Deposits of the New World District, in Elliot, J.E., ed., Guidebook for the Red Lodge-Beartooth Mountains-Stillwater area: 17th annual Field Conference, Tobacco Root Geological Society, Red Lodge, Mont., August 20-22, 1992, pp. 1-19.

Furniss, G., J.T. Gurrieri, (In Press) An Empirical Model for Estimating Pre-mining Water Quality in Catchments with Acidic Drainage and Ferricrete.

Furniss, G., N.W. Hinman, G.A. Doyle, D.D. Runnells, 1999, Radiocarbon-dated Ferricrete Provides a Record of Natural Acid Rock Drainage and Paleoclimatic Changes. Environmental Geology 37:102-106.

Gambrell, R.P., 1994. Trace and Toxic Metals in Wetlands – A Review, J. Environ. Qual. 23:883-891.

Gammons, C.H., S.A. Wood, D.A. Nimick, 2005. Diel Behavior of Rare Earth Elements in a Mountain Stream with Acidic to Neutral pH, Geochim. Cosmochim. Acta 69:3747-3758.

Gammons, C.H., D.A. Nimick, S.R. Parker, T.E. Cleasby, R.B. McCleskey, 2005. Diel Behavior of Iron and Other Trace Metals in a Mountain Stream with Acidic to Neutral pH: Fisher Creek, Montana, USA: Geochim. Cosmochim. Acta 69:2505-2516.

Goldberg, E.D., 1963. Geochronology with ^{210}Pb in "Radioactive Dating". International Atomic Energy Agency Symposium Proceeding, Vienna 1962, p. 121-131.

Gurrieri, J.T., G. Furniss, 2003, Ferricrete Study Results, an Update, USFS public meetings, January 14 & 15, Bozeman.

Gurrieri, J.T., 1998, Distribution of Metals in Water and Sediment and Effects on Aquatic Biota in the Upper Stillwater River Basin, Montana. Journal of Geochemical Exploration 64:83-100.

Hansen P.L., R.D. Pfister, K. Boggs, B.J. Cook, J. Joy, D.K. Hinckley, 1995. Classification and Management of Montana's Riparian and Wetland Sites. Montana Forest and Conservation Experiment Station, School of Forestry, The University of Montana, May, 1995. Miscellaneous Publication no. 54.

Heyden, C.J. von der, M.G. New, 2004. Sediment Chemistry: A History of Mine Contaminant Remediation and an Assessment of Processes and Pollution Potential, Journal of Geochemical Exploration 82:35-57.

Hinman, N.W., D. Alt, G. Furniss, 2000, Getting Background Chemistry of Mineral-rich Drainages: A Study of Two Montana Mining Districts, Report No. 200, Montana University System Water Center, Bozeman.

Hren, M.T., C.P. Chamberlain, F.J. Magilligan, 2001. A Combined Flood Surface and Geochemical Analysis of Metal Fluxes in a Historically Mined Region: A Case Study from the New World Mining District, Montana. Environmental Geology 40:1334-1346.

Hydrometrics, 1994, Daisy Creek Sediment Metals Characterization. Prepared by Hydrometrics, Inc. for Crown Butte Mines, Inc.

Johnson, T.W., L. Meinert, 1994. Au-Cu-Ag Skarn and Replacement Mineralization in the McLaren Deposit. New World District, Park County Montana. Econ. Geol 89:969-993.

Kalnicky, D.J., R. Singhvi, 2001. Field Portable XRF Analysis of Environmental Samples, Journal of Hazardous Materials 83:93-122.

Kimball, B.A., D.A. Nimick, L.J. Gerner, R.L. Runkel, 1999. Quantification of Metal Loading in Fisher Creek by Tracer Injection and Synoptic Sampling, Park County, Montana. August 1997: U.S. Geological Survey Water-Resources Investigations Report 99-4119, 40 p.

Kotarba, A., E. Lokas, P. Wachniew, 2002. ^{210}Pb Dating of Young Holocene Sediments in High-Mountains Lakes of the Tatra Mountains. Geochronometria 40:73-77.

Licciardi, J.M., P.U. Clark, E.J. Brook, K.L. Pierce, M.D. Kurz, D. Elmore, P. Sharma, 2001. Cosmogenic ^{3}He and ^{10}Be Chronologies of the Late Pinedale Northern Yellowstone Ice Cap, Montana, USA. Geology: December, 2001.

Lovering, T.S., 1929. The New World or Cooke City Mining District, Park County, Montana. U.S. Geol. Survey Bull. 911-A, 1-87.

MacHardy-Mitman, K.A., 2002. The Potential for Natural Wetlands to Remediate Copper Contaminated Water. Masters Thesis, Montana Tech of the University of Montana.

Matagi, S.V., D. Swai, R. Mugabe, 1998. A Review of Heavy Metal Removal Mechanisms in Wetlands, Afr. J. Trop. Hydrobiol. Fish. 8:23-35.

Maxim Technologies, Inc., 1999. Site-Wide Sampling and Analysis Plan, Appendix B of the Overall Project Work Plan, New World Mining District Response and Restoration Action. Prepared for: USDA Forest Service Northern Region Missoula, Montana, November 1999.

Maxim Technologies, Inc., 2001. McLaren Pit Response Action Engineering Evaluation/Cost Analysis, New World Mining District Response and Restoration Action. Prepared for: USDA Forest Service Northern Region Missoula, Montana, July 2001.

Maxim Technologies, Inc., 2003. Surface Water Summary - 2003, New World Mining District Response and Restoration Project, Prepared for the USDA Forest Service Northern Region Missoula, Montana, January, 2004.

Maxim Technologies Inc., 2005. Sediment Characterization - Daisy and Fischer Creeks, New World Mining District Response and Restoration Project. Prepared for: USDA Forest Service Northern Region Missoula, Montana, March, 2005.

Maxim Technologies Inc., 2005. Stillwater Groundwater Results, New World Mining District Response and Restoration Project, Prepared for: USDA Forest Service Northern Region Missoula, Montana, August, 2005.

Maxim Technologies, Inc., 2007. Surface Water Summary – 2006 (Draft), New World Mining District Response and Restoration Project, Prepared for the USDA Forest Service Northern Region Missoula, Montana, January, 2007.

Marcus, W.A., G.A. Meyer, D.R. Nimmo, 2001. Geomorphic Control of Persistent Mine Impacts in a Yellowstone Park Stream and Implications for the Recovery of Fluvial Systems. Geology 29:355-358.

Metesh, J., A. English, J. Lonn, E. Kendy, C. Parrett, 1999. Hydrology of the Upper Soda Butte Creek Basin, Montana with Sections on Climate and Streamflow in Soda Butte Creek. Montana Bureau of Mines and Geology Report of Investigation 7.

Meyer, G.A., 2001. Recent Large-magnitude Floods and Their Impact on Valley-floor Environments of Northeastern Yellowstone. Geomorphology 40:271-290.

Meyer, G.A., J.L. Pierce, 2003. Climatic Controls on Fire-induced Sediment Pulses in Yellowstone National Park and Central Idaho: a Long-term Perspective. Fire Ecology and Management 178:89-104.

Meyer, G.A., S.G. Wells, A.J. Jull, 1995. Fire and Alluvial Chronology in Yellowstone National Park: Climatic and Intrinsic Controls on Holocene Geomorphic Processes. GSA Bulletin, v. 107, no. 10, p. 1211-1230.

Nimick, D.A., T.E. Cleasby, 2001. Quantification of Metal Loads by Tracer Injection and Synoptic Sampling in Daisy Creek and the Stillwater River, Park County, Montana: U.S. Geological Survey Water-Resources Investigations Report 00-4262, 51 p.

Oldfield, F., P.G. Appleby, 1984. Empirical Testing of ^{210}Pb Models for Lake Sediments. In: E.Y. Haworth & J.W.G. Lund (eds.), Lake Sediments in Environmental History: Studies in Palaeolimnology and Palaeoecology in Honour of Winifred Tutin. University of Minnesota Press, Minneapolis, pp 93-124.

Pierce, K. L., 1979. History and Dynamics of Glaciation in the Northern Yellowstone National Park Area; U.S. Geological Survey Professional Paper 729-F, 90 p.

Poage, M., D.J. Sjostrom, J. Goldberg, C.P. Chamberlain, G. Furniss, 2000. Isotopic Evidence for Holocene Climate Change in Northern Rockies for Goethite-rich Ferricrete Chronosequence, Chemical Geology 166:327-340.

Ranville, M., D. Rough, A.R. Flegal, 2004. Metal Attenuation at the Abandoned Spenceville Copper Mine, Applied Geochemistry 19:803-815.

Ritchie, J.C., J.R. McHenry, 1990. Application of Radioactive Fallout Cesium-137 for Measuring Soil Erosion and Sediment Accumulation Rates and Patterns: A Review, Journal of Environmental Quality 19:215-233.

Robbins, J.A., 1978. Geochemical and Geophysical Applications of Radioactive Lead. In: Nriagu, J.O. (Eds.). Biogeochemistry of Lead in the Environment. Elsevier Scientific, Amsterdam: p 285-393.

Robbins, J.A., and Edgington, D.N., 1975. Determination of Recent Sedimentation Rates in Lake Michigan Using ^{210}Pb and ^{137}Cs. Geochim. Cosmochim. Acta. 39:285-304.

Robbins, J.A., J.R. Krezoski, S.C. Mozley, 1977. Radioactivity in Sediments in the Great Lakes: Post-depositional Redistribution by Deposit-feeding Organisms. Earth planet. Sci. Lett. 36:325-333.

Runnels, D.D., T.A. Shepherd, E.E. Angino, 1992. Metals in Water Determining Natural Background Concentrations in Mineralized Areas, Environ. Sci. Technol. 26:2316-2323.

Shacklette, H.T., J.C. Hamilton, J.G. Boerugen, J.M. Bowles, 1971. Elemental Composition of Surficial Materials in the Conterminous United States. USGS Professional Paper 574-D.

Shukla, B.S., 2002. Sedimentation Rate Through Environmental Radioactivity (Models and Applications). Environmental Research & Publications Inc., Ontario, Canada.

Sonderegger, J.L., J.J., Jr., Wallace, G.L., Jr., Higgins, 1975. Acid Mine Drainage Control - Feasibility Study, Cooke City, Montana. Montana Bureau of Mines and Geology Open File Report 23, 197 p.

Stumm, W., J.P. Morgan, 1996. Aquatic Chemistry, 3rd ed., Wiley-Interscience, New York.

U.S. Department of Agriculture, National Resources Conservation Service, Soil Survey Laboratory Methods Manual, Soil Survey Investigations Report No. 42, National Soil Survey Center, Version 30, January, 1996.

U.S. EPA Environmental Technology Verification Report, Superfund Innovation Technology Evaluation Program Final Demonstration Plan for the Evaluation of Field Portable X-Ray Fluorescence Technologies, March, 1995.

U.S. EPA Environmental Technology Verification Report, XRF Technologies for Measuring Trace Elements in Soil and Sediment, Niton XLi 700 Series XRF analyzer, EPA/540/R-06/004, February, 2006.

U.S. EPA Method 3050B, 1996. Acid Digestion of Sediments, Sludges, and Soils. www.epa.gov/SW-846/pdfs/3050b.pdf.

Webster, J.G., P.J. Swedlund, K.S. Webster, 1998. Trace Metal Adsorption onto an Acid Mine Drainage Iron (III) Oxyhydroxyl Sulfate: Environmental Science and Technology, 32:1361-1368.

Weis, J.S., P. Weis, 2004. Metal Uptake, Transport and Release by Wetland Plants: Implications for Phytoremediation and Restoration, Environment International 30:685-700.

Wildeman, T., G. Brodie, J. Gusek, 1993. Wetland Design for Mining Operations, BiTech Publishers Ltd, Richmond, B.C., Canada.

Whitlock, C., P.J. Bartlein, 1993. Spatial Variations of Holocene Climatic Change in the Yellowstone Region, Quaternary Research 39:231-238.

APPENDICES

APPENDIX A

METALS DATA

Survey Data for Soil Sample Locations

Table 12. Survey data for soil sample locations (NAD27 UTM Zone 12N).

Sample #	**X-Coordinate (UTM)**	**Y-Coordinate (UTM)**	**Elevation (M)**
T2-3	578636.444	4992432.266	2576.182
T2-4	578735.456	4992433.799	2576.276
T2-7	579039.853	4992434.114	2575.709
T2-8	579142.488	4992434.086	2575.222
T3-3	578635.904	4992335.113	2576.234
T3-4	578736.835	4992332.915	2575.767
T3-5	578836.707	4992330.882	2575.499
T3-6	578938.255	4992332.759	2575.405
T3-7	579038.925	4992333.592	2575.289
T3-8	579142.297	4992334.386	2575.054
T3-9	579243.919	4992339.780	N.A.
T3-10	579344.400	4992332.553	2575.831
T4-3	578635.097	4992238.055	2577.904
T4-4	578735.136	4992238.388	2575.984
T4-5	578836.496	4992238.674	2575.569
T4-6	578937.734	4992235.519	2575.432
T4-7	579038.436	4992236.968	2575.545
T4-8	579140.544	4992238.068	2575.240
T4-9	579241.561	4992236.830	2575.856
T5-4	578735.983	4992137.168	2577.928
T5-5	578835.968	4992135.089	2575.938
T5-6	578935.394	4992130.757	2575.819
T5-7	579037.804	4992132.349	2575.709
T5-8	579140.038	4992132.910	2576.011
T5-9	579238.611	4992132.975	2577.410
T6-5	578835.666	4992037.284	2576.468
T6-6	578939.048	4992038.186	2575.975
T6-7	579037.184	4992039.108	2576.167
T6-8	579141.684	4992036.053	2576.426
T6-9	579240.456	4992038.197	2576.435
T6-10	579340.233	4992036.855	2580.065
T7-5	578841.042	4991941.471	N.A.
T7-6	578939.649	4991954.021	2578.866
T7-7	579040.378	4991935.044	2578.740
T7-8	579143.086	4991936.990	2578.656
T7-9	579242.741	4991938.178	2579.118
T7-10	579344.256	4991938.124	2579.586

Table 12. Survey data for soil sample locations (continued).

Sample #	X-Coordinate (UTM)	Y-Coordinate (UTM)	Elevation (M)
T8-7	579040.429	4991836.413	2579.939
T8-8	579143.300	4991835.836	2579.460
T8-10	579343.774	4991836.546	2579.417
T9-5	578840.685	4991743.159	N.A.
T9-6	578940.329	4991738.150	2582.987
T9-7	579039.657	4991741.004	2581.286
T9-8	579142.629	4991738.397	2580.582
T9-9	579241.531	4991738.652	2580.080
T9-10	579344.552	4991737.750	2580.093
T10-6	578939.749	4991632.663	2585.171
T10-7	579038.389	4991634.456	2582.676
T10-8	579140.021	4991636.263	2581.009
T10-9	579242.967	4991635.266	2580.843
T10-10	579343.721	4991633.464	2580.655
T11-6	578937.297	4991535.056	2583.037
T11-7	579039.916	4991533.811	2580.650
T11-8	579142.397	4991534.886	2579.650
T11-9	579239.751	4991533.902	2579.364
T11-10	579341.007	4991534.019	2580.132
T12-6	578938.757	4991433.485	2582.866
T12-7	579036.846	4991433.569	2580.961
T12-8	579142.674	4991432.369	2580.397
T12-9	579242.111	4991433.857	2580.147
T12-10	579343.779	4991434.619	2581.510
T13-7	579038.181	4991334.677	2581.851
T13-8	579142.143	4991333.375	2581.909
T13-9	579242.114	4991334.074	2581.757
T14-7	579039.129	4991230.944	2583.515
T14-8	579141.372	4991233.634	2583.159
T15-7	579039.115	4991138.420	2584.707
T11-9	579239.933	4991534.071	2581.460
T11-E1	579239.825	4991533.115	2581.560
T11-E2	579239.556	4991532.188	2581.510
T11-E4	579239.128	4991530.154	2581.610
T8-5	578839.236	4991838.808	2581.334

Table 12. Survey data for soil sample locations (continued).

Sample #	**X-Coordinate (UTM)**	**Y-Coordinate (UTM)**	**Elevation (M)**
T8-6	578940.373	4991839.077	2580.066
T11-E22	579236.125	4991512.636	2581.400
T11-E29	579234.979	4991505.684	2581.250
T11-E37	579234.275	4991498.053	2581.230
T11-E46	579232.649	4991488.975	2581.970
T11-W0	579241.300	4991542.789	2581.560
T11-W1	579241.325	4991543.567	2581.570
T11-W2	579241.616	4991544.423	2581.590
T11-W4	579241.769	4991546.465	2581.630
T11-W7	579241.945	4991549.769	2581.640
T11-W11	579242.411	4991553.596	2581.490
T11-W16	579242.606	4991558.203	2581.300
T11-W22	579243.508	4991564.451	2582.770
T11-W29	579243.567	4991571.555	2581.520
T11-W37	579243.493	4991579.387	2580.920
T11-W46	579243.720	4991588.317	2581.080
T8-E0	579253.940	4991834.289	2579.540
T8-E1	579254.493	4991833.488	2579.570
T8-E2	579257.252	4991832.321	2579.450
T8-E4	579259.878	4991830.799	2581.650
T8-E7	579263.694	4991829.111	2581.430
T8-E11	579268.453	4991827.659	2579.560
T8-E16	579273.914	4991825.409	2579.720
T8-E22	579280.078	4991822.237	2579.640
T8-E29	579287.499	4991819.137	2579.600
T8-E37	579295.876	4991815.626	2579.840
T8-E46	N.A.	N.A.	N.A.
T8-9	579240.907	4991840.118	2579.570
T8-W1	579240.278	4991840.981	2579.540
T8-W2	579239.645	4991841.213	2579.520
T8-W4	579237.177	4991841.682	2579.700
T8-W7	579234.512	4991842.835	2579.630
T8-W11	579230.728	4991844.057	2579.540
T11-E7	579238.620	4991527.295	2581.690
T11-E11	579237.703	4991523.234	2581.500
T11-E16	579236.941	4991518.420	2581.500
T6-8	579143.857	4992039.582	2578.510

Table 12. Survey data for soil sample locations (continued).

Sample #	X-Coordinate (UTM)	Y-Coordinate (UTM)	Elevation (M)
T6-W1	579142.815	4992039.676	2578.510
T6-W2	579141.892	4992039.648	2578.590
T6-W4	579139.747	4992039.755	2578.570
T6-W7	579136.802	4992039.478	2578.620
T6-W11	579132.935	4992039.776	2578.610
T6-W16	579127.821	4992039.748	2578.560
T6-W22	579121.986	4992039.673	2578.490
T6-W29	579114.718	4992040.012	2578.500
T6-W37	579106.863	4992039.406	2578.320
T6-W46	579097.576	4992039.144	2578.340
T6-W56	579087.929	4992038.922	2578.280
T6-W67	579077.072	4992038.748	2578.300
T6-W79	579065.010	4992038.551	2578.200
T6-W92	579052.261	4992038.283	2578.240
T6-7	579041.709	4992037.966	2578.280
T8-W46	579197.721	4991855.903	2579.070
T4-7	579039.500	4992242.600	2577.630
T4-A1	579038.734	4992243.209	2577.640
T4-A2	579037.989	4992243.958	2577.630
T4-A4	579036.441	4992245.125	2577.590
T4-A7	579034.177	4992247.264	2577.550
T4-A11	579031.286	4992249.824	2577.550
T4-A16	579027.309	4992252.943	2577.470
T4-A22	579022.950	4992257.083	2577.670
T4-A29	579017.890	4992261.878	2577.580
T4-A37	579011.958	4992267.200	2577.480
T4-A46	579004.958	4992272.893	2577.740
T4-A56	578997.490	4992279.645	2577.620
T4-A67	578989.190	4992286.763	2577.860
T4-A79	578980.291	4992294.725	2577.720
T4-A92	578970.939	4992303.742	2577.640
T4-A106	578960.517	4992313.335	2577.480
T4-A121	578949.892	4992323.977	2577.690
T3-6	578938.369	4992334.732	2577.72
T8-W16	579225.930	4991845.754	2579.37
T8-W22	579220.735	4991847.829	2579.22
T8-W29	579213.890	4991850.161	2579.30
T8-W37	579206.169	4991852.758	2579.12
T8-W46	579197.721	4991855.903	2579.07
T4-B1	579040.259	4992243.209	2577.60
T4-B2	579040.891	4992243.998	2577.55

Table 12. Survey data for soil sample locations (continued).

Sample #	**X-Coordinate (UTM)**	**Y-Coordinate (UTM)**	**Elevation (M)**
T4-B4	579042.361	4992245.158	2577.56
T4-B7	579044.639	4992247.385	2577.56
T4-B11	579047.622	4992249.931	2577.57
T4-B16	579051.538	4992253.216	2577.58
T4-B22	579056.031	4992257.031	2577.59
T4-B29	579061.254	4992261.467	2577.60
T4-B37	579067.275	4992266.543	2577.60
T4-B46	579074.096	4992272.542	2577.59
T4-B56	579081.699	4992278.903	2577.60
T4-B67	579089.930	4992286.271	2577.57
T4-B79	579099.003	4992294.312	2577.49
T4-B92	579108.759	4992302.990	2577.46
T4-B106	579119.175	4992312.676	2577.41
T4-B121	579129.633	4992322.354	2577.12
T3-8	579142.183	4992333.320	2577.26
T4-C1	579040.259	4992242.051	2577.62
T4-C2	579040.982	4992241.482	2577.63
T4-C4	579042.532	4992240.271	2577.65
T4-C7	579044.740	4992238.270	2577.65
T4-C11	579047.891	4992235.749	2577.70
T4-C16	579051.526	4992232.435	2577.75
T4-C22	579055.566	4992227.783	2577.69
T4-C29	579060.550	4992222.938	2577.68
T4-C37	579065.705	4992216.860	2577.76
T4-C46	579071.560	4992210.018	2577.78
T4-C56	579077.946	4992202.393	2577.58
T4-C67	579084.961	4992194.025	2577.80
T4-C79	579093.049	4992184.992	2577.66
T4-C92	579101.124	4992174.848	2577.82
T4-C106	579110.406	4992164.122	2577.84
T4-C121	579120.200	4992152.617	2577.70
T5-8	579139.423	4992133.080	2578.15
T4-D1	579038.772	4992241.844	2577.67
T4-D2	579038.140	4992241.234	2577.67
T4-D4	579036.714	4992239.828	2577.66
T4-D7	579034.448	4992237.406	2577.66
T4-D11	579031.890	4992234.732	2577.66
T4-D16	579028.273	4992231.229	2577.64
T4-D22	579024.016	4992226.960	2577.62
T4-D29	579019.101	4992222.399	2577.57
T4-D37	579013.182	4992216.733	2577.65
T4-D46	579006.932	4992210.271	2577.62

Table 12. Survey data for soil sample locations (continued).

Sample #	X-Coordinate (UTM)	Y-Coordinate (UTM)	Elevation (M)
T4-D56	578999.819	4992203.163	2577.69
T4-D67	578991.984	4992195.430	2577.66
T4-D79	578983.325	4992187.126	2577.67
T4-D92	578973.570	4992177.583	2577.54
T4-D106	578963.943	4992167.989	2577.52
T4-D121	578953.362	4992157.478	2577.82
T5-6	578942.623	4992146.528	2578.03

XRF:ICP Results

Table 13. XRF Data for soil samples collected in 2003.

Sample ID	Cd (mg/kg)	Cr (mg/kg)	Cu (mg/kg)	Fe (mg/kg)	Mn (mg/kg)	Ni (mg/kg)	Pb (mg/kg)	Zn (mg/kg)
T2-3	-13.87	55.15	6.05	22581.24	748.28	-152.89	81.29	43.51
T2-4	-12.99	-105.09	-45.44	23204.45	1110.84	-95.47	64.40	38.49
T2-7	-45.15	-46.09	-18.89	8076.27	243.66	-104.76	61.04	26.62
T2-8	-22.55	-40.92	101.65	25179.28	536.84	-71.45	92.89	71.94
T3-3	-58.00	97.32	-10.79	7409.71	294.53	-100.66	80.66	3.96
T3-4	-68.31	136.82	-8.98	5348.89	193.06	-72.67	101.93	8.69
T3-5	-8.51	-89.60	53.06	16999.70	246.75	-61.96	109.71	88.53
T3-6	1.58	-113.96	256.53	22433.02	414.54	-151.41	136.28	179.90
T3-7	-21.10	344.73	104.71	19171.97	442.65	-95.15	94.23	156.32
T3-8	-11.14	129.19	114.26	29074.43	505.11	-198.61	135.22	151.33
T3-9	-6.88	7.07	109.64	24134.58	877.29	-120.55	115.16	114.87
T3-10	-7.71	20.04	-4.65	19945.26	1081.76	-25.24	88.33	49.50
T4-3	2.18	419.03	-14.66	25118.20	947.28	-138.27	81.81	79.27
T4-4	-41.78	149.47	-9.94	10551.83	189.12	-75.67	69.26	19.74
T4-5	-16.64	241.29	145.31	25844.78	975.30	-205.03	81.25	122.89
T4-6	-27.96	6.79	25.86	16190.81	349.18	-98.03	81.37	109.17
T4-7	1.97	-254.20	361.62	51939.14	937.96	-168.19	123.55	111.66
T4-8	-11.34	-111.02	54.51	24448.38	585.95	-171.75	108.53	109.87
T4-9	-33.86	166.23	84.52	14615.96	366.82	-157.15	77.54	45.15
T5-4	-11.91	246.11	-7.58	24299.85	1021.74	-131.21	46.75	59.43
T5-5	-6.79	125.14	78.27	24272.58	1247.05	-176.93	95.57	107.32
T5-6	4.17	-108.92	27.97	23347.55	515.56	-142.20	78.22	69.23
T5-7	-26.60	-72.77	43.03	24002.47	337.38	-96.23	113.44	59.89
T5-8	-14.79	301.99	99.12	24876.23	896.92	-174.28	121.03	63.25
T5-9	-10.19	232.82	-12.01	18186.11	614.33	-123.74	56.16	43.93
T6-5	3.83	53.37	96.90	48793.41	627.22	-140.98	96.53	56.43
T6-6	-8.15	142.96	29.76	34303.43	956.24	-87.46	65.44	70.96
T6-7	-6.09	203.26	206.49	27339.07	641.74	-69.03	113.32	125.57
T6-8	-10.65	119.06	196.31	26070.43	946.89	-72.37	121.88	132.69
T6-9	-9.67	284.18	62.50	32234.35	1136.05	-128.65	81.78	52.14
T6-10	-11.07	95.83	-9.39	23199.57	824.96	-74.87	57.55	53.45
T7-5	-5.01	375.69	-15.06	29893.88	901.92	-130.09	84.30	58.96
T7-6	-5.61	42.75	63.51	28782.06	901.37	-106.11	128.52	80.13
T7-7	-13.72	2.78	-15.78	24892.30	589.06	-18.40	85.91	76.14
T7-8	-11.43	-6.36	42.11	24052.40	838.14	-213.65	125.46	123.71
T7-9	1.62	-109.18	94.95	29287.70	1347.11	-102.38	90.32	121.84
T7-10	-15.44	202.46	-46.34	22297.59	874.06	-207.50	83.68	63.04
T8-5	15.54	151.55	-52.89	24346.18	847.82	-35.01	67.61	49.24
T8-6	2.37	50.54	-32.53	26483.96	930.13	-133.09	93.02	54.77
T8-7	3.37	-16.82	-48.98	31307.42	961.42	-30.65	58.42	76.94
T8-8	-19.62	183.64	-0.65	20795.38	834.81	-163.63	83.11	94.80
T8-9	-7.13	24.66	451.22	30062.96	1055.40	-101.93	106.84	134.81

Table 13. XRF Data for soil samples collected in 2003 (continued).

Sample ID	Cd (mg/kg)	Cr (mg/kg)	Cu (mg/kg)	Fe (mg/kg)	Mn (mg/kg)	Ni (mg/kg)	Pb (mg/kg)	Zn (mg/kg)
T8-10	-20.32	265.37	23.41	27496.36	392.40	-87.55	102.22	81.01
T9-5	-10.95	45.04	-53.78	19701.72	1010.49	-181.71	58.09	46.34
T9-6	-20.10	390.36	-22.48	20361.31	711.91	-117.08	60.32	29.98
T9-7	0.07	-32.48	-16.50	25058.97	949.49	-186.78	92.14	60.88
T9-8	-14.04	-76.39	62.95	25351.48	1083.72	-107.50	87.27	98.30
T9-9	-19.46	-185.06	47.21	24985.07	1105.28	-149.71	108.21	143.26
T9-10	-25.65	-110.45	111.83	24120.38	703.18	-19.23	111.17	115.22
T10-6	-9.64	56.59	-42.64	21931.04	1070.03	-35.71	32.87	88.38
T10-7	-15.15	70.38	-23.10	21596.97	781.58	-7.84	55.75	35.49
T10-8	-9.81	-131.02	143.74	23098.50	1067.69	-90.18	109.49	83.60
T10-9	-23.44	257.47	41.35	28206.31	735.98	-109.14	104.00	113.77
T10-10	-16.21	75.50	43.39	21177.76	865.06	-144.77	102.92	78.55
T11-6	4.41	-42.56	-35.86	25024.83	963.61	-127.39	67.78	54.43
T11-7	-3.76	34.98	-19.69	28472.47	996.48	-95.78	79.56	20.96
T11-8	-22.89	85.64	6.93	21889.44	974.59	-89.18	97.71	80.12
T11-9	-28.38	-57.25	492.81	24974.84	962.51	-85.50	93.75	81.69
T11-10	-12.37	75.57	-35.81	24615.71	1006.57	-84.64	75.13	103.96
T12-6	-5.07	106.74	-44.67	22058.60	887.32	-186.41	69.59	76.70
T12-7	-11.12	18.05	83.62	25221.71	954.14	-152.13	113.48	104.52
T12-8	-2.73	36.01	321.84	27359.13	773.59	-151.55	108.69	125.32
T12-9	-25.37	148.43	50.41	22347.27	725.78	-184.92	89.64	108.42
T12-10	-2.22	-274.75	17.57	21327.92	1111.71	-148.02	107.10	78.56
T13-7	-18.36	154.69	157.78	25009.27	1210.77	-117.00	119.69	147.27
T13-8	-3.13	-14.17	74.94	28770.29	1289.02	-121.23	133.74	170.05
T13-9	-24.37	58.80	19.74	21955.28	740.74	-158.48	81.04	101.28
T14-7	-1.49	-167.12	-15.54	25262.14	1482.96	-146.05	76.38	51.56
T14-8	-16.46	85.34	42.46	21321.37	905.07	-101.08	93.18	71.53
T15-7	-5.16	36.11	58.86	25540.95	1107.26	-182.61	109.30	107.07

Table 14. ICP Data for soil samples collected in 2003.

Sample ID	Cd (mg/kg)	Cr (mg/kg)	Cu (mg/kg)	Fe (%)	Mn (mg/kg)	Ni (mg/kg)	Pb (mg/kg)	Zn (mg/kg)
T2-3	1.05	41.72	22.26	2.75	383.88	28.56	31.57	75.46
T2-4	0.98	29.33	16.59	2.66	961.59	26.74	26.95	78.26
T2-7	0.56	22.89	32.13	1.09	30.38	19.04	14.49	16.8
T2-8	1.05	53.34	237.86	3.22	139.93	39.27	80.78	119.77
T3-3	1.33	10.22	16.73	1.16	37.52	9.73	11.97	23.17
T3-4	1.19	6.3	9.59	0.66	25.69	7.07	12.6	19.88
T3-5	1.33	50.4	128.17	2.79	116.9	28.07	99.05	179.48
T3-6	1.26	44.52	504.28	2.72	195.65	40.95	122.29	242.48
T3-7	1.12	47.95	233.17	2.59	176.05	32.97	99.68	209.3
T3-8	1.68	42	210.49	3.21	172.83	35.98	110.25	201.6
T3-9	1.54	31.01	196.56	2.96	802.2	39.48	89.74	167.37
T3-10	1.26	29.54	67.62	2.50	1176	23.38	42.35	96.67
T4-3	0.84	40.04	23.94	2.74	938.7	33.46	30.45	101.71
T4-4	1.4	13.86	38.15	1.41	33.88	20.37	17.64	26.95
T4-5	1.89	40.32	369.81	3.71	779.1	49.28	99.68	230.09
T4-6	0.91	45.71	158.9	2.43	201.74	31.43	72.24	182.91

Table 14. ICP Data for soil samples collected in 2003 (continued).

Sample ID	Cd (mg/kg)	Cr (mg/kg)	Cu (mg/kg)	Fe (%)	Mn (mg/kg)	Ni (mg/kg)	Pb (mg/kg)	Zn (mg/kg)
T4-7	1.68	40.95	592.13	6.38	280.35	44.66	95.41	243.39
T4-8	1.26	38.08	197.19	2.88	152.88	29.89	93.31	172.97
T4-9	1.05	35.91	135.31	1.86	100.31	17.99	41.58	86.17
T5-4	0.7	37.73	22.96	2.84	1012.76	32.41	29.54	96.95
T5-5	1.19	40.74	206.64	3.32	1639.61	44.52	85.89	161.35
T5-6	0.77	50.05	128.59	2.44	210.35	46.55	44.52	125.3
T5-7	1.05	51.24	159.11	3.47	109.27	33.25	115.57	162.82
T5-8	0.91	36.96	203.35	3.13	576.59	37.73	97.72	168.98
T5-9	0.91	24.08	44.38	1.86	568.96	17.08	36.4	92.89
T6-5	1.4	45.36	177.94	5.74	143.57	39.27	77.63	142.17
T6-6	1.4	69.65	133.7	4.36	471.59	67.27	49.49	155.68
T6-7	0.84	46.62	407.19	3.42	261.17	46.9	87.36	210.07
T6-8	1.33	41.86	348.04	3.35	873.46	44.17	118.65	219.94
T6-9	1.75	43.75	189.98	3.67	967.54	54.25	58.87	149.1
T6-10	0.84	43.96	43.68	2.66	922.32	43.96	50.54	104.51
T7-5	0.98	66.36	20.3	3.51	745.92	56	30.94	123.48
T7-6	2.17	46.55	206.08	3.46	849.24	48.16	95.48	171.71
T7-7	0.91	59.01	28.77	2.51	215.95	55.37	34.51	123.06
T7-8	1.4	45.5	189.84	3.12	640.99	41.02	100.03	193.55
T7-9	1.05	32.48	215.88	3.19	1170.19	41.09	102.13	171.85
T7-10	1.12	41.3	41.09	2.78	908.53	32.76	46.9	97.3
T8-5	1.12	47.11	17.5	2.28	566.44	43.89	16.73	74.41
T8-6	1.05	57.4	20.93	2.68	742.14	57.75	36.05	117.39
T8-7	0.91	63.77	26.74	3.21	728.91	70.07	27.44	124.46
T8-8	0.7	29.82	137.69	2.65	952.91	28.49	63.7	146.72
T8-9	1.68	32.34	822.78	3.74	945.07	42.7	90.58	213.43
T8-10	1.12	43.12	143.29	3.61	113.47	29.33	105.49	137.48
T9-5	0.49	15.12	12.18	2.35	1181.39	14.7	31.29	90.93
T9-6	0.49	50.54	17.08	2.40	613.62	48.16	18.83	89.25
T9-7	0.91	57.89	21.84	2.77	838.53	55.65	28.98	118.93
T9-8	1.75	30.52	127.05	2.88	979.23	35.91	66.85	174.79
T9-9	1.26	36.96	162.33	3.24	806.33	38.64	92.61	206.78
T9-10	1.33	35	190.75	3.19	611.24	31.29	111.02	171.5
T10-6	0.7	54.04	18.97	2.52	739.55	52.36	24.71	120.96
T10-7	1.19	57.33	18.62	2.47	707	53.83	22.96	89.04
T10-8	1.54	27.58	225.05	2.67	883.96	38.64	64.47	133.63
T10-9	1.82	33.25	165.76	3.64	714.49	34.23	103.46	194.53
T10-10	1.54	33.32	152.32	2.91	898.66	45.5	72.52	154.35
T11-6	1.33	59.36	23.8	2.48	702.59	55.65	36.26	108.71
T11-7	1.33	62.3	24.71	2.86	683.62	66.85	23.1	84.07
T11-8	1.05	30.31	115.29	2.75	864.57	41.23	57.4	126.07
T11-9	1.61	33.53	910.42	3.31	929.6	40.95	95.9	215.6
T11-10	1.12	32.83	43.12	2.89	958.09	29.89	58.03	150.36
T12-6	1.19	32.48	18.69	2.59	926.24	29.33	37.24	144.76
T12-7	1.19	34.09	165.27	3.22	934.57	35.14	98.91	201.11
T12-8	1.19	33.32	459.83	3.19	662.9	40.11	91.77	186.48
T12-9	1.68	34.51	184.31	3.13	891.31	33.46	82.46	168.14
T12-10	1.12	32.2	51.66	2.78	1223.11	28.84	56.77	147.63

Table 14. ICP Data for soil samples collected in 2003 (continued).

Sample ID	Cd (mg/kg)	Cr (mg/kg)	Cu (mg/kg)	Fe (%)	Mn (mg/kg)	Ni (mg/kg)	Pb (mg/kg)	Zn (mg/kg)
T13-7	1.47	33.04	234.01	3.03	1069.32	38.57	86.94	230.72
T13-8	1.96	28.35	153.93	2.97	1113.7	34.16	91.07	198.31
T13-9	1.05	30.1	100.03	2.83	857.36	28.91	67.55	167.72
T14-7	0.98	35.77	57.54	3.00	1145.97	37.73	42.63	108.15
T14-8	1.89	25.2	192.92	2.86	963.48	28.98	69.44	179.27
T15-7	1.19	35.56	201.39	3.15	922.25	40.11	101.85	171.85

Table 15. XRF Data for soil samples collected in 2004.

Transect ID	Depth (cm)	As (mg/kg)	Cd (mg/kg)	Cr (mg/kg)	Cu (mg/kg)	Fe (mg/kg)	Mn (mg/kg)	Pb (mg/kg)	Zn (mg/kg)
T11-9	0-10	3	10	1	2359	51279	2126	146	263
T11-9	10-20	-2	0	61	2131	44868	1940	146	285
T11-9	20-30	-3	14	-5	1219	35483	1709	138	184
T11-9	30-40	4	20	-140	488	42360	1937	123	158
T11-9	40-50	-6	15	-454	292	42869	1714	146	145
T11-9	50-75	0	12	86	239	41521	1281	139	125
T11-E1	0-10	5	3	-60	3631	50900	1758	126	350
T11-E1	10-20	5	0	32	1643	40545	1658	130	240
T11-E1	20-30	5	0	43	520	38152	1472	106	143
T11-E1	30-40	-1	11	272	340	40726	1744	128	156
T11-E1	40-50	2	7	169	259	44212	1679	140	117
T11-E1	50-75	30	25	-71	178	51928	1671	123	84
T11-E2	0-10	-19	2	326	4470	58848	2195	183	452
T11-E2	10-20	-4	1	-40	2483	42716	1987	139	289
T11-E2	20-30	5	17	220	733	36182	1699	120	183
T11-E2	30-40	-11	7	-87	208	41623	1544	141	107
T11-E2	40-50	0	9	-87	159	44950	1798	156	108
T11-E2	50-75	19	17	-104	136	56213	1832	147	109
T11-E2	75-100	-8	9	111	91	35813	1484	129	137
T11-E4	0-10	3	3	175	3502	47756	2064	118	355
T11-E4	10-20	-14	-12	354	1123	29392	1270	137	222
T11-E4	20-30	-6	-3	-12	268	28188	1316	134	154
T11-E4	30-40	-6	9	87	91	30480	1510	138	144
T11-E4	40-50	-17	9	-314	168	33656	1952	143	110
T11-E4	50-75	-5	0	-51	59	27749	1647	97	83
T11-E4	75-100	-20	9	172	63	30480	1693	144	66
T11-E7	0-10	2	-14	175	2439	31178	2315	103	372
T11-E7	10-20	3	31	115	1536	34439	2194	93	207
T11-E7	20-30	2	18	-400	624	35307	1654	95	117
T11-E7	30-40	-4	17	276	149	31567	1566	132	147
T11-E7	40-50	-16	16	-9	131	29656	1430	134	92

Table 15. XRF Data for soil samples collected in 2004 (continued).

Transect ID	Depth (cm)	As (mg/kg)	Cd (mg/kg)	Cr (mg/kg)	Cu (mg/kg)	Fe (mg/kg)	Mn (mg/kg)	Pb (mg/kg)	Zn (mg/kg)
T11-E7	50-75	4	14	286	88	27356	1360	98	92
T11-E7	75-100	2	0	213	115	26269	1245	85	96
T11-E11	0-10	15	-21	95	3458	43837	1651	75	341
T11-E11	10-20	-8	-8	8	631	30134	1425	131	156
T11-E11	20-30	-8	16	-64	204	31105	1237	134	99
T11-E11	30-40	-23	6	-164	217	33968	1699	163	117
T11-E11	40-50	-6	15	-213	145	33821	1844	145	168
T11-E11	50-75	-7	11	296	91	33569	1722	117	112
T11-E16	0-10	1	-1	18	2873	42270	2067	139	319
T11-E16	10-20	-8	-9	1	462	31177	1682	133	164
T11-E16	20-30	-11	-5	135	189	30000	1338	132	119
T11-E16	30-40	-17	14	-61	88	30886	1904	129	94
T11-E16	40-50	-13	17	20	154	30246	1494	129	102
T11-E22	0-10	-2	5	-392	4924	66132	2266	141	420
T11-E22	10-20	-4	2	-144	3215	46532	1817	136	298
T11-E22	20-30	0	0	-32	203	31142	1318	119	113
T11-E22	30-40	-13	3	-168	306	35095	2168	148	141
T11-E22	40-50	-11	12	227	160	31319	1347	142	100
T11-E22	50-75	-15	8	64	116	33004	1734	134	131
T11-E29	0-10	-19	-5	83	4217	52782	1460	151	265
T11-E29	10-20	3	-20	113	1389	29727	1172	107	186
T11-E29	20-30	-4	19	269	151	30116	1808	127	113
T11-E29	30-40	-9	2	-82	160	33298	1606	116	136
T11-E29	40-50	-4	7	13	151	33386	1637	120	117
T11-E29	50-75	-9	6	-374	162	32522	1611	111	74
T11-E37	0-10	-13	16	179	1225	39359	1921	149	269
T11-E37	10-20	2	3	14	386	38854	2304	140	229
T11-E37	20-30	-2	-9	-219	505	41843	2406	129	175
T11-E37	30-40	-5	7	47	1625	70586	4296	152	388
T11-E37	40-50	-4	29	-143	2528	91791	6003	158	494
T11-E37	50-75	6	29	-52	2560	95519	6469	153	401
T11-E37	75-100	21	21	-122	2260	86994	7436	126	458
T11-E46	0-10	-6	-30	73	312	14312	964	93	121
T11-E46	10-20	-7	-4	98	148	30002	1259	118	171
T11-E46	20-30	8	-1	129	208	35354	1694	131	168
T11-E46	30-40	10	3	-109	390	38944	1851	128	237
T11-E46	40-50	-1	6	-205	438	42350	2594	152	232
T11-E46	75-100	-3	21	153	801	51365	2861	189	387
T11-W0	0-10	0	16	-97	1294	51865	2567	172	289
T11-W0	10-20	-9	-2	-123	1318	45970	2155	184	214
T11-W0	20-30	0	7	-104	2192	53154	2811	171	364

Table 15. XRF Data for soil samples collected in 2004 (continued).

Transect ID	Depth (cm)	As (mg/kg)	Cd (mg/kg)	Cr (mg/kg)	Cu (mg/kg)	Fe (mg/kg)	Mn (mg/kg)	Pb (mg/kg)	Zn (mg/kg)
T11-W0	30-40	5	13	171	2884	59006	3802	149	529
T11-W0	40-50	-3	17	388	3424	50902	3787	150	469
T11-W1	0-10	1	6	-275	1111	42935	1912	172	255
T11-W1	10-20	9	7	63	1585	47282	1922	154	286
T11-W1	20-30	9	20	169	1734	48563	2562	123	264
T11-W1	30-40	-10	-4	-142	2340	37137	1846	129	287
T11-W1	40-50	-9	9	-67	1718	37450	1727	159	217
T11-W1	50-75	19	4	-107	1085	51007	2271	114	255
T11-W2	0-10	-1	7	-97	4776	56462	2767	128	478
T11-W2	10-20	-10	18	232	5247	56716	2563	148	493
T11-W2	20-30	13	-5	35	357	26858	1379	101	165
T11-W2	30-40	-3	3	133	415	30482	1567	134	184
T11-W2	40-50	8	1	74	237	30969	1474	106	135
T11-W2	50-75	-12	12	71	108	32559	1548	181	122
T11-W2	75-100	-7	17	54	179	31413	1393	130	125
T11-W4	0-10	-8	-1	70	4656	55501	2664	116	458
T11-W4	10-20	4	-21	27	1364	28532	1428	103	272
T11-W4	20-30	-6	13	331	138	29255	1453	121	143
T11-W4	30-40	-13	-7	-28	167	26204	1220	120	145
T11-W4	40-50	-4	-7	191	365	28760	1289	141	142
T11-W4	50-75	-4	16	168	134	29872	1724	124	124
T11-W4	75-100	-10	13	366	63	28312	1715	134	112
T11-W7	0-10	6	11	463	6124	82866	3123	143	665
T11-W7	10-20	-7	-10	-265	4080	43772	2271	135	389
T11-W7	20-30	-10	-12	90	425	30771	1705	160	214
T11-W7	30-40	6	1	201	518	32022	1688	117	203
T11-W7	40-50	-12	19	-118	497	36605	2116	153	148
T11-W7	50-75	-9	30	-323	153	33011	1625	115	100
T11-W11	0-10	4	8	94	2270	45679	1888	123	291
T11-W11	10-20	-15	5	75	150	31010	1429	179	116
T11-W11	20-30	-8	24	98	240	34520	1785	131	144
T11-W11	30-40	-9	19	221	79	32366	1510	127	98
T11-W11	40-50	-11	7	54	153	35184	1652	148	99
T11-W11	50-75	-16	11	-229	84	33418	1936	124	110
T11-W11	75-100	-8	3	18	74	32929	1551	144	130
T11-W16	0-10	-3	-3	-51	3036	48595	1699	132	374
T11-W16	10-20	13	6	176	300	29413	1151	114	119
T11-W16	20-30	1	-7	-188	148	29060	702	140	138
T11-W16	30-40	3	-1	-10	260	28016	923	132	144
T11-W16	40-50	-10	4	130	123	31515	1162	139	90
T11-W16	50-75	-7	-4	-26	179	32389	1754	126	131
T11-W16	75-100	-12	-4	24	125	32719	1789	149	131

Table 15. XRF Data for soil samples collected in 2004 (Continued).

Transect ID	Depth (cm)	As (mg/kg)	Cd (mg/kg)	Cr (mg/kg)	Cu (mg/kg)	Fe (mg/kg)	Mn (mg/kg)	Pb (mg/kg)	Zn (mg/kg)
T11-W22	0-10	6	-4	198	770	31251	904	128	193
T11-W22	10-20	-11	-2	27	201	32319	1411	138	157
T11-W22	20-30	-11	8	-69	234	30366	1343	147	131
T11-W22	30-40	4	11	163	159	31045	1641	124	118
T11-W29	0-10	-7	-43	369	2244	17137	2052	84	443
T11-W29	10-20	-11	9	33	86	31909	1533	163	103
T11-W29	20-30	-8	-2	-11	152	31681	1487	134	106
T11-W29	30-40	0	9	521	145	33764	1588	154	164
T11-W29	40-50	-5	7	-41	114	32389	1560	145	120
T11-W29	50-75	-5	10	295	88	30614	1392	130	125
T11-W37	0-10	-4	-26	52	546	16354	587	89	114
T11-W37	10-20	13	1	110	102	29732	999	105	105
T11-W37	20-30	-16	10	-75	89	31296	1369	155	111
T11-W37	30-40	0	18	-439	114	33104	1739	129	106
T11-W37	40-50	8	20	-240	141	38872	1745	152	144
T11-W37	50-75	-12	7	319	115	36559	1580	178	136
T11-W46	0-10	-18	-56	183	2377	7885	2786	98	350
T11-W46	10-20	-1	-24	27	117	21132	716	113	166
T11-W46	20-30	-5	20	-365	69	31922	1145	104	68
T11-W46	30-40	-12	10	142	151	31181	2001	108	111
T11-W46	40-50	-5	1	175	89	31598	1591	109	119
T4-7	0-10	-10	-23	204	30	12187	526	74	25
T4-7	10-20	-2	-27	126	37	14043	555	92	72
T4-7	20-30	10	2	-159	210	73254	2005	123	85
T4-7	30-40	12	9	-734	485	143030	3563	132	119
T4-7	40-50	17	22	-673	624	144322	3839	169	221
T4-7	50-75	-1	9	131	481	53309	1439	141	160
T4-7	75-100	-8	29	-353	341	60083	1612	101	125
T4-A1	0-10	-11	-46	149	13	8468	381	81	51
T4-A1	10-20	-10	-24	20	40	12400	364	95	67
T4-A1	20-30	-6	-17	-37	126	18887	533	119	125
T4-A1	30-40	-9	8	192	278	35392	980	136	123
T4-A1	40-50	7	19	-219	174	65535	1805	99	117
T4-A1	50-75	16	18	50	538	71596	2621	132	199
T4-A1	75-100	-7	3	-564	433	84158	2294	130	174
T4-A2	0-10	-35	-71	65	4	2759	280	106	101
T4-A2	10-20	-13	-37	232	55	7663	313	78	42
T4-A2	20-30	-13	-22	-65	146	11260	324	110	41
T4-A2	30-40	-8	-10	126	100	16369	602	132	113
T4-A2	40-50	-20	-14	111	299	24684	778	189	152
T4-A2	50-75	-7	17	10	445	49175	1343	155	129
T4-A2	75-100	-5	17	-309	541	22752	777	130	231

Table 15. XRF Data for soil samples collected in 2004 (continued).

Transect ID	Depth (cm)	As (mg/kg)	Cd (mg/kg)	Cr (mg/kg)	Cu (mg/kg)	Fe (mg/kg)	Mn (mg/kg)	Pb (mg/kg)	Zn (mg/kg)
T4-A4	0-10	-38	-75	42	-10	1656	216	112	55
T4-A4	10-20	-38	-75	98	3	1660	154	115	63
T4-A4	20-30	-18	-50	-5	29	5275	224	93	43
T4-A4	30-40	-3	-28	-4	110	9422	384	79	89
T4-A4	40-50	-5	2	250	168	20297	629	132	89
T4-A4	50-75	-4	-5	338	256	35770	1020	129	150
T4-A4	75-100	-10	-12	-9	369	40152	1153	129	192
T4-A7	0-10	-12	-43	83	-2	11547	564	83	58
T4-A7	10-20	-5	-17	116	42	13800	621	87	61
T4-A7	20-30	-6	-7	-29	150	20265	779	126	123
T4-A7	30-40	-6	11	124	438	51754	1596	118	184
T4-A7	40-50	25	18	-492	713	139460	4473	112	143
T4-A7	50-75	12	27	-107	691	198282	5589	161	225
T4-A7	75-100	2	25	-246	1098	98464	2894	144	332
T4-A11	0-10	-10	-34	242	25	12172	349	80	54
T4-A11	10-20	-18	-30	45	34	12399	373	103	42
T4-A11	20-30	-3	-9	-67	87	19517	620	108	141
T4-A11	30-40	-15	1	307	295	33842	1179	162	83
T4-A11	40-50	13	-10	83	497	46524	1417	116	202
T4-A11	50-75	12	17	-558	922	85838	2674	145	389
T4-A11	75-100	-12	6	-141	588	59110	1576	161	212
T4-A16	0-10	-25	-63	99	-8	7890	422	105	39
T4-A16	10-20	-7	-30	139	13	10706	418	81	62
T4-A16	20-30	-7	-27	52	58	12934	320	99	68
T4-A16	30-40	1	-5	161	272	28864	880	124	178
T4-A16	40-50	-10	11	357	612	60679	1787	153	168
T4-A16	50-75	1	31	-116	701	85488	2162	143	274
T4-A16	75-100	-10	12	-170	675	80300	2316	157	271
T4-A22	0-10	-23	-63	212	-10	7131	354	99	52
T4-A22	10-20	0	-37	55	12	10644	211	65	74
T4-A22	20-30	-3	-22	222	78	16273	504	98	102
T4-A22	30-40	-8	7	70	448	31771	865	147	204
T4-A22	40-50	-3	11	-653	657	86625	2373	172	113
T4-A22	50-75	-4	18	-457	665	106521	2884	182	174
T4-A22	75-100	2	27	-196	842	87590	2724	155	248
T4-A29	0-10	-26	-64	73	16	6758	361	87	79
T4-A29	10-20	-11	-32	150	-16	10458	351	99	64
T4-A29	20-30	-7	5	96	98	18196	636	118	139
T4-A29	30-40	4	-9	50	154	23178	669	106	145
T4-A29	40-50	-2	6	95	240	32648	932	132	163
T4-A29	50-75	1	10	-4	217	52574	1489	112	132
T4-A29	75-100	-19	4	-53	88	14128	366	109	150

Table 15. XRF Data for soil samples collected in 2004 (continued).

Transect ID	Depth (cm)	As (mg/kg)	Cd (mg/kg)	Cr (mg/kg)	Cu (mg/kg)	Fe (mg/kg)	Mn (mg/kg)	Pb (mg/kg)	Zn (mg/kg)
T4-A37	0-10	-26	-77	40	14	1983	181	92	78
T4-A37	10-20	-26	-67	97	0	2725	201	95	71
T4-A37	20-30	-15	-47	-12	24	6107	287	83	63
T4-A37	30-40	-6	-16	76	70	11791	489	81	92
T4-A37	40-50	-7	-8	-139	56	20107	598	121	112
T4-A37	50-75	-17	3	107	60	23737	683	112	116
T4-A37	75-100	-8	19	-228	350	61915	1456	129	137
T4-A46	0-10	-29	-69	155	-14	3539	249	102	110
T4-A46	10-20	-26	-62	155	-8	8300	327	109	91
T4-A46	20-30	-15	-30	190	-12	11732	542	81	63
T4-A46	30-40	-11	-5	-1	43	15338	506	114	139
T4-A46	40-50	-12	-5	127	39	23018	654	126	171
T4-A46	50-75	-15	5	33	-5	25453	887	108	121
T4-A56	0-10	-39	-76	234	-4	1702	166	115	66
T4-A56	10-20	-34	-71	185	-5	3038	214	123	62
T4-A56	20-30	-8	-43	240	13	12429	587	87	51
T4-A56	30-40	7	12	23	20	29461	1064	68	124
T4-A56	40-50	-8	12	307	46	33544	813	94	90
T4-A56	50-75	-15	-5	157	39	36532	822	117	103
T4-A56	75-100	-14	-11	188	113	22539	605	102	145
T4-A67	0-10	-32	-69	68	-19	4294	350	105	62
T4-A67	10-20	-11	-42	85	-3	11774	404	83	63
T4-A67	20-30	-10	-4	197	-7	20326	638	93	107
T4-A67	30-40	-4	12	-215	37	23794	788	120	149
T4-A67	40-50	3	2	-69	34	31926	1086	106	157
T4-A67	50-75	-12	21	-159	53	46022	1132	118	125
T4-A79	0-10	-11	-57	197	14	8439	347	77	89
T4-A79	10-20	-10	-51	8	6	10681	440	87	101
T4-A79	20-30	4	-16	280	-30	20469	717	91	115
T4-A79	30-40	-12	-1	353	-12	23174	696	98	123
T4-A79	40-50	-10	5	-115	52	22449	631	121	158
T4-A79	75-100	-7	10	-101	80	23150	813	101	119
T4-A92	0-10	-30	-70	109	-6	1998	204	103	84
T4-A92	10-20	-33	-74	43	26	1635	151	108	58
T4-A92	20-30	-31	-74	100	3	3970	277	114	72
T4-A92	30-40	-6	-41	-28	-12	11130	494	84	87
T4-A92	40-50	-9	-8	-66	10	18553	543	79	84
T4-A92	50-75	-20	7	-15	-62	39602	1057	101	145
T4-A92	75-100	-20	40	-60	-50	214678	4841	114	-18
T4-A106	0-10	-33	-67	47	-8	2114	231	105	78
T4-A106	10-20	-33	-70	-19	15	1703	192	111	91
T4-A106	20-30	-28	-66	54	1	4075	251	119	63

Table 15. XRF Data for soil samples collected in 2004 (continued).

Transect ID	Depth (cm)	As (mg/kg)	Cd (mg/kg)	Cr (mg/kg)	Cu (mg/kg)	Fe (mg/kg)	Mn (mg/kg)	Pb (mg/kg)	Zn (mg/kg)
T4-A106	30-40	-25	-21	100	54	9346	313	92	71
T4-A106	40-50	-11	11	-35	139	34713	795	174	214
T4-A106	50-75	9	11	-150	237	48751	1257	129	140
T4-A121	0-10	-31	-66	175	-12	5970	587	104	76
T4-A121	10-20	-7	-14	157	81	16425	523	99	139
T4-A121	20-30	-8	-5	-73	204	24538	799	132	268
T4-A121	30-40	7	-13	-106	216	31314	890	110	163
T4-A121	40-50	1	4	-46	469	53973	1336	145	190
T4-A121	50-75	4	30	-341	611	69979	1958	131	163
T3-6	0-10	-29	-71	100	2	5189	298	110	53
T3-6	10-20	-10	-37	302	17	10346	262	85	100
T3-6	20-30	-18	-19	191	64	14522	532	108	101
T3-6	30-40	-12	-1	64	91	19634	578	123	156
T3-6	40-50	-8	3	-14	204	23936	675	151	213
T3-6	50-75	-7	-1	-268	414	45365	1608	144	245
T3-6	75-100	-2	13	232	708	44666	1525	159	239
T4-B1	0-10	-10	-46	-79	-11	15291	543	94	27
T4-B1	10-20	-17	-10	-168	29	18994	445	108	53
T4-B1	20-30	-9	17	-40	217	89791	1934	146	96
T4-B1	30-40	-1	35	-66	362	155810	3623	130	19
T4-B1	40-50	14	64	-1221	218	230235	6073	101	40
T4-B1	50-75	4	27	-630	340	128167	3835	111	196
T4-B1	75-100	-6	50	-364	353	125145	3080	121	182
T4-B2	0-10	-13	-23	-148	-3	14944	581	93	29
T4-B2	10-20	-10	-23	193	-4	15102	410	104	78
T4-B2	20-30	-2	-16	214	164	29050	879	105	80
T4-B2	30-40	-19	31	-543	463	133098	3218	153	115
T4-B2	40-50	-13	30	-408	367	129995	3515	147	123
T4-B2	50-75	10	36	-319	258	142584	3997	94	86
T4-B2	75-100	11	33	-362	437	114233	2990	90	133
T4-B4	0-10	-28	-56	33	-28	11855	596	102	36
T4-B4	10-20	-2	-22	232	-6	14783	584	70	43
T4-B4	20-30	-5	-10	-18	24	19099	768	114	73
T4-B4	30-40	-15	3	-26	163	32946	993	133	111
T4-B4	40-50	-1	20	-328	669	85968	2550	135	234
T4-B4	50-75	13	36	-254	874	100265	2626	137	227
T4-B4	75-100	15	18	-303	646	73450	2045	85	206
T4-B7	0-10	-13	-55	181	-6	12951	618	79	46
T4-B7	10-20	-7	-22	28	21	17124	592	76	39
T4-B7	20-30	11	2	-301	281	50107	1594	101	112
T4-B7	30-40	23	53	-1064	453	221226	5333	136	109
T4-B7	40-50	29	49	-406	600	220478	6227	164	164

Table 15. XRF Data for soil samples collected in 2004 (continued).

Transect ID	Depth (cm)	As (mg/kg)	Cd (mg/kg)	Cr (mg/kg)	Cu (mg/kg)	Fe (mg/kg)	Mn (mg/kg)	Pb (mg/kg)	Zn (mg/kg)
T4-B7	50-75	23	35	-617	563	170685	4575	148	152
T4-B7	75-100	-8	40	172	817	135803	3490	160	281
T4-B11	0-10	-31	-71	224	-3	2419	275	106	93
T4-B11	10-20	-34	-65	103	-6	4592	277	122	74
T4-B11	20-30	-15	-35	59	58	8834	330	86	64
T4-B11	30-40	-18	-5	87	98	16463	469	149	132
T4-B11	40-50	-4	0	-67	106	21208	508	124	105
T4-B11	50-75	-3	-5	-367	380	61213	1541	115	135
T4-B11	75-100	-6	5	145	310	53454	1310	126	118
T4-B16	0-10	-18	-68	-8	-14	3117	250	72	102
T4-B16	10-20	-31	-75	48	1	1705	139	101	108
T4-B16	20-30	-15	-33	31	39	8706	407	106	90
T4-B16	30-40	-15	-6	56	113	11046	576	107	95
T4-B16	40-50	-4	-6	109	106	17182	657	129	167
T4-B16	50-75	-12	8	-238	195	42250	1264	162	143
T4-B22	0-10	-31	-67	-16	7	3094	279	108	83
T4-B22	10-20	-32	-66	22	11	3462	241	112	100
T4-B22	20-30	-7	-34	-114	24	9609	370	83	94
T4-B22	30-40	-14	-19	42	90	14878	524	108	144
T4-B22	40-50	-12	0	317	60	18648	514	152	141
T4-B22	50-75	-8	6	-283	255	49750	1394	148	191
T4-B22	75-100	8	17	187	197	55219	1247	150	199
T4-B29	0-10	-40	-68	159	3	2797	250	120	94
T4-B29	10-20	-33	-71	144	13	1970	198	105	82
T4-B29	20-30	-16	-62	124	9	4692	244	104	79
T4-B29	30-40	-12	-25	159	26	10329	381	70	74
T4-B29	40-50	-15	-5	120	112	20727	697	144	175
T4-B29	50-75	-17	3	-143	79	21795	609	136	147
T4-B29	75-100	-4	4	248	135	46600	1060	132	164
T4-B37	0-10	-30	-69	88	-13	2980	243	99	109
T4-B37	10-20	-36	-74	101	-12	1824	176	116	92
T4-B37	20-30	-22	-59	53	1	4849	288	92	104
T4-B37	30-40	-14	-22	41	65	10537	376	94	109
T4-B37	40-50	-6	-1	440	43	18630	410	137	148
T4-B37	50-75	-16	0	-113	141	30872	759	153	148
T4-B37	75-100	-13	-3	-266	111	42960	1187	123	156
T4-B46	0-10	-31	-69	62	2	3244	246	103	105
T4-B46	10-20	-34	-71	137	5	3165	225	114	95
T4-B46	20-30	-8	-42	193	50	7543	411	79	65
T4-B46	30-40	-9	-9	115	209	18413	621	119	172
T4-B46	40-50	-14	-5	-54	171	16523	549	152	129
T4-B46	50-75	-7	-15	114	204	31455	933	122	143

Table 15. XRF Data for soil samples collected in 2004 (continued).

Transect ID	Depth (cm)	As (mg/kg)	Cd (mg/kg)	Cr (mg/kg)	Cu (mg/kg)	Fe (mg/kg)	Mn (mg/kg)	Pb (mg/kg)	Zn (mg/kg)
T4-B46	75-100	-6	16	1	163	53044	1612	126	148
T4-B56	0-10	-26	-62	160	-8	3437	183	91	108
T4-B56	10-20	-30	-70	133	15	2054	159	103	67
T4-B56	20-30	-30	-70	130	3	2237	192	112	92
T4-B56	30-40	-13	-54	21	5	6144	317	81	80
T4-B56	40-50	-4	-15	64	96	11096	529	91	90
T4-B56	50-75	0	5	-112	135	20585	583	143	168
T4-B56	75-100	-2	9	-123	142	29200	908	126	169
T4-B67	0-10	-25	-77	106	4	2075	177	89	72
T4-B67	10-20	-35	-76	84	-12	1601	217	107	48
T4-B67	20-30	-39	-76	217	-9	1732	197	123	54
T4-B67	30-40	-21	-56	34	29	5131	296	92	75
T4-B67	40-50	-8	-21	234	71	12903	411	117	135
T4-B67	50-75	-19	2	42	181	24823	622	163	155
T4-B67	75-100	-11	-7	401	190	45331	1198	150	165
T4-B79	0-10	-19	-58	97	5	5265	288	89	55
T4-B79	10-20	-7	-34	-76	-8	9015	272	76	74
T4-B79	20-30	-12	-7	80	47	13617	295	122	157
T4-B79	30-40	-20	6	92	173	20497	695	167	129
T4-B79	40-50	-18	9	30	262	30727	1004	149	123
T4-B79	50-75	-22	5	12	196	29211	1175	143	88
T4-B79	75-100	-18	8	179	98	45736	1894	135	81
T4-B92	0-10	-18	-50	79	10	6313	361	93	97
T4-B92	10-20	-13	-25	218	-9	9995	321	98	115
T4-B92	20-30	-5	14	278	59	18751	382	120	184
T4-B92	30-40	-8	11	-196	69	21828	770	138	132
T4-B92	40-50	-13	4	-50	28	21457	748	117	96
T4-B92	50-75	-15	10	-25	3	17033	324	112	90
T4-B92	75-100	1	-2	314	161	19025	654	96	111
T4-B100	0-10	-8	-36	27	3	12236	1543	86	76
T4-B100	10-20	-7	-22	239	73	18213	810	101	60
T4-B100	20-30	-6	11	-88	160	20371	840	133	130
T4-B100	30-40	-19	6	143	93	26738	1077	154	126
T4-B100	40-50	-8	10	107	140	61913	1776	137	95
T4-B100	50-75	-6	24	-102	64	91973	2550	123	100
T4-B100	75-100	-7	5	72	220	55028	1418	131	119
T4-B106	0-10	-9	-39	-163	141	11422	613	90	84
T4-B106	10-20	-6	-15	100	15	11525	458	97	113
T4-B106	20-30	-3	-12	191	52	21180	677	115	162
T4-B106	30-40	11	18	48	120	37469	968	123	144
T4-B106	40-50	-8	1	159	148	34358	932	156	120
T4-B106	50-75	1	-2	385	132	25029	649	137	185

Table 15. XRF Data for soil samples collected in 2004 (continued).

Transect ID	Depth (cm)	As (mg/kg)	Cd (mg/kg)	Cr (mg/kg)	Cu (mg/kg)	Fe (mg/kg)	Mn (mg/kg)	Pb (mg/kg)	Zn (mg/kg)
T4-B106	75-100	-14	8	67	163	21863	713	151	176
T4-B121	0-10	-9	-37	107	41	9915	599	110	94
T4-B121	10-20	-2	1	-106	73	12780	430	112	96
T4-B121	20-30	-7	0	-277	-26	14087	614	101	115
T4-B121	30-40	-11	15	-120	-20	14512	524	99	91
T4-B121	40-50	-4	6	2	41	32119	759	127	52
T4-B121	50-75	-11	0	37	77	21928	605	122	75
T4-B121	75-100	-1	2	-37	562	26584	806	120	315
T3-8	0-10	-11	-2	-193	82	14489	614	108	99
T3-8	10-20	-10	-13	-158	72	16871	602	119	116
T3-8	20-30	-29	-4	59	70	22659	624	154	135
T3-8	30-40	9	3	-103	75	27713	879	106	145
T3-8	40-50	-11	12	-169	239	36642	1374	149	176
T3-8	50-75	-12	14	-248	261	39172	1602	142	149
T3-8	75-100	-6	-2	233	292	25719	735	145	168
T4-C1	0-10	-19	-54	136	-4	9079	564	81	30
T4-C1	10-20	-7	-24	308	34	14451	522	91	58
T4-C1	20-30	1	-5	-30	94	23253	479	122	112
T4-C1	30-40	5	35	-473	411	87814	2362	124	141
T4-C1	40-50	12	40	233	651	125154	3516	118	133
T4-C1	50-75	17	68	161	447	151788	4061	115	104
T4-C1	75-100	5	12	-324	744	80669	2003	109	255
T4-C2	0-10	-14	-55	23	2	15710	632	93	44
T4-C2	10-20	-8	-27	112	31	14106	448	77	26
T4-C2	20-30	-2	-9	275	47	17608	500	110	91
T4-C2	30-40	-12	5	265	362	53653	1443	141	106
T4-C2	40-50	10	40	-141	895	154830	4117	161	268
T4-C2	50-75	12	18	-25	865	114856	3044	157	245
T4-C2	75-100	2	17	-259	842	96124	2466	146	318
T4-C4	0-10	-10	-41	-95	21	13510	521	85	52
T4-C4	10-20	0	-9	1	105	23929	815	90	108
T4-C4	20-30	-8	-8	58	97	24167	752	123	126
T4-C4	30-40	-13	11	-186	632	98292	3108	164	232
T4-C4	40-50	-16	43	-336	744	122499	3687	164	210
T4-C4	50-75	0	31	-569	444	146157	4182	113	90
T4-C4	75-100	-5	48	-180	181	125490	3017	99	42
T4-C7	0-10	-16	-48	5	-19	13307	551	93	53
T4-C7	10-20	-16	-15	31	129	25075	660	115	96
T4-C7	20-30	-2	-16	150	145	26929	710	101	112
T4-C7	30-40	-3	-4	146	187	31828	932	105	109
T4-C7	40-50	-15	29	116	687	230393	5297	203	206
T4-C7	50-75	11	21	-482	732	136007	3425	135	250

Table 15. XRF Data for soil samples collected in 2004 (continued).

Transect ID	Depth (cm)	As (mg/kg)	Cd (mg/kg)	Cr (mg/kg)	Cu (mg/kg)	Fe (mg/kg)	Mn (mg/kg)	Pb (mg/kg)	Zn (mg/kg)
T4-C7	75-100	-10	34	-118	949	88400	2322	143	217
T4-C11	0-10	-5	-45	121	-5	11299	414	86	39
T4-C11	10-20	-6	-3	115	126	15952	585	109	59
T4-C11	20-30	-19	-2	72	87	21877	678	148	82
T4-C11	30-40	9	-5	-46	334	26974	1090	92	112
T4-C11	40-50	-3	13	167	627	58674	1615	149	221
T4-C11	50-75	22	18	-271	903	141245	4018	132	345
T4-C11	75-100	-8	29	183	1110	64685	1640	170	333
T4-C16	0-10	-11	-50	69	0	8919	375	80	30
T4-C16	10-20	-12	-21	303	30	16468	506	114	72
T4-C16	20-30	-9	-9	304	119	29586	905	138	108
T4-C16	30-40	-9	4	254	412	32834	1051	126	183
T4-C16	40-50	10	15	224	717	91997	2229	131	210
T4-C16	50-75	-1	11	-553	1015	100117	3023	166	341
T4-C16	75-100	11	15	-261	1102	86391	2585	118	362
T4-C22	0-10	-6	-14	22	14	16208	592	96	81
T4-C22	10-20	0	-32	114	29	17309	457	86	70
T4-C22	20-30	-14	3	41	82	21337	615	143	107
T4-C22	30-40	-5	-11	198	219	22144	671	115	85
T4-C22	40-50	-7	4	-72	474	71620	1741	156	212
T4-C22	50-75	-14	37	-283	801	189067	4821	196	349
T4-C22	75-100	-8	19	-396	1405	96683	1970	137	315
T4-C29	0-10	-7	-26	-156	5	13950	537	102	69
T4-C29	10-20	-16	-33	1	27	14897	486	124	61
T4-C29	20-30	-2	-8	178	130	26438	702	120	132
T4-C29	30-40	0	2	181	436	37899	1222	114	197
T4-C29	40-50	10	4	-47	1158	69105	2522	134	328
T4-C29	50-75	17	19	-2	1516	115742	3187	119	333
T4-C29	75-100	-1	3	-308	1254	73059	2120	132	226
T4-C37	0-10	-11	-26	134	46	12218	483	107	59
T4-C37	10-20	-18	-15	96	24	12126	310	121	89
T4-C37	20-30	-6	-3	-60	165	21295	812	127	69
T4-C37	30-40	-11	2	458	445	23908	1118	142	119
T4-C37	40-50	-11	35	507	1140	64108	1836	163	377
T4-C37	50-75	2	28	-1073	1774	226876	6002	144	258
T4-C37	75-100	-10	36	-473	1370	196280	4947	173	256
T4-C46	0-10	-19	-55	56	-9	9068	386	97	61
T4-C46	10-20	-11	-47	67	0	10069	338	86	44
T4-C46	20-30	-3	5	71	76	24207	733	130	98
T4-C46	30-40	3	-15	-121	253	42850	1311	132	145
T4-C46	40-50	3	4	-210	324	44070	1655	113	127
T4-C46	50-75	14	24	-352	584	101982	3102	110	166

Table 15. XRF Data for soil samples collected in 2004 (continued).

Transect ID	Depth (cm)	As (mg/kg)	Cd (mg/kg)	Cr (mg/kg)	Cu (mg/kg)	Fe (mg/kg)	Mn (mg/kg)	Pb (mg/kg)	Zn (mg/kg)
T4-C46	75-100	-17	7	-2	248	11662	344	136	135
T4-C56	0-10	-8	-28	150	22	10039	444	92	98
T4-C56	10-20	-11	-12	191	33	14690	434	128	101
T4-C56	20-30	3	-16	-206	79	24371	701	128	92
T4-C56	30-40	1	4	10	130	25242	927	141	39
T4-C56	40-50	-9	16	-95	269	71975	1770	129	95
T4-C56	50-75	-20	3	15	702	31859	735	148	204
T4-C56	75-100	-12	8	-38	197	15167	380	99	135
T4-C67	0-10	-13	-22	266	39	12551	498	105	87
T4-C67	10-20	-5	-42	79	38	11920	448	82	59
T4-C67	20-30	-13	-10	196	125	18209	507	140	84
T4-C67	30-40	-5	-3	20	117	29543	717	114	121
T4-C67	40-50	3	-3	74	197	37959	1260	140	154
T4-C67	50-75	-4	21	213	175	38734	1223	168	151
T4-C67	75-100	-6	0	34	313	16927	402	158	203
T4-C79	0-10	4	-32	200	41	14736	418	93	128
T4-C79	10-20	-2	-10	103	60	17333	619	128	107
T4-C79	20-30	-6	-18	-31	72	16853	441	100	100
T4-C79	30-40	3	12	175	16	39152	1252	158	94
T4-C79	40-50	3	6	25	42	45352	1641	118	86
T4-C79	50-75	7	3	-379	108	58514	2048	110	122
T4-C79	75-100	-10	-2	119	197	20429	735	137	157
T4-C92	0-10	-2	-24	53	46	14831	666	94	118
T4-C92	10-20	-1	-4	-3	75	23352	832	114	128
T4-C92	20-30	9	16	-185	124	25000	643	138	148
T4-C92	30-40	-7	11	355	56	27495	883	132	100
T4-C92	40-50	-9	5	31	144	55761	1673	149	99
T4-C92	50-75	-5	17	-109	188	40159	1324	127	124
T4-C92	75-100	-11	-6	289	147	23298	1098	136	151
T4-C106	0-10	-16	-16	165	81	13536	444	113	100
T4-C106	10-20	-8	-7	130	63	17327	609	121	88
T4-C106	20-30	7	-21	-284	81	21760	631	113	96
T4-C106	30-40	2	-10	-201	124	30749	1207	111	102
T4-C106	40-50	1	34	501	17	227432	12919	152	61
T4-C106	50-75	-6	22	-158	166	80434	3089	113	52
T4-C106	75-100	-6	9	-64	128	22592	974	109	153
T4-C121	0-10	6	-18	52	117	16070	504	82	103
T4-C121	10-20	-12	2	-60	33	18917	610	133	110
T4-C121	20-30	-3	4	216	96	25983	737	143	137
T4-C121	30-40	-9	0	-184	121	22510	815	136	144
T4-C121	40-50	-5	1	270	97	19748	835	118	147
T4-C121	50-75	-8	16	-89	92	20610	689	120	134

Table 15. XRF Data for soil samples collected in 2004 (continued).

Transect ID	Depth (cm)	As (mg/kg)	Cd (mg/kg)	Cr (mg/kg)	Cu (mg/kg)	Fe (mg/kg)	Mn (mg/kg)	Pb (mg/kg)	Zn (mg/kg)
T4-C121	75-100	3	9	290	90	21201	604	114	107
T5-8	0-10	-3	-8	259	33	22201	928	113	160
T5-8	10-20	3	9	79	48	30638	1458	125	120
T5-8	20-30	-8	11	221	120	29536	1548	106	89
T5-8	30-40	-13	23	124	78	30048	1744	123	107
T4-D1	0-10	-24	-57	23	-17	9939	483	101	47
T4-D1	10-20	-12	-32	83	-15	15531	456	82	52
T4-D1	20-30	-3	-4	-149	155	24730	752	105	115
T4-D1	30-40	-10	33	-153	295	86619	2202	155	62
T4-D1	40-50	-21	45	-521	80	98601	2527	115	80
T4-D1	50-75	11	14	-185	117	52192	1626	77	95
T4-D1	75-100	2	1	-49	169	65726	1610	88	77
T4-D2	0-10	-31	-67	150	-21	6527	387	97	100
T4-D2	10-20	-17	-55	144	-15	5447	257	92	97
T4-D2	20-30	-8	-25	161	31	12166	519	98	80
T4-D2	30-40	-10	-10	-11	58	16021	683	106	103
T4-D2	40-50	-31	1	-125	44	24679	811	164	129
T4-D2	50-75	16	13	-180	276	105403	2245	118	135
T4-D2	75-100	-18	7	-178	276	35749	1010	115	83
T4-D4	0-10	-22	-65	153	1	7141	388	93	66
T4-D4	10-20	-12	-36	66	10	10795	501	93	40
T4-D4	20-30	-7	-19	-99	59	14051	510	109	93
T4-D4	30-40	6	-2	39	362	35663	832	124	117
T4-D4	40-50	20	35	67	438	132723	3435	113	252
T4-D4	50-75	17	15	88	502	77170	2022	138	327
T4-D4	75-100	-7	22	-87	498	48154	1348	111	154
T4-D7	0-10	-23	-68	176	5	3727	243	85	98
T4-D7	10-20	-36	-62	72	-8	5235	237	114	57
T4-D7	20-30	-13	-41	69	41	9035	381	91	46
T4-D7	30-40	-6	-9	154	79	17054	570	135	127
T4-D7	40-50	1	8	482	381	30609	983	157	146
T4-D7	50-75	-5	29	32	194	67423	1748	140	224
T4-D7	75-100	-9	15	-277	626	51124	1366	150	254
T4-D11	0-10	-22	-63	126	-14	8091	467	89	58
T4-D11	10-20	-15	-46	138	-6	9393	474	91	55
T4-D11	20-30	-4	-17	264	34	14380	530	94	82
T4-D11	30-40	6	9	-157	662	58696	1696	121	191
T4-D11	40-50	5	10	244	738	73323	2414	111	176
T4-D11	50-75	-10	24	204	843	84204	2283	161	248
T4-D11	75-100	7	23	65	935	106428	3492	163	263
T4-D16	0-10	-12	-54	121	-6	6689	340	76	54

Table 15. XRF Data for soil samples collected in 2004 (continued).

Transect ID	Depth (cm)	As (mg/kg)	Cd (mg/kg)	Cr (mg/kg)	Cu (mg/kg)	Fe (mg/kg)	Mn (mg/kg)	Pb (mg/kg)	Zn (mg/kg)
T4-D16	10-20	-6	-21	26	0	10200	442	78	77
T4-D16	20-30	-6	-4	64	49	19352	704	126	123
T4-D16	30-40	-9	11	-6	328	30425	855	146	185
T4-D16	40-50	6	14	-220	471	76483	2057	148	158
T4-D16	50-75	5	28	-2	522	89987	2485	149	167
T4-D16	75-100	-2	10	-105	992	53392	2134	153	366
T4-D22	0-10	-19	-52	-26	-4	11600	427	92	46
T4-D22	10-20	-12	-38	151	22	12716	479	77	41
T4-D22	20-30	-3	-9	61	65	15399	580	104	81
T4-D22	30-40	-21	0	184	354	21599	869	162	196
T4-D22	40-50	-14	-7	-39	349	24392	1081	152	185
T4-D22	50-75	5	12	-28	355	92164	2992	160	228
T4-D22	75-100	-7	36	-87	621	81986	2573	174	342
T4-D29	0-10	-16	-45	126	-15	8449	327	79	56
T4-D29	10-20	-13	-19	168	41	10999	364	83	71
T4-D29	20-30	-5	-12	227	42	16830	518	115	144
T4-D29	30-40	-1	17	-178	467	39274	1134	151	249
T4-D29	40-50	-6	8	-113	457	43181	1350	145	230
T4-D29	50-75	8	19	-218	1226	60613	1675	188	425
T4-D29	75-100	-14	11	196	754	46910	1206	170	350
T4-D37	0-10	-24	-61	154	6	4683	259	105	109
T4-D37	10-20	-6	-28	147	15	10257	404	85	114
T4-D37	20-30	-16	-10	213	16	14428	551	111	163
T4-D37	30-40	-8	-15	223	52	18049	558	111	194
T4-D37	40-50	-2	1	134	327	25747	767	155	163
T4-D37	50-75	-3	0	-390	570	48663	1702	150	215
T4-D37	75-100	-11	6	-49	261	22549	727	132	151
T4-D46	0-10	-15	-47	219	-10	10738	594	86	78
T4-D46	10-20	-13	-14	76	47	16915	532	91	127
T4-D46	20-30	-15	-1	32	52	19097	696	130	173
T4-D46	30-40	-6	-3	-187	179	29960	744	164	247
T4-D46	40-50	-9	7	114	462	37291	1340	160	252
T4-D46	50-75	-20	8	5	397	41643	1441	141	204
T4-D46	75-100	3	31	-229	822	89551	2212	153	323
T4-D56	0-10	-26	-68	53	-16	3501	365	87	66
T4-D56	10-20	-37	-73	98	9	2529	295	115	75
T4-D56	20-30	-7	-41	291	14	8209	341	84	137
T4-D56	30-40	-19	-3	-75	38	14843	419	124	145
T4-D56	40-50	-14	-18	222	89	22821	764	131	194
T4-D56	50-75	-1	2	168	441	33387	1028	152	181
T4-D56	75-100	7	7	-413	482	44699	1287	155	235
T4-D67	0-10	-7	-53	31	7	11293	536	76	62

Table 15. XRF Data for soil samples collected in 2004 (continued).

Transect ID	Depth (cm)	As (mg/kg)	Cd (mg/kg)	Cr (mg/kg)	Cu (mg/kg)	Fe (mg/kg)	Mn (mg/kg)	Pb (mg/kg)	Zn (mg/kg)
T4-D67	10-20	2	-29	102	-6	18152	610	64	50
T4-D67	20-30	-19	6	-129	-13	23600	817	97	102
T4-D67	30-40	-5	-4	93	80	20708	634	130	135
T4-D67	40-50	-4	-8	-16	75	22399	803	125	153
T4-D67	50-75	-5	-15	50	111	18998	636	106	172
T4-D67	75-100	0	5	155	378	24594	783	131	245
T4-D79	0-10	-21	-62	32	-9	9264	508	91	93
T4-D79	10-20	-15	-49	45	18	7400	458	97	75
T4-D79	20-30	-11	-9	15	37	13944	422	88	103
T4-D79	30-40	-19	4	-199	32	17983	390	138	123
T4-D79	40-50	-6	7	450	43	30100	752	116	153
T4-D79	50-75	1	3	189	266	30364	811	144	258
T4-D79	75-100	12	-2	55	422	46047	1569	152	288
T4-D92	0-10	-29	-62	58	9	4744	296	102	111
T4-D92	10-20	-5	-50	193	11	8684	338	84	119
T4-D92	20-30	1	9	66	-37	19971	801	80	93
T4-D92	30-40	-20	4	85	-33	26405	751	87	86
T4-D92	40-50	4	11	181	-2	29082	794	70	89
T4-D92	50-75	-14	-2	137	-29	30528	1018	93	140
T4-D92	75-100	-2	44	-831	384	137679	3692	139	267
T4-D106	0-10	-9	-27	160	25	16188	509	84	54
T4-D106	10-20	-5	4	359	59	23555	850	100	119
T4-D106	20-30	6	0	188	333	27884	702	138	175
T4-D106	30-40	-8	10	-105	366	23960	791	138	232
T4-D106	40-50	11	-4	91	389	35575	1321	120	222
T4-D106	50-75	-9	7	-375	372	56727	1646	156	176
T4-D106	75-100	-7	8	-755	429	89123	2071	163	154
T4-D121	0-10	-6	-24	10	1	13321	1283	83	52
T4-D121	10-20	-1	-12	-4	114	16884	1260	99	73
T4-D121	20-30	-13	9	132	125	20850	1313	117	111
T4-D121	30-40	-8	7	346	191	25719	1430	103	90
T4-D121	40-50	-8	9	321	303	23042	1807	132	168
T4-D121	50-75	-22	9	-126	227	29477	1422	127	158
T4-D121	75-100	-13	17	16	208	44129	1295	127	146
T5-6	0-10	-25	-64	27	-1	8351	540	94	86
T5-6	10-20	-10	-13	226	-11	15176	444	79	88
T5-6	20-30	-22	-8	57	111	16247	598	122	100
T5-6	30-40	-2	-6	171	64	21237	576	104	123
T5-6	40-50	-17	9	-142	107	29787	937	125	145
T5-6	50-75	-3	13	295	48	32870	1048	128	108
T5-6	75-100	-16	8	-243	41	41884	1306	144	99
T6-8	0-10	0	-16	208	922	22975	1421	104	175

Table 15. XRF Data for soil samples collected in 2004 (continued).

Transect ID	Depth (cm)	As (mg/kg)	Cd (mg/kg)	Cr (mg/kg)	Cu (mg/kg)	Fe (mg/kg)	Mn (mg/kg)	Pb (mg/kg)	Zn (mg/kg)
T6-8	10-20	-2	-11	-29	147	23110	881	123	163
T6-8	20-30	-14	-11	-97	105	21365	807	117	140
T6-8	30-40	-3	11	-56	73	33808	1648	142	178
T6-8	40-50	3	11	134	187	26063	1110	133	187
T6-8	50-75	2	2	139	372	29945	1136	130	227
T6-8	75-100	3	9	130	308	14658	581	116	111
T6-W1	0-10	1	-16	29	440	23503	1370	112	176
T6-W1	10-20	0	-4	-181	439	25607	1122	118	154
T6-W1	20-30	2	-8	114	64	27812	885	118	116
T6-W1	30-40	-3	-1	-86	199	31523	1130	141	123
T6-W1	40-50	-4	15	66	239	23413	1066	146	198
T6-W1	50-75	-2	17	-117	231	25483	871	130	127
T6-W1	75-100	4	15	147	390	29783	983	146	181
T6-W2	0-10	-11	-19	54	294	28435	1324	145	140
T6-W2	10-20	-3	-8	133	117	27840	1150	129	149
T6-W2	20-30	8	-8	200	84	31643	1233	121	133
T6-W2	30-40	-19	-2	-430	179	24107	1102	153	170
T6-W2	40-50	-18	7	-79	347	19775	827	164	254
T6-W2	50-75	-9	22	58	310	22489	1153	122	157
T6-W2	75-100	-13	7	-87	434	23593	918	151	181
T6-W4	0-10	-12	-45	-51	648	14031	1003	96	173
T6-W4	10-20	-1	-3	277	103	29665	1202	131	149
T6-W4	20-30	9	-10	-115	113	25262	885	96	159
T6-W4	30-40	1	3	291	184	20587	805	116	205
T6-W4	40-50	-8	13	96	231	18227	552	128	158
T6-W4	50-75	-1	5	184	415	26715	730	128	168
T6-W4	75-100	-7	14	-130	334	33626	926	119	114
T6-W7	0-10	-2	-41	252	444	12707	1274	87	230
T6-W7	10-20	-10	-10	82	80	26268	1161	127	96
T6-W7	20-30	-7	-1	-223	100	18333	803	134	154
T6-W7	30-40	-8	-1	-15	236	19887	631	124	211
T6-W7	40-50	-3	8	45	290	26505	864	104	169
T6-W7	50-75	11	1	-54	598	43351	1190	134	217
T6-W7	75-100	-18	5	23	404	36926	963	154	149
T6-W11	0-10	-6	-6	188	197	21386	724	132	140
T6-W11	10-20	-7	-13	-305	141	21255	620	132	110
T6-W11	20-30	5	-10	-51	197	22290	604	118	187
T6-W11	30-40	-9	21	77	256	22273	683	130	145
T6-W11	40-50	-22	6	-147	126	21510	502	109	61
T6-W11	50-75	20	-3	74	159	36899	1065	69	72
T6-W11	75-100	-9	10	118	160	33608	917	91	74
T6-W16	0-10	-7	-18	27	116	17948	715	121	81

Table 15. XRF Data for soil samples collected in 2004 (continued).

Transect ID	Depth (cm)	As (mg/kg)	Cd (mg/kg)	Cr (mg/kg)	Cu (mg/kg)	Fe (mg/kg)	Mn (mg/kg)	Pb (mg/kg)	Zn (mg/kg)
T6-W16	10-20	0	-23	66	22	17306	610	105	124
T6-W16	20-30	-9	11	345	165	19442	543	115	127
T6-W16	30-40	-4	-3	-46	368	15658	529	106	207
T6-W16	40-50	-13	7	-459	177	13886	486	96	104
T6-W16	50-75	1	10	-240	174	25365	728	72	106
T6-W16	75-100	-9	-2	-236	612	46864	1741	145	266
T6-W22	0-10	-3	-6	-99	44	21315	857	109	73
T6-W22	10-20	5	-4	-48	89	18434	554	89	95
T6-W22	20-30	-17	-7	-87	140	20277	848	140	120
T6-W22	30-40	-13	0	-226	269	16405	596	136	232
T6-W22	40-50	-13	14	-285	180	16253	720	110	110
T6-W22	50-75	3	26	65	478	30803	1553	128	263
T6-W22	75-100	-10	17	38	937	79151	2027	165	257
T6-W29	0-10	5	-32	22	95	17265	647	96	132
T6-W29	10-20	-8	-7	-64	148	21279	629	116	165
T6-W29	20-30	-8	-5	39	289	22862	725	141	253
T6-W29	30-40	-12	9	118	427	26167	829	145	246
T6-W29	40-50	9	3	165	573	41801	1119	158	343
T6-W29	50-75	-2	7	105	761	36735	1025	160	314
T6-W29	75-100	-2	0	-285	706	26161	768	145	285
T6-W37	0-10	-6	-19	144	61	20052	941	107	106
T6-W37	10-20	-3	-9	-273	137	18713	786	101	86
T6-W37	20-30	7	5	14	200	22551	763	113	184
T6-W37	30-40	-9	16	68	521	45536	1286	146	232
T6-W37	40-50	-13	16	167	795	34278	836	165	298
T6-W37	50-75	10	4	-36	987	40785	1173	144	283
T6-W37	75-100	-7	1	206	721	15143	296	131	339
T6-W46	0-10	-2	-23	289	41	16300	760	91	89
T6-W46	10-20	-3	-10	-138	81	18456	563	110	145
T6-W46	20-30	-14	-7	-219	364	22041	607	130	209
T6-W46	30-40	0	9	-267	518	40534	1242	133	228
T6-W46	40-50	-5	-1	-80	650	27342	834	138	274
T6-W46	50-75	-6	6	-10	849	32658	921	143	299
T6-W46	75-100	-17	10	-35	328	12794	394	122	152
T6-W56	0-10	-28	-65	-34	7	7791	364	112	94
T6-W56	10-20	-8	-54	147	64	11273	451	90	45
T6-W56	20-30	-11	-14	-170	68	18779	686	111	89
T6-W56	30-40	-13	11	-287	23	36244	1076	116	73
T6-W56	40-50	-12	-8	93	20	49065	1478	107	53
T6-W56	50-75	-6	22	-255	39	48604	1406	90	57
T6-W56	75-100	-6	-2	-94	73	34283	922	79	109
T6-W67	0-10	-33	-66	-88	28	8600	392	106	69

Table 15. XRF Data for soil samples collected in 2004 (continued).

Transect ID	Depth (cm)	As (mg/kg)	Cd (mg/kg)	Cr (mg/kg)	Cu (mg/kg)	Fe (mg/kg)	Mn (mg/kg)	Pb (mg/kg)	Zn (mg/kg)
T6-W67	10-20	-18	-54	62	96	10893	302	107	73
T6-W67	20-30	-11	-26	117	39	16974	534	117	95
T6-W67	30-40	-16	11	344	61	42632	1022	154	48
T6-W67	40-50	-2	-5	-670	0	68212	1954	113	2
T6-W67	50-75	1	26	-389	-48	66193	1424	83	44
T6-W67	75-100	-14	-3	-3	54	32677	958	105	74
T6-W79	0-10	0	-29	-56	116	14717	489	89	102
T6-W79	10-20	-4	-25	62	48	11403	444	88	56
T6-W79	20-30	-12	-32	-321	41	11078	382	108	59
T6-W79	30-40	-20	-3	-300	-23	25690	703	98	85
T6-W79	40-50	-15	-3	-121	21	26722	666	85	49
T6-W79	50-75	-17	-3	-221	79	20216	842	115	138
T6-W79	75-100	-14	1	96	124	13142	334	99	113
T6-W92	0-10	-5	-46	272	157	13039	441	96	135
T6-W92	10-20	-7	-31	177	237	16464	555	102	101
T6-W92	20-30	5	-12	-120	144	21267	814	87	133
T6-W92	30-40	6	-17	-106	66	28653	752	72	46
T6-W92	40-50	-16	-6	102	125	22700	659	129	38
T6-W92	50-75	-17	11	41	33	23830	795	108	77
T6-W92	75-100	1	1	-237	125	16380	652	111	135
T6-7	0-10	-15	-55	-26	19	8688	533	98	108
T6-7	10-20	-12	-4	168	35	14536	595	98	104
T6-7	20-30	-7	5	175	274	21333	646	139	173
T6-7	30-40	2	13	205	182	56177	1718	130	136
T6-7	40-50	4	11	-55	297	46183	1466	133	180
T6-7	50-75	-1	-2	12	266	29188	823	143	214
T6-7	75-100	0	-3	-31	343	28358	865	144	157
T8-E0	0-10	0	21	-69	1395	47476	2164	149	255
T8-E0	10-20	1	1	88	1730	37972	1901	112	263
T8-E0	20-30	15	10	276	1383	36089	1749	106	184
T8-E0	30-40	-6	29	15	913	37907	1764	157	202
T8-E0	40-50	9	12	318	260	38568	1868	131	105
T8-E0	50-75	-8	5	301	171	30276	834	125	100
T8-E0	75-100	-1	25	37	148	27819	726	133	152
T8-E1	0-10	-3	-13	142	2062	39615	2051	118	236
T8-E1	10-20	7	2	128	1497	37783	1915	136	251
T8-E1	20-30	5	17	-231	1225	37489	2319	143	195
T8-E1	30-40	-13	8	-228	1021	40040	2032	168	215
T8-E1	50-75	-5	5	99	134	27482	1140	119	99
T8-E1	75-100	-14	2	-227	117	30654	787	134	86
T8-E2	0-10	-1	21	46	2260	43208	2005	141	272
T8-E2	10-20	8	6	-118	1801	39983	2162	113	281

Table 15. XRF Data for soil samples collected in 2004 (continued).

Transect ID	Depth (cm)	As (mg/kg)	Cd (mg/kg)	Cr (mg/kg)	Cu (mg/kg)	Fe (mg/kg)	Mn (mg/kg)	Pb (mg/kg)	Zn (mg/kg)
T8-E2	20-30	-7	-11	12	632	35780	1498	141	169
T8-E2	30-40	9	9	-258	149	27807	1340	106	136
T8-E2	40-50	-12	8	-221	111	29669	1248	149	163
T8-E2	50-75	-13	-9	88	125	29138	864	147	93
T8-E2	75-100	-7	5	53	202	27961	1255	120	135
T8-E4	0-10	-3	1	39	1456	43890	2068	140	225
T8-E4	10-20	-21	-2	206	1443	35545	1489	148	187
T8-E4	20-30	-2	2	5	509	28876	1219	125	141
T8-E4	30-40	-1	-4	88	222	32467	1575	130	92
T8-E4	40-50	-1	6	-267	89	31818	1625	131	145
T8-E4	50-75	-9	9	-50	130	30629	1588	93	101
T8-E7	0-10	9	0	39	1314	36064	1699	114	261
T8-E7	10-20	2	-11	16	162	23617	1212	121	105
T8-E7	20-30	-4	10	51	122	31181	1553	127	118
T8-E7	30-40	-18	11	73	146	29032	925	152	100
T8-E7	40-50	-8	-2	54	116	25034	853	116	105
T8-E7	50-75	-9	1	178	127	24302	841	120	122
T8-E11	0-10	12	-16	290	501	26534	932	116	142
T8-E11	10-20	-8	10	169	122	26255	1141	126	114
T8-E11	20-30	-5	9	-243	52	30362	1844	132	118
T8-E11	30-40	3	6	126	182	31161	1880	107	110
T8-E11	40-50	-5	9	-81	140	30150	1482	126	119
T8-E11	50-75	-12	1	-72	109	29015	1473	117	96
T8-E16	0-10	3	-6	193	264	27148	1247	116	128
T8-E16	10-20	-4	-6	86	86	26676	1007	126	106
T8-E16	20-30	-13	-7	-250	111	26682	1178	129	136
T8-E16	30-40	2	8	-11	104	25629	1427	111	70
T8-E16	40-50	-6	5	65	38	25285	1403	84	90
T8-E16	50-75	-21	-4	52	51	25370	1318	117	71
T8-E22	0-10	9	-31	-43	131	18903	747	97	96
T8-E22	10-20	-2	-3	145	72	27771	1259	124	116
T8-E22	20-30	-14	-10	155	47	23969	1412	100	91
T8-E22	30-40	-15	10	96	90	31271	1377	108	102
T8-E29	0-10	8	5	-55	92	27005	969	114	101
T8-E29	10-20	-5	-11	159	78	28315	1332	99	136
T8-E29	20-30	-12	14	-329	82	27964	1430	110	108
T8-E29	30-40	-12	10	-259	52	27514	1498	107	80
T8-E37	0-10	-6	-1	30	117	26688	1420	131	114
T8-E37	10-20	-12	-6	-8	122	27122	1386	135	108
T8-E37	20-30	-6	3	294	103	27713	1331	131	122
T8-E37	30-40	-11	-6	163	76	26621	1490	114	88

Table 15. XRF Data for soil samples collected in 2004 (continued).

Transect ID	Depth (cm)	As (mg/kg)	Cd (mg/kg)	Cr (mg/kg)	Cu (mg/kg)	Fe (mg/kg)	Mn (mg/kg)	Pb (mg/kg)	Zn (mg/kg)
T8-E37	40-50	-7	11	139	100	28722	1581	101	92
T8-E46	0-10	6	-14	213	90	29566	1487	122	129
T8-E46	10-20	-5	-10	261	25	24954	1159	118	129
T8-E46	20-30	-7	3	-69	101	25118	1066	98	87
T8-E46	30-40	-13	25	-42	53	30537	1472	103	96
T8-E46	40-50	-5	17	13	121	31850	1794	112	99
T8-E46	50-75	-15	-2	-118	40	26414	1381	113	79
T8-9	0-10	-3	17	-401	919	44227	1902	126	236
T8-9	10-20	-3	2	190	824	39328	1606	133	159
T8-9	20-30	3	13	-27	268	30499	1519	108	140
T8-9	30-40	-20	6	235	232	32772	1491	150	151
T8-9	40-50	-9	10	302	139	30748	1825	137	125
T8-9	50-75	-8	-1	-43	114	32081	1449	105	75
T8-W1	0-10	15	-2	150	827	40056	1899	123	195
T8-W1	10-20	-2	-4	337	874	33897	1535	139	170
T8-W1	20-30	1	3	163	1114	34658	1805	124	207
T8-W1	30-40	-7	8	-101	637	36057	1975	122	143
T8-W1	40-50	-5	-2	172	166	29406	1339	105	88
T8-W1	50-75	-16	-1	90	155	27585	1374	138	120
T8-W2	0-10	4	-14	-107	832	38110	1866	116	206
T8-W2	10-20	-11	-3	-47	1329	40139	2142	161	186
T8-W2	20-30	-7	8	-185	862	34131	1466	126	187
T8-W2	30-40	1	17	130	179	35759	1636	87	103
T8-W2	40-50	-5	10	16	286	36196	1603	129	100
T8-W2	50-75	-8	3	22	193	31616	1478	115	133
T8-W4	0-10	10	12	-121	896	45646	2149	140	214
T8-W4	10-20	12	6	70	992	36956	1543	119	184
T8-W4	20-30	-6	6	160	726	37257	1564	144	155
T8-W4	30-40	5	-2	75	293	32278	1707	137	123
T8-W4	40-50	-12	13	91	172	28261	1377	116	100
T8-W4	50-75	-17	11	-29	82	25366	1171	109	108
T8-W7	0-10	-2	0	-218	1042	44120	2271	162	223
T8-W7	10-20	-12	4	-113	1118	37443	1909	134	246
T8-W7	20-30	7	9	117	506	28537	1398	97	159
T8-W7	30-40	-4	5	-152	186	30710	1576	112	141
T8-W7	40-50	-6	5	186	223	29595	1576	117	95
T8-W11	0-10	-7	17	41	970	47290	2328	162	233
T8-W11	10-20	0	16	210	1013	43202	1910	141	185
T8-W11	20-30	-16	-4	345	637	36602	1790	163	141
T8-W11	30-40	-8	-6	-193	378	31670	1505	132	119

Table 15. XRF Data for soil samples collected in 2004 (continued).

Transect ID	Depth (cm)	As (mg/kg)	Cd (mg/kg)	Cr (mg/kg)	Cu (mg/kg)	Fe (mg/kg)	Mn (mg/kg)	Pb (mg/kg)	Zn (mg/kg)
T8-W16	0-10	11	23	348	936	41346	2037	144	149
T8-W16	10-20	11	-6	112	835	37414	1737	122	171
T8-W16	20-30	-15	8	-17	466	35975	1741	145	132
T8-W16	30-40	-12	14	39	114	32872	1551	113	112
T8-W16	40-50	-13	5	141	146	29592	1372	123	115
T8-W22	0-10	7	0	169	1195	41598	1527	137	213
T8-W22	10-20	-5	14	200	701	36871	1614	141	162
T8-W22	20-30	-2	9	-303	326	28918	1301	112	117
T8-W22	30-40	-8	-4	44	151	30125	1671	111	104
T8-W22	40-50	10	-1	-217	12	27200	1482	62	110
T8-W22	50-75	-12	-11	43	62	25757	1501	116	77
T8-W29	0-10	-7	6	-365	816	39557	1590	134	188
T8-W29	10-20	-15	16	-413	1130	43834	2470	167	242
T8-W29	20-30	6	9	-203	806	34048	1766	104	218
T8-W29	30-40	-15	-1	-445	559	30058	1555	102	148
T8-W37	0-10	-2	9	-140	989	41185	2078	143	196
T8-W37	10-20	-2	-2	98	1002	40924	1763	131	211
T8-W37	20-30	-13	25	117	456	32116	1816	115	131
T8-W46	0-10	-13	-36	79	966	26392	873	120	194
T8-W46	10-20	-13	19	12	675	37383	1443	158	145
T8-W46	20-30	-11	-6	117	331	21079	795	144	141
T8-W46	30-40	-13	2	-202	60	24587	1078	135	104
T8-W46	40-50	-8	4	-149	76	32536	1240	140	76
T8-W46	50-75	-2	0	-90	85	19794	733	112	131
T8-W46	75-100	-16	11	-219	124	31679	952	126	76
T19-9	0-10	17	26	-161	1067	77344	3014	171	226
T19-9	10-20	-4	10	-339	890	57269	2567	195	195
T19-9	20-30	-1	18	57	618	39249	2015	157	313
T19-9	40-40	-4	0	464	148	24651	701	156	133
T20-9	0-10	-13	1	78	-9	24130	1191	93	48
T20-9	10-20	-10	4	110	-68	26881	1130	80	51
T20-9	20-30	-11	33	380	-49	31436	1810	85	82
T20-9	30-40	3	17	963	-42	45821	8684	97	40
T20-9	40-50	-9	14	-66	-37	33417	1938	88	21

Table 16. ICP Data for soil samples collected in 2004.

Transect ID	Depth (cm)	As (mg/kg)	Cd (mg/kg)	Cr (mg/kg)	Cu (mg/kg)	Fe (%)	Pb (mg/kg)	Mn (mg/kg)	Zn (mg/kg)
T3-6	0-10	3	<1	3	17	0.7	19	92	71
T3-6	10-20	5	1	22	76	1.4	41	81	118
T3-6	20-30	2	<1	33	106	1.8	51	119	167
T3-6	30-40	3	<1	40	175	2.3	75	144	199
T3-6	40-50	5	<1	39	352	2.6	95	199	227
T3-6	50-75	14	<1	41	716	4.9	88	655	291
T3-6	75-100	12	1	36	838	4.4	93	583	282
T4-A1	0-10	5	<1	12	38	1.2	29	74	43
T4-A1	10-20	3	<1	30	107	1.5	53	75	79
T4-A1	20-30	4	<1	38	184	2.2	75	98	131
T4-A1	30-40	9	<1	40	407	4.2	82	160	161
T4-A1	40-50	16	1	35	351	7.3	67	420	188
T4-A1	50-75	23	1	29	687	7.5	92	720	288
T4-A1	75-100	16	1	26	594	7.5	72	326	230
T4-C37	0-10	5	<1	18	69	1.3	47	154	50
T4-C37	10-20	3	<1	30	117	1.5	61	128	85
T4-C37	20-30	4	<1	38	250	2.4	82	214	106
T4-C37	30-40	4	<1	40	563	2.7	86	373	128
T4-C37	40-50	10	4	31	1564	6.5	104	589	459
T4-C37	50-75	27	3	22	1957	14.3	87	559	423
T4-C37	75-100	22	4	22	1805	14.0	87	467	389
T4-D106	0-10	11	<1	27	47	1.8	30	164	79
T4-D106	10-20	5	<1	51	94	2.4	45	199	138
T4-D106	20-30	9	<1	38	378	3.3	101	229	246
T4-D106	30-40	8	<1	38	481	2.7	93	305	265
T4-D106	40-50	16	<1	37	519	3.9	90	451	283
T4-D106	50-75	11	1	33	526	5.7	91	311	232
T4-D106	75-100	14	1	28	545	7.6	84	180	242
T6-W1	0-10	11	1	34	180	3.4	87	229	180
T6-W1	10-20	9	2	32	575	3.0	79	473	189
T6-W1	20-30	11	1	36	189	3.5	90	238	186
T6-W1	30-40	12	<1	34	232	3.5	95	495	176
T6-W1	40-50	6	<1	33	284	2.5	89	563	217
T6-W1	50-75	10	1	24	331	2.5	63	288	154
T6-W1	75-100	13	<1	32	564	3.2	93	223	216
T6-W29	0-10	9	2	31	165	2.3	69	271	185
T6-W29	10-20	7	<1	36	188	2.4	74	182	224
T6-W29	20-30	5	<1	35	301	2.2	75	170	251
T6-W29	30-40	9	1	33	501	2.8	84	219	281
T6-W29	40-50	21	1	35	665	4.4	110	194	367
T6-W29	50-75	14	1	32	913	3.8	101	199	355
T6-W29	75-100	11	1	34	955	3.0	108	165	329

Table 16. ICP Data for soil samples collected in 2004 (continued).

Transect ID	Depth (cm)	As (mg/kg)	Cd (mg/kg)	Cr (mg/kg)	Cu (mg/kg)	Fe (%)	Pb (mg/kg)	Mn (mg/kg)	Zn (mg/kg)
T8-E4	0-10	15	2	25	1855	4.8	92	1075	286
T8-E4	10-20	15	2	26	2082	4.6	93	979	298
T8-E4	20-30	14	<1	29	703	3.6	82	662	196
T8-E4	30-40	11	<1	29	197	3.3	76	848	156
T8-E4	40-50	9	<1	27	186	3.1	64	771	133
T8-E4	50-75	9	<1	26	219	3.6	54	873	141
T8-W4	0-10	16	2	21	1043	4.9	114	1043	260
T8-W4	10-20	15	1	27	1244	4.3	90	775	220
T8-W4	20-30	13	<1	26	875	3.8	83	711	189
T8-W4	30-40	11	<1	26	424	3.5	96	847	155
T8-W4	40-50	9	<1	27	178	3.0	55	739	119
T8-W4	50-75	11	1	33	153	2.9	47	755	114
T11-E37	0-10	13	2	25	1231	4.1	88	1129	279
T11-E37	10-20	14	1	25	546	3.9	84	1475	251
T11-E37	20-30	14	<1	23	625	4.4	72	1207	253
T11-E37	30-40	14	2	25	1661	6.2	77	1882	428
T11-E37	40-50	17	3	23	2719	7.8	85	2826	513
T11-E37	50-75	25	4	23	2934	8.2	85	2962	526
T11-E37	75-100	38	4	25	2392	7.4	76	4078	565
T11-E7	0-10	14	4	23	3086	3.7	75	1427	430
T11-E7	10-20	10	2	24	1450	3.3	54	1044	248
T11-E7	20-30	10	2	25	594	3.5	55	953	167
T11-E7	30-40	11	1	27	189	3.3	67	841	151
T11-E7	40-50	10	<1	28	219	3.3	61	866	142
T11-E7	50-75	6	<1	29	147	2.6	46	719	104
T11-E7	75-100	7	1	26	160	2.8	47	827	117
T11-W7	0-10	16	6	25	7088	7.1	105	1327	775
T11-W7	10-20	14	5	24	5839	7.0	97	1198	691
T11-W7	20-30	14	2	28	477	3.2	75	960	248
T11-W7	30-40	12	1	27	539	3.2	80	870	212
T11-W7	40-50	13	1	25	533	3.6	95	1109	199
T11-W7	50-75	9	<1	26	202	3.5	66	890	137
T19-9	0-10	23	3	16	1291	8.1	126	942	319
T19-9	10-20	21	2	19	1152	6.5	152	1185	291
T19-9	20-30	16	2	18	691	3.8	96	931	295
T19-9	40-40	9	<1	18	225	2.7	87	254	158
T20-9	0-10	9	<1	38	26	2.6	34	523	83
T20-9	10-20	8	<1	41	25	2.8	29	538	80
T20-9	20-30	9	<1	47	21	2.8	31	853	70
T20-9	30-40	23	2	33	34	4.8	56	7778	120
T20-9	40-50	7	<1	46	25	2.8	32	958	73

Carbon and Nitrogen Results

Table 17. Carbon and nitrogen data for soil samples collected in 2004.

Transect ID	Depth (cm)	Carbon (%)	Nitrogen (%)		Transect ID	Depth (cm)	Carbon (%)	Nitrogen (%)
T3-6	0-10	46.79	1.798		T6-W29	0-10	14.57	1.082
T3-6	10-20	19.99	1.184		T6-W29	10-20	6.80	0.587
T3-6	20-30	7.84	0.666		T6-W29	20-30	3.04	0.298
T3-6	30-40	2.48	0.208		T6-W29	30-40	1.67	0.170
T3-6	40-50	1.00	0.107		T6-W29	40-50	1.13	0.107
T3-6	50-75	0.72	0.064		T6-W29	50-75	0.88	0.067
					T6-W29	75-100	1.06	0.105
T4-A1	0-10	32.45	1.974					
T4-A1	10-20	13.18	1.082		T8-E4	0-10	4.08	0.249
T4-A1	20-30	4.65	0.403		T8-E4	10-20	5.33	0.311
T4-A1	30-40	1.85	0.164		T8-E4	20-30	5.54	0.348
T4-A1	40-50	1.30	0.118		T8-E4	30-40	3.22	0.190
T4-A1	50-75	0.57	0.056		T8-E4	40-50	2.94	0.145
T4-A1	75-100	0.64	0.057		T8-E4	50-75	0.96	0.065
T4-C37	0-10	24.33	1.665		T8-W4	0-10	3.00	0.177
T4-C37	10-20	12.31	0.989		T8-W4	10-20	2.94	0.208
T4-C37	20-30	2.79	0.264		T8-W4	20-30	3.07	0.209
T4-C37	30-40	1.86	0.168		T8-W4	30-40	2.02	0.159
T4-C37	40-50	0.95	0.081		T8-W4	40-50	0.91	0.072
T4-C37	50-75	0.68	0.058		T8-W4	50-75	0.82	0.063
T4-C37	75-100	0.60	0.058					
					T11-E37	0-10	7.47	0.491
T4-D106	0-10	25.39	1.501		T11-E37	10-20	3.01	0.238
T4-D106	10-20	5.34	0.358		T11-E37	20-30	0.78	0.065
T4-D106	20-30	1.24	0.105		T11-E37	30-40	1.23	0.113
T4-D106	30-40	0.79	0.059		T11-E37	40-50	1.40	0.107
T4-D106	40-50	0.71	0.063		T11-E37	50-75	1.03	0.095
T4-D106	50-75	0.51	0.048		T11-E37	75-100	1.28	0.099
T4-D106	75-100	0.56	0.053					
					T11-E7	0-10	0.20	0.779
T6-W1	0-10	15.13	0.928		T11-E7	10-20	4.98	0.248
T6-W1	10-20	9.14	0.650		T11-E7	20-30	1.65	0.087
T6-W1	20-30	4.96	0.441		T11-E7	30-40	4.33	0.274
T6-W1	30-40	2.96	0.262		T11-E7	40-50	2.63	0.162
T6-W1	40-50	1.28	0.135		T11-E7	50-75	0.69	0.045
T6-W1	50-75	0.52	0.049		T11-E7	75-100	0.52	0.037
T6-W1	75-100	0.94	0.066					

Table 17. Carbon and nitrogen data for soil samples collected in 2004 (continued).

Transect ID	Depth (cm)	Carbon (%)	Nitrogen (%)		Transect ID	Depth (cm)	Carbon (%)	Nitrogen (%)
T11-W7	0-10	11.51	0.630		T19-9	0-10	2.27	0.128
T11-W7	10-20	12.07	0.725		T19-9	10-20	1.51	0.102
T11-W7	20-30	7.26	0.464		T19-9	20-30	3.48	0.186
T11-W7	30-40	6.88	0.439		T19-9	40-40	5.69	0.298
T11-W7	40-50	1.96	0.160					
T11-W7	50-75	0.67	0.043		T20-9	0-10	9.34	0.770
					T20-9	10-20	6.78	0.587
					T20-9	20-30	1.29	0.131
					T20-9	30-40	1.64	0.158
					T20-9	40-50	0.62	0.065

Stream Sediment Chemistry Data

Table 18. Stream sediment data for lower Daisy Creek and upper Stillwater River.

Sample ID	Ag (mg/kg)	As (mg/kg)	Cd (mg/kg)	Cr (mg/kg)	Cu (mg/kg)	Hg (mg/kg)	Pb (mg/kg)	Zn (mg/kg)
DSC-11000	<20	23	2	13	2060	<0.5J	86	404
DSC-11430	<20	14	<2	14	1140	<0.5J	83	297
DSC-12000	<20	16	2	17	2030	<0.5J	76	401
DSC-13000	<20	13	<2	15	1440	<0.5J	69	324
DSC-13490	<20	16	<2	17	1110	<0.5J	88	287
DSC-14000	<20	17	<2	18	1110	<0.5J	82	312
DSC-15000	<20	17	<2	16	1180	<0.5J	64	320
DSC-15675	<20	14	<2	16	1220	<0.5J	54	321

J signifies estimated values for Hg (mercury).

ANOVA Results

Table 19. ANOVA significance results between pre-mining and post-mining metal concentrations for the marsh soils.

Levene's Test of Equality of Error Variances

Dependent Variable	F	df1	df2	Sig.
Copper	4.973	1	32	.033
Lead	.242	1	32	.626
Zinc	2.224	1	32	.146

Tests the null hypothesis that the error variance of the dependent variable is equal across groups.

Tests of Between-Subjects Effects

Dependent Variable: Copper

Source	Type III Sum of Squares	df	Mean Square	F	Sig.
Corrected Model	1444216.085[a]	1	1444216.085	6.924	.013
Intercept	2924281.261	1	2924281.261	14.019	.001
PrePost	1444216.085	1	1444216.085	6.924	.013
Error	6674908.298	32	208590.884		
Total	18764731.000	34			
Corrected Total	8119124.382	33			

[a] R Squared = .178 (Adjusted R Squared = .152)

Dependent Variable: Lead

Source	Type III Sum of Squares	df	Mean Square	F	Sig.
Corrected Model	3746.477[a]	1	3746.477	10.079	.003
Intercept	88110.006	1	88110.006	237.035	.000
PrePost	3746.477	1	3746.477	10.079	.003
Error	11894.964	32	371.718		
Total	210357.000	34			
Corrected Total	15641.441	33			

[a] R Squared = .240 (Adjusted R Squared = .216)

Dependent Variable: Zinc

Source	Type III Sum of Squares	df	Mean Square	F	Sig.
Corrected Model	143982.438[a]	1	143982.438	12.975	.001
Intercept	617003.144	1	617003.144	55.600	.000
PrePost	143982.438	1	143982.438	12.975	.001
Error	355112.298	32	11097.259		
Total	2327719.000	34			
Corrected Total	499094.735	33			

[a] R Squared = .288 (Adjusted R Squared = .266)

Table 20. ANOVA significance results between pre-mining and post-mining metal concentrations for the floodplain soils.

Levene's Test of Equality of Error Variances

Dependent Variable	F	df1	df2	Sig.
Copper	3.298	1	38	.077
Lead	.005	1	38	.942
Zinc	.028	1	38	.869

Tests the null hypothesis that the error variance of the dependent variable is equal across groups.

Tests of Between-Subjects Effects

Dependent Variable: Copper

Source	Type III Sum of Squares	df	Mean Square	F	Sig.
Corrected Model	4722438.400[(a)]	1	4722438.400	2.160	.150
Intercept	49195240.000	1	49195240.000	22.499	.000
Pre-Post Mining	4722438.400	1	4722438.400	2.160	.150
Error	83088867.600	38	2186549.147		
Total	137006546.000	40			
Corrected Total	87811306.000	39			

[a] R Squared = .054 (Adjusted R Squared = .029)

Dependent Variable: Lead

Source	Type III Sum of Squares	df	Mean Square	F	Sig.
Corrected Model	632.025[(a)]	1	632.025	2.340	.134
Intercept	241647.025	1	241647.025	894.645	.000
PrePost	632.025	1	632.025	2.340	.134
Error	10263.950	38	270.104		
Total	252543.000	40			
Corrected Total	10895.975	39			

[a] R Squared = .058 (Adjusted R Squared = .033)

Dependent Variable: Zinc

Source	Type III Sum of Squares	df	Mean Square	F	Sig.
Corrected Model	8497.225[(a)]	1	8497.225	.328	.570
Intercept	2585214.025	1	2585214.025	99.738	.000
PrePost	8497.225	1	8497.225	.328	.570
Error	984963.750	38	25920.099		
Total	3578675.000	40			
Corrected Total	993460.975	39			

[a] R Squared = .009 (Adjusted R Squared = -.018)

Table 21. ANOVA results (LSD) for copper concentrations by depth in the marsh.

(I) PrePost	(J) PrePost	Mean Difference (I-J)	Std. Error	Sig.	95% Confidence Interval	
					Lower Bound	Upper Bound
0-10	10-20	6.3049	40.77390	.877	-73.7750	86.3849
	20-30	-46.8860	40.77390	.251	-126.9659	33.1939
	30-40	-181.0860(*)	40.77390	.000	-261.1659	-101.0061
	40-50	-298.4410(*)	40.77390	.000	-378.5209	-218.3611
	50-75	-405.9396(*)	40.89365	.000	-486.2548	-325.6245
	75-100	-464.6456(*)	41.39835	.000	-545.9520	-383.3393
10-20	0-10	-6.3049	40.77390	.877	-86.3849	73.7750
	20-30	-53.1909	40.77390	.193	-133.2709	26.8890
	30-40	-187.3909(*)	40.77390	.000	-267.4709	-107.3110
	40-50	-304.7459(*)	40.77390	.000	-384.8259	-224.6660
	50-75	-412.2446(*)	40.89365	.000	-492.5597	-331.9295
	75-100	-470.9506(*)	41.39835	.000	-552.2569	-389.6442
20-30	0-10	46.8860	40.77390	.251	-33.1939	126.9659
	10-20	53.1909	40.77390	.193	-26.8890	133.2709
	30-40	-134.2000(*)	40.77390	.001	-214.2799	-54.1201
	40-50	-251.5550(*)	40.77390	.000	-331.6349	-171.4751
	50-75	-359.0536(*)	40.89365	.000	-439.3688	-278.7385
	75-100	-417.7596(*)	41.39835	.000	-499.0660	-336.4533
30-40	0-10	181.0860(*)	40.77390	.000	101.0061	261.1659
	10-20	187.3909(*)	40.77390	.000	107.3110	267.4709
	20-30	134.2000(*)	40.77390	.001	54.1201	214.2799
	40-50	-117.3550(*)	40.77390	.004	-197.4349	-37.2751
	50-75	-224.8536(*)	40.89365	.000	-305.1688	-144.5385
	75-100	-283.5596(*)	41.39835	.000	-364.8660	-202.2533
40-50	0-10	298.4410(*)	40.77390	.000	218.3611	378.5209
	10-20	304.7459(*)	40.77390	.000	224.6660	384.8259
	20-30	251.5550(*)	40.77390	.000	171.4751	331.6349
	30-40	117.3550(*)	40.77390	.004	37.2751	197.4349
	50-75	-107.4986(*)	40.89365	.009	-187.8138	-27.1835
	75-100	-166.2046(*)	41.39835	.000	-247.5110	-84.8983
50-75	0-10	405.9396(*)	40.89365	.000	325.6245	486.2548
	10-20	412.2446(*)	40.89365	.000	331.9295	492.5597
	20-30	359.0536(*)	40.89365	.000	278.7385	439.3688
	30-40	224.8536(*)	40.89365	.000	144.5385	305.1688
	40-50	107.4986(*)	40.89365	.009	27.1835	187.8138
	75-100	-58.7060	41.51629	.158	-140.2440	22.8320
75-100	0-10	464.6456(*)	41.39835	.000	383.3393	545.9520
	10-20	470.9506(*)	41.39835	.000	389.6442	552.2569
	20-30	417.7596(*)	41.39835	.000	336.4533	499.0660
	30-40	283.5596(*)	41.39835	.000	202.2533	364.8660
	40-50	166.2046(*)	41.39835	.000	84.8983	247.5110
	50-75	58.7060	41.51629	.158	-22.8320	140.2440

Based on observed means.

* The mean difference is significant at the .05 level.

Table 22. ANOVA results (LSD) for lead concentrations by depth in the marsh.

(I) PrePost	(J) PrePost	Mean Difference (I-J)	Std. Error	Sig.	95% Confidence Interval	
					Lower Bound	Upper Bound
0-10	10-20	-2.9339	2.22126	.187	-7.2965	1.4286
	20-30	-11.7006(*)	2.22126	.000	-16.0632	-7.3380
	30-40	-18.8718(*)	2.22126	.000	-23.2344	-14.5092
	40-50	-25.9786(*)	2.22126	.000	-30.3412	-21.6160
	50-75	-24.2841(*)	2.22779	.000	-28.6595	-19.9088
	75-100	-24.3073(*)	2.25528	.000	-28.7366	-19.8779
10-20	0-10	2.9339	2.22126	.187	-1.4286	7.2965
	20-30	-8.7667(*)	2.22126	.000	-13.1292	-4.4041
	30-40	-15.9379(*)	2.22126	.000	-20.3004	-11.5753
	40-50	-23.0447(*)	2.22126	.000	-27.4072	-18.6821
	50-75	-21.3502(*)	2.22779	.000	-25.7256	-16.9748
	75-100	-21.3733(*)	2.25528	.000	-25.8027	-16.9440
20-30	0-10	11.7006(*)	2.22126	.000	7.3380	16.0632
	10-20	8.7667(*)	2.22126	.000	4.4041	13.1292
	30-40	-7.1712(*)	2.22126	.001	-11.5338	-2.8086
	40-50	-14.2780(*)	2.22126	.000	-18.6406	-9.9154
	50-75	-12.5835(*)	2.22779	.000	-16.9589	-8.2082
	75-100	-12.6067(*)	2.25528	.000	-17.0360	-8.1773
30-40	0-10	18.8718(*)	2.22126	.000	14.5092	23.2344
	10-20	15.9379(*)	2.22126	.000	11.5753	20.3004
	20-30	7.1712(*)	2.22126	.001	2.8086	11.5338
	40-50	-7.1068(*)	2.22126	.001	-11.4694	-2.7442
	50-75	-5.4123(*)	2.22779	.015	-9.7877	-1.0370
	75-100	-5.4355(*)	2.25528	.016	-9.8648	-1.0061
40-50	0-10	25.9786(*)	2.22126	.000	21.6160	30.3412
	10-20	23.0447(*)	2.22126	.000	18.6821	27.4072
	20-30	14.2780(*)	2.22126	.000	9.9154	18.6406
	30-40	7.1068(*)	2.22126	.001	2.7442	11.4694
	50-75	1.6945	2.22779	.447	-2.6809	6.0698
	75-100	1.6713	2.25528	.459	-2.7580	6.1007
50-75	0-10	24.2841(*)	2.22779	.000	19.9088	28.6595
	10-20	21.3502(*)	2.22779	.000	16.9748	25.7256
	20-30	12.5835(*)	2.22779	.000	8.2082	16.9589
	30-40	5.4123(*)	2.22779	.015	1.0370	9.7877
	40-50	-1.6945	2.22779	.447	-6.0698	2.6809
	75-100	-.0231	2.26171	.992	-4.4651	4.4189
75-100	0-10	24.3073(*)	2.25528	.000	19.8779	28.7366
	10-20	21.3733(*)	2.25528	.000	16.9440	25.8027
	20-30	12.6067(*)	2.25528	.000	8.1773	17.0360
	30-40	5.4355(*)	2.25528	.016	1.0061	9.8648
	40-50	-1.6713	2.25528	.459	-6.1007	2.7580
	50-75	.0231	2.26171	.992	-4.4189	4.4651

Based on observed means.

* The mean difference is significant at the .05 level.

Table 23. ANOVA results (LSD) for zinc concentrations by depth in the marsh.

(I) PrePost	(J) PrePost	Mean Difference (I-J)	Std. Error	Sig.	95% Confidence Interval	
					Lower Bound	Upper Bound
0-10	10-20	-2.0019	9.81255	.838	-21.2737	17.2699
	20-30	-33.3322(*)	9.81255	.001	-52.6040	-14.0603
	30-40	-58.0378(*)	9.81255	.000	-77.3096	-38.7659
	40-50	-80.9220(*)	9.81255	.000	-100.1939	-61.6502
	50-75	-104.1138(*)	9.84136	.000	-123.4422	-84.7853
	75-100	-116.6929(*)	9.96282	.000	-136.2599	-97.1259
10-20	0-10	2.0019	9.81255	.838	-17.2699	21.2737
	20-30	-31.3303(*)	9.81255	.001	-50.6021	-12.0584
	30-40	-56.0359(*)	9.81255	.000	-75.3077	-36.7640
	40-50	-78.9201(*)	9.81255	.000	-98.1920	-59.6483
	50-75	-102.1119(*)	9.84136	.000	-121.4403	-82.7834
	75-100	-114.6910(*)	9.96282	.000	-134.2579	-95.1240
20-30	0-10	33.3322(*)	9.81255	.001	14.0603	52.6040
	10-20	31.3303(*)	9.81255	.001	12.0584	50.6021
	30-40	-24.7056(*)	9.81255	.012	-43.9774	-5.4338
	40-50	-47.5898(*)	9.81255	.000	-66.8617	-28.3180
	50-75	-70.7816(*)	9.84136	.000	-90.1100	-51.4532
	75-100	-83.3607(*)	9.96282	.000	-102.9277	-63.7937
30-40	0-10	58.0378(*)	9.81255	.000	38.7659	77.3096
	10-20	56.0359(*)	9.81255	.000	36.7640	75.3077
	20-30	24.7056(*)	9.81255	.012	5.4338	43.9774
	40-50	-22.8843(*)	9.81255	.020	-42.1561	-3.6124
	50-75	-46.0760(*)	9.84136	.000	-65.4044	-26.7476
	75-100	-58.6551(*)	9.96282	.000	-78.2221	-39.0881
40-50	0-10	80.9220(*)	9.81255	.000	61.6502	100.1939
	10-20	78.9201(*)	9.81255	.000	59.6483	98.1920
	20-30	47.5898(*)	9.81255	.000	28.3180	66.8617
	30-40	22.8843(*)	9.81255	.020	3.6124	42.1561
	50-75	-23.1918(*)	9.84136	.019	-42.5202	-3.8633
	75-100	-35.7708(*)	9.96282	.000	-55.3378	-16.2039
50-75	0-10	104.1138(*)	9.84136	.000	84.7853	123.4422
	10-20	102.1119(*)	9.84136	.000	82.7834	121.4403
	20-30	70.7816(*)	9.84136	.000	51.4532	90.1100
	30-40	46.0760(*)	9.84136	.000	26.7476	65.4044
	40-50	23.1918(*)	9.84136	.019	3.8633	42.5202
	75-100	-12.5791	9.99121	.209	-32.2018	7.0436
75-100	0-10	116.6929(*)	9.96282	.000	97.1259	136.2599
	10-20	114.6910(*)	9.96282	.000	95.1240	134.2579
	20-30	83.3607(*)	9.96282	.000	63.7937	102.9277
	30-40	58.6551(*)	9.96282	.000	39.0881	78.2221
	40-50	35.7708(*)	9.96282	.000	16.2039	55.3378
	50-75	12.5791	9.99121	.209	-7.0436	32.2018

Based on observed means.

* The mean difference is significant at the .05 level.

Table 24. ANOVA results (LSD) for copper concentrations by depth in the floodplain.

(I) PrePost	(J) PrePost	Mean Difference (I-J)	Std. Error	Sig.	95% Confidence Interval	
					Lower Bound	Upper Bound
0-10	10-20	920.7731(*)	223.60653	.000	480.4306	1361.1156
	20-30	1592.5656(*)	223.60653	.000	1152.2231	2032.9081
	30-40	1697.5129(*)	224.87343	.000	1254.6755	2140.3502
	40-50	1740.0493(*)	232.04746	.000	1283.0843	2197.0143
	50-75	1872.0663(*)	245.26741	.000	1389.0676	2355.0650
	75-100	1761.5063(*)	333.97334	.000	1103.8213	2419.1913
10-20	0-10	-920.7731(*)	223.60653	.000	-1361.1156	-480.4306
	20-30	671.7925(*)	223.60653	.003	231.4500	1112.1350
	30-40	776.7397(*)	224.87343	.001	333.9023	1219.5771
	40-50	819.2762(*)	232.04746	.000	362.3112	1276.2412
	50-75	951.2932(*)	245.26741	.000	468.2944	1434.2919
	75-100	840.7332(*)	333.97334	.012	183.0482	1498.4182
20-30	0-10	-1592.5656(*)	223.60653	.000	-2032.9081	-1152.2231
	10-20	-671.7925(*)	223.60653	.003	-1112.1350	-231.4500
	30-40	104.9472	224.87343	.641	-337.8902	547.7846
	40-50	147.4837	232.04746	.526	-309.4813	604.4487
	50-75	279.5007	245.26741	.256	-203.4981	762.4994
	75-100	168.9407	333.97334	.613	-488.7443	826.6257
30-40	0-10	-1697.5129(*)	224.87343	.000	-2140.3502	-1254.6755
	10-20	-776.7397(*)	224.87343	.001	-1219.5771	-333.9023
	20-30	-104.9472	224.87343	.641	-547.7846	337.8902
	40-50	42.5365	233.26852	.855	-416.8332	501.9061
	50-75	174.5534	246.42298	.479	-310.7209	659.8278
	75-100	63.9935	334.82290	.849	-595.3645	723.3514
40-50	0-10	-1740.0493(*)	232.04746	.000	-2197.0143	-1283.0843
	10-20	-819.2762(*)	232.04746	.000	-1276.2412	-362.3112
	20-30	-147.4837	232.04746	.526	-604.4487	309.4813
	30-40	-42.5365	233.26852	.855	-501.9061	416.8332
	50-75	132.0170	252.98666	.602	-366.1830	630.2170
	75-100	21.4570	339.68270	.950	-647.4713	690.3853
50-75	0-10	-1872.0663(*)	245.26741	.000	-2355.0650	-1389.0676
	10-20	-951.2932(*)	245.26741	.000	-1434.2919	-468.2944
	20-30	-279.5007	245.26741	.256	-762.4994	203.4981
	30-40	-174.5534	246.42298	.479	-659.8278	310.7209
	40-50	-132.0170	252.98666	.602	-630.2170	366.1830
	75-100	-110.5600	348.84727	.752	-797.5358	576.4158
75-100	0-10	-1761.5063(*)	333.97334	.000	-2419.1913	-1103.8213
	10-20	-840.7332(*)	333.97334	.012	-1498.4182	-183.0482
	20-30	-168.9407	333.97334	.613	-826.6257	488.7443
	30-40	-63.9935	334.82290	.849	-723.3514	595.3645
	40-50	-21.4570	339.68270	.950	-690.3853	647.4713
	50-75	110.5600	348.84727	.752	-576.4158	797.5358

Based on observed means.

* The mean difference is significant at the .05 level.

Table 25. ANOVA results (LSD) for lead concentrations by depth in the floodplain.

(I) PrePost	(J) PrePost	Mean Difference (I-J)	Std. Error	Sig.	95% Confidence Interval	
					Lower Bound	Upper Bound
0-10	10-20	-2.8789	2.99580	.337	-8.7784	3.0207
	20-30	1.5795	2.99580	.598	-4.3200	7.4791
	30-40	.7921	3.01278	.793	-5.1409	6.7250
	40-50	-.7669	3.10889	.805	-6.8891	5.3554
	50-75	2.6458	3.28601	.421	-3.8253	9.1168
	75-100	-3.8531	4.47446	.390	-12.6645	4.9584
10-20	0-10	2.8789	2.99580	.337	-3.0207	8.7784
	20-30	4.4584	2.99580	.138	-1.4411	10.3580
	30-40	3.6709	3.01278	.224	-2.2621	9.6039
	40-50	2.1120	3.10889	.498	-4.0103	8.2342
	50-75	5.5246	3.28601	.094	-.9464	11.9957
	75-100	-.9742	4.47446	.828	-9.7856	7.8373
20-30	0-10	-1.5795	2.99580	.598	-7.4791	4.3200
	10-20	-4.4584	2.99580	.138	-10.3580	1.4411
	30-40	-.7875	3.01278	.794	-6.7205	5.1455
	40-50	-2.3464	3.10889	.451	-8.4687	3.7758
	50-75	1.0662	3.28601	.746	-5.4048	7.5373
	75-100	-5.4326	4.47446	.226	-14.2440	3.3788
30-40	0-10	-.7921	3.01278	.793	-6.7250	5.1409
	10-20	-3.6709	3.01278	.224	-9.6039	2.2621
	20-30	.7875	3.01278	.794	-5.1455	6.7205
	40-50	-1.5590	3.12525	.618	-7.7134	4.5955
	50-75	1.8537	3.30149	.575	-4.6478	8.3552
	75-100	-4.6451	4.48584	.301	-13.4790	4.1887
40-50	0-10	.7669	3.10889	.805	-5.3554	6.8891
	10-20	-2.1120	3.10889	.498	-8.2342	4.0103
	20-30	2.3464	3.10889	.451	-3.7758	8.4687
	30-40	1.5590	3.12525	.618	-4.5955	7.7134
	50-75	3.4127	3.38943	.315	-3.2621	10.0874
	75-100	-3.0862	4.55095	.498	-12.0482	5.8759
50-75	0-10	-2.6458	3.28601	.421	-9.1168	3.8253
	10-20	-5.5246	3.28601	.094	-11.9957	.9464
	20-30	-1.0662	3.28601	.746	-7.5373	5.4048
	30-40	-1.8537	3.30149	.575	-8.3552	4.6478
	40-50	-3.4127	3.38943	.315	-10.0874	3.2621
	75-100	-6.4988	4.67374	.166	-15.7027	2.7050
75-100	0-10	3.8531	4.47446	.390	-4.9584	12.6645
	10-20	.9742	4.47446	.828	-7.8373	9.7856
	20-30	5.4326	4.47446	.226	-3.3788	14.2440
	30-40	4.6451	4.48584	.301	-4.1887	13.4790
	40-50	3.0862	4.55095	.498	-5.8759	12.0482
	50-75	6.4988	4.67374	.166	-2.7050	15.7027

Based on observed means.

* The mean difference is significant at the .05 level.

Table 26. ANOVA results (LSD) for zinc concentrations by depth in the floodplain.

(I) PrePost	(J) PrePost	Mean Difference (I-J)	Std. Error	Sig.	95% Confidence Interval	
					Lower Bound	Upper Bound
0-10	10-20	70.8055(*)	19.70911	.000	31.9928	109.6181
	20-30	122.0666(*)	19.70911	.000	83.2540	160.8792
	30-40	121.8948(*)	19.82078	.000	82.8623	160.9273
	40-50	135.0732(*)	20.45311	.000	94.7954	175.3509
	50-75	147.4850(*)	21.61834	.000	104.9126	190.0574
	75-100	109.3049(*)	29.43705	.000	51.3353	167.2745
10-20	0-10	-70.8055(*)	19.70911	.000	-109.6181	-31.9928
	20-30	51.2612(*)	19.70911	.010	12.4485	90.0738
	30-40	51.0894(*)	19.82078	.011	12.0568	90.1219
	40-50	64.2677(*)	20.45311	.002	23.9899	104.5455
	50-75	76.6796(*)	21.61834	.000	34.1071	119.2520
	75-100	38.4994	29.43705	.192	-19.4702	96.4690
20-30	0-10	-122.0666(*)	19.70911	.000	-160.8792	-83.2540
	10-20	-51.2612(*)	19.70911	.010	-90.0738	-12.4485
	30-40	-.1718	19.82078	.993	-39.2043	38.8607
	40-50	13.0065	20.45311	.525	-27.2712	53.2843
	50-75	25.4184	21.61834	.241	-17.1540	67.9908
	75-100	-12.7617	29.43705	.665	-70.7314	45.2079
30-40	0-10	-121.8948(*)	19.82078	.000	-160.9273	-82.8623
	10-20	-51.0894(*)	19.82078	.011	-90.1219	-12.0568
	20-30	.1718	19.82078	.993	-38.8607	39.2043
	40-50	13.1783	20.56074	.522	-27.3114	53.6681
	50-75	25.5902	21.72019	.240	-17.1828	68.3632
	75-100	-12.5899	29.51193	.670	-70.7070	45.5271
40-50	0-10	-135.0732(*)	20.45311	.000	-175.3509	-94.7954
	10-20	-64.2677(*)	20.45311	.002	-104.5455	-23.9899
	20-30	-13.0065	20.45311	.525	-53.2843	27.2712
	30-40	-13.1783	20.56074	.522	-53.6681	27.3114
	50-75	12.4119	22.29873	.578	-31.5004	56.3242
	75-100	-25.7683	29.94029	.390	-84.7289	33.1923
50-75	0-10	-147.4850(*)	21.61834	.000	-190.0574	-104.9126
	10-20	-76.6796(*)	21.61834	.000	-119.2520	-34.1071
	20-30	-25.4184	21.61834	.241	-67.9908	17.1540
	30-40	-25.5902	21.72019	.240	-68.3632	17.1828
	40-50	-12.4119	22.29873	.578	-56.3242	31.5004
	75-100	-38.1801	30.74807	.215	-98.7315	22.3712
75-100	0-10	-109.3049(*)	29.43705	.000	-167.2745	-51.3353
	10-20	-38.4994	29.43705	.192	-96.4690	19.4702
	20-30	12.7617	29.43705	.665	-45.2079	70.7314
	30-40	12.5899	29.51193	.670	-45.5271	70.7070
	40-50	25.7683	29.94029	.390	-33.1923	84.7289
	50-75	38.1801	30.74807	.215	-22.3712	98.7315

Based on observed means.

- The mean difference is significant at the .05 level.

APPENDIX B

SOIL AGE DATA

Methods of ^{210}Pb Age Calculation

The ^{210}Pb dating technique is based on the exponential decline in the activity of ^{210}Pb in buried sediment (Goldberg, 1963). Radioactive ^{210}Pb falls to the earth's surface with precipitation and then is buried by sediment deposition. The amount of ^{210}Pb activity in the soil corresponds to the length of time since exposure to the atmosphere. The dating technique works for sediments buried up to a maximum of 150 years. The key assumption of the dating technique is that there has been no post-depositional mobility of lead in the soil profile (Heyden et al., 2004). The activities of ^{210}Pb, ^{226}Ra, and ^{137}Cs in the soil samples are included in the analysis. The ^{226}Ra activity equals the "supported" ^{210}Pb activity in the soil samples, since ^{210}Pb also forms from the radioactive decay of the ^{226}Ra that is naturally present in the soil. The "unsupported" or excess ^{210}Pb activity that was originally deposited from the atmosphere equals the measured total ^{210}Pb activity minus the ^{226}Ra activity. The exponential decline of this "unsupported" ^{210}Pb activity represents the activity curve used to calculate sedimentation rates and sediment ages.

The most common methods for calculating ^{210}Pb dates and sedimentation rates are the Constant Initial Concentration (CIC) and the Constant Rate of Supply (CRS) models (Appleby et al., 1978; Shukla, 2003). Both the CIC and CRS models assume a constant rate of supply of unsupported ^{210}Pb to the sediment. The CIC model also assumes a constant sedimentation rate, whereas the CRS model assumes a variable sedimentation rate. The CIC model requires soil porosity and density of the dry sediment to calculate the mass depth, which accounts for soil compaction (Shukla, 2003).

The CRS model uses the following formula to calculate soil ages:

$$T_{age} = 1/\lambda * \ln (A(0) / A(x))$$

where A(0) is the total amount of unsupported ^{210}Pb activity present in the core, A(x) is the amount of unsupported ^{210}Pb activity present in the core below depth x, and λ is the radioactive decay constant for ^{210}Pb. The CRS model assumes a constant rate of supply of unsupported ^{210}Pb to the sediment, but the sedimentation rate changes over time. The CRS does not require porosity and mass measurements. The CIC model uses the following formula to calculate soil ages:

$$T_{age} = 1/\lambda * \ln (C(0) / C(x))$$

where C(0) is the total amount of unsupported ^{210}Pb activity present at the surface, and C(x) is the amount of unsupported ^{210}Pb activity present in the core at depth x, and λ is the radioactive decay constant for ^{210}Pb. The CIC model assumes that the initial unsupported ^{210}Pb activity at the surface is constant over time. The radioactive decay constant of ^{210}Pb, with a half-life of 22.26 years, and is calculated using the following formula:

$$\lambda = \log 2 / 22.26 = 0.3114$$

The sedimentation rate for each depth was calculated using the following formula:

$$r_n = (h_n - h_{n-1}) / (t_n - t_{n-1})$$

where h and t are the midpoint depth and age of layer n and layer n -1.

The activity of ^{137}Cs is also included in the ^{210}Pb analysis as an independent marker for calibrating the ^{210}Pb sediment ages. The ^{137}Cs activity is a product of atmospheric thermonuclear testing and provides some insight into the erosional processes

occurring in the watershed. The ^{137}Cs isotope has been shown to be mobile in the soil profile, and therefore is not reliable isotope for age dating (Church et al., 1999). The level of ^{137}Cs activity in the atmosphere peaked in the late 1950's and early 1960's (due to atmospheric nuclear testing) and has declined to non-detectable levels in the present atmosphere (Church et al., 1999). A typical soil core will reflect this change in ^{137}Cs activity and show a peak in measured activity in the subsurface. When the highest ^{137}Cs activity is in the shallowest sediments, this suggests that ^{137}Cs has been eroded from elsewhere in the watershed and re-deposited on the floodplain (Ritchie et al., 1990). Other possibilities are that that the upper layers of sediment have been eroded and the expected peak is exposed at the surface or that there has been no sediment deposition since the ^{137}Cs was deposited.

^{210}Pb Activity Profiles

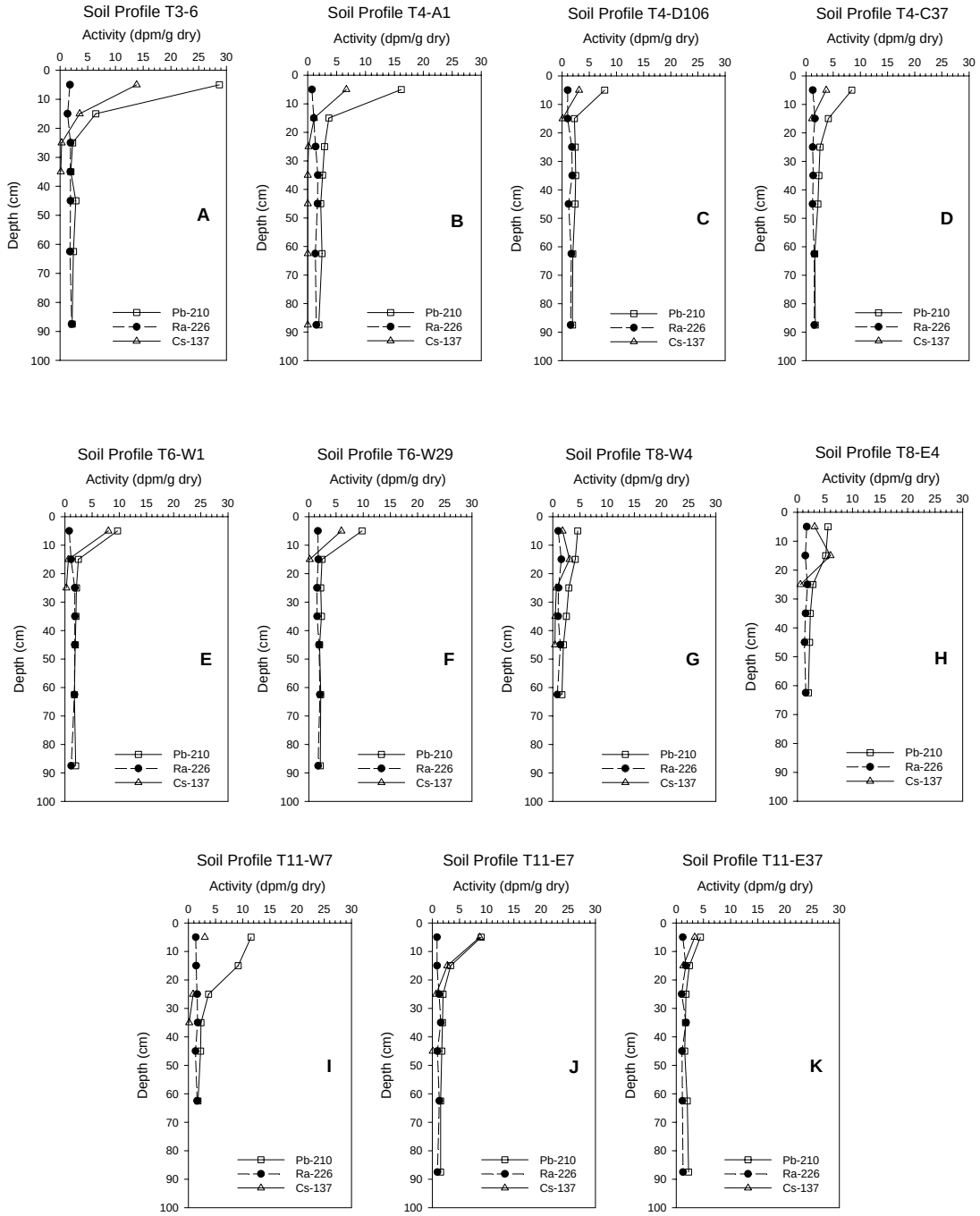


Figure 31. (a)-(k) Plots of all the ^{210}Pb profiles for the Stillwater wetland.

USGS ^{210}Pb Analysis

Table 27. Data and ages from ^{210}Pb analysis.

Site ID	Depth	^{210}Pb	+/-	^{226}Ra	+/-	^{137}Cs	+/-	Excess	Years
T11-E37	0-10	4.460	0.072	1.210	0.033	3.397	0.039	3.251	1987
T11-E37	10-20	2.431	0.043	1.769	0.021	1.312	0.023	0.663	1950
T11-E37	20-30	1.792	0.058	1.003	0.037	ND	ND	0.789	1912
T11-E37	30-40	1.706	0.062	1.804	0.038	ND	ND	-0.098	1874
T11-E37	40-50	1.573	0.066	1.064	0.046	ND	ND	0.509	1836
T11-E37	50-75	2.028	0.073	1.151	0.047	ND	ND	0.877	1770
T11-E37	75-100	2.263	0.062	1.259	0.039	ND	ND	1.004	1675
T11-E7	0-10	9.004	0.152	0.858	0.043	8.747	0.097	8.147	1987
T11-E7	10-20	3.363	0.087	0.875	0.040	2.769	0.051	2.488	1950
T11-E7	20-30	1.975	0.077	1.253	0.036	0.680	0.032	0.723	1913
T11-E7	30-40	1.883	0.045	1.571	0.023	ND	ND	0.312	1876
T11-E7	40-50	1.748	0.055	0.931	0.033	0.085	0.007	0.818	1839
T11-E7	50-75	1.523	0.050	1.303	0.025	ND	ND	0.220	1774
T11-E7	75-100	1.521	0.059	0.954	0.039	ND	ND	0.568	1681
T11-W7	0-10	11.547	0.235	1.376	0.088	3.021	0.078	10.171	1996
T11-W7	10-20	9.178	0.181	1.428	0.082	ND	ND	7.750	1975
T11-W7	20-30	3.713	0.121	1.615	0.092	0.865	0.037	2.098	1955
T11-W7	30-40	2.311	0.072	1.699	0.069	0.147	0.011	0.612	1934
T11-W7	40-50	1.615	0.070	1.307	0.035	ND	ND	0.308	1913
T11-W7	50-75	1.782	0.070	1.619	0.075	ND	ND	0.163	1877
T3-6	0-10	28.711	1.080	ND	ND	13.820	0.523	ND	ND
T3-6	10-20	6.451	0.209	0.674	0.088	3.570	0.107	5.777	ND
T3-6	20-30	2.282	0.084	1.037	0.055	0.292	0.019	1.245	ND
T3-6	30-40	2.420	0.093	1.323	0.040	0.154	0.017	1.097	ND
T3-6	40-50	2.179	0.083	1.118	0.034	ND	ND	1.062	ND
T3-6	50-75	2.497	0.096	1.333	0.040	ND	ND	1.164	ND
T3-6	75-100	2.196	0.064	1.169	0.044	ND	ND	1.027	ND
T4-A1	0-10	15.034	0.350	0.722	0.050	6.669	0.167	14.313	1979
T4-A1	10-20	3.301	0.111	1.050	0.038	1.110	0.045	2.251	1924
T4-A1	20-30	2.527	0.097	1.356	0.041	0.131	0.016	1.171	1869
T4-A1	30-40	2.567	0.096	1.753	0.047	ND	ND	0.815	1814
T4-A1	40-50	2.253	0.087	1.705	0.087	ND	ND	0.547	1759
T4-A1	50-75	2.138	0.089	1.306	0.042	ND	ND	0.832	1664
T4-A1	75-100	1.493	0.057	0.752	0.023	ND	ND	0.741	1527
T4-C37	0-10	8.430	0.162	1.259	0.038	3.731	0.076	7.170	1993
T4-C37	10-20	4.121	0.096	1.651	0.036	1.119	0.035	2.469	1966
T4-C37	20-30	2.569	0.056	1.240	0.109	ND	ND	1.329	1938
T4-C37	30-40	2.372	0.081	1.325	0.054	ND	ND	1.046	1911
T4-C37	40-50	2.178	0.040	1.210	0.026	ND	ND	0.968	1884
T4-C37	50-75	1.608	0.069	1.528	0.039	ND	ND	0.080	1837
T4-C37	75-100	1.718	0.059	1.529	0.032	ND	ND	0.189	1769

Table 27. Data and ages from ^{210}Pb analysis (continued).

Site ID	Depth	^{210}Pb	+/-	^{226}Ra	+/-	^{137}Cs	+/-	Excess	Years
T4-D106	0-10	7.844	0.142	1.039	0.034	3.133	0.063	6.806	1982
T4-D106	10-20	2.272	0.082	1.027	0.048	0.091	0.010	1.245	1934
T4-D106	20-30	2.433	0.071	1.808	0.036	ND	ND	0.625	1886
T4-D106	30-40	2.494	0.081	1.882	0.040	ND	ND	0.613	1837
T4-D106	40-50	2.387	0.086	1.189	0.053	ND	ND	1.198	1789
T4-D106	50-75	1.992	0.072	1.720	0.039	ND	ND	0.272	1705
T4-D106	75-100	1.915	0.060	1.577	0.032	ND	ND	0.338	1584
T6-W1	0-10	9.704	0.199	0.789	0.053	7.996	0.118	8.916	1976
T6-W1	10-20	2.478	0.078	1.144	0.047	0.641	0.025	1.334	1916
T6-W1	20-30	2.122	0.075	1.828	0.042	0.259	0.019	0.293	1856
T6-W1	30-40	2.028	0.079	1.844	0.044	ND	ND	0.184	1796
T6-W1	40-50	1.914	0.075	1.827	0.043	ND	ND	0.086	1736
T6-W1	50-75	1.731	0.078	1.769	0.046	ND	ND	-0.038	1630
T6-W1	75-100	1.992	0.078	1.156	0.052	ND	ND	0.837	1480
T6-W29	0-10	9.793	0.197	1.667	0.096	5.989	0.098	8.127	1968
T6-W29	10-20	2.438	0.085	1.755	0.081	0.173	0.014	0.684	1891
T6-W29	20-30	1.815	0.075	1.496	0.040	ND	ND	0.318	1814
T6-W29	30-40	1.903	0.080	1.522	0.042	ND	ND	0.381	1737
T6-W29	40-50	1.969	0.079	1.889	0.086	ND	ND	0.081	1660
T6-W29	50-75	2.200	0.064	2.030	0.070	ND	ND	0.171	1525
T6-W29	75-100	1.343	0.051	0.674	0.021	ND	ND	0.669	1333
T8-E4	0-10	5.552	0.133	1.700	0.084	3.130	0.063	3.852	1999
T8-E4	10-20	5.131	0.131	1.430	0.042	6.005	0.100	3.701	1985
T8-E4	20-30	2.795	0.097	1.844	0.092	0.546	0.027	0.952	1971
T8-E4	30-40	2.325	0.093	1.473	0.043	ND	ND	0.853	1956
T8-E4	40-50	2.196	0.068	1.304	0.031	ND	ND	0.892	1942
T8-E4	50-75	1.994	0.072	1.524	0.070	ND	ND	0.471	1917
T8-W4	0-10	4.577	0.120	1.010	0.049	1.806	0.047	3.567	2001
T8-W4	10-20	4.150	0.097	1.588	0.035	3.099	0.060	2.562	1990
T8-W4	20-30	2.947	0.076	1.078	0.124	0.662	0.022	1.869	1980
T8-W4	30-40	2.492	0.075	0.976	0.042	0.460	0.020	1.516	1969
T8-W4	40-50	1.958	0.060	1.405	0.028	0.418	0.020	0.554	1959
T8-W4	50-75	1.684	0.070	0.849	0.043	ND	ND	0.836	1941

^{14}C Calibration Plots – Beta Analytic Memo

December 13, 2005

Ms. Mary Beth Marks
Gallatin National Forest
USDA
PO Box 140
Bozeman, MT 59771 USA

RE: Radiocarbon Dating Results For Samples STILLWATER PS1 #20, STILLWATER PS2 #5, STILLWATER PS2 #6, STILLWATER PS2 #7, STILLWATER PS3 #2, STILLWATER PS4 #16, STILLWATER PS5 #13

Dear Ms. Marks:

Enclosed are the radiocarbon dating results for seven samples recently sent to us. They each provided plenty of carbon for accurate measurements and all the analyses went normally. The report sheet also contains the method used, material type, and applied pretreatments and, where applicable, the two-sigma calendar calibration range.

You will notice that Beta-210353 (STILLWATER PS5 #13) is reported with the units "pMC" rather than BP. "pMC" stands for "percent modern carbon". Results are reported in the pMC format when the analyzed material had more ^{14}C than did the modern (AD 1950) reference standard. The source of this "extra" ^{14}C in the atmosphere is thermo-nuclear bomb testing which on-set in the 1950s. Its presence generally indicates the material analyzed was part of a system that was respiring carbon after the on-set of the testing (AD 1950s). On occasion, the two sigma lower limit will extend into the time region before this "bomb-carbon" onset (i.e. less than 100 pMC). In those cases, there is some probability for 18th, 19th, or 20th century antiquity.

We analyzed these samples on a sole priority basis. No students or intern researchers who would necessarily be distracted with other obligations and priorities were used in the analyses. We analyzed them with the combined attention of our entire professional staff.

Information pages are also enclosed with the mailed copy of this report. If you have any specific questions about the analyses, please do not hesitate to contact us.

Our invoice has been sent separately. Our copy is enclosed. Thank you for your prior efforts in arranging payment. As always, if you have any questions or would like to discuss the results, don't hesitate to contact me.

Sincerely,

Darden Hood

Table 28. Results of ^{14}C analysis from Beta Analytic.

Ms. Mary Beth Marks
Gallatin National Forest

Report Date: 12/13/2005
Material Received: 11/4/2005

Sample Data	Measured Radiocarbon Age	13C/12C Ratio	Conventional Radiocarbon Age(*)
Beta - 210347	3350 +/- 40 BP	-25.7 o/oo	3340 +/- 40 BP
SAMPLE : STILLWATER PS1 #20 ANALYSIS : AMS-Standard delivery MATERIAL/PRETREATMENT : (peat): acid/alkali/acid 2 SIGMA CALIBRATION : Cal BC 1720 to 1520 (Cal BP 3670 to 3470)			
Beta - 210348	2770 +/- 40 BP	-26.2 o/oo	2750 +/- 40 BP
SAMPLE : STILLWATER PS2 #5 ANALYSIS : AMS-Standard delivery MATERIAL/PRETREATMENT : (peat): acid/alkali/acid 2 SIGMA CALIBRATION : Cal BC 990 to 820 (Cal BP 2940 to 2770)			
Beta - 210349	5470 +/- 40 BP	-26.3 o/oo	5450 +/- 40 BP
SAMPLE : STILLWATER PS2 #6 ANALYSIS : AMS-Standard delivery MATERIAL/PRETREATMENT : (peat): acid/alkali/acid 2 SIGMA CALIBRATION : Cal BC 4350 to 4240 (Cal BP 6300 to 6190)			
Beta - 210350	8270 +/- 40 BP	-29.1 o/oo	8200 +/- 40 BP
SAMPLE : STILLWATER PS2 #7 ANALYSIS : AMS-Standard delivery MATERIAL/PRETREATMENT : (peat): acid/alkali/acid 2 SIGMA CALIBRATION : Cal BC 7330 to 7080 (Cal BP 9280 to 9020)			
Beta - 210351	5110 +/- 40 BP	-26.4 o/oo	5090 +/- 40 BP
SAMPLE : STILLWATER PS3 #2 ANALYSIS : AMS-Standard delivery MATERIAL/PRETREATMENT : (peat): acid/alkali/acid 2 SIGMA CALIBRATION : Cal BC 3970 to 3780 (Cal BP 5920 to 5730)			

Table 28. Results of ^{14}C analysis from Beta Analytic (continued).

Sample Data	Measured Radiocarbon Age	13C/12C Ratio	Conventional Radiocarbon Age(*)
Beta - 210352	8710 +/- 40 BP	-24.2 o/oo	8720 +/- 40 BP
SAMPLE : STILLWATER PS4 #16 ANALYSIS : AMS-Standard delivery MATERIAL/PRETREATMENT : (wood): acid/alkali/acid 2 SIGMA CALIBRATION : Cal BC 7930 to 7610 (Cal BP 9880 to 9560)			
Beta - 210353	111.1 +/- 0.4 pMC	-25.6 o/oo	111.2 +/- 0.4 pMC
SAMPLE : STILLWATER PS5 #13 ANALYSIS : AMS-Standard delivery MATERIAL/PRETREATMENT : (wood): acid/alkali/acid COMMENT: reported result indicates an age of post 0 BP and has been reported as a % of the modern reference standard, indicating the material was living within the last 50 years.			

CALIBRATION OF RADIOCARBON AGE TO CALENDAR YEARS

(Variables: C13/C12=-25.7:lab. mult=1)

Laboratory number: **Beta-210347**

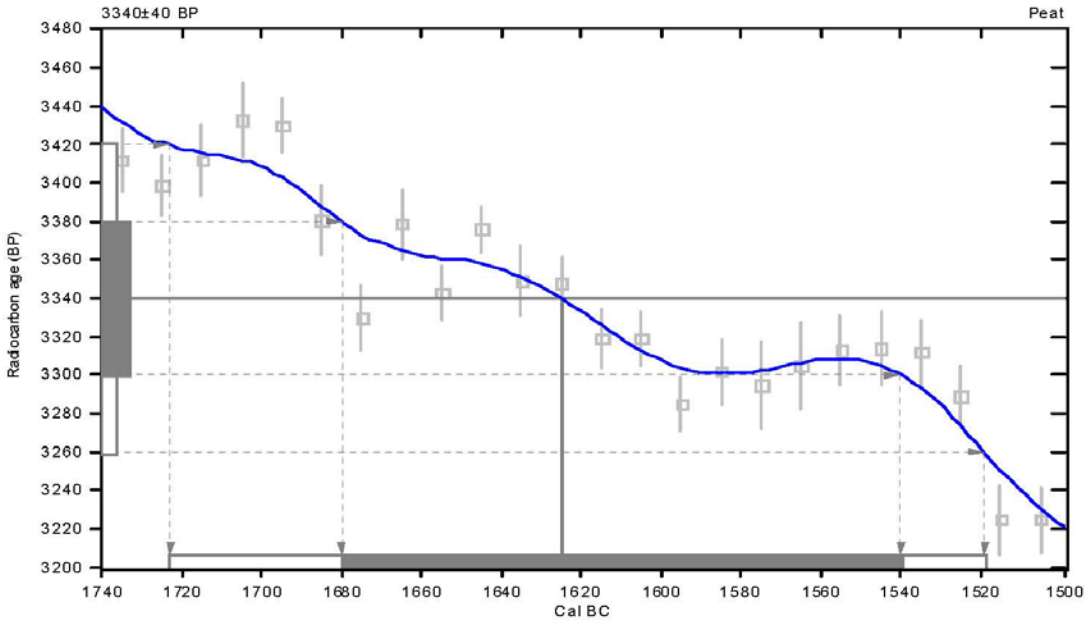
Conventional radiocarbon age: **3340±40 BP**

2 Sigma calibrated result: (95% probability) **Cal BC 1720 to 1520 (Cal BP 3670 to 3470)**

Intercept data

Intercept of radiocarbon age with calibration curve: Cal BC 1620 (Cal BP 3580)

1 Sigma calibrated result: (68% probability) Cal BC 1680 to 1540 (Cal BP 3630 to 3490)



References:

Database used
INTCAL98

Calibration Database

Editorial Comment
Stuiver, M., van der Plicht, H., 1998, Radiocarbon 40(3), pxii-xiii

INTCAL98 Radiocarbon Age Calibration
Stuiver, M., et. al., 1998, Radiocarbon 40(3), p1041-1083

Mathematics
A Simplified Approach to Calibrating C14 Dates
Talma, A. S., Vogel, J. C., 1993, Radiocarbon 35(2), p317-322

Beta Analytic Radiocarbon Dating Laboratory
4985 S.W. 74th Court, Miami, Florida 33155 • Tel: (305)667-5167 • Fax: (305)663-0964 • E-Mail: beta@radiocarbon.com

Figure 32. Calibration plot for ^{14}C ages for sample PS1 (180-190 cm).

CALIBRATION OF RADIOCARBON AGE TO CALENDAR YEARS

(Variables: C13/C12=-26.2:lab. mult=1)

Laboratory number: **Beta-210348**

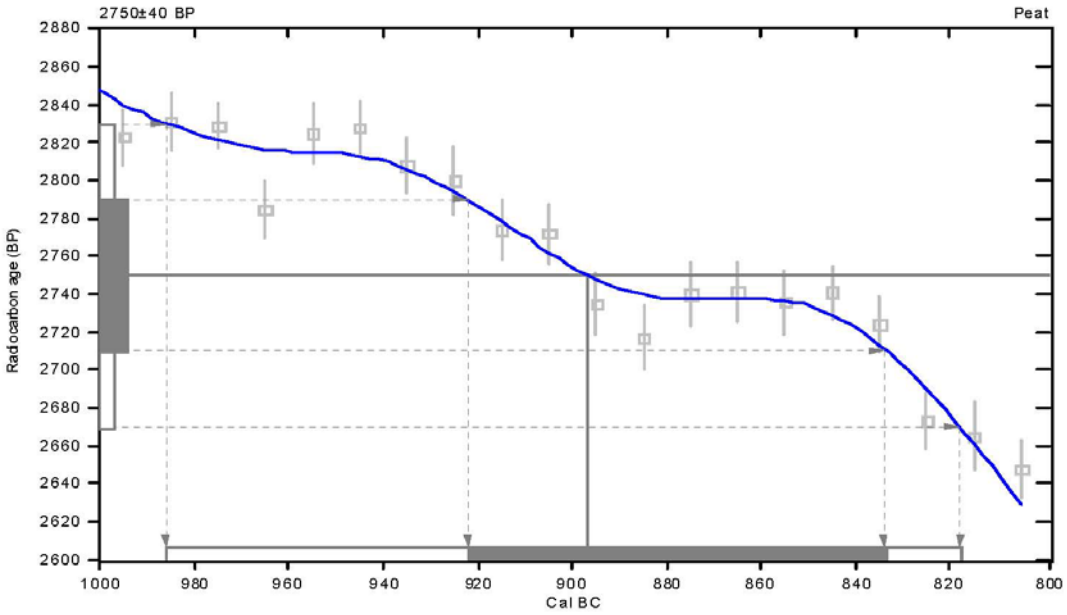
Conventional radiocarbon age: **2750±40 BP**

2 Sigma calibrated result: (95% probability) **Cal BC 990 to 820 (Cal BP 2940 to 2770)**

Intercept data

Intercept of radiocarbon age with calibration curve: Cal BC 900 (Cal BP 2850)

1 Sigma calibrated result: (68% probability) Cal BC 920 to 830 (Cal BP 2870 to 2780)



References:

Database used
INTCAL98

Calibration Database

Editorial Comment
Stuiver, M., van der Plicht, H., 1998, Radiocarbon 40(3), pxii-xiii

INTCAL98 Radiocarbon Age Calibration
Stuiver, M., et. al., 1998, Radiocarbon 40(3), p1041-1083

Mathematics

A Simplified Approach to Calibrating C14 Dates
Talma, A. S., Vogel, J. C., 1993, Radiocarbon 35(2), p317-322

Beta Analytic Radiocarbon Dating Laboratory
4985 S.W. 74th Court, Miami, Florida 33155 • Tel: (305)667-5167 • Fax: (305)663-0964 • E-Mail: beta@radiocarbon.com

Figure 33. Calibration plot for ^{14}C ages for sample PS2 (70-90 cm).

CALIBRATION OF RADIOCARBON AGE TO CALENDAR YEARS

(Variables: C13/C12=-26.3:lab. mult=1)

Laboratory number: **Beta-210349**

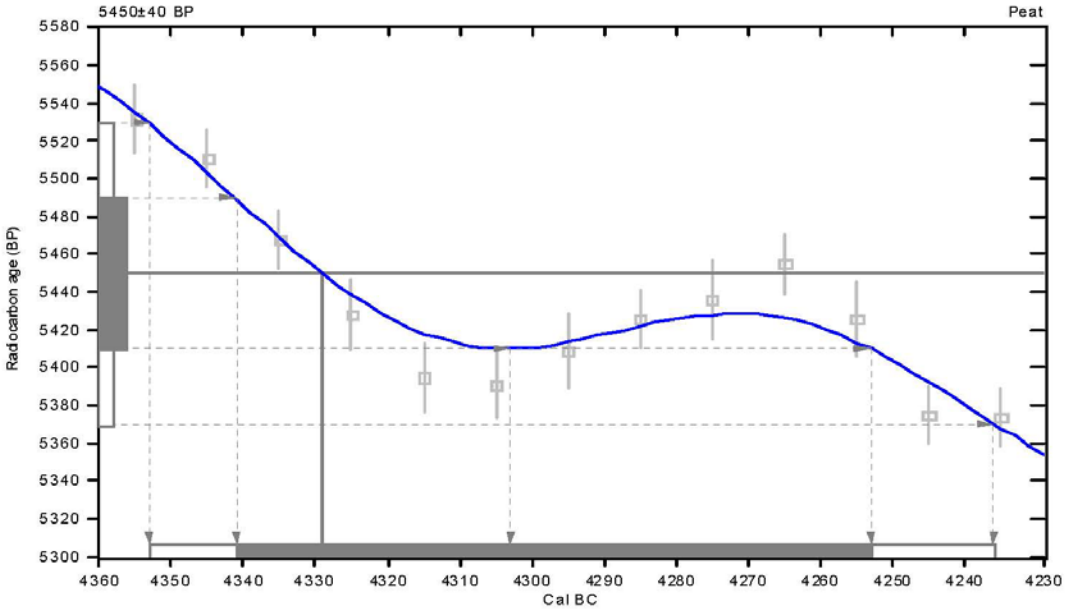
Conventional radiocarbon age: **5450±40 BP**

2 Sigma calibrated result: (95% probability) **Cal BC 4350 to 4240 (Cal BP 6300 to 6190)**

Intercept data

Intercept of radiocarbon age with calibration curve: Cal BC 4330 (Cal BP 6280)

1 Sigma calibrated results: (68% probability) Cal BC 4340 to 4300 (Cal BP 6290 to 6250) and Cal BC 4300 to 4250 (Cal BP 6250 to 6200)



References:

Database used

INTCAL98

Calibration Database

Editorial Comment

Stuiver, M., van der Plicht, H., 1998, Radiocarbon 40(3), pxii-xiii

INTCAL98 Radiocarbon Age Calibration

Stuiver, M., et. al., 1998, Radiocarbon 40(3), p1041-1083

Mathematics

A Simplified Approach to Calibrating C14 Dates

Talma, A. S., Vogel, J. C., 1993, Radiocarbon 35(2), p317-322

Beta Analytic Radiocarbon Dating Laboratory

4985 S.W. 74th Court, Miami, Florida 33155 • Tel: (305)667-5167 • Fax: (305)663-0964 • E-Mail: beta@radiocarbon.com

Figure 34. Calibration plot for ^{14}C ages for sample PS2 (90-110 cm).

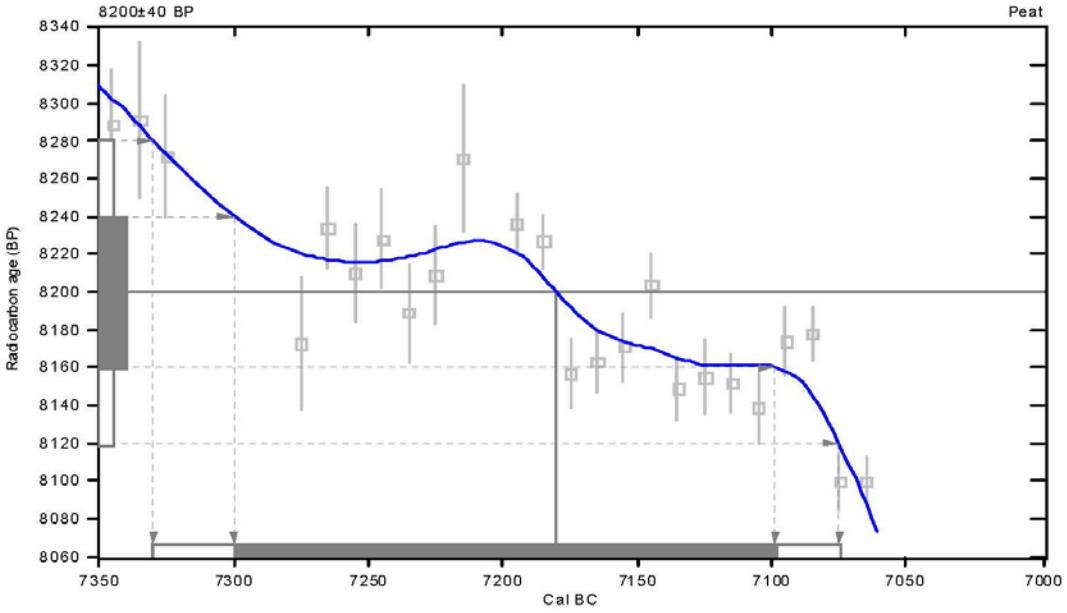
CALIBRATION OF RADIOCARBON AGE TO CALENDAR YEARS

(Variables: C13/C12=-29.1:lab. mult=1)

Laboratory number:	**Beta-210350**
Conventional radiocarbon age:	**8200±40 BP**
2 Sigma calibrated result: (95% probability)	**Cal BC 7330 to 7080 (Cal BP 9280 to 9020)**

Intercept data

Intercept of radiocarbon age with calibration curve:	Cal BC 7180 (Cal BP 9130)
1 Sigma calibrated result: (68% probability)	Cal BC 7300 to 7100 (Cal BP 9250 to 9050)



References:

Database used
INTCAL98
Calibration Database
Editorial Comment
Stuiver, M., van der Plicht, H., 1998, Radiocarbon 40(3), pxii-xiii
INTCAL98 Radiocarbon Age Calibration
Stuiver, M., et. al., 1998, Radiocarbon 40(3), p1041-1083
Mathematics
A Simplified Approach to Calibrating C14 Dates
Talma, A. S., Vogel, J. C., 1993, Radiocarbon 35(2), p317-322

Beta Analytic Radiocarbon Dating Laboratory
4985 S.W. 74th Court, Miami, Florida 33155 • Tel: (305)667-5167 • Fax: (305)663-0964 • E-Mail: beta@radiocarbon.com

Figure 35. Calibration plot for ^{14}C ages for sample PS2 (110-130 cm).

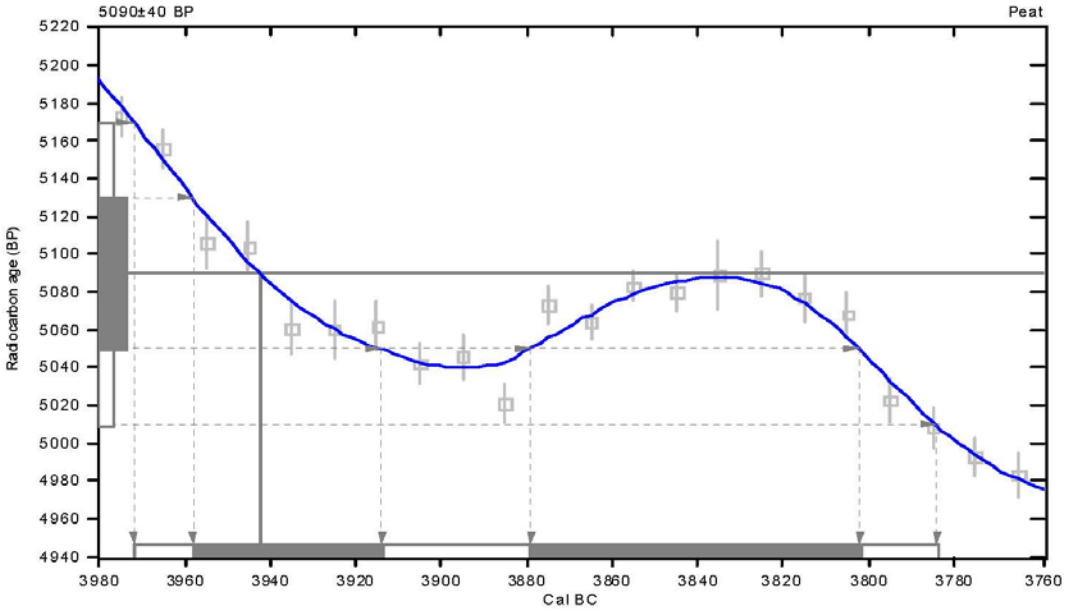
CALIBRATION OF RADIOCARBON AGE TO CALENDAR YEARS

(Variables: C13/C12=-26.4:lab. mult=1)

Laboratory number:	**Beta-210351**
Conventional radiocarbon age:	**5090±40 BP**
2 Sigma calibrated result: (95% probability)	**Cal BC 3970 to 3780 (Cal BP 5920 to 5730)**

Intercept data

Intercept of radiocarbon age with calibration curve:	Cal BC 3940 (Cal BP 5890)
1 Sigma calibrated results: (68% probability)	Cal BC 3960 to 3910 (Cal BP 5910 to 5860) and Cal BC 3880 to 3800 (Cal BP 5830 to 5750)



References:

Database used
INTCAL98
Calibration Database
Editorial Comment
Stuiver, M., van der Plicht, H., 1998, Radiocarbon 40(3), pxii-xiii
INTCAL98 Radiocarbon Age Calibration
Stuiver, M., et. al., 1998, Radiocarbon 40(3), p1041-1083
Mathematics
A Simplified Approach to Calibrating C14 Dates
Talma, A. S., Vogel, J. C., 1993, Radiocarbon 35(2), p317-322

Beta Analytic Radiocarbon Dating Laboratory

4985 S.W. 74th Court, Miami, Florida 33155 • Tel: (305)667-5167 • Fax: (305)663-0964 • E-Mail: beta@radiocarbon.com

Figure 36. Calibration plot for ^{14}C ages for sample PS3 (120-130 cm).

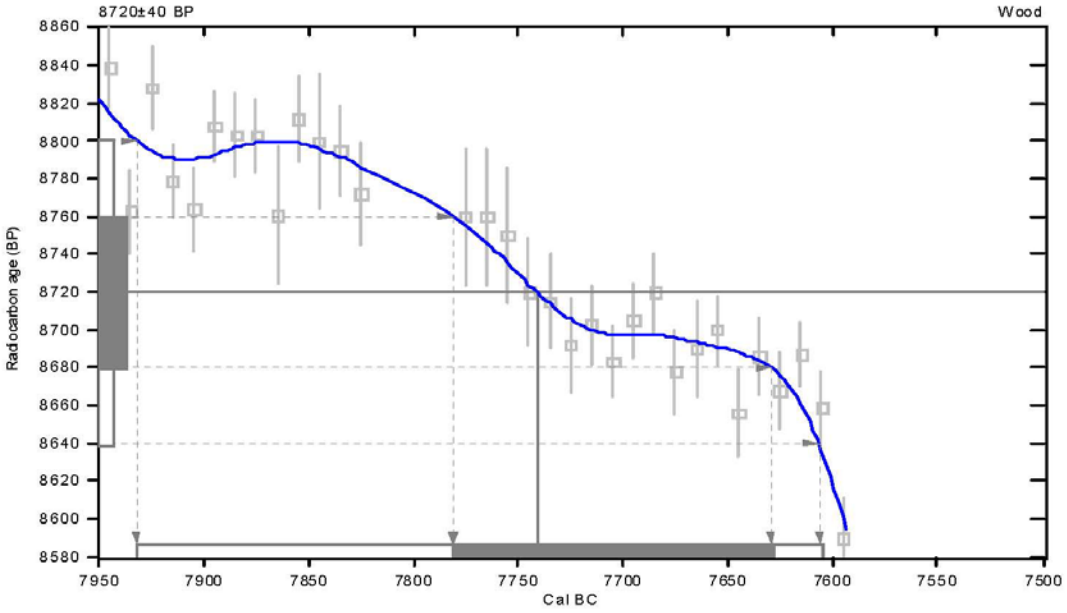
CALIBRATION OF RADIOCARBON AGE TO CALENDAR YEARS

(Variables: C13/C12=-24.2:lab. mult=1)

Laboratory number:	**Beta-210352**
Conventional radiocarbon age:	**8720±40 BP**
2 Sigma calibrated result: (95% probability)	**Cal BC 7930 to 7610 (Cal BP 9880 to 9560)**

Intercept data

Intercept of radiocarbon age with calibration curve:	Cal BC 7740 (Cal BP 9690)
1 Sigma calibrated result: (68% probability)	Cal BC 7780 to 7630 (Cal BP 9730 to 9580)



References:

Database used
INTCAL98
Calibration Database
Editorial Comment
Stuiver, M., van der Plicht, H., 1998, Radiocarbon 40(3), pxii-xiii
INTCAL98 Radiocarbon Age Calibration
Stuiver, M., et. al., 1998, Radiocarbon 40(3), p1041-1083
Mathematics
A Simplified Approach to Calibrating C14 Dates
Talma, A. S., Vogel, J. C., 1993, Radiocarbon 35(2), p317-322

Beta Analytic Radiocarbon Dating Laboratory
4985 S.W. 74th Court, Miami, Florida 33155 • Tel: (305)667-5167 • Fax: (305)663-0964 • E-Mail: beta@radiocarbon.com

Figure 37. Calibration plot for ^{14}C ages for sample PS4 (90-100 cm).

APPENDIX C

VEGETATION AND WELL DATA

Vegetation Habitat Types

On September 1, 2005, plant ecologist Marlene Renwick and I visited the Stillwater wetland to determine the dominant vegetation and habitat types of five predetermined zones based on hydrology. The following descriptions provided by Marlene Renwick give a general overview of the dominant vegetation of these zones and their associated habitat types. Habitat types are described using *Classification and Management of Montana's Riparian and Wetland Sites* by Hansen et al., (1995).

• Northwest Marsh

This area is dominated by *Salix planifolia* (planeleaf willow) with interspersed areas of *Salix wolfii* (wolf's willow) found on areas of higher ground and lower moisture. The area is a mosaic of willow thickets, marshy graminoid-willow areas dominated by *Carex aquatilis* (water sedge) and areas of standing water dominated by *Carex rostrata* (beaked sedge). Additionally, we visited one upland site within the zone where the vegetation corresponded more closely to zone 5, the upland area of the alluvial fan. Overall, the dominant habitat type for this zone is *Salix planifolia/Carex aquatilis* (planeleaf willow/water sedge).

• Beaver Pond Marsh

This area is similar overall to the description above for zone 1 with the exception of numerous areas of permanent open water dominated by *Sparganium sp.*. The dominant habitat type for this zone is *Salix planifolia/Carex aquatilis* (planeleaf

willow/water sedge). On the northern most edge of the marsh in this area, I noted successful establishment of *Abies lasiocarpa, Picea engelmannii* and *Pinus contorta* seedlings. However, since it is only on the very edge and appears to be less then 10 trees per acre, the coniferous trees were not taken into consideration for habitat type.

• Active Floodplain

This area is predominantly a dense willow thicket with the Stillwater Creek running though it. Occasionally one finds small areas free of willows which are forb dominated with incidental sedges and/or grasses. *Salix planifolia* and *Carex aquatilis* increase in occurrence and abundance near the creek and as one moves inward and north in the marsh within this zone. *Salix wolfii* dominants the periphery along the eastern edge and occasional upland areas within this zone. For the areas that I observed the most within this zone, which is the southern part, the dominant habitat type appears to be *Salix wolfii/Deschampsia cespitosa* (wolf's willow/tufted hairgrass). One could also expect to find areas within this zone more appropriately described by the *Salix planifolia/Carex aquatilis* or *Salix wolfii/Carex aquatilis* habitat types.

• Southwest Marsh

This area is dominated by *Salix wolfii* thickets with a centrally located beaver pond. Within and around the beaver pond, the habitat type is *Salix wolfii/Carex aquatilis.* The southern edge of the zone transitions into a moist alluvial fan area as described in zone 5.

• Alluvial Fan

The area of the alluvial fan can be broken into two distinct habitat types. The upland part of the alluvial fan, which adjoins the toeslope of the forested habitat above the wetland, appears to be a graminoid-forb dominated area that is not wetland associated. Dominant graminoids include *Bromus sp., Stipa sp.,* and *Phleum pratense* and the dominant forbs include *Agoseris glauca, Fragaria virginis, Aster sp.* and *Delphinium sp*. The area is largely free of willow reproduction and will likely support tree regeneration before other areas in the marsh will. A review of *Grassland and Shubland Habitat Types of Western Montana* by Mueggler and Stewart (1980) did not indicate a habitat type which adequately described this area. This area may be in transition towards a forested habitat type. As one will note on the map, a creek flows through this zone into the marsh. This area is dominated by *Picea engelmannii*, *Abies lasiocarpa*, *Salix spp*., and numerous forbs.

As the alluvial fan loses elevation and picks up moisture towards the center of the marsh, the vegetation changes to a sedge-graminoid-forb dominated area that does support willow reproduction. The graminoids in this area are different species from those described previously for the alluvial fan upland area and include *Carex sp., Deschampsia sp., Poa sp.,* and *Melica sp*.. Dominant forbs included *Angelica sp., Pedicularis groenlandica, Mertensia sp.* and *Taraxacum officinale sp.*. Due to the willow reproduction that I observed, the *Salix wolfii/Deschampsia cespitosa* habitat type is likely the best fit to describe the dominant vegetation in this area although there are certainly areas with less than 10% willow canopy cover that may key to a non-shrub habitat type.

Survey Data for Monitoring Wells and Piezometer Nests

Table 29. Survey data for monitoring wells and piezometer nest locations.

Well ID	X-Coord (UTM) (meters)	Y-Coord (UTM) (meters)	Elevation (meters)
P1	579043.434	4992198.797	2575.597
P2	579206.702	4992195.299	2575.252
P3	579131.552	4991863.504	2579.232
P4	579291.840	4991797.463	2579.674
P5	579100.428	4991561.479	2579.620
M1	578789.221	4992249.861	2575.661
M2	579044.162	4992247.367	2575.441
M3	579206.135	4992234.705	2575.136
M5	578891.570	4991939.698	2579.316
M11	579139.943	4991848.799	2579.356

Monitoring Well Chemistry Data

Table 30. Well evacuation data for monitoring well M1.

Date:	7/12/2005	**Well Depth (ft below measuring point):**	12.17
Lab:	Northern Analytical	**Depth to Water (ft):**	2.40
Sample #:	2005070149-18	**Feet of Water:**	9.77

Method :	Displacement Polyethylene Bailer
Purge Volume:	9.77 ft. x 0.163 gal/ft (2 in. well) = 1.6 gal. x 3 = 4.8 gal.
Remarks:	Poor recovery, gray-brown cloudy water, dry at 1.9 gal.
Meter:	pH - YSI556 (Calibration: 7/11/2005)
Decontamination:	Scrub (yes); Potable Water (yes); Liquinox (yes); Distilled Water (yes)

Sample Container	**Parameters**	**Preservative**
250 ml Poly	Dissolved Metals	HNO3
500 ml Poly	Commons	

Cumulative Gallons	**Temp (℃)**	**pH** (s.u.)	**SC** (µS/cm)	**DO** (mg/l)	**ORP** (millivolts)	**Other**
1.6	5.80	6.85	830	1.56	-84.90	
2.1	6.08	7.02	603	6.30	-66.80	

Table 31. Water chemistry data for monitoring well M1.

Laboratory Test	**Measured Value**	**Test Units**	**Test Method**	**Date of Analysis**
Acidity as CaCO3	<2	mg/l	305.1	07/15/2005
Alkalinity Bicarbonate as HCO3	366	mg/l	2320B	07/15/2005
Alkalinity Carbonate as CO3	0	mg/l	2320B	07/15/2005
Alkalinity Total as CaCO3	300	mg/l	2320B	07/15/2005
Chloride as Cl	2	mg/l	325.3	07/22/2005
Sulfate as SO4	7	mg/l	375.2	07/20/2005
Hardness as CaCO3	313	mg/l	2340B	08/10/2005
Specific Conductivity	562	µS/cm	2510B	07/15/2005
pH	6.8	S.U.	150.1	07/14/2005
Total Dissolved Solids	351	mg/l	160.1	07/18/2005
Aluminum as Al (Dissolved)	<0.05	mg/l	200.7	08/04/2005
Cadmium as Cd (Dissolved)	<.0001	mg/l	200.8	07/20/2005
Calcium as Ca (Dissolved)	94	mg/l	200.8	07/27/2005
Copper as Cu (Dissolved)	0.002	mg/l	200.8	07/20/2005
Iron as Fe (Dissolved)	24.5	mg/l	200.7	08/04/2005
Lead as Pb (Dissolved)	<0.001	mg/l	200.8	07/20/2005
Magnesium as Mg (Dissolved)	19	mg/l	200.8	07/27/2005
Manganese as Mn (Dissolved)	0.32	mg/l	200.8	07/20/2005
Potassium as K (Dissolved)	<1	mg/l	200.8	07/28/2005
Sodium as Na (Dissolved)	3	mg/l	200.7	08/02/2005
Zinc as Zn (Dissolved)	0.03	mg/l	200.8	07/20/2005
Cations	6.39	meq/l	1030F	08/04/2005
Anions	6.20	meq/l	1030F	07/28/2005
Cation/Anion Balance	0.19	[max 0.20]	AWWA/APHA	08/04/2005

Table 32. Well evacuation data for monitoring well M2.

Date:	7/12/2005	**Well Depth (ft below measuring point):**	11.54
Lab:	Northern Analytical	**Depth to Water (ft):**	2.42
Sample #:	2005070149-17	**Feet of Water:**	9.12
Method :	Displacement Polyethylene Bailer		
Purge Volume:	9.12 ft. x 0.163 gal/ft (2 in. well) = 1.5 gal. x 3 = 4.5 gal.		
Remarks:	Good recovery; brown-gray, cloudy water		
Meter:	pH - YSI556 (Calibration: 7/11/2005)		
Decontamination:	Scrub (yes); Potable Water (yes); Liquinox (yes); Distilled Water (yes)		

Sample Container	**Parameters**	**Preservative**
250 ml Poly	Dissolved Metals	HNO3
500 ml Poly	Commons	

Cumulative Gallons	**Temp (℃)**	**pH** (s.u.)	**SC** (µS/cm)	**DO** (mg/l)	**ORP** (millivolts)	**Other**
2.3	6.15	6.86	412	0.75	-107	
4.6	5.22	6.88	413	0.83	-98	
6.9	3.11	6.95	423	0.40	-114	Downhole

Table 33. Water chemistry data for monitoring well M2.

Laboratory Test	**Measured Value**	**Test Units**	**Test Method**	**Date of Analysis**
Acidity as CaCO3	<2	mg/l	305.1	07/15/2005
Alkalinity Bicarbonate as HCO3	220	mg/l	2320B	07/15/2005
Alkalinity Carbonate as CO3	0	mg/l	2320B	07/15/2005
Alkalinity Total as CaCO3	181	mg/l	2320B	07/15/2005
Chloride as Cl	2	mg/l	325.3	07/22/2005
Sulfate as SO4	5	mg/l	375.2	07/20/2005
Hardness as CaCO3	179	mg/l	2340B	08/10/2005
Specific Conductivity	342	µS/cm	2510B	07/15/2005
pH	6.7	S.U.	150.1	07/14/2005
Total Dissolved Solids	218	mg/l	160.1	07/18/2005
Aluminum as Al (Dissolved)	<0.05	mg/l	200.7	08/04/2005
Cadmium as Cd (Dissolved)	<0.0001	mg/l	200.8	07/20/2005
Calcium as Ca (Dissolved)	55	mg/l	200.8	07/27/2005
Copper as Cu (Dissolved)	<0.001	mg/l	200.8	07/20/2005
Iron as Fe (Dissolved)	27.4	mg/l	200.7	08/04/2005
Lead as Pb (Dissolved)	<0.001	mg/l	200.8	07/20/2005
Magnesium as Mg (Dissolved)	10	mg/l	200.8	07/27/2005
Manganese as Mn (Dissolved)	0.35	mg/l	200.8	07/20/2005
Potassium as K (Dissolved)	<1	mg/l	200.8	07/28/2005
Sodium as Na (Dissolved)	3	mg/l	200.7	08/02/2005
Zinc as Zn (Dissolved)	0.01	mg/l	200.8	07/20/2005
Cations	3.7	meq/l	1030F	08/04/2005
Anions	3.78	meq/l	1030F	07/28/2005
Cation/Anion Balance	0.08	[max 0.20]	AWWA/APHA	08/04/2005

Table 34. Well evacuation data for monitoring well M3.

Date:	7/12/2005	**Well Depth (ft below measuring point):**	5.54
Lab:	Northern Analytical	**Depth to Water (ft):**	2.19
Sample #:	2005070149-16	**Feet of Water:**	3.35
Method :	Displacement Polyethylene Bailer		
Purge Volume:	3.35 ft. x 0.163 gal/ft (2 in. well) = 0.55 gal. x 3 = 1.7 gal.		
Remarks:	Good recovery; Red-brown, cloudy water		
Meter:	pH - YSI556 (Calibration: 7/11/2005)		
Decontamination:	Scrub (yes); Potable Water (yes); Liquinox (yes); Distilled Water (yes)		

Sample Container	**Parameters**	**Preservative**
250 ml Poly	Dissolved Metals	HNO3
500 ml Poly	Commons	

Cumulative Gallons	**Temp (℃)**	**pH** (s.u.)	**SC** (µS/cm)	**DO** (mg/l)	**ORP** (millivolts)	**Other**
0.6	6.00	6.88	118	2.95	-44.6	
1.2	5.71	6.66	120	2.89	-4.7	
1.8	4.48	6.38	117	1.77	-94.2	Downhole

Table 35. Water chemistry data for monitoring well M3.

Laboratory Test	**Measured Value**	**Test Units**	**Test Method**	**Date of Analysis**
Acidity as CaCO3	<2	mg/l	305.1	07/15/2005
Alkalinity Bicarbonate as HCO3	66	mg/l	2320B	07/15/2005
Alkalinity Carbonate as CO3	0	mg/l	2320B	07/15/2005
Alkalinity Total as CaCO3	54	mg/l	2320B	07/15/2005
Chloride as Cl	<1	mg/l	325.3	07/22/2005
Sulfate as SO4	9	mg/l	375.2	07/20/2005
Hardness as CaCO3	53	mg/l	2340B	08/10/2005
Specific Conductivity	109	µS/cm	2510B	07/15/2005
pH	6.6	S.U.	150.1	07/14/2005
Total Dissolved Solids	78	mg/l	160.1	07/18/2005
Aluminum as Al (Dissolved)	<0.05	mg/l	200.7	08/04/2005
Cadmium as Cd (Dissolved)	<0.0001	mg/l	200.8	07/20/2005
Calcium as Ca (Dissolved)	18	mg/l	200.8	07/27/2005
Copper as Cu (Dissolved)	0.002	mg/l	200.8	07/20/2005
Iron as Fe (Dissolved)	0.48	mg/l	200.7	08/04/2005
Lead as Pb (Dissolved)	<0.001	mg/l	200.8	07/20/2005
Magnesium as Mg (Dissolved)	2	mg/l	200.8	07/27/2005
Manganese as Mn (Dissolved)	0.05	mg/l	200.8	07/20/2005
Potassium as K (Dissolved)	<1	mg/l	200.8	07/28/2005
Sodium as Na (Dissolved)	<1	mg/l	200.7	08/02/2005
Zinc as Zn (Dissolved)	0.04	mg/l	200.8	07/20/2005
Cations	1.06	meq/l	1030F	08/04/2005
Anions	1.27	meq/l	1030F	07/28/2005
Cation/Anion Balance	0.21	[max 0.20]	AWWA/APHA	08/04/2005

Table 36. Well evacuation data for monitoring well M5.

Date:	7/12/2005	**Well Depth (ft below measuring point):**	8.18
Lab:	Northern Analytical	**Depth to Water (ft):**	2.02
Sample #:	2005070149-14	**Feet of Water:**	6.20
Method :	Displacement Polyethylene Bailer		
Purge Volume:	6.2 ft. x 0.163 gal/ft (2 in. well) = 1.0 gal. x 3 = 3.0 gal.		
Remarks:	Bailed dry at 1.5 gal; water clear at start, turning cloudy		
Meter:	pH - YSI556 (Calibration: 7/11/2005)		
Decontamination:	Scrub (yes); Potable Water (yes); Liquinox (yes); Distilled Water (yes)		

Sample Container	**Parameters**	**Preservative**
250 ml Poly	Dissolved Metals	HNO3
500 ml Poly	Commons	

Cumulative Gallons	**Temp (℃)**	**pH** (s.u.)	**SC** (µS/cm)	**DO** (mg/l)	**ORP** (millivolts)	**Other**
1.00	8.60	6.15	280.00	2.28	9.12	
1.50	6.31	6.14	183.00	5.10	65.20	Downhole

Table 37. Water chemistry data for monitoring well M5.

Laboratory Test	**Measured Value**	**Test Units**	**Test Method**	**Date of Analysis**
Acidity as CaCO3	<2	mg/l	305.1	07/15/2005
Alkalinity Bicarbonate as HCO3	101	mg/l	2320B	07/15/2005
Alkalinity Carbonate as CO3	0	mg/l	2320B	07/15/2005
Alkalinity Total as CaCO3	83	mg/l	2320B	07/15/2005
Chloride as Cl	<1	mg/l	325.3	07/22/2005
Sulfate as SO4	<5	mg/l	375.2	07/20/2005
Hardness as CaCO3	90	mg/l	2340B	08/10/2005
Specific Conductivity	185	µS/cm	2510B	07/15/2005
pH	6.6	S.U.	150.1	07/14/2005
Total Dissolved Solids	127	mg/l	160.1	07/18/2005
Aluminum as Al (Dissolved)	<0.05	mg/l	200.7	08/04/2005
Cadmium as Cd (Dissolved)	<0.0001	mg/l	200.8	07/20/2005
Calcium as Ca (Dissolved)	26	mg/l	200.8	07/27/2005
Copper as Cu (Dissolved)	0.005	mg/l	200.8	07/20/2005
Iron as Fe (Dissolved)	1.05	mg/l	200.7	08/04/2005
Lead as Pb (Dissolved)	<0.001	mg/l	200.8	07/20/2005
Magnesium as Mg (Dissolved)	6	mg/l	200.8	07/27/2005
Manganese as Mn (Dissolved)	0.25	mg/l	200.8	07/20/2005
Potassium as K (Dissolved)	<1	mg/l	200.8	07/28/2005
Sodium as Na (Dissolved)	2	mg/l	200.7	08/02/2005
Zinc as Zn (Dissolved)	<0.01	mg/l	200.8	07/20/2005
Cations	1.88	meq/l	1030F	08/04/2005
Anions	1.66	meq/l	1030F	07/28/2005
Cation/Anion Balance	0.22	[max 0.20]	AWWA/APHA	08/04/2005

Table 38. Well evacuation data for monitoring well M11.

Date:	7/12/2005	**Well Depth (ft below measuring point):**	6.50
Lab:	Northern Analytical	**Depth to Water (ft):**	2.50
Sample #:	2005070149-15	**Feet of Water:**	4.00

Method :	Displacement Polyethylene Bailer
Purge Volume:	4.0 ft. x 0.163 gal/ft (2 in. well) = 0.65 gal. x 3 = 2.0 gal.
Remarks:	Good recovery
Meter:	pH - YSI556 (Calibration: 7/11/2005)
Decontamination:	Scrub (yes); Potable Water (yes); Liquinox (yes); Distilled Water (yes)

Sample Container	**Parameters**	**Preservative**
250 ml Poly	Dissolved Metals	HNO3
500 ml Poly	Commons	

Cumulative Gallons	**Temp (℃)**	**pH** (s.u.)	**SC** (µS/cm)	**DO** (mg/l)	**ORP** (millivolts)	**Other**
0.7	8.19	6.91	210.00	6.66	34.20	
1.4	7.18	6.81	7.18	6.21	68.30	
2.1	6.26	6.62	6.26	5.61	113.00	Downhole

Table 39. Water chemistry data for monitoring well M11.

Laboratory Test	**Measured Value**	**Test Units**	**Test Method**	**Date of Analysis**
Acidity as CaCO3	<2	mg/l	305.1	07/15/2005
Alkalinity Bicarbonate as HCO3	101	mg/l	2320B	07/15/2005
Alkalinity Carbonate as CO3	0	mg/l	2320B	07/15/2005
Alkalinity Total as CaCO3	83	mg/l	2320B	07/15/2005
Chloride as Cl	<1	mg/l	325.3	07/22/2005
Sulfate as SO4	19	mg/l	375.2	07/20/2005
Hardness as CaCO3	107	mg/l	2340B	08/10/2005
Specific Conductivity	203	µS/cm	2510B	07/15/2005
pH	6.7	S.U.	150.1	07/14/2005
Total Dissolved Solids	124	mg/l	160.1	07/18/2005
Aluminum as Al (Dissolved)	<0.05	mg/l	200.7	08/04/2005
Cadmium as Cd (Dissolved)	<0.0001	mg/l	200.8	07/20/2005
Calcium as Ca (Dissolved)	33	mg/l	200.8	07/27/2005
Copper as Cu (Dissolved)	0.004	mg/l	200.8	07/20/2005
Iron as Fe (Dissolved)	0.1	mg/l	200.7	08/04/2005
Lead as Pb (Dissolved)	<0.001	mg/l	200.8	07/20/2005
Magnesium as Mg (Dissolved)	6	mg/l	200.8	07/27/2005
Manganese as Mn (Dissolved)	0.16	mg/l	200.8	07/20/2005
Potassium as K (Dissolved)	<1	mg/l	200.8	07/28/2005
Sodium as Na (Dissolved)	1	mg/l	200.7	08/02/2005
Zinc as Zn (Dissolved)	0.06	mg/l	200.8	07/20/2005
Cations	2.18	meq/l	1030F	08/04/2005
Anions	2.06	meq/l	1030F	07/28/2005
Cation/Anion Balance	0.12	[max 0.20]	AWWA/APHA	08/04/2005